A

Dissertation Thesis

on

Effects of Gut Microbiota-host Kynurenine Pathway Interactions on *Caenorhabditis elegans* Early Ageing

Submitted to

Lancaster University

In Partial Fulfilment of the Requirements for The Degree

MASTERS by RESEARCH

In

BIOMEDICAL SCIENCE

Submitted by

Rajal Patel (36365203)

Under the guidance of

Dr Alexandre Benedetto (primary)

Dr Susan Broughton (secondary)

Bailrigg Ln, Bailrigg, Lancaster LA1 4YE, United Kingdom. 2022-2024

Dissertation Declaration

I, Rajal Patel, declare that the work submitted is my own and is not similar in concept to or based on the work of others, whether published or unpublished, except with full and proper acknowledgment.

_____

Signed by: Rajal Patel Date: 30th December 2024

Note: In accordance with the personal data and privacy protection guidelines established by Lancaster University, the originally included signatures have been intentionally omitted from this document.

TABLE OF CONTENT

ABBREVIATIONS

ARDs - Age-Related diseases

KP - Kynurenine Pathway

C. elegans - *Caenorhabditis elegans*

CeMbio - *Caenorhabditis elegans* Microbiome

CRISPR-Cas9 - Clustered Regularly Interspaced Short Palindromic Repeats, CRISPR-associated protein 9

SCFAs - Short-chain fatty acids

IBD - Inflammatory Bowel Disease

IgA - Immunoglobulin A

LPS - lipopolysaccharides

IGF - Insulin/Insulin-like Growth Factor

mTOR inhibitors - mammalian Target of Rapamycin

AMP - Adenosine monophosphate

AMPK - AMP-activated protein kinase

CNS - Central Nervous System

GBA - Gut-Brain Axis

GI - Gastrointestinal Tract

TRP – Tryptophan

KYN - Kynurenine

KYNA - Kynurenic acid

3HK - 3-hydroxykynurenine

QA - Quinolinic acid

IDO - Indoleamine 2,3-dioxygenase

TDO - Tryptophan 2,3-dioxygenase

RNAi - RNA interference

KO - Knockout

LROs - Lysosome-Related Organelles

CFU - Colony-Forming Unit

IPTG - Isopropyl-β-d-thiogalactopyranoside

Dual-RNA seq - Dual RNA sequencing

***kmo-1 (*OW478)** - Kynurenine 3-monooxygenase

***kynu-1 (*OW454)** - Kynureninase

***haao-1 (*OW479)** - 3-hydroxy anthranilate 3,4-dioxygenase

***tdo-2 (*OW717)** - Tryptophan 2,3-dioxygenase

***afmd-1 (*OW477)** - Arylformamidase

COSHH - Control of Substances Hazardous to Health

LB - Luria Bertani

SK - Streptococcus/Klebsiella Agar

NGBHI - Nutrient Gelatin Broth with Brain Heart Infusion

PVDF - Polyvinylidene difluoride

NGM - Nematode Growth Media

PM - Phenotype Microarray

PCR - Polymerase Chain Reaction

PLP - Pseudocoelomic Lipoprotein Pools

TL - Transmitted Light

sfGFP - Superfolder Green Fluorescent Protein

dTomato - Dimer Tomato

mPlum - Monomeric Plum fluorescent protein

RFP - Red Fluorescent Protein

TBE - Tris-Borate-EDTA

BF - Blue autofluorescence

ApE - A plasmid Editor

BLAST - Basic Local Alignment Search Tool

NCBI - National Center for Biotechnology Information

3HAA - 3-Hydroxyanthranilic acid

LIST OF FIGURES

LIST OF TABLES

ABSTRACT

Aging is a multifactorial process characterized by physiological decline and the onset of age-related pathologies. The gut microbiota has emerged as a major modulator of health span and longevity, influencing host biological processes. The kynurenine pathway (KP), a primary catabolic route of tryptophan, produces metabolites with roles in immune regulation and neurotoxicity, making it a potential target for aging interventions. This study investigates the interplay between gut microbiota and the KP in *Caenorhabditis elegans*, hypothesizing that KP activity influences microbial colonization dynamics and aging-related pathologies. This study also focuses on lifespan modulation, and metabolic activity. Using fluorescently tagged isolates of the CeMbio+ bacterial community i.e. *Enterobacter cloacae* (CEent1-mPlum), *Ochrobactrum vermis* (MYb71-sfGFP), *Stenotrophomonas indicatrix* (JUb19-RFP2), *Pantoea nemavictus* (BIGb0393a-mPlum), and *Enterobacter ludwigii* (MYb174-dTom), we studied colonization patterns in wild-type and KP mutant (*kmo-1, kynu-1, haao-1, tdo-2 and afmd-1*) worms under monoxenic and polyxenic conditions. It was observed that bacterial colonization is influenced by host genetic background and inter-bacterial competition. *kmo-1* and *haao-1* mutants exhibited enhanced bacterial loads and prolonged colonization, across most bacterial conditons. Certain bacterial strains (*E. cloacae, O. vermis, E. ludwigii*) were efficient colonizers, while others (*P. nemavictus, S. indicatrix*) showed lower colonization. Bacterial colonization also influenced aging pathologies, including intestinal atrophy, pharyngeal enlargement and uterine tumour formation, with monoxenic condition (*E. cloacae* and *E. ludwigii*) as well as polyxenic condition showing tissue-specific deterioration in KP mutants. Progressive pharyngeal enlargement was observed with most bacterial strains, with *E. ludwigii* showing a positive correlation between gut colonization and pharyngeal swelling. Uterine tumors appeared earlier (around 48 hours) and were generally larger under polyxenic conditions compared to monoxenic conditions. Lifespan assays showed *kmo-1* mutation affects longevity of *C. elegans* on *O. vermis* as well as on *E. coli*. Biolog Ecoplate metabolic profiling revealed that most of transformed bacterial strains phenotypically match their parental strains, maintaining strain-specific activity linked to colonization efficiency and host impact. This study underscores the complex interplay between gut microbiota, Kynurenine pathway mutations, aging and age-associated pathologies.

1 LITERATURE REVIEW

Ageing is a multifaceted process involving the gradual accumulation of biological changes within an organism, ultimately increasing susceptibility to age-related diseases (ARDs). These changes arise from intricate interactions between genetic predispositions and environmental influences. With advancements in medical science extending human lifespan, the prevalence of ARDs has grown, driving interest in understanding and targeting the ageing process. Consequently, the fields of *biogerontology* and *geroscience* have emerged to explore interventions that alleviate the burden of ARDs by directly modulating ageing mechanisms.

One promising area of investigation is the role of the gut microbiome in ageing, as research suggests that gut bacteria influence nutrient-sensing pathways; however, the precise mechanisms, particularly in model organisms and humans, remain poorly understood. To address this gap, our study investigates the impact of specific gut microbiota interventions on *Caenorhabditis elegans* mutants deficient in the Kynurenine Pathway (KP). The study aims to; examine how these mutations affect bacterial colonization, particularly the ability of CeMbio commensal strains to establish within the host; and evaluate ageing-associated parameters such as lifespan, health span, and aging pathologies.

1.1 The Journey of Aging

1.1.1 What is aging? It's impact on human's and animal's health

Aging is a complex biological process marked by a gradual decline in physiological functions and increased susceptibility to diseases, impacting humans and animals alike (Guo et al., 2022) In humans, aging leads to challenges such as higher rates of chronic diseases like cardiovascular conditions, diabetes, and dementia (Dong, et al., 2024). Similarly, aging in animals affects their behaviour, reproduction, and survival, necessitating adjustments in care and conservation practices (Gordon, et al., 2021).

At the molecular level, aging is characterized by hallmarks (see Figure 1) such as genomic instability, telomere attrition, epigenetic alterations, mitochondrial dysfunction, and impaired nutrient sensing (Zhang, et al., 2020). These hallmarks contribute to cellular senescence, chronic inflammation, and a decline in tissue repair, all of which underpin the

onset of chronic diseases. By intervening in these pathways, researchers aim to extend not only lifespan but also the years lived in good health.(López-Otín, et al., 2023).

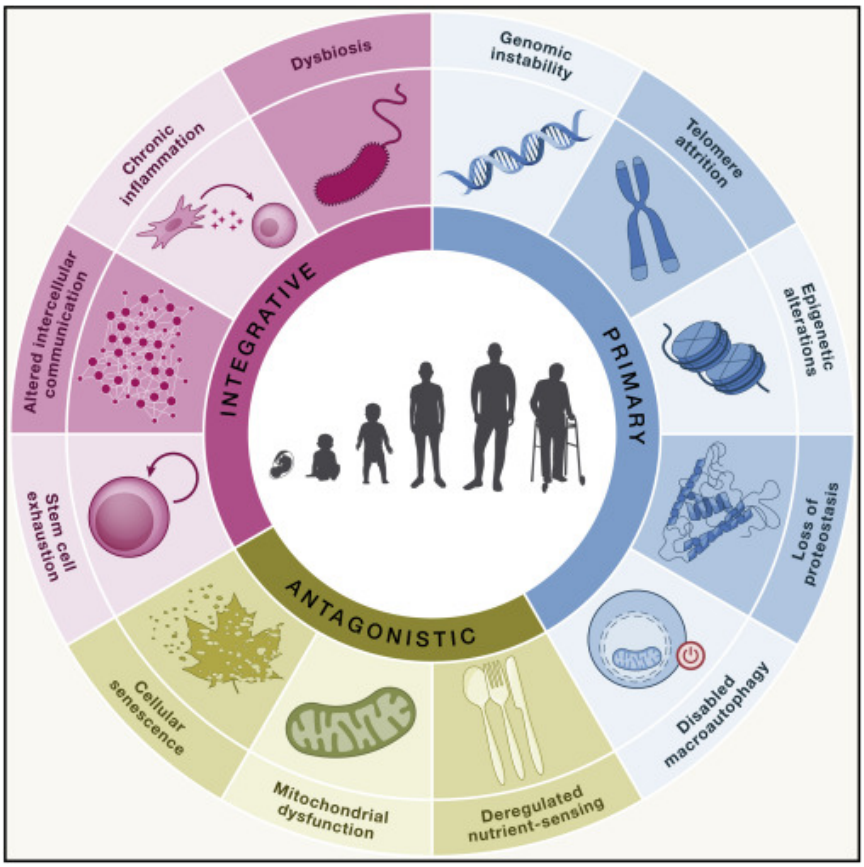

Figure 1. Hallmarks of ageing: The scheme enumerates the twelve hallmarks: genomic instability, telomere attrition, epigenetic alterations, loss of proteostasis, disabled macro autophagy, de-regulated nutrient sensing, mitochondrial dysfunction, cellular senescence, stem cell exhaustion, altered intercellular communication, chronic inflammation and dysbiosis. Image source: (López-Otín, et al., 2023)

In humans, aging results in physical and cognitive decline, raising healthcare demands and emphasizing the need for strategies promoting healthy aging (Wurm, et al., 2021). For animals, aging patterns vary across species, impacting population dynamics and care practices. Research on model organisms, such as mice and fruit flies, has revealed genetic and environmental factors influencing lifespan, offering insights into both human and animal aging (Cohen, 2017).

While advances in medicine have extended longevity, they also highlight the challenges of managing age-related issues. Ongoing research into aging mechanisms provides opportunities to enhance quality of life, supporting healthier aging across species. (Rony, et al., 2024)

1.1.2 Health span vs lifespan: the quest for longevity and quality of life

Aging is an inevitable biological process characterized by a gradual decline in physiological function, increased susceptibility to disease, and eventual mortality. Central to aging research are the concepts of lifespan and healthspan. Lifespan refers to the total duration of life, while healthspan represents the period during which an individual remains free from chronic diseases or functional decline that impairs quality of life (Fries, 2015). Although increasing lifespan has been a primary focus of aging research for decades, it is now evident that extending healthspan is of greater importance to ensure that longer lives are also lived in good health (Rollins, et al., 2017).

The compression of morbidity hypothesis proposed by Fries (1980) remains a cornerstone in understanding the importance of balancing lifespan and healthspan. Fries suggested that with effective interventions, the onset of age-related morbidity can be delayed, compressing the duration of illness and frailty into a shorter period near the end of life (Fries, 2015). This approach aims to not only extend life but also maintain functional and disease-free years, ultimately improving quality of life in aging populations. However, achieving this balance remains a significant challenge, as extending lifespan without addressing healthspan risks prolonged vulnerability to chronic diseases, frailty, and poor quality of life (Rollins, et al., 2017).

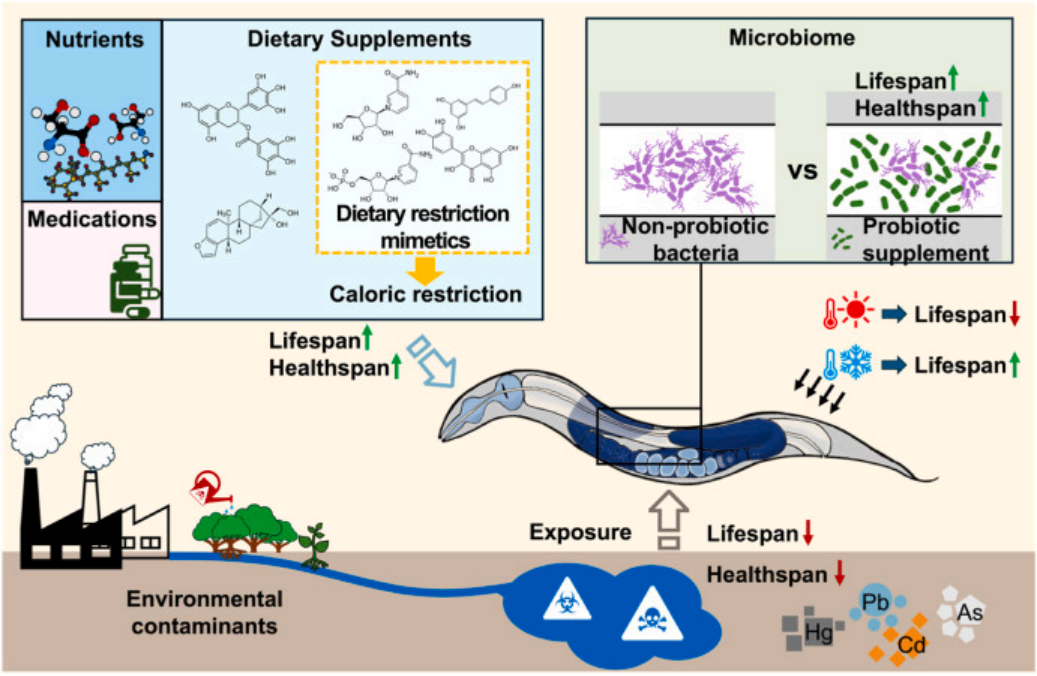

Figure 2. Factors known to regulate lifespan and healthspan in *C. elegans.* Image source: (Guo et al., 2022)

To better understand the mechanisms underlying healthspan and lifespan, aging research focuses on both intrinsic and extrinsic factors (as seen in Figure 2) that drive biological aging. Intrinsic factors include genetic predispositions, cellular senescence, and molecular damage accumulation, while extrinsic factors encompass environmental conditions, lifestyle choices, and stressors (Rollins, et. all, 2017; Keith,et al., 2014a). The interplay between these factors influences aging trajectories and determines the timing and severity of age-related diseases. Studies have shown that targeting these mechanisms can decelerate aging processes and improve healthspan (Keith, et al., 2014a).

1.1.3 Aging: a risk factor and therapeutic target

Aging is widely recognized as the primary risk factor for most chronic diseases, including cardiovascular disease, cancer, neurodegenerative disorders, and metabolic syndromes. The incidence of these conditions increases exponentially with age, making aging itself a significant contributor to morbidity and mortality (Cho & Park, 2024). Consequently, targeting the biological processes of aging has emerged as a promising strategy to prevent or delay multiple age-related diseases simultaneously, rather than addressing them individually.

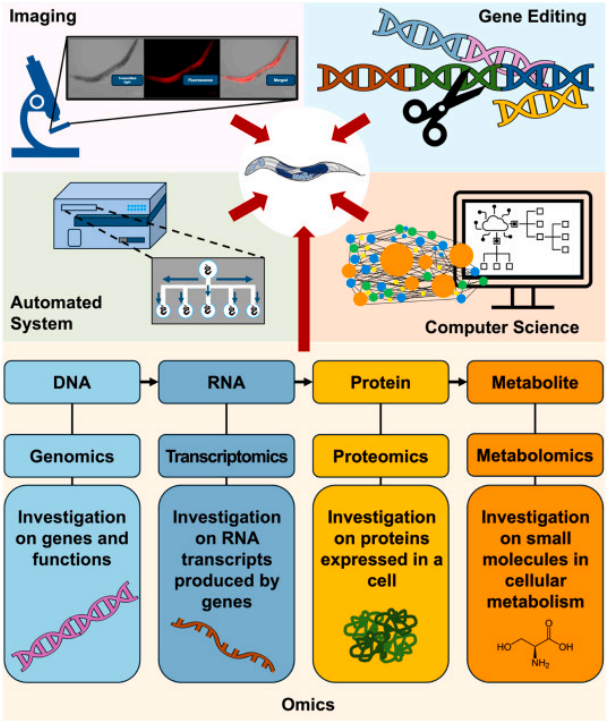

Figure 3. Application of technological advancements in healthy aging studies with *C. elegans*. Gene editing techniques, such as CRISPR, allow accurate manipulation of the *C. elegans* genome to investigate specific genes and their roles in aging. Image source: (Guo et al., 2022)

Recent advancements in biotechnology (see Figure 3) have paved the way for the development of targeted interventions to slow aging. CRISPR-Cas9 gene editing allows for precise genetic modifications to identify and manipulate longevity-related genes, offering new avenues for therapeutic intervention (Cho & Park, 2024). Similarly, innovations in molecular imaging techniques, such as fluorescence microscopy, enable real-time monitoring of age-related physiological changes, facilitating the identification of biomarkers and therapeutic targets (Cho & Park, 2024).

Looking to the future, interventions such as senolytics (drugs that selectively eliminate senescent cells), caloric restriction mimetics, and pharmacological agents targeting nutrient-sensing pathways (e.g., mTOR inhibitors) are being explored for their potential to improve healthspan (Keith, et al., 2014a). These interventions aim to address aging at its root cause, thereby reducing the burden of age-related diseases and promoting healthy longevity.

1.2 The Role of Gut Microbiome

1.2.1 Gut microbiota: an intricate ecosystem orchestrating health and ageing

The gut microbiome is a complex and dynamic community of microorganisms, including bacteria, archaea, fungi, and viruses, residing in the gastrointestinal tract. It is estimated that over 93% of the human gut microbiota consists of bacterial species belonging predominantly to the phyla *Firmicutes*, *Bacteroidetes*, *Actinobacteria*, and *Proteobacteria* (Hugon et al., 2015)This microbial composition is not static; it undergoes significant changes influenced by age, lifestyle, health status, and anatomical location within the digestive tract (Conlon & Bird, 2014).

The gut microbiota plays an important role in regulating host physiology and immune system (see Figure 4). It is essential for nutrient metabolism, digestion, and the synthesis of key biomolecules, including short-chain fatty acids (SCFAs) that promote immune regulation and maintain gut barrier integrity (Macfarlane & Macfarlane, 2003). Beyond the gastrointestinal system, the microbiome influences systemic health, impacting metabolic processes, the central nervous system, and even drug metabolism (Clayton, et al., 2008). Conversely, dysbiosis—an imbalance in microbial composition—has been linked to chronic diseases such

as obesity, diabetes, metabolic syndrome, autoimmune disorders, inflammatory bowel disease (IBD), neurodegeneration, cancer and aging (Verhaar et al., 2022). Human health may be affected by factors that alter microbiota, e.g. dietary changes and antibiotic usage, which may reduce microbiota complexity (Cabreiro & Gems, 2013)

The impact of the gut microbiome evolves throughout life. In early development, it influences immune maturation and metabolic programming, forming a foundation for long-term health (Schupack, et al., 2022). In adulthood, the microbiome supports energy balance, stress resilience, and pathogen defence. However, in older age, shifts in microbial composition are associated with systemic inflammation and age-related diseases, such as Alzheimer's pathology, further emphasizing its role in aging and frailty (Verhaar et al., 2022).

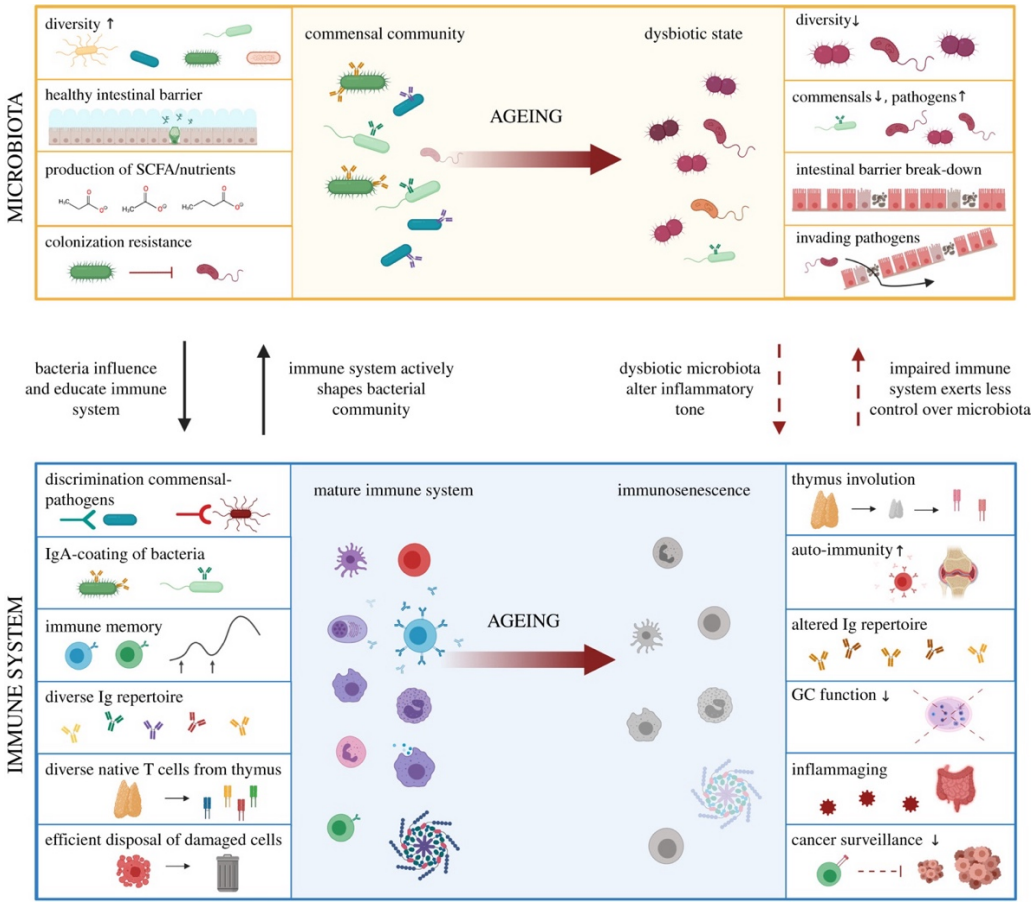

Figure 4. Modulations in the microbiota-immune system axis with aging. The figure demonstrates how aging affects the microbiota-immune system axis. The upper panel shows the transition of gut microbiota from a healthy state (characterized by high diversity, intact intestinal barrier, SCFA production, and colonization resistance) through a balanced commensal community to a dysbiotic state (marked by reduced diversity, pathogen dominance, and barrier breakdown). The lower panel illustrates parallel changes in the immune system, progressing from a mature state (with effective pathogen discrimination, IgA-coating of bacteria, diverse immune repertoire, and efficient cell disposal) to an immunosenescent state (showing thymus involution, increased autoimmunity, altered antibody profiles, reduced germinal centre function, inflammaging, and decreased cancer surveillance). Bidirectional arrows indicate the continuous interaction between these systems, which becomes impaired with age. Image source: (Popkes & Valenzano, 2020)

Despite significant advances in characterizing the human gut microbiome through large-scale omics studies, a clear definition of a "healthy" microbiome and its precise impact on aging-related mechanisms remains elusive. Establishing causal relationships between specific microbial changes and health outcomes is challenging in human studies due to confounding variables. Model organisms play a crucial role in bridging this gap by allowing controlled manipulations to uncover causal relationships between gut microbes and aging processes. Using these systems, researchers can investigate microbial influence on host physiology, immune responses, and longevity under defined conditions, offering potential strategies for improving healthspan and delaying aging-related decline (Dirksen et al., 2016).

1.2.2 Bacterial dysbiosis: A potential cause of pathology and age-related diseases

Gut dysbiosis refers to an imbalance in the microbial composition within the gut microbiome, where shifts in the diversity, abundance, or activity of microbial species disrupt the stable homeostasis necessary for host health (Haran & McCormick, 2021). Homeostasis is a state of equilibrium in the gut, where the microbiota and host immune system interact symbiotically to maintain key physiological processes, including digestion, metabolism, immune modulation, and protection against pathogens (Cabreiro & Gems, 2011; Biragyn & Ferrucci, 2018).

A healthy gut microbiome is characterized by microbial diversity and the production of essential metabolites such as short-chain fatty acids (SCFAs), which play critical role in shaping immune responses and protection of the intestinal barrier along with participating in its repair (as seen in Figure 5) (DeJong et al., 2020; Min'an Zhao et al., 2023).

However, when dysbiosis occurs, the delicate balance between the host and its gut microbiota is disrupted. This can result from both intrinsic factors (e.g., aging, host genetics) and extrinsic factors (e.g., dietary changes, antibiotics, and environmental stress) (Biragyn & Ferrucci, 2018). For instance, a Western diet high in fats and low in fiber is linked to reduced microbial diversity and increased levels of pro-inflammatory bacterial species (Haran & McCormick, 2021).

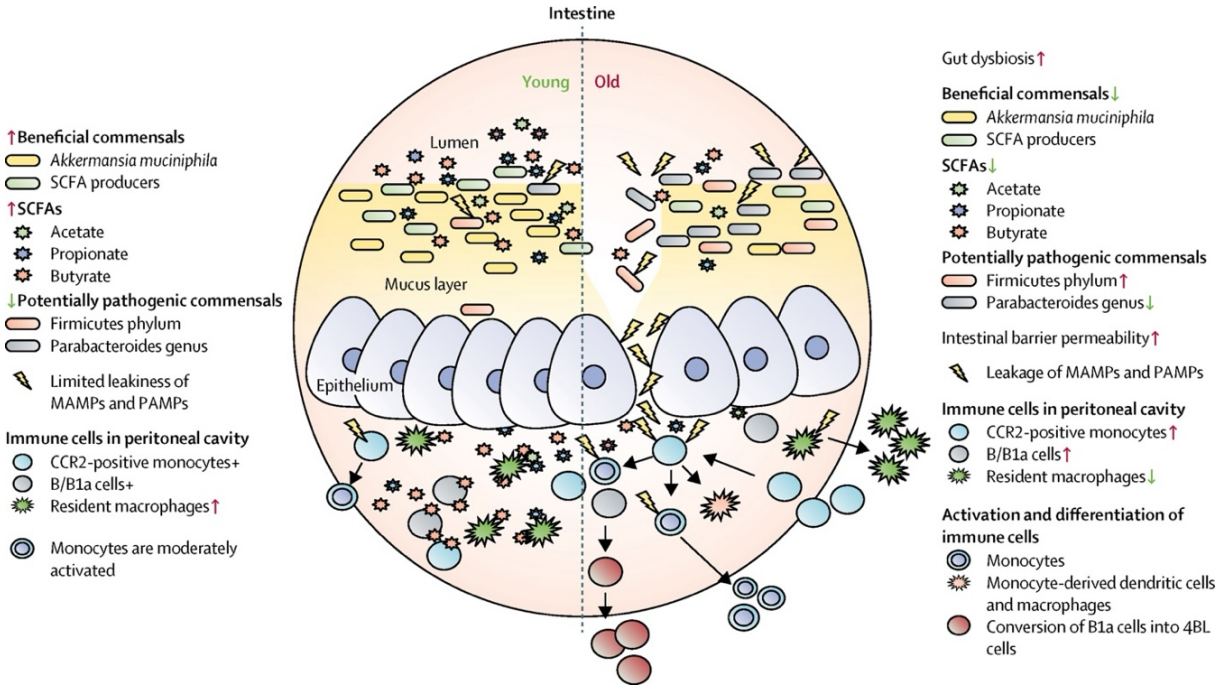

Figure 5. Gut homeostasis vs. Inflammaging and age-associated gut dysbiosis in young and old adult (Biragyn, Arya et al, 2018)

Dysbiosis can cause increased intestinal permeability (as seen in Figure 5), leading to translocation of bacterial components such as lipopolysaccharides (LPS) into the bloodstream, triggering low-grade chronic inflammation—a process known as *inflammaging* (Cani & Delzenne, 2009; Biragyn & Ferrucci, 2018). While multiple factors contribute to inflammaging, including aging-related immune dysfunction and lifestyle factors (Franceschi et al., 2018), gut dysbiosis has been identified as a key driver by promoting systemic inflammation and immune activation (O'Toole & Jeffery, 2015). Prolonged dysbiosis can disrupt bodily homeostasis, triggering local and systemic inflammatory responses linked to various age-related and inflammatory diseases, including metabolic syndrome, cardiovascular disease, asthma, inflammatory bowel disease, rheumatoid arthritis and cancers such as colorectal and prostate cancer (Min'an Zhao, et al., 2023).

Mechanistically, dysbiosis may alters several metabolic and signalling pathways involved in host physiology. Gut bacteria produce metabolites such as SCFAs, bile acids, and polyamines, which influence mitochondrial function, insulin-like signalling, and immune responses (DeJong et al., 2020). Dysbiosis can disrupt these pathways, leading to impaired metabolism, oxidative stress, and immune dysregulation, all of which accelerate aging and age-related pathologies (Haran & McCormick, 2021).

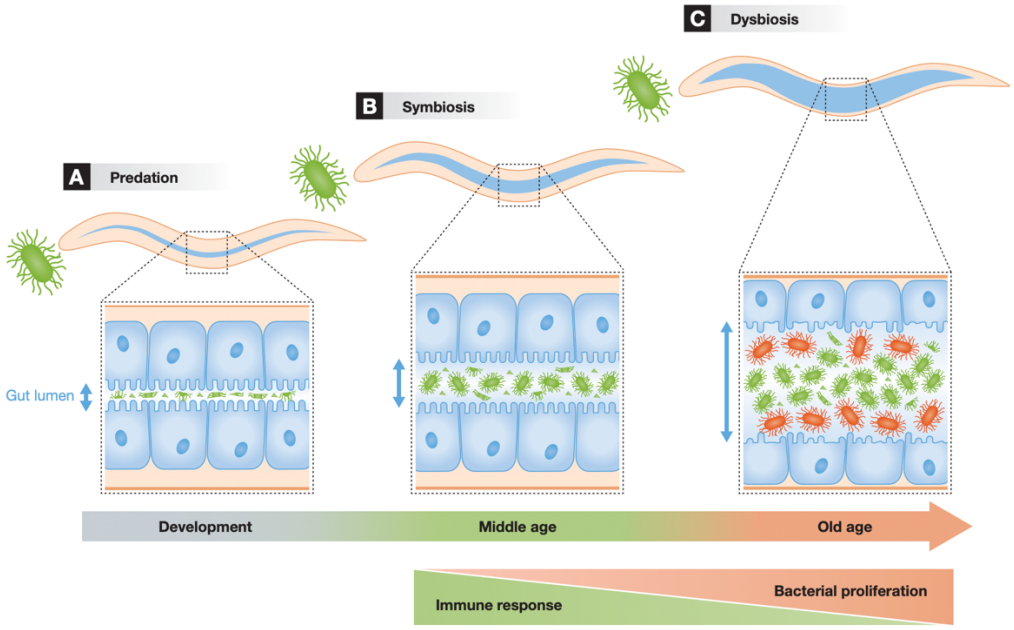

Figure 6. From hunter to prey: the changing relationship between *C. elegans* and *E. coli*. Different stages in the course of the life of the worm can serve as models to study how humans interact with their microbiota (Cabreiro & Gems, 2011)

However, it remains unclear whether a dysbiosis-like condition occurs in *C. elegans*, particularly in those maintained in monoxenic culture (Cabreiro & Gems, 2011), studies have shown that aging is associated with microbial over proliferation, intestinal lumen distension, and structural damage to the gut epithelium , including loss of microvilli and nuclei (as seen in Figure 6) (Garigan et al., 2002; McGee et al., 2011). During *C. elegans* aging, bacteria can shift to a detrimental state, termed pathobionts, which cause pathology even in the absence of invasion into intestinal cells. For example, certain bacterial strains or their secreted molecules, such as LPS, have been shown to regulate lifespan in *C. elegans* (Maier et al., 2010). By using *C. elegans* as a model system, researchers can study the causal relationships between gut dysbiosis, microbial metabolites, and host aging pathways under defined conditions. This includes identifying specific bacterial strains or molecules responsible for pathology and aging, offering potential targets for interventions such as probiotics or dietary modifications (Cabreiro & Gems, 2011; Haran & McCormick, 2021).

1.3 Kynurenine Pathway and Its Interactions

1.3.1 Metabolic pathways as central regulators of aging and age-related diseases

Nutrient-sensing pathways play a crucial role in regulating aging and age-related diseases. These pathways allow organisms to adapt their metabolism based on nutrient availability, thereby influencing growth, reproduction, and longevity. Three primary nutrient-sensing pathways are particularly significant: the Insulin/Insulin-like Growth Factor (IGF) signaling pathway, the mechanistic Target of Rapamycin (mTOR) pathway, and the AMP-activated protein kinase (AMPK) pathway (Van Der Goot & Nollen, 2013a).

The Insulin/IGF signaling pathway is a highly conserved mechanism that modulates growth and metabolism in response to nutrient levels. In model organisms such as *Caenorhabditis elegans* and *Drosophila melanogaster*, reduced activity of this pathway has been associated with increased lifespan (Van Der Goot & Nollen, 2013a).

The mTOR pathway is another critical regulator of cellular growth and metabolism. It integrates signals from nutrients, growth factors, and cellular energy status to control processes such as protein synthesis and autophagy. Inhibition of mTOR has been shown to extend lifespan in various organisms by mimicking the effects of dietary restriction (Johnson, et al., 2013).

The Kynurenine Pathway's (KP) a metabolic pathway involved in the catabolism of the amino acid tryptophan. It plays a key role in immune regulation, neurobiology, and redox balance. KP metabolites have been implicated in aging and various neurodegenerative conditions due to their effects on the central nervous system (CNS) and gut-brain axis (GBA), a network linking the gastrointestinal tract (GI) and the brain. This pathway plays a crucial role in the immune system, as alterations in the gut microbiota can influence KP metabolism, triggering inflammation and neurodegenerations. These processes are associated with disorders such as Alzheimer's and Parkinson's diseases (Kearns, 2024).

1.3.2 Tryptophan and the Kynurenine Pathway

The kynurenine (KP) and tryptophan (Trp) metabolism pathways exist in various forms across multiple species, from fruit flies (*Drosophila melanogaster*) and nematodes (*Caenorhabditis elegans*) to bacteria and plants. While these pathways may differ in complexity, they are at least partially conserved due to tryptophan's essential role in biological systems (Van Der Goot & Nollen, 2013b; Cervenka et al., 2017). Tryptophan biosynthesis was one of the last metabolic pathways to evolve and remains one of the most energy-intensive. Organisms like bacteria and plants, which can synthesize tryptophan, do so via the shikimate pathway—a process that has remained highly conserved (Gutierrez-Preciado et al., 2010, Nature Education). However, because of its high metabolic cost, mammals eventually lost this ability. Instead, they evolved mechanisms to obtain tryptophan through their diet and regulate its availability to meet their biological needs (Azmitia, 2020).

Tryptophan is an essential amino acid that humans must obtain from dietary sources, as the body cannot synthesize it. Tryptophan is critical for protein synthesis and serves as a precursor for numerous biologically important molecules, such as serotonin and melatonin (Van Der Goot & Nollen, 2013b). Serotonin, derived directly from tryptophan, is a neurotransmitter that plays a vital role in mood regulation, highlighting the importance of tryptophan in maintaining neurological and emotional health(Gao et al., 2018; Van Der Goot & Nollen, 2013b)

The majority of tryptophan (TRP) (approximately 95%) is metabolized via the kynurenine pathway (KP), which involves its conversion to kynurenine (KYN) and various downstream metabolites. These metabolites include kynurenic acid (KYNA), 3-hydroxykynurenine (3HK), and quinolinic acid (QA), which are important for various biological functions, including immune modulation, neuroprotection, and neuroinflammation (Gao et al., 2018). Approximately 1–2% of ingested tryptophan is converted to serotonin (5-HT) and melatonin via the serotonin pathway (Gao et al., 2018). Beyond serotonin synthesis, the kynurenine pathway plays a significant role in maintaining physiological functions, such as immune regulation and brain health (Gao et al., 2018; Van Der Goot & Nollen, 2013b).

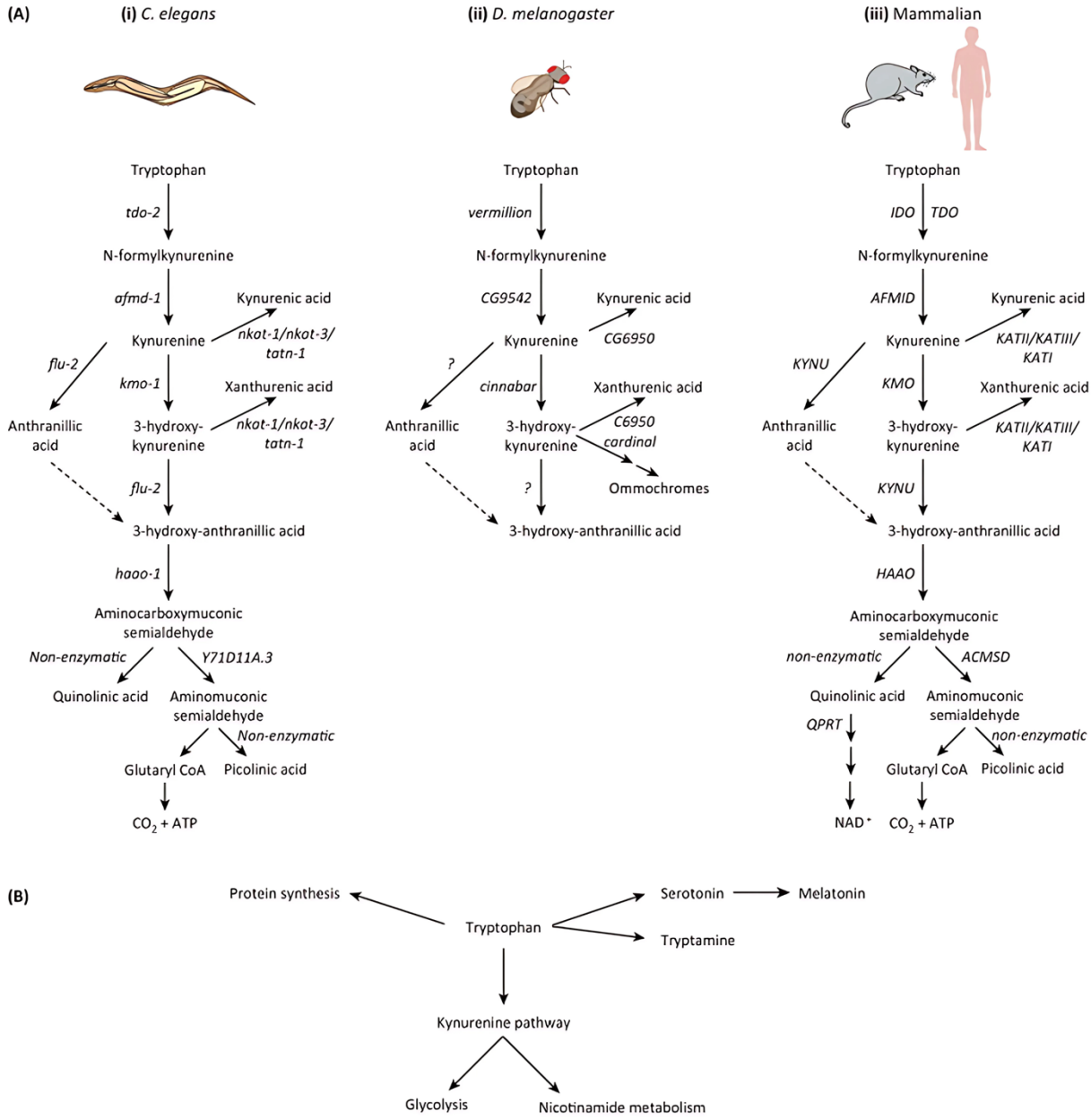

Figure 7. The kynurenine pathway (KP), which metabolises tryptophan, is conserved amongst organisms such as *Caenorhabditis elegans*, *Drosophila melanogaster* and mammals. This highlighting its fundamental role in regulating biological functions. Image source: (Van Der Goot & Nollen, 2013).

Recent studies have highlighted the emerging importance of tryptophan metabolism in aging and age-related pathologies. A notable observation is the elevated kynurenine-to-tryptophan ratio in older adults, suggesting increased tryptophan degradation through the KP with age. This metabolic shift has been associated with chronic inflammation and heightened susceptibility to neurodegenerative diseases and cancer, making tryptophan metabolism a key player in aging biolog (Van Der Goot & Nollen, 2013b). Furthermore, kynurenine metabolites, which can cross the blood-brain barrier, influence neurotransmitter systems,

underlining their neuroactive and neuroprotective properties (Kearns, 2024; Van Der Goot & Nollen, 2013b).

Furthermore, pharmacological inhibition of enzymes within the kynurenine pathway has provided direct evidence for its role in regulating age-related pathologies, with studies demonstrating that inhibiting indoleamine 2,3-dioxygenase 1 (IDO1) or tryptophan-2,3-dioxygenase (TDO) can suppress tumor growth and mitigate neurodegeneration in various models. This indicates that targeting tryptophan metabolism could be a viable strategy for promoting healthy aging and managing age-related diseases (Gao et al., 2018)

1.3.3 Role of Kynurenine Pathway in regulating host-microbiome interactions

The kynurenine pathway (KP) appears to play an important role in regulating host-microbiome interactions by influencing both microbial composition and activity within the gut microbiome. Metabolites derived from the KP, such as kynurenine and its derivatives, modulate immune responses, shaping the microbial community structure and functionality in the gut (Kearns, 2024). These interactions underscore the critical role of the KP in maintaining a balanced gut microbiota, particularly as it relates to inflammatory and metabolic processes (Nagy-Grócz, et al., 2024).

The main causes of change in gut microbiota are due to antibiotics, type of labour and suboptimal bacteria transmission from the mother (Elvers, et. al., 2020) . This may influence the levels of circulating tryptophan and kynurenine metabolism not only in the periphery but also in CNS (Kennedy, et al., 2016). A bidirectional relationship exists between tryptophan metabolism and the gut microbiota, where microbial metabolites influence host tryptophan degradation pathways, further impacting the KP (Gao et al., 2018). For example, specific microbial enzymes can alter the flux through the KP, regulating the production of key metabolites involved in neuroimmune signalling and mitochondrial function (Kearns, 2024).

This interaction is essential not only for metabolic homeostasis but also for preserving gut health, particularly during aging, when dysregulation of the KP and microbial composition are commonly observed (Nagy-Grócz, et al., 2024).

The correlation between the KP and gut microbiota offers a valuable framework for studying their mutual interactions and contributions to host health. Modulations in the KP, such as

alterations in enzyme activity or metabolite levels, can profoundly affect the ability of both host and bacterial populations to thrive and colonize the gut (Kearns, 2024). For instance, targeted pharmacological interventions in KP enzymes like indoleamine 2,3-dioxygenase (IDO) or tryptophan 2,3-dioxygenase (TDO) have shown promise in reshaping gut microbial communities, potentially improving outcomes in age-related diseases (Gao et al., 2018). The metabolite 3 HAA has been shown to extend the lifespan of *C. elegans* and improve gut integrity, while also providing resistance against bacterial infections(Espejo et al., 2024b). These findings suggest that KP metabolites may serve as regulators of both microbial dynamics and host resilience.

In conclusion, the intricate interplay between the KP and gut microbiota highlights its potential as a therapeutic target for enhancing host health and promoting a balanced microbiome. By leveraging the regulatory mechanisms of the KP, novel strategies could be developed to mitigate inflammation, support microbial diversity, and ultimately enhance healthspan during (Nagy- et al., 2024).

1.4 *Caenorhabditis elegans* as A Model for Studying Microbiota and Kynurenine Pathway Interactions

1.4.1 Modelling the human microbiota: the role of vertebrate and invertebrate model systems

August Krogh's principle, highlighting the value of specific organisms for studying biological problems, underscores the significance of model systems in research. His profound statement—"for many biological problems, there is an animal on which it can be most conveniently studied"—is often cited when animal models are chosen. Biogerontologists commonly utilize species like *Saccharomyces cerevisiae*, *Caenorhabditis elegans*, *Drosophila melanogaster*, and *Mus musculus* for microbiota studies. Despite their evolutionary divergence, these models reveal conserved processes relevant to human health and microbiota interactions (Buffenstein, et al., 2008)

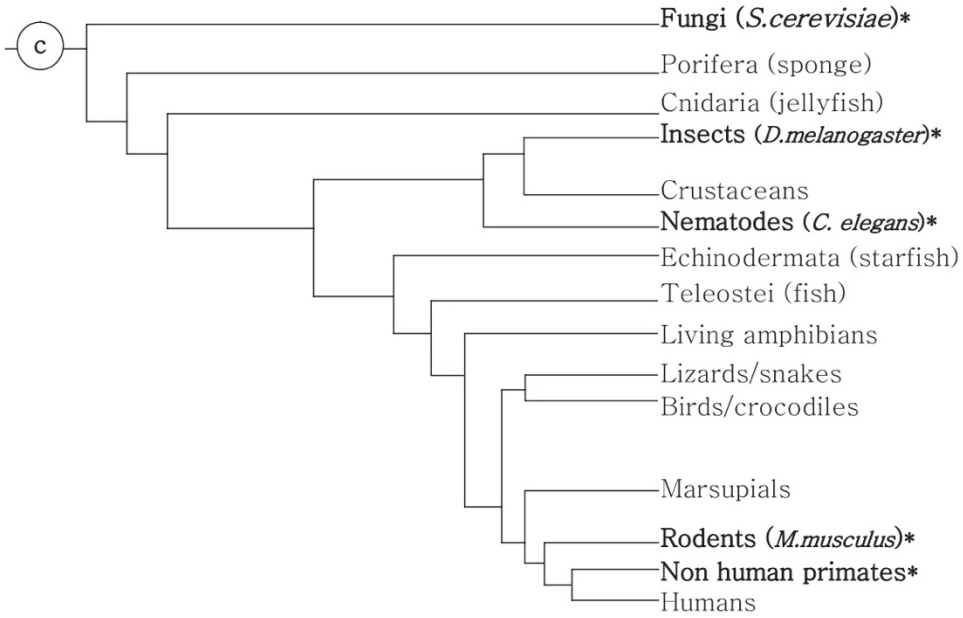

Figure 8. Phylogenetic relationships of model organisms used in aging research. "C" rep- resents a common ancestor. Animals in bold are traditional models used in aging research. Image source: (Buffenstein, et al., 2008)

Mammalian models, particularly mice, have traditionally dominated microbiome research due to their genetic similarity to humans and availability of transgenic strains (Holmes & Kristan, 2008). Mice allow for manipulation of gut microbiota through germ-free systems, dietary interventions, and bacterial transplants. However, murine studies are resource-intensive, time-consuming, limited by their complex physiology, and which may differ from humans in key aspects such as immune response, gut microbiota composition, and metabolic processes (Nguyen et al., 2015). As a result, findings from murine models may not fully reflect human microbiota-host interactions.

Invertebrate models, such as *Drosophila melanogaster* (fruit flies), and *Caenorhabditis elegans*, offer simpler and cost-effective systems for microbiome studies while retaining evolutionary conservation of key signalling pathways.

Mice (*Mus musculus*) are a cornerstone of microbiota research due to their genetic similarity to humans, with approximately 90% of their genes being homologous (Waterston et al., 2002). Their well-developed immune, respiratory, and metabolic systems make them ideal for studying host-microbe interactions and disease mechanisms, particularly through controlled experiments such as germ-free and gnotobiotic models (Rydell-Törmänen & Johnson, 2019). These models allow precise manipulation of microbial communities, enabling

researchers to investigate causal relationships between the microbiota and host physiology, including metabolic changes and disease phenotypes. For example, calorie restriction in mice has shown benefits such as improved insulin sensitivity and reduced inflammatory markers, mirroring human responses (Fontana, 2007). Despite their advantages, mice studies are time-consuming, costly, and require significant ethical considerations due to their longer lifespan (1.5–3 years) and generation time (1–2 months) (Flurkey et al., 2009).

Zebrafish (*Danio rerio*) serve as a valuable vertebrate model for studying host-microbiome interactions due to their optical transparency during early developmental stages, which allows real-time visualization of microbial colonization, gut dynamics, and host responses (Abou-Dahech & Williams, 2024a). These fish share 70% of their genes with humans, including those linked to aging-related diseases such as Alzheimer's disease(Abou-Dahech & Williams, 2024a). This unique trait enables non-invasive imaging to track microbial behaviour, host-microbiota interactions, and the establishment of microbial communities in the gut in ways not achievable with mammalian models. Additionally, zebrafish share conserved immune pathways, such as Toll-like receptors and NF-κB, that regulate host-microbiota interactions. However, differences in gut physiology, such as the absence of a stomach and a shorter gut transit time, limit the direct applicability of zebrafish models to human gut studies, as does the lack of specific human microbial species (Abou-Dahech & Williams, 2024b).

Fruit flies (Drosophila melanogaster) another extensively used model to study host-microbiome interactions, gut-brain signaling, and aging. The fruit fly is a well-established genetic model for studying human diseases, with many conserved biological traits and functional homologs for nearly 75% of human disease-related genes (Pandey & Nicolas, 2011). They possess a relatively simple gut microbiota dominated by a few bacterial species, making it easier to track microbial changes (Lee & Min, 2019). Moreover, Drosophila shares conserved pathways such as insulin/IGF-1 and JNK, which regulate longevity and microbial influences. Unlike organisms such as zebrafish larvae and *C.elegans*, which have transparent bodies that allow for real-time visualization of internal processes, *Drosophila* lacks this feature. This opacity hinders non-invasive observation of gut microbiota dynamics (Metwaly, et al.,2025). Proper isolation and recovery of the microbiota from the gut lumen often require precise dissection techniques under high-magnification microscopy. These factors make it difficult to standardize conditions for microbiome studies.

While vertebrate models like mice and zebrafish offer valuable insights into microbiome-host interactions, the complexity and cost of these models limit their scalability for large-scale studies. In contrast, *Caenorhabditis elegans* (*C. elegans*) offers a simpler, cost-effective alternative with a fully sequenced genome, short lifespan, and well-established microbiome. Its tractability allows for controlled experimental manipulation, making it an ideal model for studying microbiome dynamics in a way that is both efficient and informative (Wu et al., 2024 ;Zhang, F. et al., 2017). This makes *C. elegans* a powerful tool for microbiome research, especially in aging and disease studies.

1.4.2 Tiny worm, big impact: A model for studying host-microbiota interactions.

Caenorhabditis elegans (*C. elegans*), a nematode that was first described by the French biologist Maupass in 1900, became a pivotal model organism in the 1960s, thanks to the groundbreaking work of South African biologist Sydney Brenner (Brenner, 1973). His pioneering research on neuronal development in *C. elegans* led to its widespread use in genetics and molecular biology, earning Brenner the Nobel Prize in Medicine in 2002. *C. elegans* has since become an invaluable model for studying diverse biological processes, including host-microbiota interactions.

C. elegans, is a nematode species which are naturally found in temperate soil environments, decaying organic matter such as rotting fruits and leaves (Dirksen, et al., 2020). Its suitability stems from several factors: 40% of genes found in *C. elegans* have orthologs in humans (Radeke & Herman, 2021) , and it is relatively simple, well-characterized biology (Zhang, F. et al., 2017), small size (1.5 mm), high fertility rates (~250 eggs per worm), short lifespan (~3 weeks, 20°C), easy maintainance in laboratory setting and low cost of their food source (*E. coli*), make it cost-effective for large-scale studies (Dirksen et al., 2020).

The life cycle of *C. elegans* begins with an embryonic stage, followed by four distinct larval stages (L1–L4), and culminates in the adult stage (Figure 9). Under optimal conditions, the N2 strain completes its life cycle in approximately 3.5 days at 20°C. Alternatively, *C. elegans* can enter a dauer stage—a long-term survival state—bypassing the typical L3 larval stage (Figure 9). Its transparent body facilitates direct observation of anatomical structures and fluorescently labelled molecules, making it a valuable tool for research. Furthermore, *C. elegans* can be cryopreserved, and an extensive collection of strains is available through the

Caenorhabditis Genetics Center (https://cgc.umn.edu), solidifying its role as a prominent model organism in biomedical studies (Wu et al., 2024)

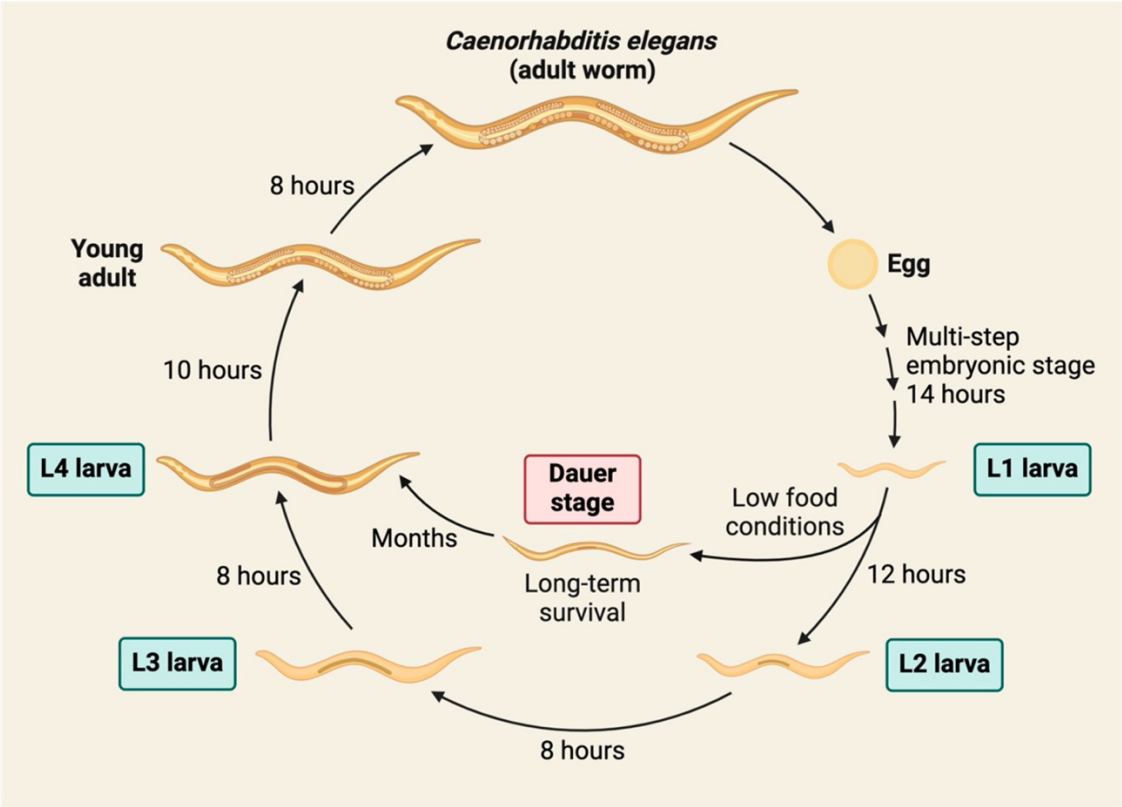

Figure 9. Schematic representation of the *Caenorhabditis elegans* life cycle: including the embryonic stage, four larval stages (L1–L4), and the adult stage. Under adverse conditions, the L3 stage can transition into a dauer state for long-term survival. The cycle is completed in approximately 3.5 days at 20°C. Image source: (Wu et al., 2024)

In nature, *C. elegans* carries a more diverse and species rich bacterial community, *dominated* by *Proteobacteria such as Enterobacteriaceae* and members of the genera *Pseudomonas, Stenotrophomonas, Ochrobactrum, and Sphingomonas* (Dirksen et al., 2016) compared to the simplified, controlled settings of laboratory experiments where it feeds predominantly on bacteria, with *Escherichia coli* to establish its microbiome. The organism's gut microbiota is primarily composed of fast-growing, Gram-negative bacteria, which are also typically found in decaying organic matter in natural environments (Zhang, F. et al., 2017). These bacteria engage in competitive metabolic interactions with the host, influencing *C. elegans'* growth and immunity (Dirksen et al., 2016). Certain bacterial strains have been identified as enhancing the fitness of *C. elegans*, offering protection against pathogenic microorganisms, thereby highlighting the crucial role of these microbial associations in supporting host

resilience against environmental stressors and infections (Radeke & Herman, 2021). Moreover, the ability to reconstruct microbiomes that mirror those naturally present in the environment and its easy traceability underscores the potential of *C. elegans* as a robust and valuable model for studying host-microbiota interactions, offering significant insights into microbial community structure and function (Wu et al., 2024).

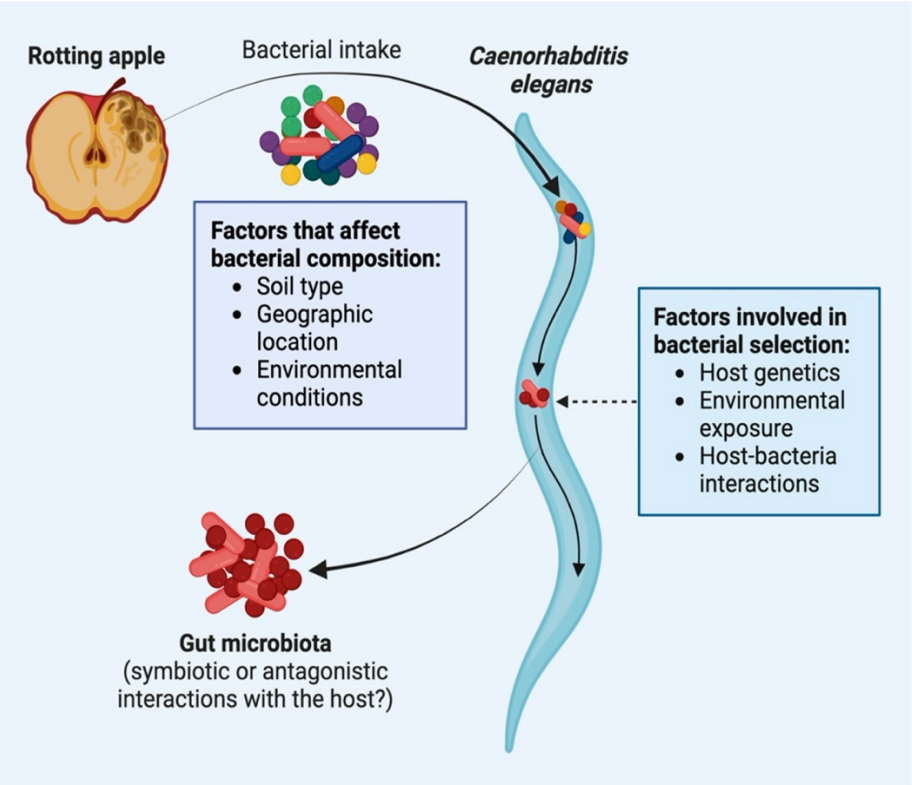

Figure 10. Factors influencing bacterial colonization and host-microbiota interactions in *C. elegans*. In their natural environment, *C. elegans* nematodes consume bacteria present on decomposing fruits, plants, and organic matter. Multiple factors impact the colonization and selection of bacteria within the gut of *C. elegans*, making it a valuable model for investigating host-microbiota interactions. Image source: (Wu et al., 2024)

1.4.1 Experimental approaches: tools and techniques to study aging and gut microbiota interactions *Caenorhabditis elegans*

Interventions for studying gut microbiome and aging in *C. elegans* have been significantly enhanced through the development of molecular tools and controlled experimental approaches. *C. elegans* is highly amenable to genetic manipulation, and its microbiome can be efficiently controlled using the bleaching protocol, which eliminates all microorganisms except nematode eggs, enabling cultivation under axenic or monoxenic conditions

(Stiernagle, 2006). Furthermore, several well-established life history readouts, such as stress resistance, lifespan, population growth, and fecundity, serve as valuable metrics for investigating *C. elegans*-microbiome interactions (Zhang, F. et al., 2017).

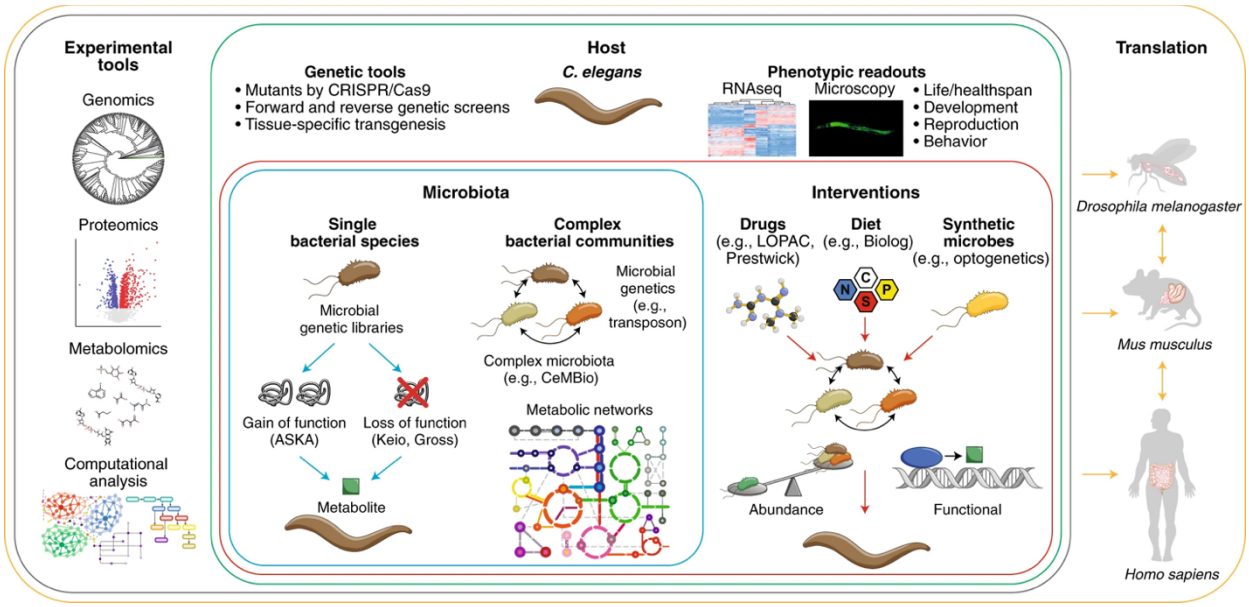

Figure 11. **Experimental approaches for studying host- gut bacterial interactions using *C. elegans*** (Backes et al.,2021). The small size of *C. elegans* and available experimental toolbox makes it an ideal organism for exploring host- gut bacterial interactions.

The availability of a complete genome sequence, combined with advanced genetic manipulation tools and techniques have been developed to investigate the gut microbiota in *C. elegans*—including RNA interference (RNAi), gene knockouts, transgenesis, and mutagenesis—has facilitated precise studies on the microbial effects on host physiology (Zhang, F. et al., 2017;Dirksen et al., 2020;Wu et al., 2024). Methods such as 16S rRNA sequencing allow for microbial community analysis, while dual RNA-seq enables simultaneous examination of gene expression in both the host and its colonizing microbes (Westermann, Gorski, & Vogel, 2012; Dirksen et al., 2020). Metabolomics and proteomics approaches help identify microbial metabolites and proteins that influence host health and aging. Additionally, tools like Biolog and EcoPlates facilitate functional phenotyping of bacteria, providing insights into their metabolic traits (Dirksen et al., 2020). Resources such as CeMbio have further streamlined research by cataloguing the natural microbiota of *C. elegans*, offering a standardized system for studying host-microbe dynamics (Dirksen et al., 2020). These

methodologies together allow researchers to explore how gut bacteria contribute to aging and health span, providing critical insights into microbial influences on host biology.

Interventions such as dietary modifications and microbiome composition analysis are currently used to investigate how microbial metabolites impact age-related pathways. These pathways include insulin/insulin growth factor (IGF)-1-like receptor, DAF-2, that dictates the gut microbiome composition in *C. elegans* (Singh & Luallen, 2024). For example, specific bacterial strains have been identified to promote longevity or delay aging in *C. elegans*, offering insights into probiotics with potential health benefits (Zhang, F. et al., 2017). This research has also enabled the exploration of classical signalling pathways, such as those involved in development, neurobiology, cell death, and aging (Markaki & Tavernarakis, 2020).

Notably, *C. elegans* shares conserved molecular pathways—like antimicrobial responses—with mammals, making it a relevant model for studying microbial interactions at the cellular and molecular levels (Radeke & Herman, 2021). Additionally, *C. elegans*' susceptibility to human pathogens such as *Pseudomonas aeruginosa*, *Staphylococcus aureus*, and *Salmonella* highlights its utility for host-pathogen interaction studies (Issi, et al., 2017). These advantages position *C. elegans* as a bridge between *in vitro* systems and mammalian models, enabling high-throughput screening of anti-aging drugs and microbiota interventions at reduced experimental costs.

1.4.2 *Caenorhabditis elegans* as a model for studying Kynurenine Pathway interactions

C. elegans has been a valuable model organism in the study of the kynurenine pathway (KP) and its role in aging and neurodegenerative diseases. Several studies have investigated the production of kynurenic acid (KYNA) and the transport of L-kynurenine within *C. elegans* neurons (Lin, et al., 2020). Research has also explored how the KP pathway influences aging in these worms, including its role in proteotoxicity associated with Alzheimer's and Parkinson's diseases (Van Der Goot & Nollen, 2013b). Moreover, *C. elegans* has been used to study rhodoquinone biosynthesis, a process linked to the KP in nematodes (Roberts Buceta et al., 2019). The Van der Goot lab has developed knockout (KO) strains of *C. elegans* to study the KP pathway, enabling researchers to explore the effects of specific genetic deletions on aging and neurodegeneration (Van Der Goot et al., 2012).

A particularly interesting phenomena associated with the KP in *C. elegans* is the "blue death." This event is marked by a wave of blue fluorescence that propagates from the head to the tail during organismal death, driven by the accumulation of anthranilic acid in lysosome-related organelles (LROs) within the gut. Anthranilic acid, a KP metabolite, exhibits natural autofluorescence at 364 nm/480 nm, making it a visually accessible marker for studying KP activity in vivo (Coburn et al., 2013)

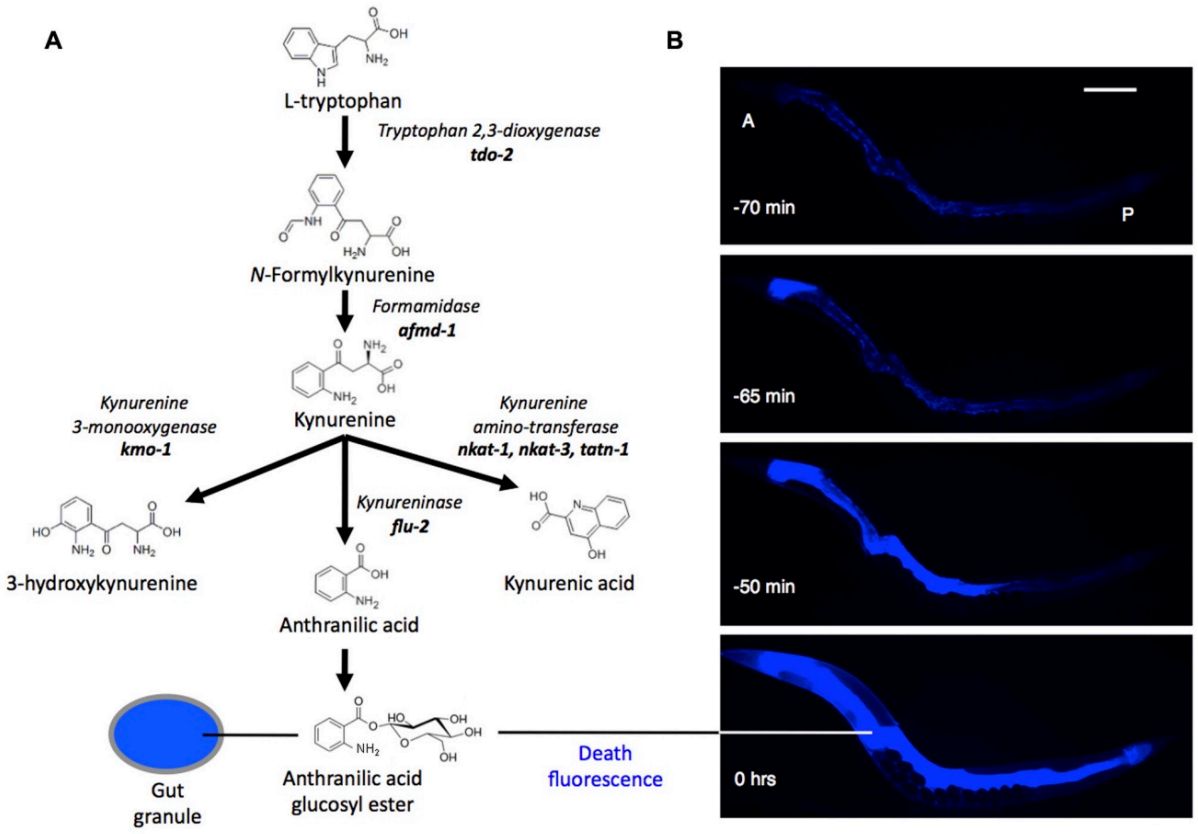

Figure 12. A. Synthesis of anthranilic acid by the kynurenine pathway. B. Death fluorescence in young adult *C. elegans* killed with a heated wire (DAPI filter). Image source: (Coburn & Gems, 2013)

The gut granules, or LROs, in *C. elegans* are specialized organelles with roles in stress responses and aging. These organelles harbor metabolites such as anthranilic acid, linking the kynurenine pathway to processes such as necrosis, stress resistance, and aging-related deterioration (Coburn et al., 2013;Coburn & Gems, 2013). Importantly, the KP's metabolic intermediates can influence healthspan and lifespan by modulating cellular stress responses, highlighting the utility of *C. elegans* for unraveling the molecular and physiological effects of these metabolites (Coburn & Gems, 2013) The transparent body of *C. elegans* further

facilitates live imaging, enabling researchers to monitor the progression of KP-related phenomena such as the blue death in real time. By leveraging the blue death as a visible endpoint and its genetic tools, *C. elegans* offers unique advantages for elucidating KP-related mechanisms and their broader implications for health and aging (Coburn & Gems, 2013)

In the lab (Benedetto, unpublished), the lysosome-related organelles (LROs) and the kynurenine pathway (KP) were found to play a role in host defence against gut bacterial pathogen. Previous work has shown that the worm's autofluorescence shifts in a kynureninase-dependent manner during infection, suggesting a role for the KP in modulating immune responses to pathogens like *Enterococcus faecalis* (Benedetto, unpublished). Furthermore, kynureninase mutants, which accumulate kynurenine metabolites, show increased resistance to *E. faecalis* infection, highlighting the potential antimicrobial properties of KP metabolites. The conserved nature of the kynurenine pathway between *C. elegans* and higher organisms including human, along with its role in regulating immune responses, highlights the significance of using *C. elegans* as a model for studying KP interactions (Coburn & Gems, 2013). Research in this organism has the potential to provide valuable insights into therapeutic strategies aimed at modulating the KP to enhance healthspan and address aging-related diseases (Coburn & Gems, 2013)

1.4.3 Current state of knowledge on *Caenorhabditis elegans* gut microbiota and aging

Research has identified a core membership of the natural microbiome in *C. elegans*, which includes several bacterial families such as *Enterobacteriaceae, Pseudomonadaceae*, and *Sphingobacteriaceae*. High-throughput sequencing techniques have been employed to analyse the gut microbiota composition in wild populations, emphasizing that specific bacterial interactions are vital for the host's health (Han et al., 2017; Zhang, et al., 2020)

Recent studies have highlighted how particular bacterial species can influence the lifespan and stress resistance of C. elegans. For instance, colonization by *Bacteroides fragilis* has been shown to significantly enhance lifespan under oxidative stress conditions, suggesting that certain commensal bacteria may play a crucial role in the aging process (Zimmermann et al., 2023;Donato et al., 2017). Additionally, *Bacillus subtilis* has been found to produce biofilms that extend the lifespan of C. elegans by more than 50%. This effect is attributed to molecules

like nitric oxide and quorum-sensing peptides produced by the bacteria, which enhance the worm's resistance to various stressors(Donato et al., 2017;Clark & Walker, 2017)

Experiments to assess colonization dynamics, researchers employed methods such as colony-forming unit (CFU) counts and 16S rRNA sequencing to evaluate the ability of these bacteria to colonize the nematode gut. The first experiment focused on individual CeMbio strains, while subsequent experiments examined community-level colonization. Results indicate that specific strains, including those from the Gammaproteobacteria and Bacteroidetes phyla, effectively colonized the gut and positively influenced host fitness (Dirksen et al., 2020) For instance, *Enterobacter cloacae* was shown to enhance reproductive success, while *Pseudomonas aeruginosa* contributed to improved growth rates.

Overall, these findings underscore the importance of specific commensal bacteria in shaping the health and aging processes of *C. elegans*. By manipulating gut microbiota through targeted bacterial strains, researchers can potentially promote health and delay aging in this model organism.

2 PROJECT BACKGROUND

2.1 Selecting experimental bacteria

The CeMbio (*C. elegans* Microbiome) collection (as shown in Figure 13)represents a significant advancement in microbiome research, offering a standardized set of 12 microbial strains selected for their relevance in *C. elegans* gut ecology. This resource allows for reproducible studies of host-microbiota interactions, including how specific microbes influence immunity, development, and aging (Dirksen et al., 2020) The extended CeMbio+ collection further diversifies microbial strains, making it ideal for studying more complex microbial dynamics and their ecological impact.

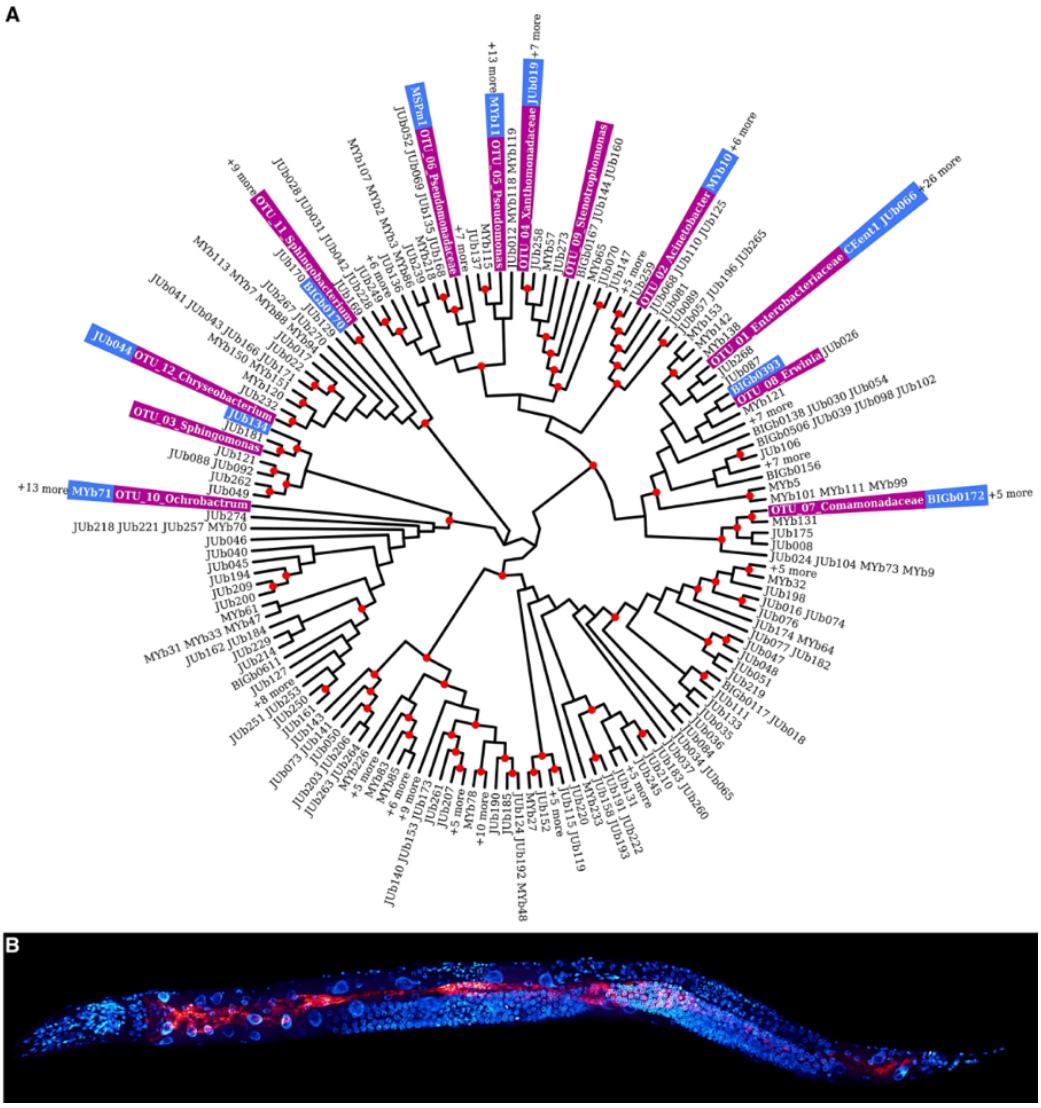

Figure 13. The CeMbio strains A. (blue) were selected by comparing 510 cultured bacteria from the *C. elegans* microbiome with the 12 most common bacterial groups (OTUs) (pink) identified from previous analysis of natural worm samples. **B.** Fluorescence in situ hybridization of C. elegans N2 colonized with the CeMbio strains [red, general bacterial probe EUB338; blue, DAPI] (Dirksen et al., 2020)

I chose to use the *CeMbio* strains for my research on gut colonization assays and aging pathologies because these well-characterized strains provide a robust framework for investigating the role of gut microbiota in modulating host health and aging. Understanding how these microbes interact with *C. elegans* and influence intestinal colonization, and age-related diseases may provide insights into potential therapeutic targets for supporting host health and longevity (Dirksen et al., 2020)

2.2 Bacterial transformation using Tn-7 triparental matting for *Caenorhabditis elegans* gut colonisation assay

Fluorescently transformed CeMbio+ have revolutionized the understanding of the colonisation dynamics in *C. elegans* and how the mutation of different pathways can affect this microbial community dynamics, as these engineered strains enables real-time *in-vivo*, visualization and tracking of bacterial populations within the host. This technique has been crucial in understanding microbial community establishment during *C. elegans* development. (Zhang, F. et al., 2017) used fluorescently labelled probiotics to investigate their colonization efficiency and persistence in the nematode gut. Similarly, (Zhao et al., 2017) used RFP tagged *E. faecalis* to investigate the causes of death in *C. elegans* due to pharyngeal infections when exposed to bacteria and it revealed two distinct modes of death, one that largely occurs earlier in life than the other.

The goal of this protocol is to transform the target bacteria to express fluorescent protein and gentamicin resistance while eliminating vector bacteria or untransformed bacteria through gentamicin treatment and activation of the kill switch via IPTG (isopropyl-β-d-thiogalactopyranoside) exposure. Combined with advanced imaging techniques, these approaches have allowed for three-dimensional mapping of microbial distributions within *C. elegans* GI tract and quantifying the bacterial load through fluorescence intensity measurements. By utilising distinct fluorophores expressed by each bacterium, it becomes feasible to track single isolate colonisation as well as co-colonisation of bacterial community in a single worm. Hence, bacteria transformation using the Tn7 kill switch counterselection system streamlines transformation across diverse bacteria lineages, including novel and uncharacterized bacteria, using a standardised protocol.

2.3 Metabolic Phenotyping of Transformed and Parental Bacterial Strains Using Biolog Phenotypic Microarrays and EcoPlates

This study aimed to assess the metabolic diversity and functional capacity of transformed bacterial strains using Biolog EcoPlates, specifically to determine their ability to utilize various carbon substrates. This approach was used to evaluate potential metabolic shifts resulting from genetic manipulation and to phenotype the transformed strains based on their substrate utilization patterns. Meanwhile, the Biolog Phenotypic Microarray (PM) assays enable in-depth phenotypic analysis of pure bacterial isolates, assessing their ability to utilize a wide range of substrates, making them ideal for metabolic and stress-response studies. This high-throughput system allows researchers to analyse metabolic capabilities and phenotypic changes across various substrates in a single experiment. The standard Biolog PM plates contain a variety of different substrates, such as carbon and nitrogen sources, heavy metals, antibiotics, etc. Together, these assays provided a robust framework to determine whether bacterial transformation significantly altered the metabolic phenotype compared to parental strains. This ensured that any observed effects on *C. elegans* aging pathologies could be reliably attributed to bacterial colonization rather than artifacts arising from genetic manipulation.

2.4 Using *Caenorhabditis elegans* Kynurenine Pathway mutants for studying gut-microbiota

This study aims to investigate the impact of kynurenine pathway mutations on *C. elegans* gut colonisation by commensal bacteria and vice-versa along with its potential link to aging-related pathologies. Gut microbes impact nutrition, immunity, and behavior (Sekirov et al., 2010) and can prevent pathogen colonization (Kamada et al., 2014). Understanding microbial colonization dynamics can reveal how communities establish, evolve, and maintain stability (Koenig et al., 2010). Commensal colonization affects host metabolism (Tremaroli & Bäckhed, 2012), kynurenine pathway in *C. elegans* is involved in modulating immune responses upon infection. Mutations in key enzymes of this pathway, such as kynurenine 3-monooxygenase (*kmo-1*), can alter the worm's susceptibility to bacterial colonization and infection (Van Der Goot et al., 2012). Studying gut colonisation can provide insights into metabolic disorders, potential interventions and development of novel probiotics (O'Toole, et al., 2017).

Polyxenic models are essential for understanding microbial competition, community dynamics, and host-microbe relationships in a biologically relevant context, as highlighted in studies exploring microbial ecology and host physiology in multi-microbe environments (Koenig et al., 2010; Sekirov et al., 2010).

2.5 Studying aging pathologies in *Caenorhabditis elegans* colonised with CeMbio strains

Investigating age-associated pathologies in *C. elegans*, such as intestinal atrophy, pharyngeal deterioration, development of uterine tumors and bacterial accumulation within the gut, provides critical insights into the biological mechanisms of ageing. The gastrointestinal (GI) tract in *C. elegans* undergoes functional decline—evident through slowed pharyngeal pumping and defecation—and morphological deterioration, including gut lining damage and muscle weakening, which mimic ageing-related changes observed in more complex organisms (Garigan et al.). Another well-documented hallmark of *C. elegans* aging is development of uterine tumors (Ezcurra et al., 2018). As *C. elegans* hermaphrodites age, their germline switches from producing sperm to producing oocytes. After sperm depletion, unfertilized oocytes accumulate in the uterus and undergo extensive cellular hypertrophy, forming large tumor-like masses that can fill the entire body cavity. This proliferation of oocytes leads to the development of the uterine tumors observed in aged hermaphrodites, despite their large size, tumors are believed not to be a direct cause of mortality (Wang et al., 2018).

Studying these pathologies helps address a key question: *does bacterial accumulation drive the development of ageing-related pathologies, or is the decline in gut function a consequence of ageing itself?* Understanding this relationship is crucial, as gut microbiota manipulation represents a promising intervention for improving both lifespan and health span. By exploring how microbial colonization influences ageing phenotypes in *C. elegans*, this research can shed light on broader host-microbe dynamics and potential therapeutic strategies for mitigating age-related decline in humans (Cabreiro & Gems, 2013; O'Toole & Jeffery, 2015).By combining these morphological measurements of ageing pathologies with bacterial colonization data, the aim was to investigate the potential causal relationship between bacterial presence and age-related tissue deterioration.

2.6 Using DualRNA-seq for studying host-microbe interactions

Dual RNA sequencing (dual-RNA seq) enables the simultaneous transcriptomic profiling of both *C. elegans* and associated bacterial strains (CeMbio commensals or pathogens), providing a detailed view of their molecular interactions. This technique allows for the identification of host gene expression changes in response to bacterial colonization, as well as bacterial transcriptional adaptations within the worm gut environment. By capturing these bidirectional interactions, dual-RNA seq offers a powerful approach to understanding how specific bacterial strains influence *C. elegans* physiology, immune responses, and metabolic pathway.

This unbiased approach can uncover novel interaction mechanisms, regulatory networks, and previously unknown genes or RNA molecules involved in the interaction. It is particularly valuable in studying infectious diseases, symbiotic relationships, and host-microbe interactions in various biological systems (Westermann, et al., 2012).

2.7 Studying lifespan assay of *Caenorhabditis elegans* Kynurenine Pathway mutants on CeMbio strain

A lifespan assay in *C. elegans* is an experimental method provide a quantitative measure of longevity of these nematode worms, allowing researchers to compare the effects of different interventions or genetic modifications on lifespan. It can help elucidate how various environmental factors (e.g., diet, temperature, stress) along with gut microbiome influence an organism's longevity and screen for compounds that might extend lifespan, potentially leading to interventions for age-related diseases in humans (Keith, et al., 2014).

2.8 Objective

This project aims to investigate how manipulations of the gut microbiota can influence the aging process in *Caenorhabditis elegans* Kynurenine Pathway (KP) mutants, and conversely, how alterations in the kynurenine pathway affect microbial colonization and host aging. To achieve this, the study will evaluate gut bacterial colonization, worm lifespan, and aging-related pathologies, while also examining changes in host gene expression induced by microbial colonization. The goal is to identify specific gut microbe or microbial community that could promote or delay aging in this model organism.

3 MATERIALS

The following section outlines the experimental materials and key equipment (Table 1), and medium recipes (Table 2) used in this study.

3.1 Key Resource Table

Table 1 presents a complete list of all materials and resources using a layout adapted from the STAR Methods guidelines (Cell Press).

Table 1. Study materials and equipment. A. Environmental bacterial strains, B. Tn7 transformation strains, C. *Caenorhabditis elegans* strains, D. Chemicals and Reagents, E. Commercial assay kits F. Consumables, G. Laboratory equipment, H. Software

No.	Reagent/Resource	Source	Identifier/Product code
A.	**Environmental bacterial strains**		
1	*Acinetobacter guillouiae*	Schulenburg Lab, University of Kiel	MYb10
2	*Chryseobacterium sp.*	Schulenburg Lab, University of Kiel	MYb317
3	*Comamonas piscis*	Schulenburg Lab, University of Kiel	BIGb0172
4	*Comamonas sp.*	Schulenburg Lab, University of Kiel	MYb396
5	*Comamonas sp. B-9*	Schulenburg Lab, University of Kiel	MYb21
6	*Enterobacter cloacae*	Schulenburg Lab, University of Kiel	CEent1
7	*Enterobacter ludwigii*	Schulenburg Lab, University of Kiel	MYb174
8	*Escherichia coli*	Schulenburg Lab, University of Kiel	OP50
9	*Lelliottia amnigena*	Schulenburg Lab, University of Kiel	JUb66
10	*Ochrobactrum vermis*	Schulenburg Lab, University of Kiel	MYb71
11	*Pantoea nemavictus*	Schulenburg Lab, University of Kiel	BIGb0393
12	*Pseudomonas fluorescens*	Schulenburg Lab, University of Kiel	MYb115
13	*Pseudomonas lurida*	Schulenburg Lab, University of Kiel	MYb11
14	*Pseudomonas sp.*	Schulenburg Lab, University of Kiel	MYb330
15	*Sphingobacterium multivorum*	Schulenburg Lab, University of Kiel	BIGb0170
16	*Stenotrophomonas indicatrix*	Schulenburg Lab, University of Kiel	JUb19
B.	**Bacteria for Tn7 transformation**		
17	*Escherichia coli* SM10/pTn7xKS-dTomato	Guillemin Lab, University of Oregon	SM10/pTn7xKS-dTomato
18	*Escherichia coli* SM10/pTn7xKS-mPlum	Guillemin Lab, University of Oregon	SM10/pTn7xKS-mPlum
19	*Escherichia coli* SM10/pTn7xKS-sfGFP	Guillemin Lab, University of Oregon	SM10/pTn7xKS-sfGFP
20	*Escherichia coli* SM10/pTNS2	Guillemin Lab, University of Oregon	SM10/pTNS2
C.	***Caenorhabditis elegans* strains**		
26	Wild type	Ellen Nollen lab, ERIBA - UMCG	N2OW
27	*tdo-2(zg218)*	Ellen Nollen lab, ERIBA - UMCG	OW717
28	*kynu-1 (tm4924)*	Ellen Nollen lab, ERIBA - UMCG	OW454

29	*afmd -1 (tm4547)*	Ellen Nollen lab, ERIBA - UMCG	OW477
30	*kmo-1 (tm4529)*	Ellen Nollen lab, ERIBA - UMCG	OW478
31	*haao-1 (tm4627)*	Ellen Nollen lab, ERIBA - UMCG	OW479
D.	**Chemicals and Reagents**		
32	16S-1495r Reverse Primer	Merck Group	SY201035515-012
33	16S-27f Forward Primer	Merck Group	SY201035515-01
34	Agar, ash 2-4.5%	Sigma-Aldrich	A7002
35	Agarose (DNA/RNA/Genetic Analysis Grade)	Fisher	BP1356
36	Ampicillin Sodium salt	Fisher	10419313
37	Bleach, Sodium Hypochlorite solution, Chlorine 10 to 15% (Honeywell)	Fisher	BP1356
38	Calcium Chloride ($CaCl_2$)	Fisher	C5080
39	Cholesterol, >99%	Fisher	11493310
40	DNA GEL STAIN, SYBR SAFE(TM)	Fisher	10328162
41	Ethanol (Absolute)	Fisher	10437341
42	Gel loading dye, Purple (6X)	New England Biolabs	10043349
43	Gentamicin Sulphate, 600I.U./mg, 10 g	Alfa Aesar	J62834
44	Glycerol (Molecular Biology)	Fisher	BP229-1
45	GoTaq(R) Green Master Mix	Promega	M7122
46	Isopropyl β- d-1-thiogalactopyranoside (IPTG)	Melford	MB1008
47	Levamisole	Sigma-Aldrich	L9756
48	LB Agar Lennox (BD Difco)	Fisher	11778842
49	LB Broth Miller (Invitrogen)	Fisher	11558866
50	Magnesium Sulphate ($MgSO_4$)	Fisher	22189-08-8
51	Potassium Phosphate Monobasic (KH_2PO_4)	Sigma-Aldrich	P0662-500g
52	Potassium Phosphate Dibasic (K_2HPO_4)	Fisher	P3786-500g
53	Silicone grease	-	-
54	Sodium chloride (NaCl)	Sigma-Aldrich	7647-14-5
55	Sodium Hydroxide, Pellets (NaOH)	Fisher	S/4920/53
56	Sodium Phosphate, Disbasic, anhydrous (Na_2HPO_4)	Fisher	7558-79-4
57	Sodium pyruvate	Sigma-Aldrich	14170
58	Tryptone	Fisher	12787099
59	Yeast Extract	Fisher	10225203
E.	**Commercial assay kits**		
60	Direct-zol™ RNA MiniPrep with Zymo-Spin™ IIC Columns (Capped)	Cambridge Bioscience	R2052
61	Qubit RNA HS Assay Kit	Thermo-fisher	Q32852
62	Purple 1 kb Plus DNA Ladder	Quick-Load, New England Biolabs	N0550G
63	Biolog Phenotype plates	TechnoPath	PM 1,2A,3,4,5,6,7,8,9 & 10
F.	**Consumables**		

64	Autoclavable bottle (for media preparation and bacteria culture)	Duran	GL45
65	Bunsen Burner, Natural Gas, 13 mm	SLS	BUR3000
66	Bunsen Burner, Natural Gas, 3mm	SLS	BUR3300
67	Centrifuge tube conical PP, sterile 15 mL flatcap	Fisher	11849650
68	Centrifuge tube conical PP, sterile 50 mL flatcap	Fisher	11512303
69	Cotton Swab Woodstick, Single in Peel Pouch	SLS	SWA2034
70	Coverslips 22 mm x 22 mm	VWR	MIC3104
71	Cryotube 2ml, Int.Thread, Sterile	Fisher	11321675
72	Distriman repetitive pipette	Gilson	F164001
73	Distritips 12.5mL	Gilson	F164150
74	Filter disc 0.45µm pore size, 25mm	EMD Millipore	HAWP02500
75	Filter tips 20µL	Starlab	S1123-1810-C
76	Filter tips 200µL	Starlab	S1120-8810-C
77	Filter tips 1000µL	Starlab	S1122-1830-C
78	Filter tips 10-20µL	Starlab	S1120-3810-C
79	Inoculating loop, 1µL, sterile	Fisher	OS1-01
80	Microcentrifuge tubes, 1.5mL	Fisher	FB74031
81	Microcentrifuge tubes, RNAse-free 1.5mL	Fisher	15432545
82	Micropipette 0.5-10µL,	Gilson	FA10002M
83	Micropipette 2-20µL	Gilson	F144056M
84	Micropipettes 20-200µL	Gilson	FA10005M
85	Micropipettes 10-100µL	Gilson	F144057M
86	Micropipettes 10-1000µL	Gilson	F144059M
87	Microscope slides - plain	Medline	D100002
88	Pasteur Pipette, 150 mm	Fisher	11546963
90	Petri dish 60 x 15mm	Fisher	150288
91	Petri dish 150 x 15 mm	Fisher	168381
92	Petri dish (vented) 100 x 15 mm	Fisher	150350
93	Petri dish (non-vented) For bacteria growing 100 x 15 mm	Falcon, Corning	351029
94	Platinum Wire, 50 cm, 0.3 mm	Fisher	P/3600/89
95	Precellys bulk beads 0.1 mm Zirconium oxide beads	VWR	P000927-LYSK0-A
96	Serological Pipette 5mL	VWR/Corning	612-3702/4051
97	Serological Pipette 50mL	VWR/Corning	612-3696
98	Serological Pipette 25mL	VWR/Corning	612-3698/4251
99	Serological Pipette 10mL	VWR/Corning	612-3700/4101
100	Syringe Membrane Filter, 0.2 um	Fisher	15181499
101	Tape Autoclave	Fisher	12739135

G. Laboratory equipment			
102	Benchtop centrifuge	Beckman coulter	Allegra X-15R
103	Cell disruption- Homogenizer	MP Biomedicals	116005500
104	Fluorescence microscope – Fluorescence light source	Zeiss	CoolLED PE-4000
105	Fluorescence microscope- Automated XYZ stage	Zeiss	AxioZoom V16
106	Fluorescence microscopy – Camera	Zeiss	Axiocam 512 Mono-Camera
107	Fluorescence microscopy – Lens	Zeiss	PlanNeoFluar Z 1x/0.25 FWD 56mm
108	Fluorescence microscopy – Lens (Gut colonised worms)	Zeiss	PlanNeoFluar Z 2.3x/0.57 FWD 10.6mm
109	Gel-Bright gel analyser - Agarose gel electrophoresis	Thermo Scientific	iBright CL750 Imaging System
110	Laminar air flow cabinet	Air Science	PCR-24-A
111	Microcentrifugation (>1 mL)	Eppendorf	5415R
112	Microvolume centrifuge tubes	Sarstedt	72.690.001
113	PCR tubes	ThermoFisher	AB0350
114	Purified water source	Milli-Q	IQ 7000
115	Shaker Incubator	Infors HT	Unitron AJ254
116	Stereo Microscope (Light) 7.5x-60x	Leica	M80 with TL3000 Light Base (1x)
117	Thermal cycler	Bio-Rad	PTC tempo thermal cycler
	Tube revolver rotator	Thermo Scientific	CAT#88881001
118	UV-visible spectrophoto meter	Thermo Scientific	-
119	Visible range cuvettes	Kartell Labware	01938-00
120	Vortexer	Scientific Industries	SI-0266
H. Software			
121	ApE- A plasmid editor	M. Wayne Davis	Version 3.1.4
122	Excel	Microsoft Corporation	Version 16.83
123	Fiji – ImageJ2	Open-source image processing software	Version 2.9.0
124	GraphPad Prism	2D graphing and statistics software	Version 9.3.0
125	Nucleotide BLAST	National Institute of Health	blast.ncbi.nlm.nih.gov
126	4Peaks-sequence analysis	Nucleobytes	Version 1.8
127	UGene-sequence alignment tool	Unipro	Version 49.1
128	ZEN Pro	ZEISS	Version 2.6

3.2 Media Preparation

This section provides the recipes for the preparation of both bacteriological and *C. elegans* media.

Table 2. Medium recipes for A. Bacterial handling, B. Caenorhabditis elegans handling, C. Molecular biology assays, D. Antibiotic and drug stock solutions.

No.	Media type	Component	Weight/Volume	Final volume
A. Bacterial handling				
1	Luria Bertani broth (Miller's)	LB powder	25g	1 Litre
		MilliQ water	1000mL	
2	Luria Bertani agar (Lennox)	Agar	32g	1 Litre
		MilliQ water	1000mL	
3	LB + Glycerol (20%)	LB broth	800mL	1 Litre
		Glycerol	200mL	
4	LB + IPTG (1mM)/ Gentamicin (60ug/ mL)/ Ampicillin (100ug/ mL)	LB powder	25g	1 Litre
		MillIQ water	1000mL	
		*Respective Antibiotic	1mL	
B. *Caenorhabditis elegans* handling				
4	OP_{50} media	Tryptone	5g	1 Litre
		Yeast extract	2.5g	
		MilliQ	1000mL	
		After powder dissolve completely, aliquot into 100 mL bottles.		
5	1M $MgSO_4$ $7H_2O$	$MgSO_4$	246.4g	1 Litre
		MilliQ	1000mL	
6	1M KH_2PO_4	KH_2PO_4	136g	1 Litre
		MilliQ	900mL	
		Adjust pH to 6.0 using KOH pellets	≅ 14-16g	
		Fill bottle up to 1L after pH is adjusted, autoclave.		
7	1M $CaCl_2$ $2H_2O$	$CaCl_2$	29.40g	200 Millilitre
		MilliQ	200mL	
8	Cholesterol (5mg/ mL)	Cholesterol	5mg	1 Millilitre
		100% ethanol	1mL	
		Vortex until all cholesterol powder is dissolved.		

9	M9 Buffer	NaCl	5g	1 Litre
		KH_2PO_4	3g	
		Na_2HPO_4 anhydrous	5.6g	
		MilliQ water	1000mL	
		*1M $MgSO_4$	1mL	
10	Nematode growing media (NGM)	1M NaCl	3g	1 Litre
		Agar	17g	
		Tryptone	2.5g	
		Millipore water	1000mL	
		*1M KH_2PO_4	25mL	
		*1M $MgSO_4$	1mL	
		*1M $CaCl_2$	1mL	
		*Cholesterol (5mg/ mL)	1mL	
11	Freezing medium	NaCl	1.17g	200 Millilitre
		KH_2PO_4	1.36g	
		100% Glycerol	60mL	
		MilliQ water	140mL	
		*1M $MgSO_4$	60µL	
C. Molecular biology media preparation				
12	Gel electrophoresis	Agarose	1g	100 Millilitre
		1X TBE buffer	100mL	
		*SYBR safe gel stain	10µL	
D. Antibiotics and drug stock solutions				
13	1M IPTG aliquots	IPTG	238.3mg	1 Millilitre
		MilliQ water	1mL	
14	Gentamicin Sulphate aliquots	Gentamicin	60mg	1 Millilitre
		MilliQ water	1mL	
15	Ampicillin aliquots	Ampicillin	100mg	1 Millilitre
		MilliQ water	1mL	
16	Levamisole 0.2%	Levamisole	100mg	50 Millilitre
		M9 buffer	50mL	
All the media once prepared as mentioned above, are autoclaved at 121°C for 20 minutes at 15 psi.				
*Reagents are added after the autoclave/heating and once the media is cooled to below 60°C				

4 METHODS

All experimental procedures were conducted in accordance with standard laboratory safety practices and in an aseptic environment as required. Prior to initiating any laboratory work described herein, comprehensive safety training was completed, with all relevant risk assessments and COSHH (Control of Substances Hazardous to Health) forms read and signed. Glassware, culture media, and relevant equipment were sterilized by autoclaving at 121°C for 20 minutes at 15 psi. Where heat sterilization was not appropriate, media and solutions were sterilised by filtration through 0.22µm filters. Sterile work took place either on a bleach- and 70% ethanol-sanitised bench within the sterility cone of a Bunsen burner, or in a biosafety cabinet. Hazardous and volatile substances were handled in a fume hood.

4.1 Bacterium Handling and Maintenance

4.1.1 Antibiotics preparation

All antibiotics were weighed and mixed with purified water (Milli-Q), vortexed, and then filtered through a polyvinylidene difluoride (PVDF) membrane syringe filter to sterilize the solution. The filtered solution was either used immediately or aliquoted into 1 mL portions and stored at -20°C for later use.

4.1.2 Bacterium medium preparation

All the components/reagents for growing bacterial cultures in liquid and solid media were first weighted and combined in autoclavable glass bottles (Duran). The bottles were loosely capped and taped with autoclave tape to confirm sterilization. Once autoclaved the bottled were taken out and allowed to cool down to 55-60°C. After which, reagents or antibiotics were added (Table 2). For agar-based medium plates, the media were kept liquid at 55-60°C in a water bath, until pouring (30 mL per 100 mm diameter dish, or 80 mL per 150 mm diameter dish). All culture media and poured plates were cooled to room temperature before use or stored at 4°C.

4.1.3 Growing bacterial clones from a frozen stock

Using a sterile inoculation loop, bacteria were scraped off from stocks kept at -80°C in cryogenic vials and streaked onto a fresh agar-based medium plate in aseptic conditions and incubated at the permissive growth temperature (25 or 37°C depending on the strain, see Table 3, for 48 or 24 hours, respectively). Following plate growth, single clones were picked under a stereomicroscope to start liquid bacterium cultures for later plate seeding, or to generate clean maintenance plates by streaking onto new agar-based medium plates.

4.1.4 Bacterium maintenance and culture preparation

For weekly maintenance of bacterial strains, a clean colony of each bacterium was picked from its maintenance plate using a sterile inoculation loop and streaked onto a new culture plate, followed by incubation at 25°C for 48h or 37°C for 24 hours, depending on the bacterial strain and stored lid-down in a vented box at 4°C.

For worm assay plate seeding, single colonies from freshly maintained bacterial plates were inoculated into 10 mL of liquid growth medium in a 15 mL falcon (ThermoFisher). Liquid cultures were allowed to grow at 25°C for up to 48h or 37°C for up to 24 hours, depending on the bacterial strain, on a tube rotator placed inside the incubator or in a shaking incubator, respectively, to avoid sedimentation. Depending on the assay, saturated liquid grown cultures were then used to seed plates or as a starter to grow large batches of bacteria to a specific optical density. Media and culture conditions required for growing environmental strains, donors and helper strains (for Tn7 transformation) and fluorescently tagged strains are mentioned below in Table 3.

Table 3. Bacterial media and culture conditions

No.	Bacterium type	Media type	Temperature (°C)
1	Environmental bacterial strains (recipients)	LB broth/ LB agar	25
2	Escherichia coli SM10/pTn7xKS strain (donors)	LB broth/ LB agar + Gentamicin 60mg/ mL treated	37
3	Escherichia coli SM10/pTNS2 (helpers)	LB broth/ LB agar + Ampicillin treated	37
4	Fluorescently tagged strains (transformed)	LB broth/ LB agar + 1mM IPTG + Gentamicin 60mg/ mL treated	25
5	*Escherichia coli* OP_{50} (worm food)	OP_{50} medium/NGM plates	37
*Antibiotics are added 1 mL per 1000 mL of liquid or solid media			

4.1.5 Bacterium glycerol stock preservation

For cryopreservation of bacterial strains, bacteria were grown on agar media for up to 5 days at room temperature to ensure they are devoid of any contamination and/or that they express homogenously high levels of fluorescent proteins. Then, the whole bacterial lawn was collected with a sterile cotton swab and resuspended into sterile LB broth + 20% glycerol in a sterile cryovial under aseptic conditions and stored at -80°C for future use.

4.2 *Caenorhabditis elegans* Handling And Maintenance

C. elegans handling took place on bleach- and 70% ethanol-sanitised laboratory benchtops. The *C. elegans* strains used were procured from the Nollen laboratory (Netherlands) as detailed in Table 1.

4.2.1 *Caenorhabditis elegans* bacterial food preparation

C. elegans strains in laboratory settings are usually grown in monoxenic conditions on *E. coli* strain OP50 as food source (Brenner, 1974). OP50 *E. coli* is a slow-growing Uracil auxotroph strain that forms thin lawn on NGM plates, which does not suffocate worms and facilitates direct observation under a stereomicroscope (Stiernagle, 2006). To prepare OP50 *E. coli* cultures, single colonies were picked from a freshly streaked plate grown at 37°C overnight, grown in 10 mL OP50 medium (see Table 3) as described in (4.1.4) *E. coli* OP50 cultures were stored at 4°C while being tested by seeding 3-5 NGM plates and observing their growth (24h at 37°C followed by 48h at 20-25°C) to ensure absence of contamination. Confirmed clean liquid cultured were then used to seed worm assay plates as required.

To prepare fluorescently tagged bacterial cultures for worm gut colonisation assays, three independent fluorescent bacterial clones were seeded into 10 mL of LB broth media supplemented with gentamicin (60 µg/mL) and IPTG (1 mM/mL) and incubated at 25°C under agitation (tube rotator) for 48 hours, ensuring proper aeration. On Day 3, the bacterial suspensions were seeded onto NGM plates and incubated at 20°C for about 48h and checked for fluorophore expression under fluorescent microscope (method 4.5.3), and the clone with the best expression was selected for seeding the experimental NGM plates.

Bacterial maintenance plates and liquid cultures were stored at 4°C. They were typically used within the week but can remain usable for up to three weeks (Byerly, Cassada, & Russell, 1976).

4.2.2 Preparation and seeding of NGM petri plates

C. elegans strains are maintained on NGM (Nematode Growth Media) agar plates (prepared as mentioned in Table 2, (Brenner, 1974). These are typically using 10 mL of medium per 60 mm diameter vented Petri dish. Upon pouring in aseptic conditions, plates are allowed to cool down and dry overnight lid on, on a sanitised benchtop or in a biosafety cabinet. NGM plates for *C. elegans* maintenance are then typically seeded with 100 µL of saturated *E. coli* OP50 culture and grown overnight at 37°C. Once brought back to room temperature, they can be used for stock maintenance of worm strains or for worm experiments. To ensure NGM plates are not contaminated, seeding liquid cultures (whether for OP50 or other bacterial strains) are first tested as described in (4.2.1). To seed large batches of plates, the laboratory uses a Distriman (Gilson) fitted with a 12.5 mL Distritip set to dispense 100 µL at a time. Seeded plates are allowed to dry before incubating them lid-down in a vented box at 37°C overnight. To seed large batches of plates, the laboratory uses a Distriman (Gilson) fitted with a 12.5 mL Distritip set to dispense 100 µL at a time. Seeded plates are allowed to dry before incubating them lid-down in a vented box at 37°C overnight.

4.2.3 Seeding fluorescently tagged CeMbio+ bacterial strains onto NGM plates

Fluorescently tagged CeMbio strains , for studying *C. elegans* commensal gut colonisation and lifespan assays, were generated using the Tn7 counterselection method (mentioned in 4.5.2). Experimental plates for gut colonization assay-monoxenic conditions, were seeded with 100 µL of fluorescently tagged bacteria cultures (prepared using 4.1.4) of interest. For cocktail/polyxenic conditions, three fluorescently tagged-bacterial cultures were seeded separately (as shown in Figure 14. c), with each drop of 30 µL constituting to a single bacterium culture. Plates were allowed to dry and incubate lid-down at 25°C for the initial 24 hours and then shifted to 20°C for another 24-48h, to ensure a robust expression of the fluorophores.

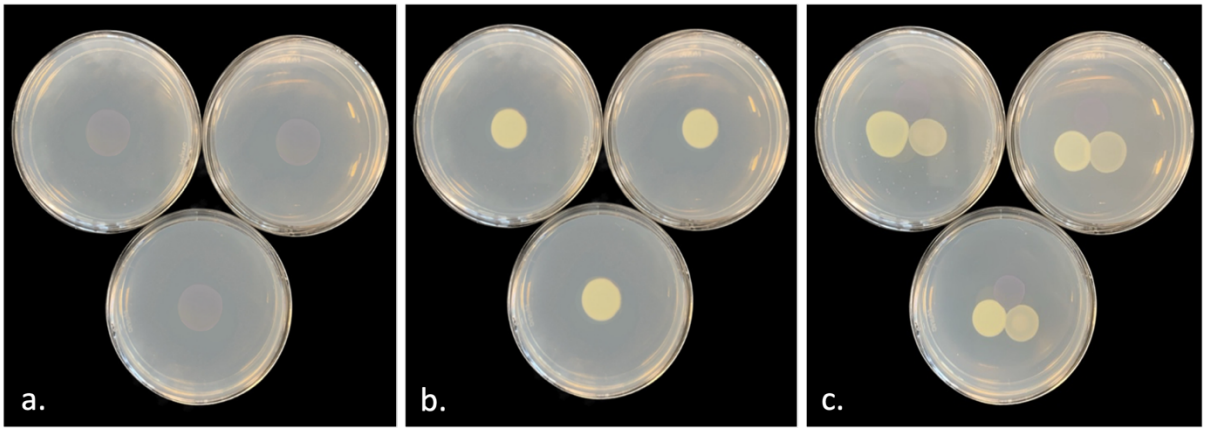

Figure 14. Seeded NGM plates: This figure illustrates the pattern of seeding NGM plates for different conditions: **a.** CEent1 mPlum, **b.** MYb71 sfGFP (monoxenic conditions) and **c.** CEent1 mPlum + MYb71 sfGFP + JUb19 RFP2 (polyxenic condition) incubated at 20-25°C for 48-72 hours.

4.2.4 Transferring of worms onto NGM plates

C. elegans is transparent and can be visualized using a dissecting stereomicroscope equipped with a transmitted light source. Using a Leica M80 light microscope, equipped with standard 10x eyepieces and a 1x lens, 7.5x-60x magnification were used to pick worms with a worm picker, made using a 1-inch 32-gauge platinum wire fused by melting the tip of a glass pasteur pipet. As platinum wire can be flame sterilised between the transfers, it helps in eliminating any kind of contamination. To avoid agar poking and killing of worm, the end of the wire was flattened using a hammer. To this flattened surface (on the lower bottom) a blob of *E.coli*, from the seeded plate was created, before gently touching it on to the top of the worm. This bacterial paste act as a sticky media to which the worms get stick to and such like many worms can be transferred at the same time (Stiernagle, 2006).

4.2.5 *Caenorhabditis elegans* strain maintenance

C. elegans stock were typically maintained on NGM (Nematode Growth Medium) agar plates pre-seeded with OP50 *E.coli* cultures and grown at 20°C. *C. elegans* has a rapid life cycle of about 3.5 days at 20°C, from one-cell embryo to a fertile adult, it takes about 5.5 days at 15°C. Taking advantage of this (as worms can be grown between 15°C and 25°C) the life cycle of the worms were altered depending on the experimental requirements (Fay, 2005).

For stock maintenance of *C. elegans* strains, about 3-4 L1 stage worms were picked and transferred to a pre-seeded NGM plate. These transfers were done at interval of 15-20 days and two plates per strains were maintained, to recover in case of contamination. To amplify larger populations, the "chunking" method was also used (wherein a sterilised scalpel was used to move a chunk of agar from an old plate to a fresh one). This is useful for transferring worms burrowed into the agar, as it will allow the worms to crawl out of chunk and spread out onto the bacterial lawn (Stiernagle, 2006).

4.2.6 Handling of contaminated *Caenorhabditis elegans* stocks

While pouring, seeding plates, or when transferring worms, it is best to keep the amount of time and angle of opening the lid to a minimum. This reduces chances of contamination but occasionally worm stocks might get contaminated with moulds, yeasts or other bacteria (Stiernagle, 2006). Two decontaminations methods were used here.

4.2.6.1 "Chunking and diluting"

It's easy to get rid of mould contaminations using the "chunking" method (Stiernagle, 2006) This process is repeated several times as needed by serial transferring until the contamination is completely gone.

4.2.6.2 "Egg prep": Bleaching

For bacterial and yeast contaminations, sodium hypochlorite solution (1mL 5 N NaOH + 2 mL bleach 5%; 0.45M NaOCl) was used to kill the contaminants and gravid worms leaving clean eggs behind Briefly, gravid worms are collected and washed off from the contaminated plates using 1 mL of distilled water fer for each plate, collecting in15 mL falcon tubes, followed by spinning it down at 1500rpm for 1 min (Beckman coulter Allegra X-15R centrifuge), removing and discarding the supernatant, and resuspending in 2mL of distilled water total. Next, depending of pellet size 200 to 500uL of sodium hypochlorite solution were quickly added and mixed using vortex or shaking vigorously by hand for 3 to 5min, regularly checking for worm lysis and egg release under a stereo microscope. Once most adult worm carcasses are broken down and egg released in solution, 10 mL of M9 buffer were added immediately to stop the bleaching process and tubes were swiftly spined down at 1500 rpm for 1 min (Prolonged exposure to bleach can eventually be harmful to eggs). The egg pellet is then

washed serial times, before being resuspended in final 100µl of M9 buffer and distributed across seeded NGM plates for simple maintenance. For L1 synchronization, eggs are instead left on an unseeded NGM plate for 15h (20C) or 20h (15C) to allow all eggs to hatch, releasing developmentally matched L1 animals for future experiments. .

4.2.7 Freezing of worm stocks

C. elegans stock were frozen using freezing media, which was prepared as mentioned in (Table 2) the key to successful freezing is to use animals at the right developmental stage of life cycle i.e. young larval stage L1-L2 as they survive freezing best (Stiernagle, 2006). About 2-3 medium sized or 5-6 small sized NGM plate containing number of freshly starved L1-L2 worms were wash with 3 mL M9 buffer. To this was added equal volume of freezing medium, mixed well and aliquoted 1 mL into 1.8 mL cryovials each, labelled with strain name and date.

4.3 Egg Lay: Synchronization of Worm Populations by Egg Laying

Some experiments including gut colonisation assays require synchronous populations of worm strains using the egg lay technique. This generates a collection of plates with eggs from the same 24hr window providing a constant supply of worms at similar life cycle, without having experienced the stress of bleaching, which can be a confounding factor in subsequent lifespan, stress or infection assays.

Egg lay is initiated by picking 15-20 L4 worms and transferring them onto NGM plates pre-seeded with the OP50 E. coli, . They are then transferred onto new OP50-seeded NGM plates every 24h for 3 days. To maintain a constant supply of synchronous worm populations, new l4 animals are selected every 3 days to repeat the process.

As hermaphrodites reaches a peak of progeny production on day 2 of adulthood and displays a rapid decline in progeny production (Scharf, et al., 2021) they are no longer transferred after day 3 and were instead heat killed. This process ensures that every day, enough synchronised L4 are available to initiate gut colonisation assays.

4.4 Biolog Phenotype Microarray and EcoPlates

For this thesis, selected strains were analysed using Biology Phenotypic Microarray (PM) and Biolog Ecoplates designed to test metabolic phenotype and substrate utilisation by the transformed and parental strains. Specifically, plates PM1, 2A, 3, 4, 6, 7, 8, 9, and 10 were utilized to evaluate Carbon, Nitrogen, Peptide nitrogen, Sulphur, and Phosphorous utilization, Osmolarity and pH susceptibility. PM5 plates were utilised to study Biosynthetic pathway/nutrient stimulation. The assay followed Biolog's prescribed protocol, with some modifications. The substrates are pre-dispensed and dried, requiring only inoculation with bacteria and a buffer containing a dye, colorimetric indicator enables rapid and quantitative assessment of bacterial metabolism over time. As bacteria grow and metabolize the substrates, they reduce a tetrazolium dye, producing a purple colour that can be measured spectrophotometrically (Shubin, et al., 2016).

Bacterial strains were cultured on LB agar at 20°C for 48h prior to the experiment. Bacterial suspensions were prepared to an OD600 of 0.337, then diluted in inoculating fluid IF-0a to achieve an OD of 0.37. Further dilution was performed using either IF-0a dye A or IF-10a dye A mix. Each plate was inoculated with 100 µl of the prepared culture and was incubated in the Omnilog Biolog plate reader for 96 hours. Colour changes were recorded every 15 minutes throughout the incubation period.

The Omnilog data software was employed for preliminary data visualization, from which three key metrics were extracted. Here we report maximum growth as it is less susceptible to variations associated with initial variability in cell density.

4.5 Tn-7 Mediated Bacterial Transformation

Bacterial transformation was carried out using methodologies adapted from a Tn7 kill switch counterselection system (Wiles et al., 2018). Tn7 transformation is a sophisticated method for introducing specific genetic elements into the genome of target bacteria, utilizing a triparental *E. coli* SM10 conjugation system. This approach involves three bacterial strains: the recipient (the target strain, sensitive to gentamicin), the donor (resistant to gentamicin and carrying a tn7-tagging vector with a kill switch), and the helper (gentamicin-sensitive, providing the transposase function). The goal of this protocol is to transform the target

bacteria to express fluorescent protein and gentamicin resistance while eliminating vector bacteria or untransformed bacteria through gentamicin treatment and activation of the kill switch via IPTG (isopropyl-β-d-thiogalactopyranoside) exposure. Once transformed, the identity of the fluorescent bacteria was reconfirmed through 16S sequencing.

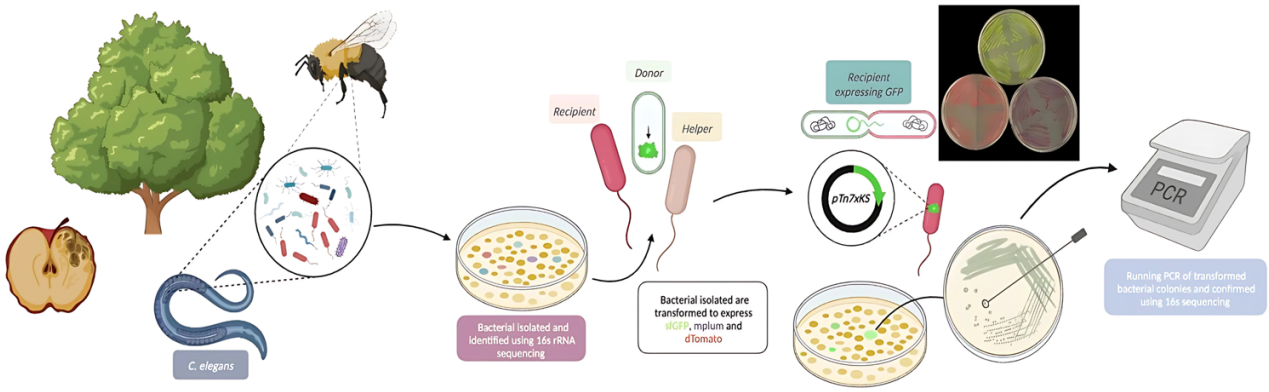

Figure 15. Schematic diagram depicting methodology for Tn7 kill switch counterselection system. Right from collection of bacterial community from worms in the wild, followed by isolation, bacterial transformation using Tn7 kill switch, PCR amplification and 16s sequencing. Illustration created with BioRender.com

4.5.1 Bacteria selected for transformation

Below mentioned are the bacterial strains used for transformation using Tn7 counterselection system. . Detailed information including genomic sequences is mentioned in appendix 10.1

Table 4. Bacteria used for triparental suicide vector counterselection system

No.	Bacteria	Identifier	Function/Context	Source
1	*Comamonas piscis*	BIGb0172	Recipient Bacterium (CeMbio)	Schulenburg Lab, University of Kiel
2	*Sphingobacterium multivorum*	BIGb0170	Recipient Bacterium (CeMbio)	Schulenburg Lab, University of Kiel
3	*Comamonas sp. B-9*	MYb21	Recipient Bacterium (CeMbio)	Schulenburg Lab, University of Kiel
4	*Chryseobacterium sp.*	Myb317	Recipient Bacterium (CeMbio)	Schulenburg Lab, University of Kiel
5	*Escherichia coli* SM10/pTn7xKS-dTomato	SM10/pTn7xKS-dTomato	Donor Bacteria (Transformation)	Guillemin Lab, University of Oregon
6	*Escherichia coli* SM10/pTn7xKS-mPlum	SM10/pTn7xKS-mPlum	Donor Bacteria (Transformation)	Guillemin Lab, University of Oregon
7	*Escherichia coli* SM10/pTn7xKS-sfGFP	SM10/pTn7xKS-sfGFP	Donor Bacteria (Transformation)	Guillemin Lab, University of Oregon
8	*Escherichia coli SM10/pTNS2*	SM10/pTNS2	Helper Bacteria (Transformation)	Guillemin Lab, University of Oregon

4.5.2 Tn7 counterselection selection

To transform a recipient bacterium of interest, this method uses three parent donor strain (Tn7xKSmPlum, Tn7xKSsfGFP and Tn7xKSdTomato) and a helper strain (SM10/pTNS2). Prior to conjugation the bacterial cultures of, recipients in plain LB broth, donors in LB + Gentamicin 60mg/ mL (each donor per tube) and helper strain in LB + Ampicillin 100ug/mL, were grown overnight at 25°C, 37ºC and 37ºC respectively (using method 4.1.4). Once incubated these cultures were diluted by ratio of 1:50 (for donors and helper bacteria) and 1:100 (for recipient bacteria) using 5 mL fresh LB broth and were again incubated at same temperature conditions for 3-4 hours. Bacteria were allowed to grow to an OD_{600} between 0.4 to 0.6, which was confirmed using spectrophotometer. Strains were then mixed, in a sterile microcentrifuge tube, in a ratio of 1:1:1 (Donor:Helper:Recipient), with 500µL of each bacterium. To remove any antibiotics from the mixture, the mixture is centrifuged at 7000 g and washed with 1 mL of LB broth. This step is repeated several times, with the last wash followed by resuspending the pellet in 25µL of LB broth and pipetted onto a sterile 0.45 µm filter disc placed on a LB agar plate, once dried plates were incubated at 25°C for 24h. The filter disc provides as a stage for the conjugation/mating to take place and transferring of the fluorophore.

After incubation, mating disc was collected in 50 mL falcon tube using sterile forceps and the bacterial lawn over it was resuspended by vortexing in 1 mL of 0.7% NaCl solution. 100µL of the suspension was then spreaded onto three LB agar + $IPTG_{60}$ (1mM IPTG + G 60mg/ mL) plates each while the other three plates were spreaded with 10-fold higher concentration. Plates were dried and incubated at 25°C for 24-72hrs. Once bacterial growth was apparent (as shown in figure 2a) the plates were screened for fluorescence under a fluorescence microscope (AxioZoomV16, Zeiss) method for screening as described in 2.5.3. Colonies that show uniform fluorescence expressions were then streaked (refer figure 2b) twice onto plain LB agar plates and once on LB agar + $IPTG_{60}$ plates with the same incubation conditions to ensure fluorophore expression is not lost and to check for any contamination. This is a convenient way to verify that the Tn*7* transposon has chromosomally integrated, and the tagging vector has been lost (Wiles et al., 2018). Transformed bacteria with stable fluorescence expression confirmed through fluorescence microscopy were then processed further for colony PCR and 16s-sequencing.

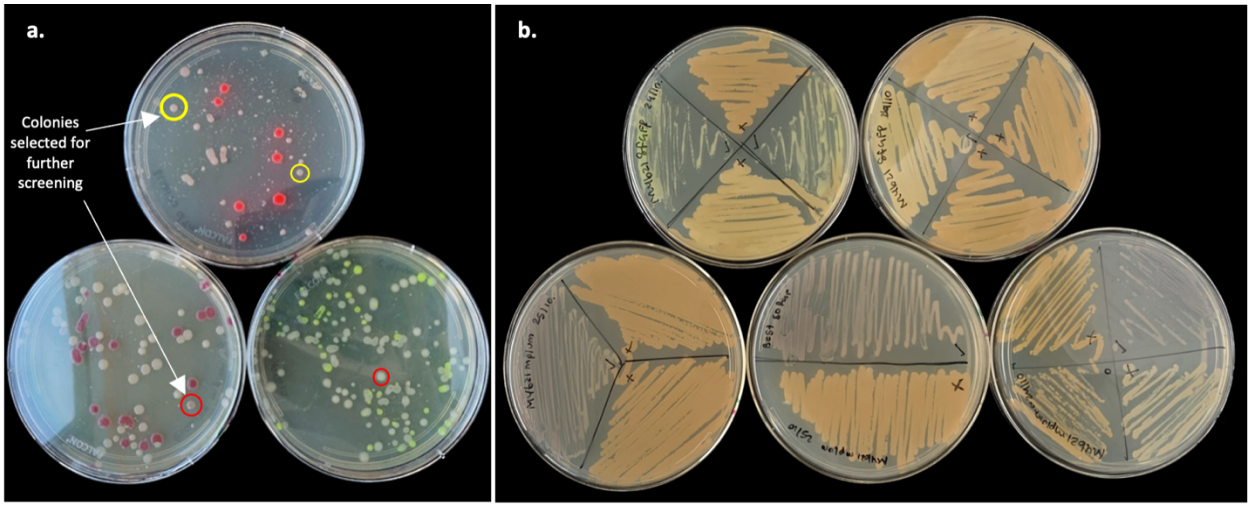

Figure 16. The images presented show fluorescently tagged bacteria: a. transformed bacterial colonies on LB agar plates obtained after mating with three fluorophore proteins. These colonies were further screened using fluorescent microscope **b.** and serially streaked onto LB and LB + IPTG60 agar plates to confirm stable expression of the fluorophores

4.5.3 Screening the transformed bacterial plates

This approach allowed for the efficient identification and isolation of bacterial strains that had successfully incorporated and expressed the desired fluorescent proteins. Transformed bacteria are screened using fluorescence microscope, AxioZoom V16 (Zeiss Ltd.) with automated XYZ stage equipped with PlanNeoFluar Z 1x/0.25 FWD 56mm Objective (Zeiss Ltd.), a PE-4000 (CoolLED) fluorescence light source, an Axiocam 512 Mono, and operated by the Zen Blue 2.6 (Zeiss Ltd.) software.

Plates with tagged bacteria were positioned on the microscope stage and were brought into focus (approx. 7x magnification) using transmitted light (TL) illumination. Fine adjustments were made using stage's XY position controlled via the joystick to locate regions of interest. Once in focus, the light source was switched from TL to the appropriate fluorescence channel (

Table 5) causing the fluorescent proteins within the transformed bacteria to emit light at specific wavelengths. The excitation and emission wavelengths for each fluorescent protein are detailed in

Table 5 below. Colonies exhibiting strong and uniform fluorescence were identified as potential positive transformants. To confirm the success of the transformation and verify the

bacterial identity, the selected fluorescent colonies were subjected to 16s DNA Sanger sequencing (4.5.6).

Table 5. Fluorescence imaging conditions for Tn7 transformed bacteria

Fluorescent protein	Excitation light	Emission light	Exposure time
Bacterial morphology	Contrasted transillumination	Transmitted light (TL)	2ms
sfGFP	470nm	499-529nm	10ms
dTom	550nm	580-605nm	12ms
mPlum	595nm	615-760nm	32ms
*Exposure time were adjusted as per need for controlled fluorescence illumination			

4.5.4 PCR amplification

Colony PCR is used to quickly screen bacterial colonies for the presence of a specific DNA sequence, here it confirms the successful insertion of insertion of the Tn*7* transposon at the *attTn7* site (Wiles et al., 2018). It allows rapid screening of many colonies, which is crucial when working with large numbers of transformants for verifying successful DNA insertions in cloning experiments. Colony PCR amplification was done using the 16s-27f and 16s-1495r primers (Merck Group), GoTaq Green mastermix (Promega), transformed bacterial colony as a DNA template and nuclease free water. A total of 25µL (GoTaq green + 27f primer + 1495r primer + nuclease free water) per reaction is prepared in 1.5 mL PCR tubes to which a single transformed colony (DNA template) is added in sterile condition, using the same loop, is streaked on LB + $IPTG_{60}$ agar plate to have a copy of colony for freezing later upon confirmation. *E.coli* OP_{50} is used as positive control and for negative control reaction mixture with no DNA template is used. PCR tubes are then places inside the thermal cycler for amplification. Recipe table for preparing reaction mixture and thermal cycler settings are mentioned in the Table 6 and Table 7.

Table 6. Recipe table for preparing reaction mixture for colony PCR amplification

Component	Volume/reaction	Volume x12 reactions	Final concentration
GoTaq green mix	12.5µL	150µL	1x
27f primer	1.0µL	12µL	0.1-10µM
1495r primer	1.0µL	12µL	0.1-10µM
DNA template	Single colony	-	-
Nuclease free water	10.5µL	126µL	-
Total reaction mixture	**25µL**	**300µL**	-

Table 7. Thermal cycler settings for running PCR amplification

Temperature(°C)	Time	No. of cycles
95	5min.	1
94	30sec.	30
58	30sec.	30
72	40sec	30
74	10min	1
4	∞	1

4.5.5 Agarose gel electrophoresis

Gel electrophoresis is performed after colony PCR in the Tn7 counterselection technique for confirming the presence of the fluorescent protein gene by showing a band of the expected size. 1% Agarose gel was prepared by dissolving 1gm of agarose powder in 100 mL of 1x TBE (Tris-Borate-EDTA) buffer in an Erlenmeyer flask and microwaved. The flask was taken out every 30 seconds and swirl to ensure complete dissolving of agarose powder. After which mixture was allowed to cool down a bit and 10µL of SYBR safe gel stain (Fisher) was added to it and again swirled to give it a proper mix. Agarose gel bed was made by pouring the mixture into gel cast and combo for the wells, assembly. It was then covered and allowed to cool down till the gel solidifies.

The solid gel was then placed in an electrophoresis chamber and filled with 1x TBE buffer until it covered the top of the gel. Each well contained 5µL of amplified DNA, whereas the last 3 wells contain 5µL of positive control, negative control and 1 kb Plus DNA ladder (New England Biolabs) for molecular weight referencing. The agarose gel is run at 90v for 50min after which it is imaged using a Gel-Bright gel analyser (Thermo Fisher).

4.5.6 DNA purification and 16s bacterial DNA Sanger sequencing

Based on the results from gel electrophoresis, only the samples for which bands are obtained at around ≅ 1468 bp were selected for further processing. The selected amplified samples were sent to Source Bioscience, Cambridge for DNA purification and 16s sanger sequencing.

4.5.7 Analysis of sanger sequencing

Once sanger sequences were received, a specific region or part of the sequence was selected based on the peaks formed as the height of the peaks were direct measurement of the intensity of the fluorescence. For both 27f and 1495r sequences, peaks analysis was done used using 4peaks software and the sequences were edited using ApE- A plasmid editor

software. These edited forward and reverse sequences were then aligned using UGene software- sequence alignment tool. The aligned sequences were then analysed using Nucleotide BLAST (National Institute of Health) to identify bacterial classification. Successful bacterial transformation was concluded when the taxonomical classification of the aligned sequences matched with the top 3 BLAST results with more than 90% identical sequences and a close to zero expectation value. The confirmed sample strain is then frozen using the (method .) agar copy plate streaked while inoculating colony for PCR.

4.6 *Caenorhabditis elegans* Microbial Gut Colonisation Assay and Imaging

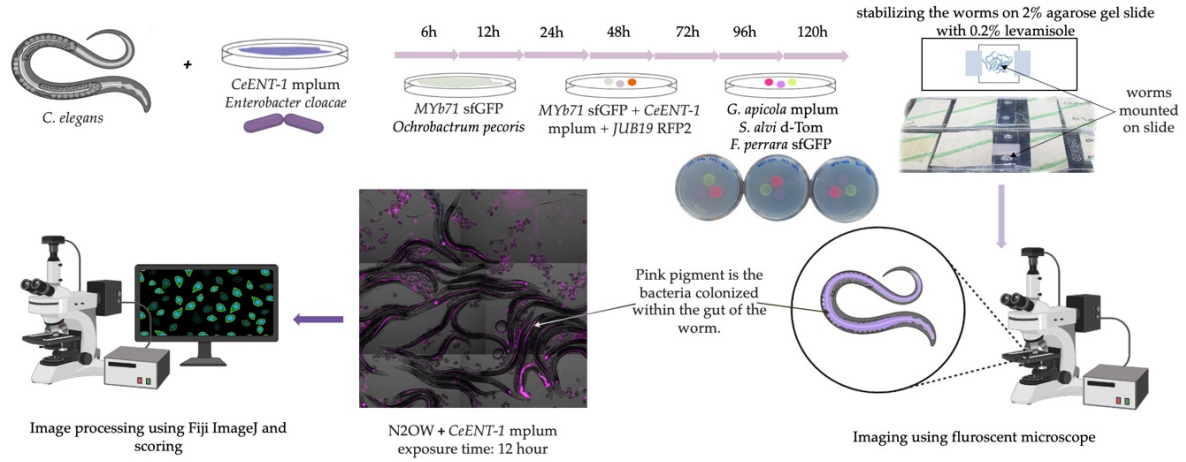

Figure 17. Schematic representation of the *C. elegans* gut colonization assay using fluorescently tagged CeMbio strains. The process begins with bacterial media preparation, followed by exposing OP_{50} pre-feed L4+24h day1 adult *C. elegans* to the bacteria and allowing gut colonization over six days. Worms are then mounted and imaged at given time-points (i.e. 6,12,24,48,72,120 hour)using fluorescence microscopy to visualize bacterial colonization within the gut. Illustration created with BioRender.com.

4.6.1 Bacterial media preparation for gut colonisation assay

While the study initially planned to transform and utilise as many commensal bacteria as possible, to study it's impacts on worm health, these bacteria were not ready during the time of experiment. As such, selection of bacteria was limited to those previously transformed and confirmed via sequencing in our laboratory. Ultimately, the fluorescently tagged bacteria selected for gut colonisation studies are mentioned below in the Table 8.

Bacterial cultures were prepared using method 4.1.4, in LB + $IPTG_{60}$ and incubated at 25°C for 24h. These cultures were then used for seeding 60 x 15mm NGM agar plates using method 4.2.3, and incubated at 15°C-20°C for 24-48h.

Table 8. Fluorescently tagged commensal bacteria used for gut colonisation assay

No.	Bacterium strain	Identifier	Fluorophore	Source
1	*Enterobacter cloaca*	CEent1	mPlum	ABA lab, Lancaster University
2	*Ochrobactrum vermis*	MYb71	sfGFP	ABA lab, Lancaster University
3	*Enterobacter ludwigii*	MYb174	dTomato	ABA lab, Lancaster University
4	*Pantoea nemavictu*	BIGb0393	mPlum	ABA lab, Lancaster University
5	*Stenotrophomonas indicatrix*	JUb19	RFP2	Schulenburg Lab, University of Kiel

4.6.2 Pre-conditioning of Caenorhabditis elegans with Escherichia coli OP50

As this method requires synchronous population of worms, egg lay is setup before the experiment (as mentioned in 4.3). Once the worms are grown to L4 stage, about 50-60 worms are transferred onto *E.coli* OP50 pre-seeded NGM plate and incubated at 25°C for 24 hours, these worms are then transferred onto experimental plates. N2 from the Nolan laboratory (designated as N2OW) was used as the *C. elegans* control strain to maintain a consistent genetic background with that of the mutants. Whereas all the *C. elegans* Kynurenine Pathway (KP) mutant strains used for the experiment are mentioned below, with detailed genetic information found Table 9.

Table 9. Genotypes of *C. elegans* Kynurenine Pathway mutant strain

Gene	Allele(s)	Chromosome	Enzyme function	Strain	Additional Information
kmo-1	*tm4529*	V	Kynurenine 3-monooxygenase	OW478	Catalyses the hydroxylation of L-kynurenine to 3-hydroxykynurenine. Predicted to be located mitochondria and involved in NAD metabolic process and kynurenine metabolic process. Mutation affects innate immunity *(WB:WBGene00011089)*
kynu-1	*tm4924*	X	Kynureninase	OW454	Catalyses the cleavage of L-kynurenine and 3-hydroxykynurenine to anthranilic acid and 3-hydroxyanthranilic acid, respectively. Predicted to be located in cytoplasm. kynu-1 mutations could disrupt these signalling pathways, affecting worms' ability to communicate and regulates its commensal bacteria *(WB:WBGene00015802)*
haao-1	*tm4627*	V	3-hydroxy anthranilate 3,4-dioxygenase	OW479	Catalyses the oxidative ring opening of 3-hydroxyanthranilate to 2-amino-3-carboxymuconate semialdehyde. Predicted to be active in cytoplasm *(WB:WBGene00010595)*
tdo-2	*zg218*	III	Tryptophan 2,3-dioxygenase	OW717	Catalyses the first and rate-limiting step of tryptophan degradation. Mutation affects lifespan and stress resistance *(WB:WBGene00016201)*
afmd-1	*tm4547*	IV	Arylformamidase	OW477	Converts N-formyl-kynurenine to L-kynurenine. Less studied compared to other KP enzymes in C. elegans *(WB:WBGene00017051)*

4.6.3 Gut Colonisation assay: exposing *Caenorhabditis elegans to* CeMbio strains

For gut colonisation assay, L4 + 24h day 1 adult worms grown on *E.coli* (day1 adults at 25C) were transferred onto fluorescently tagged bacteria seeded plates (4.2.4) with 50-60 worms per plate. About four plates per strain of *C. elegans* were prepared, to have enough stock of

worms for imaging throughout the experiment. The time of first transfer is designated as the 0-hour timepoint. Worms were maintained on fluorescent bacterial plates at 25°C for the entire duration of the experiment. At specific timepoints (6, 12, 24, 48, 72, 96, and 120 hours), worms were mounted onto microscope slides for imaging using a Zeiss AxioZoom V16 setup. Worms were mounted in the same order as their initial transfer onto experimental plates.

For mounting, approximately 15-30 worms per strain were transferred onto a 2% agarose gel bed, set between 2 coverslips (22x22mm^2 borosilicate coverslips, VWR) placed 0.5cm apart on the microscope slide (Medline). Once placed, the worms were then immobilized by using approx. 2-10µL of 0.2% levamisole (Sigma-Aldrich) and finally secured with a coverslip, sealed using silicon grease to prevent desiccation. Throughout the experiment, adult and gravid adults were transferred every1-2 days onto new fluroscent bacteria seeded plates to separate them from their progeny.

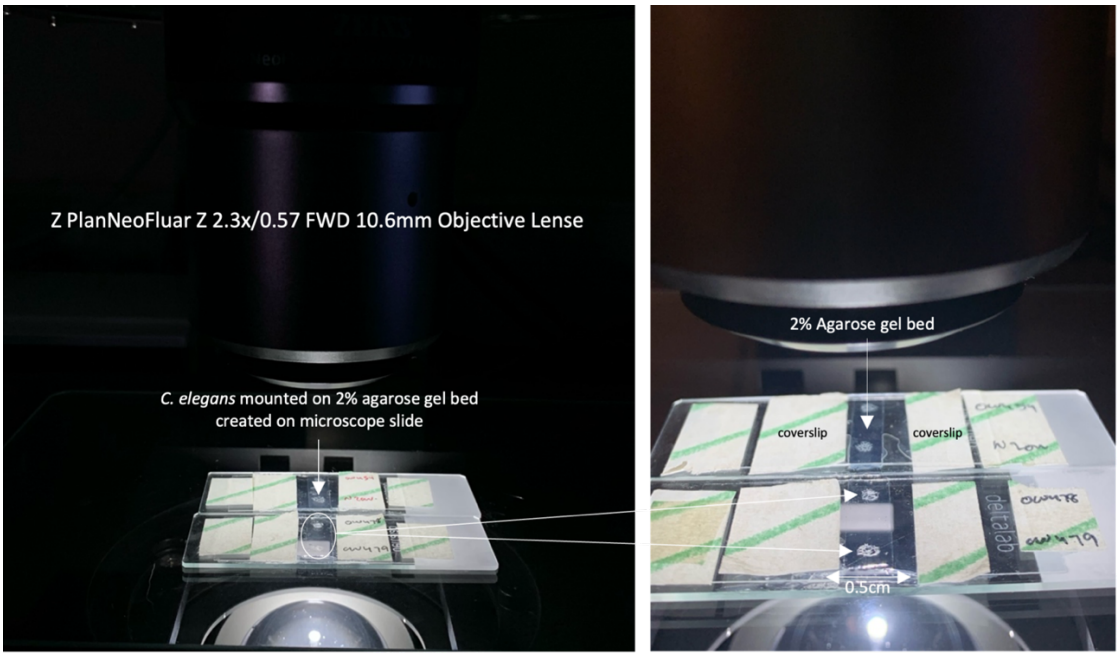

Figure 18. Immobilization and mounting of infected *C. elegans* onto microscopic slide, using 2% levamisole for fluorescence imaging of commensal gut colonised bacteria using AxioZoom V16 (Zeiss Ltd.)

4.6.4 Fluorescence microscopy: Image acquisition

For Fluorescence imaging, an AxioZoom V16 (Zeiss Ltd.) with automated XYZ stage equipped with Z PlanNeoFluar Z 2.3x/0.57 FWD 10.6mm Objective (Zeiss Ltd.), a PE-4000 (CoolLED)

fluorescence light source and an Axiocam 512 Mono, all operated by the Zen Blue 2.6 (Zeiss Ltd.) software was used. ~15-30 mounted worms per slide were imaged at 80 times magnification, using the combined multichannel Z-stacking and tiling mode to automatically acquire, dTomato (Dimer tomato), sfGFP (Superfolder green fluorescent protein), RFP (Red Fluorescent Protein), mPlum (monomeric Plum fluorescent protein), gut blue autofluorescence (BF), and transmitted light (TL) as specified in

Table 5.

Z-stack acquisition was centred on the mid-section of the mounted worms, acquiring image across the worm in 17 slices 3 microns apart, and sequentially performed for each fluorescence channel. Tiles were set with an 8% surface overlap for optimal stitching (covering the entire area with mounted worms), images were acquired at 80x magnification, setting camera gain a 2x, binning at 1x, and image depth at 16-bit. For monoxenic conditions, a single image per slide was sufficient to acquire 3 channels at a time: BF/mPlum/TL. Whereas, for bacterial cocktail conditions, two sets of images were collected per slide: BF/mPlum/TL and sfGFP/RFP/TL, in rapid succession.

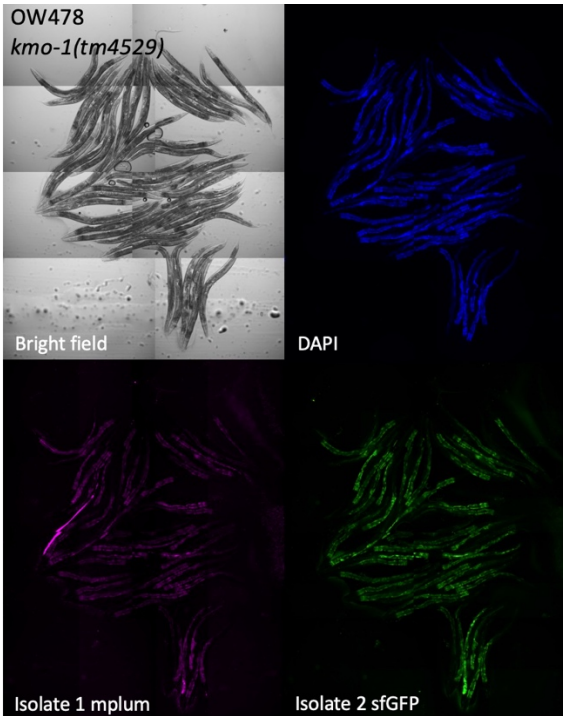

Figure 19. Multichannel image of bacteria gut colonised *C. elegans* acquired using Z-stack acquisition at 80x magnification using AxioZoom V16 (Zeiss Ltd.). Each image acquired contains different fluorophore protein

4.6.5 Image processing

The raw images (Figure 19) taken in previous step were multichannel tiled image hyperstacks (~8-16Gb per file) which were then pre-processed on a PC imaging station (12 cores and 192 Gb SDRAM) using Fiji splitting channels, optimising signal-to-noise ratio (applying background removal and normalising to the maximal signal across all slides for each fluorophore independently, followed by a median filter to remove single bright pixels). To improve file handling, images were then resembled from 16-bit to 8-bit and maximal projections were performed for all fluorescence channels while the midsection slice was kept for the TL channel, creating composite multichannel XY images, and reducing file size to ~60-120Mb. All images were batch-processed using macros (Appendix 10.3) in Fiji (Schindelin et al., 2013). Fiji: an open-source platform for biological-image analysis to ensure treatment consistency.

4.6.6 Image analysis using Fiji ImageJ software

Once the images were processed, they were analysed for the gut colonised commensal bacteria and aging pathologies using Fiji ImageJ. For each individual worm, the extent of bacterial gut colonisation was scored based on a combination of signal intensity and location within the animal as specified in Table 10. Scoring was performed blinded (not knowing what worm strain was being scored) and repeated at least twice, including a scoring uniformity check by another lab member.

Table 10. Scoring scale for gut colonised bacteria

Score	Specifications/ Location within the worm
0	Only mouth or no staining inside the worm
1	Small portion of anterior or posterior only
2	Several dots or small portions along gut
3	Continuous thin gut staining
4	Clearly enlarged filled posterior gut
5	Clearly enlarged filled anterior gut
6	Clearly enlarged filled both anterior and posterior gut
7	Continuous and enlarged throughout or very severely enlarged at places
8	Continuous and enlarged throughout or very severely enlarged at places and clear staining outside gut
9	Pharynx invaded and significant portion of the gut clearly enlarged filled
10	Very deteriorated worm with bacteria in multiple locations outside the gut
11	Nearing death, appearing lysed, GFP all around
12	Sac of GFP undiscernible organs

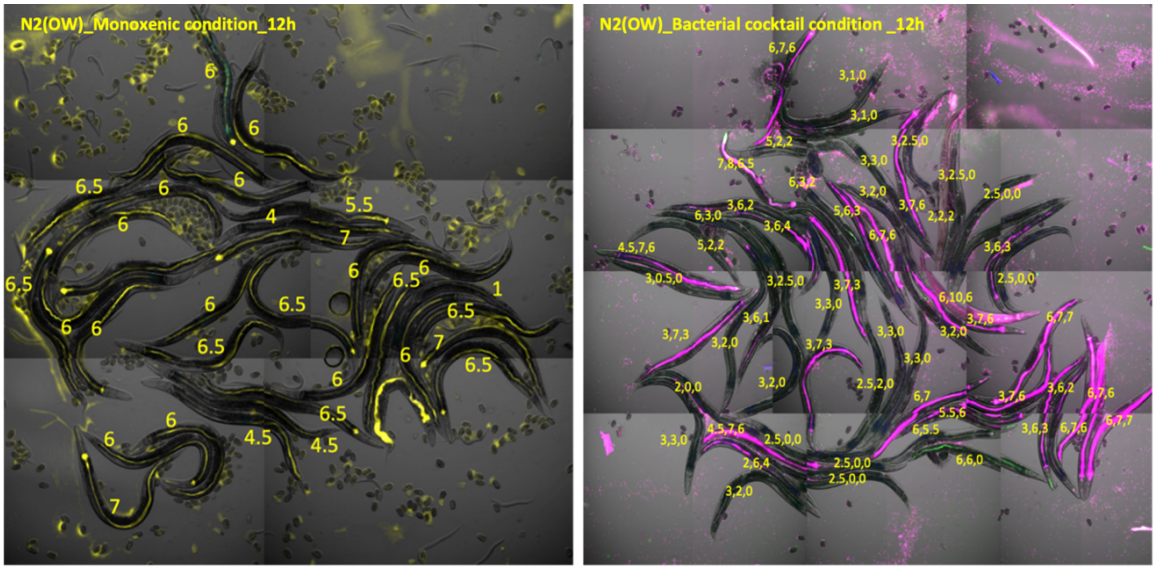

Figure 20. Manual scoring of the acquired images from gut colonisation assay. The images shown above serves as an example for the scoring system used, where Right image: *C. elegans* N2(OW) (control) is allowed colonisation in presence of single bacterium strain (monoxenic condition), Left image: whereas in bacterial cocktail condition the same *C. elegans* strain is allowed colonisation in presence of 3 commensal bacteria, the scoring for which are separated by commas in the same image.

4.7 Measuring Aging Pathologies

To better understand the functional relevance of microbiota gut colonisation changes in the context of the impact on the KP mutant *C. elegans* ageing (Van Der Goot et al., 2012), we next measured main age-related pathologies (Ezcurra, Benedetto et al, 2018) including (1) intestinal atrophy, (2) gut lumen dilation, (3) uterine tumour size, and (4) pharyngeal size and infection status (Zhao et al., 2017).

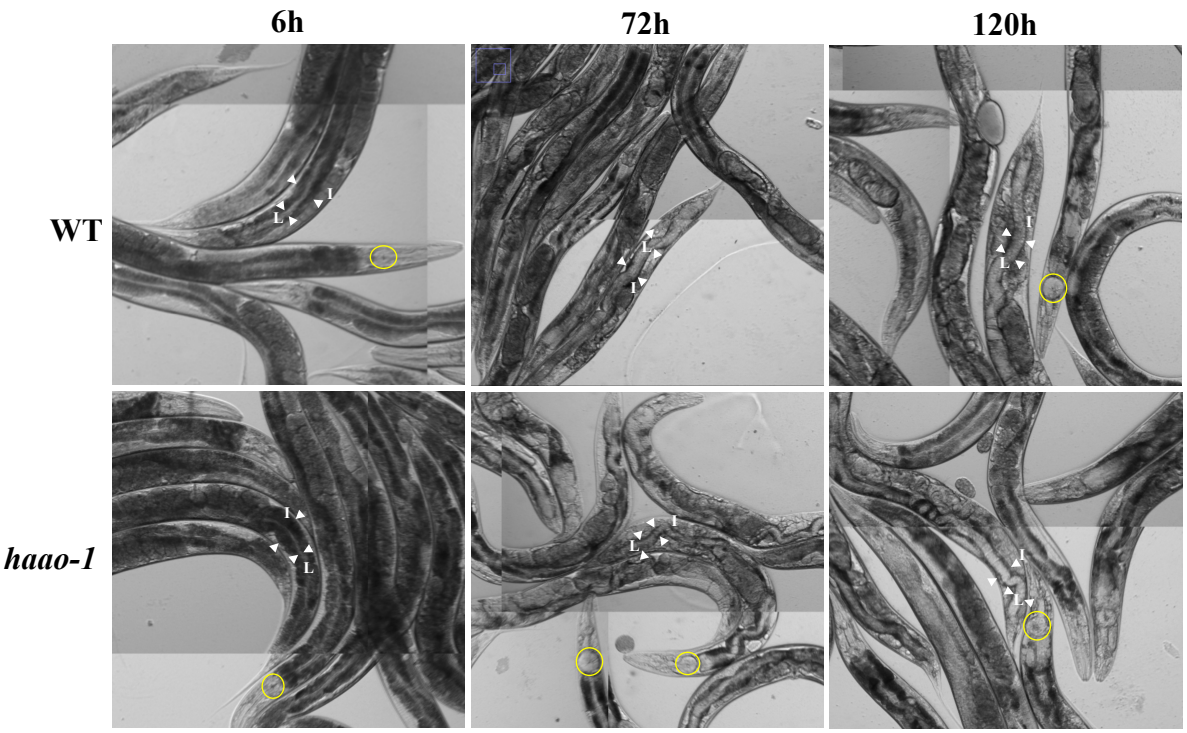

Figure 21. ***C. elegans*** **age-pathologies quantification post-exposure to fluorescently tagged CeMbio bacterial strains.** Bright field images acquired at 6,72 and 120-hours post-exposure to fluorescently tagged isolates of CeMbio strains were analysed for development of age-related pathologies. A manual planimetric analysis was performed using tools in Fiji software. White arrows at posterior end of the worm indicates measurement of intestinal Lumen width (L), Intestinal width (I), and body width for determining intestinal atrophy. Pharyngeal changes and tumor development were quantified by manual tracing of pharyngeal circumference (as seen in yellows circles) and tumor boundaries (as seen in green line) to determine cross-sectional area at defined time points.

Bright-field (TL) images, as described in section 4.6.4, were used for analysis. From each image, 12 worms were randomly selected, and their pharyngeal size, uterine tumor dimensions, and gut width were measured using Fiji ImageJ software. Intestinal atrophy was quantified by measuring the intestinal width at a point posterior to the uterine tumors, subtracting the lumenal width and dividing by the body width (Ezcurra, Benedetto et al, 2018). Pharyngeal size was determined by measuring the circumference of the pharynx, which tends to shrink with age and swollen when infected (Zhao et al., 2017) . Uterine tumor size, known to increase with age, was directly quantified by outlining the tumour area. These measurements provided insights into how bacterial colonization influences key aging pathologies in *C. elegans.*

4.8 Lifespan Assay

4.8.1 *C. elegans* lifespan assay on fluorescent CeMBio bacterium

Lifespan assays require synchronised populations of worms to begin with, for which standard egg-lay technique was performed (as mentioned in 4.3) using *C. elegans* N2OW (wildtype) as control and *kmo-1* (OW478) mutants as experimental model, to obtain age-synchronised L4 young adult worms. NGM plates were seeded with CeMbio strain *Ochrobactrum vermis* (MYb71) (as 4.2.3) and OP50 *E.coli* and about 30 worms per plate were transferred to 4 plates per condition and incubated at 25°C throughout. Worms were transferred to fresh MYb71 sfGFP and OP50 *E.coli* -seeded plates every 24h for first five days and later alternate days to avoid intergenerational mixing. Worm's survival was scored (dead, alive, censored) starting from day 1 daily until all animals were dead. The data was analysed, and lifespan graphs were made using GraphPad Prism.

4.9 Dual-RNA sequencing of *Caenorhabditis elegans* and associated microbes

4.9.1 Dual-RNAseq sample collection

C. elegans worms were grown on NGM plates with OP50 bacteria until they reached the L4+24 hours day 1 adult stage. Worms were exposed to the commensal and pathogenic bacteria, *E.coli* and *P. aeruginosa* on SK plates, another set of *E. faecalis* and *E.coli* on NGBHI plates and CeMbio strains on LB plates . Samples were collected at designated time points (0, 2, 4, 6, and 12 hours post-exposure). Worms were washed with M9 buffer and tetramisole to remove bacteria and paralyze the worms. Final washes were performed with cold MiliQ water. 200µL of worm suspension was transferred to a sample tube for each time point. Samples were centrifuged and the supernatant was removed, leaving 50µL of worms. 950µL of TRI reagent was added to each worm pellet. Samples were snap-frozen in liquid nitrogen and stored at -80°C for future (Dual-RNA seq extraction)

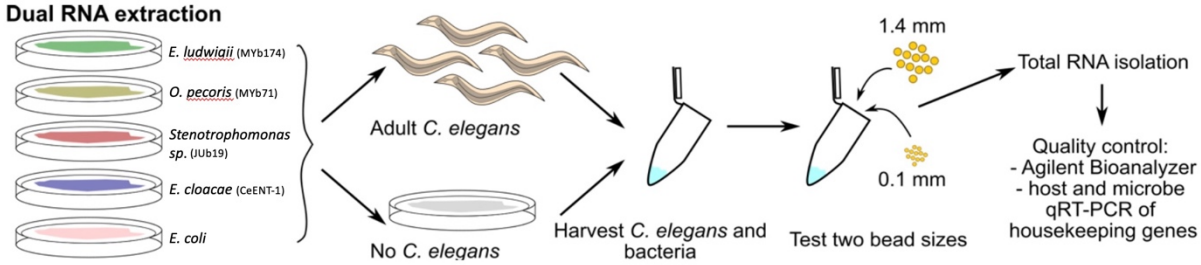

Figure 22. Dual RNA extraction methodology for *C. elegans* and bacterial samples. Two sets of samples are harvested containing C. elegans with bacteria and bacteria alone. Once harvested samples are homogenised using 0.1mm beads for RNA extraction, followed by total RNA isolation. Quality control is performed using Agilent Bioanalyzer and qRT-PCR of housekeeping genes for both host and microbe samples.

4.9.2 Total RNA extraction

The protocol for RNA extraction from *C. elegans* samples was adapted from the Zymo Research Direct-zol RNA Miniprep kit (Cambridge Bioscience). Extraction was carried out under RNase-free conditions, inside a biosafety cabinet equipped with laminar downflowand sterile DNAse/RNAse-free handling of materials was ensured throughout. Initially, samples were subjected to freeze-thaw cycles in liquid nitrogen and an ice water bath to facilitate cellular disruption. Homogenization (MP biomedicals) was then performed by bead-beating the samples with 0.1 mm Zirconium oxide beads (VWR) in Tri Reagent solution. The homogenized samples were centrifuged, and the supernatant was transferred to fresh RNase-free tubes. Subsequently, an equal volume of 70% ethanol was added, and the mixture was carefully loaded onto Zymo-Spin IC Columns for RNA purification.

After centrifugation and flow-through removal, an on-column DNase I treatment was performed by incubating the columns with a master mix of DNase I and buffer. The columns were then washed with RNA Prewash and RNA Wash Buffer, followed by elution of the purified RNA using DNase/RNase-free water. The eluates were divided into aliquots, snap-frozen in liquid n2and stored at -80°C for further analysis.

Quantification of the extracted RNA was carried out using the Qubit RNA HS Assay Kit (ThermoFisher). A master mix of Qubit RNA HS Reagent and Buffer was prepared, and standards and diluted samples were added to separate Qubit assay tubes. After a brief incubation, the samples were measured using the Qubit 2.0 Fluorometer, and RNA concentrations were calculated based on the standard curve.

Qualification of the extracted RNA was assessed by agarose gel electrophoresis. A 1% RNase-free agarose gel was prepared in TBE buffer and stained with SYBR Safe (as mentioned in 4.5.5). After loading the RNA samples and 5uL of 1kb plus DNA ladder (Thermofisher)marker, electrophoresis was performed at 120 Volts for 45 minutes. RNA integrity was visualized by examining the banding patterns on a UV transilluminator.

4.10 Statistical analysis

The statistical approach was designed to evaluate the significance of observed differences across experimental conditions, identify correlations between gut colonization and aging pathologies, and determine the impact of bacterial strains on *C. elegans* aging.

Gut colonization images and measured aging pathologies were systematically recorded using Microsoft Excel (Version 16.83), ensuring standardized and consistent data entry. Graphical representations were generated using GraphPad Prism (Version 9.3.0). Statistical significance was defined as $P < 0.05$.

Data was analysed using the following statistical approaches:

- Biolog Data Analysis: EcoPlate data were analysed using multiple T-tests to identify significant differences in bacterial metabolic activity across conditions.
- Gut Colonization Analysis: A two-way ANOVA with post-hoc Tukey's correction was performed to evaluate the effects of bacterial strain and *C. elegans* genotype on gut colonization levels, identifying specific differences between groups.
- Pathology Analysis:

    1. Intestinal Atrophy and Pharyngeal Size: Two-way ANOVA followed by Tukey's multiple comparisons test was used to compare groups. Linear regression was applied to identify trends, with Pearson's regression (95% confidence intervals) used to visualize these trends. Nonparametric Spearman correlation tests were conducted to assess the strength and significance of the relationship between pharyngeal size and bacterial colonization scores.
    2. Uterine Tumors: Two-way ANOVA followed by Bonferroni's multiple comparisons test was used to evaluate group differences in tumor size.

- Lifespan Analysis: Survival curves were compared using the log-rank test to determine the effects of bacterial strains and host genotypes on lifespan.

5 RESULTS

This section presents the finding from the experiments carried out for Biolog plate, bacterial transformations, *C. elegans* Kynurenine pathway mutant's gut colonisation by fluorescently tagged isolates of CeMbio+ community namely *Enterobacter cloacae* mPlum (CEent1-mPlum), *Ochrobactrum vermis* sfGFP (MYb71-sfGFP), *Pantoea nemavictus* mPlum (BIGb0393a-mPlum), *Enterobacter ludwigii* dTom (MYb174-dTom) and *Stenotrophomonas indicatrix* RFP2 (JUb19-RFP2) and dual-RNAseq. Along with the impact of those bacteria on *C. elegans* health and ageing, by quantifying the aging-pathologies.

5.1 Tn7-Mediated Fluorescent Tagging Of CeMbio+ Bacterial Strains For Tracking Gut Colonization In *Caenorhabditis elegans*

To be able to visualise microbial colonization dynamics within *C. elegans* and understanding the influence of kynurenine pathway (KP) gene mutations during early aging, we opted for a time-lapse microscopy approach. To enable real-time imaging of bacterial colonization *in-vivo*, under both monoxenic and polyxenic conditions, a Tn7-driven triparental matting technique was employed to insert fluorescent proteins (mPlum, dTomato, sfGFP) into CeMbio gut commensals. This approach allows for spatial tracking of single- and multi-species colonization dynamics (provided that combined bacterial strains are tagged with non-overlapping fluorophores) and facilitates associating microbial persistence with host pathologies.

Few bacterial strains were tagged previously in the lab (as mentioned in Table 11), and I thus aimed to continue generating more CeMbio+ fluorescently tagged strains for which we had failed to generate successful transformants. I notably focused on those that further needed to be transformed (see Table 12). However, bacterial transformation still revealed challenging despite multiple optimization attempts.

When observed under fluorescence microscope, *Comamonas sp. B-9* mPlum (MYb21-mPlum) and *Comamonas sp. B-9* sfGFP (MYb21-sfGFP) bacterial colonies expressed homogenous and most promising fluorophore protein expression. Fewer colonies expressing signs of transformations were also found for *Sphingobacterium multivorum* dTom (BIGb170-dTom),

Comamonas piscis sfGFP (BIGb172-sfGFP) and *Chryseobacterium sp*. mPlum (MYb317-mPlum) bacteria, these were further screened based on antibiotic profile test and quantified using PCR and agarose gel electrophoresis.

Table 11. List of previously transformed CeMbio bacterial strains

No.	Identifier	Strain Taxonomy	Fluorophore	Fluorescent Clone Generation	Stable Fluorescence Expression
1	MYb11	*Pseudomonas lurida*	dTomato	Yes	Yes
2	MYb71	*Ochrobactrum vermis*	sfGFP	Yes	Yes
3	MYb11	*Pseudomonas lurida*	mPlum	Yes	Yes
4	CEent1	*Enterobacter cloacae*	dTomato	Yes	Yes
5	MYb186	*Enterobacter sp.*	sfGFP	Yes	Yes
6	BIGb0393	*Pantoea nemavictus*	mPlum	Yes	Yes
7	CEent1	*Enterobacter cloacae*	mPlum	Yes	Yes
8	MYb11	*Pseudomonas lurida*	sfGFP	Yes	Yes
9	CEent1	*Enterobacter cloacae*	sfGFP	Yes	Yes
10	JUb66	*Llelliota amnigena*	sfGFP	Yes	Yes
11	MYb186	*Enterobacter sp. 638*	sfGFP	Yes	Yes

Table 12. List of bacteria transformation carried out

No.	Identifier	Strain Taxonomy	Fluorophore	Fluorescent Clone Generation	Stable Fluorescence Expression
1	BIGb0170	*Sphingobacterium multivorum*	dTom	Yes	No
2	BIGb0170	*Sphingobacterium multivorum*	sfGFP	Yes	No
3	BIGb0170	*Sphingobacterium multivorum*	mPlum	No	No
4	BIGb0172	*Comamonas piscis*	dTom	Yes	No
5	BIGb0172	*Comamonas piscis*	sfGFP	No	No
6	BIGb0172	*Comamonas piscis*	mPlum	No	No
7	MYb21	*Comamonas sp. B-9*	mPlum	Yes	No
8	MYb21	*Comamonas sp. B-9*	sfGFP	Yes	No
9	MYb21	*Comamonas sp. B-9*	dTom	No	No
10	MYb317	*Chryseobacterium sp.*	dTom	Yes	No
11	MYb317	*Chryseobacterium sp.*	mPlum	Yes	No
12	MYb317	*Chryseobacterium sp.*	sfGFP	Yes	No

As expected, the transformed bacteria gained gentamicin resistance. From the previous work done it in the lab and given antibiotic profile test, most of the bacteria of interest were found to be gentamicin sensitive (which was the prerequisite for bacterial transformation). BIGb0170, BIGb0172, MYb21 and MYb317 were streaked (onto LB+G_{60}, LB+IPTG, LB agar

plates) before and after transformation to ensure that the bacteria were susceptible to the antibiotics and gained resistance only after the transformation.

Results for colony PCR amplification followed by agarose gel electrophoresis shows band formation corresponding to the expected insert site i.e. ≈1468bp was verified against the ladder. Replicates with brightest bands (as shown in the Figure 23 below) were further sent for 16S DNA sanger sequencing (Source biosciences).

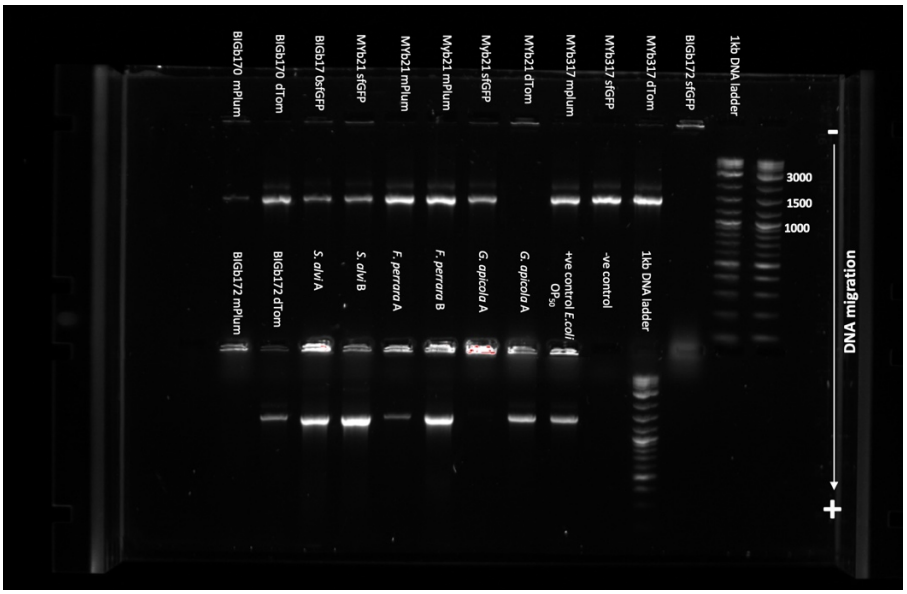

Figure 23. Agarose gel electrophoresis: Fluorescently transformed commensal bacteria. Agarose gel image shows band formation after bacterial transformation of *Sphingobacterium multivorum, Comamonas piscis, Comamonas sp. B-9,* and *Chryseobacterium sp.* with tagged fluorophore proteins, along with a positive control (*E. coli* OP50), a negative control, and a 1 kb DNA ladder for reference. Complete strain details and fluorophore information are provided in Table 12.

Once 16S DNA sequences were received, 4peaks software was used for analysing DNA sequencing chromatograms to determine the nucleotide sequence from raw sequencing data. Once analysed, ApE (A plasmid Editor) software was used to edit and refine the selected part from the raw sequence. Both the reverse and forward sequences were aligned using UGene software-sequence alignment tool. Using BLAST (Basic Local Alignment Search Tool) on NCBI, these aligned sequences were used for comparing to sequence databases and calculating the statistical significance of matches to the target organism. The sequences for which the %identical came up 90% or more were considered successfully transformed bacteria as they resemble to the (recipient) bacteria's pre-transformed genome. The table below gives a detail information on bacteria antibiotic profile pre- and post-transformation sequence confirmation using BLAST and final confirmation and identification via MALDI.

Table 13. Molecular characterization of transformed bacteria: 16S sequencing and MALDI-TOF Analysis

No.	Identifier	Strain Taxonomy	Antibiotic profile (Gentamicin)	Sequencing match	Forward sequence			Reverse sequence			MALDI TOF
					Sequence aligned	E Value	% Identical	Sequence aligned	E Value	% Identical	
1	BIGb0170 dTom	*Sphingobacterium multivorum*	Resistant	No	*Escherichia coli*	0.0	97.28%	*Escherichia coli*	0.0	98.22%	*Escherichia coli*
2	BIGb0170 sfGFP	*Sphingobacterium multivorum*	Resistant	No	*Escherichia coli*	0.0	98.35%	*Escherichia coli*	0.0	98.21%	*Escherichia coli*
3	BIGb0172 dTom	*Comamonas piscis*	Resistant	No	*Escherichia coli*	0.0	97.90%	*Escherichia coli*	0.0	98.26%	*Escherichia coli*
4	MYb21 mPlum	*Comamonas sp. B-9*	Resistant	No	*Escherichia sp.*	0.0	97.90%	*Escherichia coli*	0.0	98.21%	*Escherichia coli*
5	MYb21 sfGFP	*Comamonas sp. B-9*	Resistant	No	*Escherichia sp.*	0.0	98.50%	*Escherichia sp.*	0.0	97.56%	*Escherichia coli*
6	MYb317 dTom	*Chryseobacterium sp.*	Resistant	No	*Escherichia coli*	0.0	97.26%	*Escherichia sp.*	0.0	98.59%	*Escherichia coli*
7	MYb317 mPlum	*Chryseobacterium sp.*	Resistant	No	*Escherichia coli*	0.0	97.79%	*Escherichia coli*	0.0	97.37%	*Escherichia coli*
8	MYb317 sfGFP	*Chryseobacterium sp.*	Resistant	No	*Escherichia sp.*	0.0	97.49%	*Escherichia sp.*	0.0	98%	*Escherichia coli*

The majority of transformation attempts yielded unsuccessful results, 8 fluorescent bacteria were produced but were identified as *Escherichia sp.* or had improper fluorescent protein encoding gene integration revealed by unstable fluorescence expression observed under fluorescence microscopy. As for the remaining 4 bacteria, no fluorescent clones were generated. Ultimately the unsuccessfully transformed bacteria were discarded. Multiple repeats for this experiment were carried out each time, adjusting transformation parameters, but yet no successful outcomes were reported (reasons that might have occurred which resulted unsuccessful transformations are discussed later). These outcomes highlight the challenges encountered in the transformation process and the need for further optimization.

5.2 Fluorescently-Tagged CeMbio+ Isolates Phenotypically Match Their Parent Isolate

To investigate the relationship between bacterial gut colonization and the development of aging pathologies in *C. elegans*, it was crucial to ensure that fluorescent tagging of bacterial strains did not introduce unintended phenotypic changes. However, transposon-mediated insertion can potentially alter endogenous bacterial gene expression, leading to unintended metabolic or physiological changes. These alterations might influence the colonization capacity, virulence, bacterial metabolism, substrate utilization, and overall phenotypic traits.

To address this concern, bacterial strains both parental and transformed versions were subjected to phenotypic characterization using antibiotic resistance assays, Biolog EcoPlates, and Phenotypic Microarray (PM) assays. By applying these methods, it was possible to ensure that the new fluorescing bacteria would be a good model to study their corresponding parent isolate.

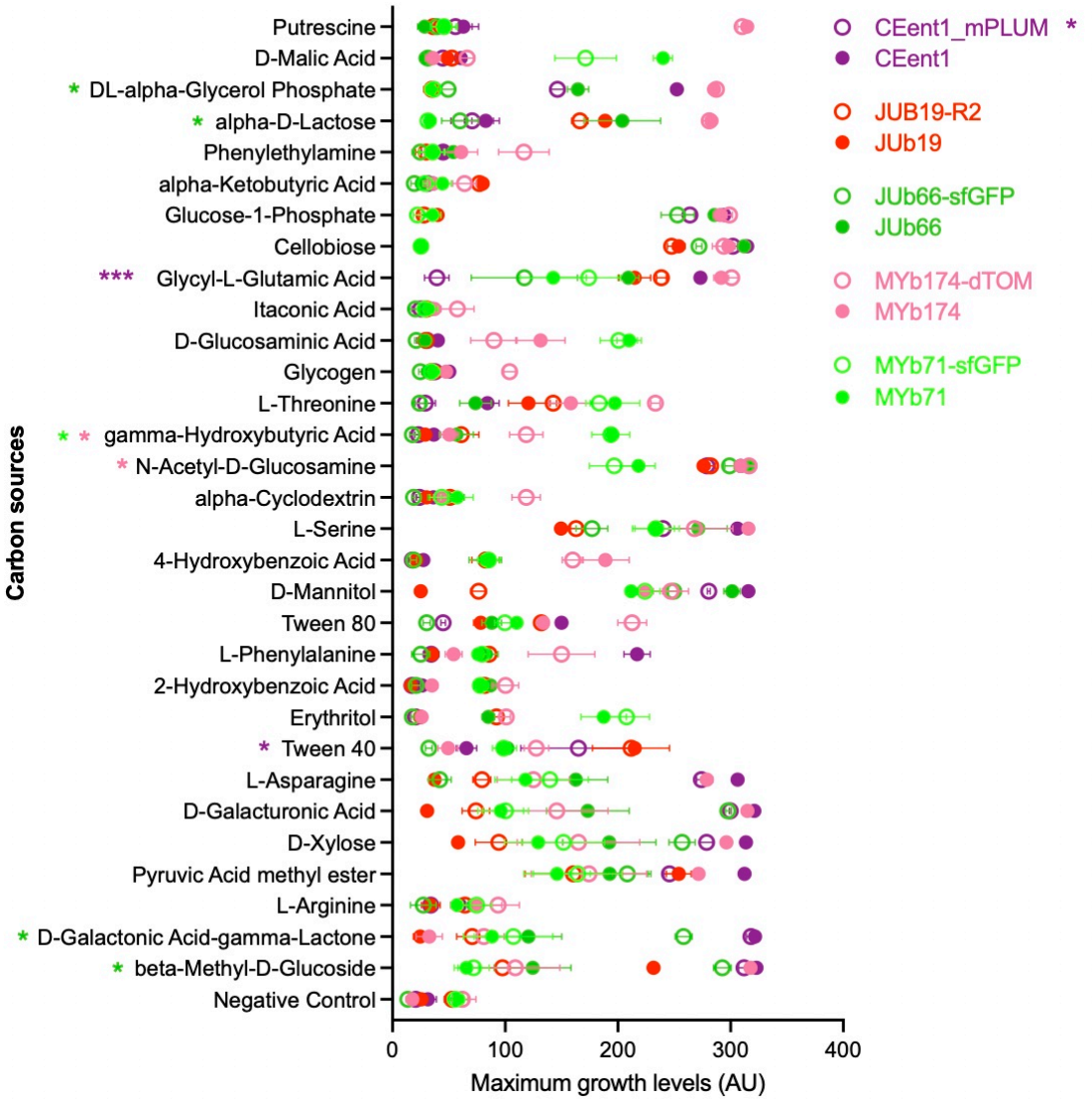

Figure 24. Metabolic Phenotyping of Transformed and Parental Bacterial Strains Using Biolog EcoPlates. The figure illustrates the metabolic activity of transformed bacterial strains (e.g., *Enterobacter cloacae* mPlum, *Stenotrophomonas indicatrix* RFP2, *Lelliottia amnigena* sfGFP, *Enterobacter ludwigii* dTomato, and *Ochrobactrum vermis* sfGFP) compared to their respective parental strains (CEent1, JUb19, JUb66, MYb174, and MYb71) across a range of 31 carbon sources. Error bars denote standard deviations from biological replicates. Statistical significance was determined using multiple t-tests, with significant differences marked by asterisks : * $p<0.05$, ** $p<0.01$, *** $p<0.001$ between the transformed and parental strains. These results highlight variations in metabolic capabilities due to the transformation process, which may influence bacterial phenotypes relevant to colonization and host interactions.

The Biolog EcoPlate results highlight notable differences in carbon source utilization among the bacterial strains and their fluorescent derivatives. *Enterobacter cloacae* mPlum (CEent1-mPlum) exhibited a potential functional divergence from its parent strain CEent1, suggesting it might have distinct effects on the host. Similarly, *Lelliottia amnigena* GFP (JUb66-GFP) demonstrated enough variation from JUb66 in substrate utilization, warranting further investigation to confirm these differences through additional repeats. In contrast, the fluorescent derivatives *Stenotrophomonas indicatrix* RFP2 (JUb19-RFP2), *Enterobacter ludwigii* dTom (MYb174-dTomato), and *Ochrobactrum vermis* (MYb71-sfGFP) closely mirrored the metabolic profiles of their respective parent strains, indicating they are likely representative of their non-fluorescent counterparts. These observations underscore the importance of assessing functional equivalence in modified strains for host-microbe interaction studies

5.3 In Monoxenic Conditions, Mutation Of Kynurenine Pathway Enzymes Differentially Affect Commensal Bacterium Gut Colonisation In *Caenorhabditis elegans* And *Vice Versa*

Gut colonization by commensal bacteria significantly influences host health, affecting nutrition, immunity, behaviour, metabolism (Sekirov, et al., 2009; Tremaroli & Bäckhed, 2012) and even helps in preventing pathogen colonization (Kamada, et al., 2014). Investigating gut colonization can reveal how microbial communities establish, evolve, and maintain stability over time (Koenig et al., 2010). Studying gut colonisation can provide insights into metabolic disorders, potential interventions and development of novel probiotics (O'toole, et al., 2017).

The Kynurenine Pathway (KP), a primary tryptophan metabolic pathway has proven to be a potential target for increasing both lifespan and health-span. 3-Hydroxyanthranilic acid (3 HAA) is a metabolite of KP, which is found to extend lifespan in *C. elegans.* Accumulation of 3 HAA in *C. elegans* also shows improved gut integrity and resistance to bacterial infection (Espejo et al., 2024).

To determine whether the *C. elegans* Kynurenine Pathway (KP) can differentially impact gut colonisation rate by CeMbio+ isolates, we first exposed *E. coli* OP50-raised *C. elegans* day-one adult worms to fluorescently tagged bacteria in monoxenic conditions (see method 4.6.3). For

this, we focused on a subset of CeMbio+ strains we had previously successfully tagged and characterised: CEent1-mPlum, MYb71-sfGFP, BIGb0393a-mPlum, MYb174-dTom and JUB19-RFP2. The experiment was performed on wild type (WT), *tdo-2 , afmd -1 , kynu-1, kmo-1* and *haao-1* kynurenine pathway (Figure 25) mutants. Fluorescent microscopy imaging between 6h and 120h post-exposure revealed that all the bacteria tested colonise the *C. elegans* gut well, and that KP mutants displayed altered gut colonisation patterns as hypothesised.

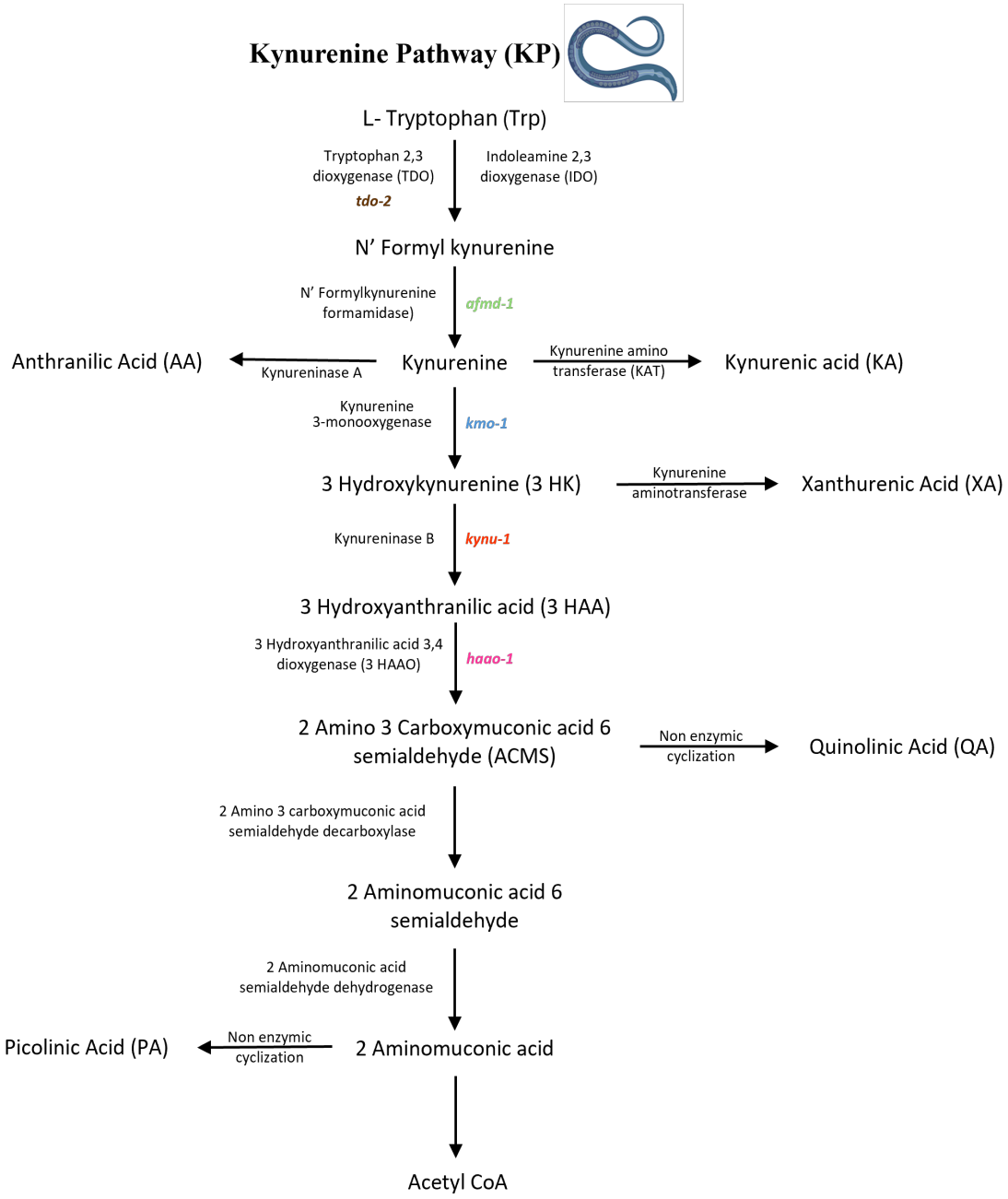

Figure 25. Map of Kynurenine Pathway: in *C. elegans* with each enzyme knock out point labelled with the corresponding colour to the mutants represented in gut colonisation graphs below. Illustration created with BioRender.com

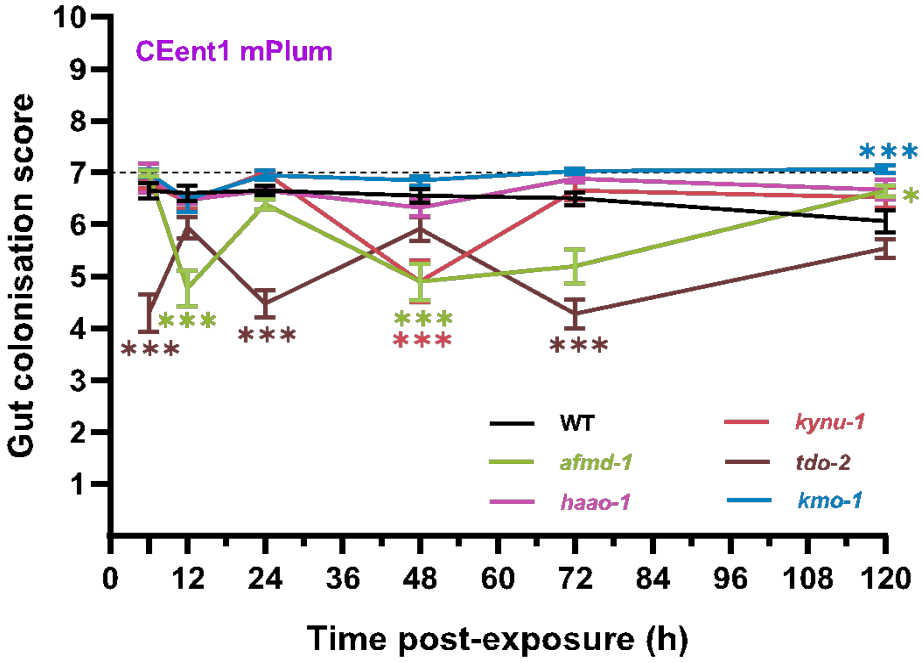

Figure 26. Gut colonisation rate of monoxenic *Enterobacter cloacae* in naïve control versus kynurenine pathway mutant *C. elegans* adults. *C. elegans* day 1 adult worms were raised on *E. coli* OP50 bacteria and transferred onto NGM plate seeded with fluorescently-tagged isolate of the CeMbio community *E. hormaechei,* expressing the genetically-encoded fluorescent protein mPlum (https://www.fpbase.org/protein/mplum/) (see methods). Fluorescence images were acquired at 6, 12, 24, 48, 72 and 120 hours post-exposure, and a visual score of 0-12 was given to quantify the extent of the gut colonisation (see Table 10). The experiment was carried out on two different weeks (N=2), imaging and measuring 25-50 worms per condition. Error bars indicate the standard error of the mean. Differences were assessed by 2-way ANOVA with post-hoc Tukey's correction for multiple comparisons. Differences were deemed significant for $p<0.05$. Asterisks indicate significant differences compared to wild-type control: * $p<0.05$, ** $p<0.01$, *** $p<0.001$.

In particular, *Enterobacter cloacae* (CEent1-mPlum) revealed a strong monoxenic coloniser, reaching maximal colonisation at 6h in all worm strains except for mutants of the first enzyme in the KP pathway tdo-2, which showed reduced gut colonisation at all time points (Figure 26). Mutation of the next enzyme in the KP pathway afmd-1 also reduced *Enterobacter cloacae* gut colonisation extent at 12h, 48h and 72h. Conversely, kmo-1 mutants displayed slightly, yet significantly, higher gut colonisation at 120h post-exposure, compared to all other genotypes.

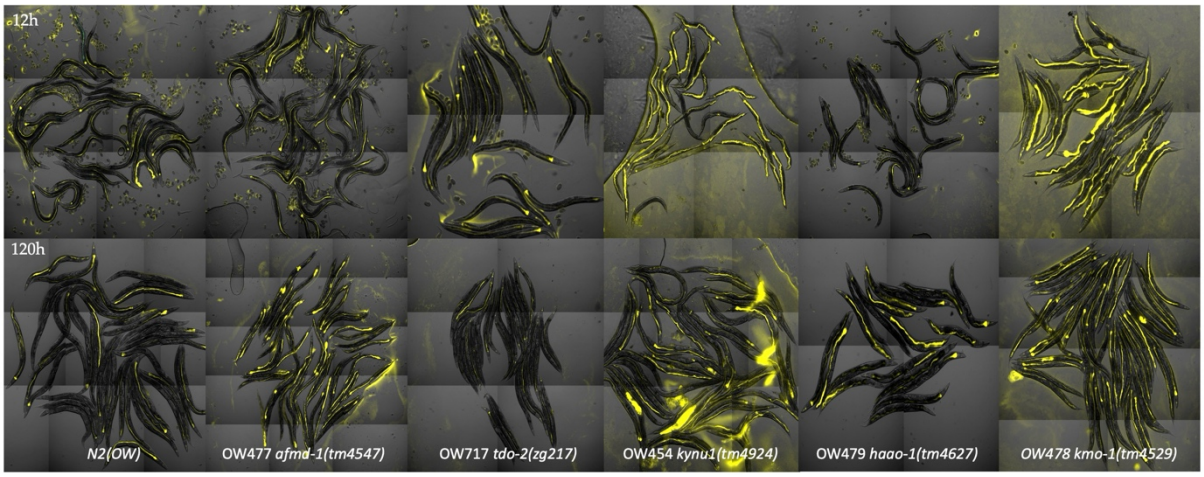

Figure 27. Kynurenine Pathway mutant *C.elegans* gut colonised by *Enterobacter cloacae (CEent1-mPlum).* Images showing the bacterial load present at 12h and 120h across wildtype and Kynurenine pathway mutants.

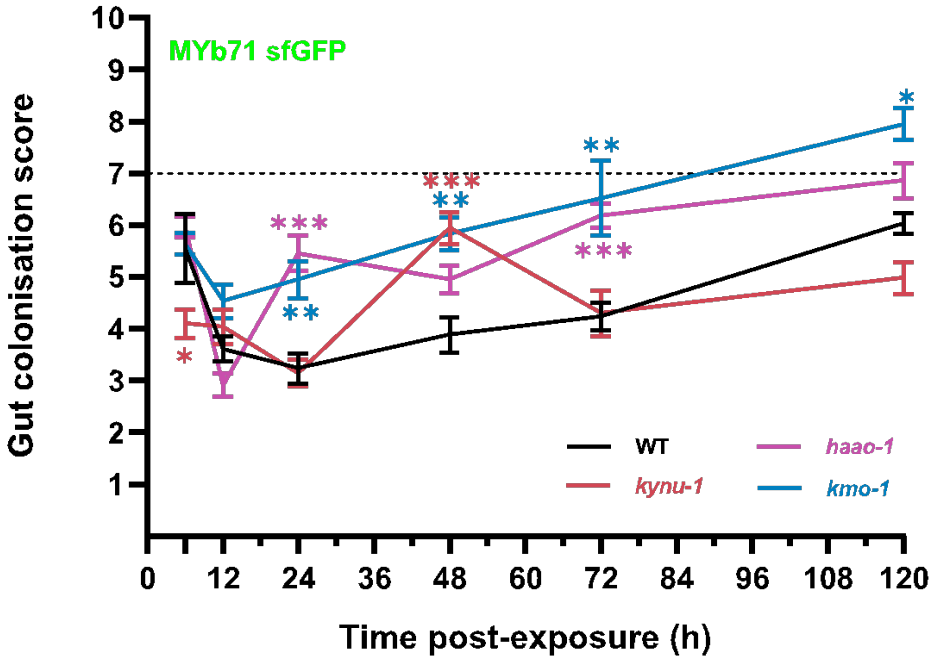

Figure 28. Gut colonisation rate of monoxenic *Ochrobactrum vermis* in naïve control versus kynurenine pathway mutant *C. elegans* adults. *C. elegans* day 1 adult worms were raised on *E. coli* OP50 bacteria and transferred onto NGM plate seeded with fluorescently-tagged isolate of the CeMbio community *O. vermis*, expressing the genetically-encoded fluorescent protein sfGFP (https://www.fpbase.org/protein/superfolder-gfp/) (see methods). Fluorescence images were acquired at 6, 12, 24, 48, 72 and 120 hours post-exposure, and a visual score of 0-12 was given to quantify the extent of the gut colonisation (see Table 10). The experiment was carried out on two different weeks (N=2), imaging and measuring 25-50 worms per condition. Error bars indicate the standard error of the mean. Differences were assessed by 2-way ANOVA with post-hoc Tukey's correction for multiple comparisons. Differences were deemed significant for $p<0.05$. Asterisks indicate significant differences compared to wild-type control: * $p<0.05$, ** $p<0.01$, *** $p<0.001$.

Ochrobactrum vermis (MYb71-sfGFP) revealed a very good but slower monoxenic coloniser than *Enterobacter cloacae* (CEent1-mPlum), displaying an initially rapid colonisation followed

by a decrease between 6h and 24h, before repopulating the gut of wild type worms following a linear growth pattern until the 120h timepoint (Figure 28). kynu-1 showed an initial lower colonisation rate than other worm strains before peaking at 48h and subsequently receding. Conversely kmo-1 mutants displayed sustained git colonisation beyond wild type levels from 12h onwards, albeit still following a linear growth pattern, reaching pathogenic levels (gut colonisation score >7) at 120h. haao-1 mutants also displayed increased gut colonisation levels by *Ochrobactrum vermis* compared to wild type and kynu-1 worms.

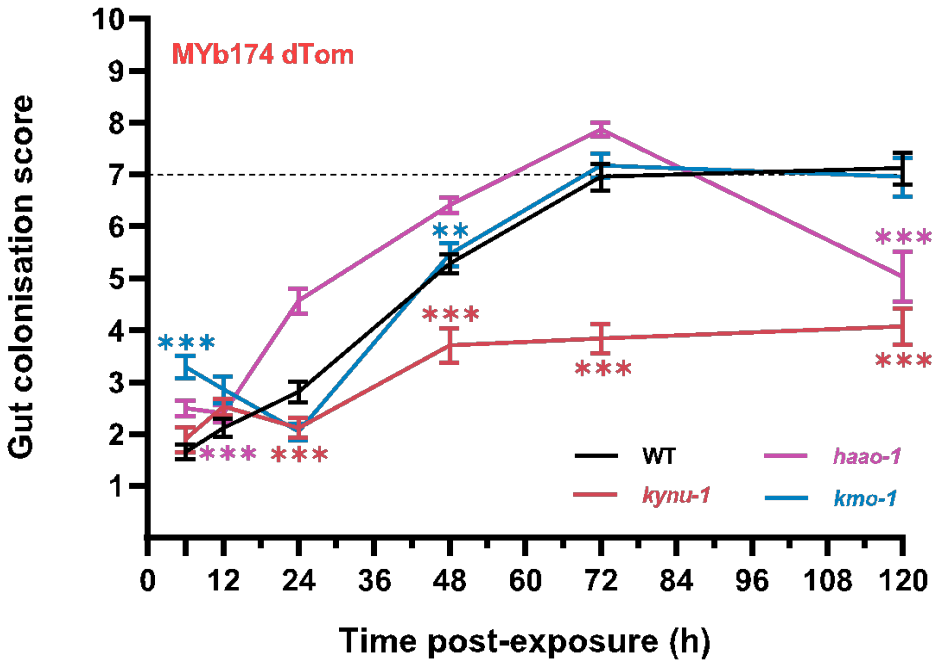

Figure 29. Gut colonisation rate of monoxenic *Enterobacter ludwigii* in naïve control versus kynurenine pathway mutant *C. elegans* adults. *C. elegans* day 1 adult worms were raised on *E. coli* OP50 bacteria and transferred onto NGM plate seeded with fluorescently-tagged isolate of the CeMbio community *E. ludwigii*, expressing the genetically-encoded fluorescent protein dTomato (https://www.fpbase.org/protein/dtomato/) (see methods). Fluorescence images were acquired at 6, 12, 24, 48, 72 and 120 hours post-exposure, and a visual score of 0-12 was given to quantify the extent of the gut colonisation (see Table 10). The experiment was carried out on two different weeks (N=2), imaging and measuring 25-50 worms per condition. Error bars indicate the standard error of the mean. Differences were assessed by 2-way ANOVA with post-hoc Tukey's correction for multiple comparisons. Differences were deemed significant for $p<0.05$. Asterisks indicate significant differences compared to wild-type control: * $p<0.05$, ** $p<0.01$, *** $p<0.001$.

Contrasting with the phylogenetically related *Enterobacter cloacae* (CEent1-mPlum), *Enterobacter ludwigii* (MYb174-dTomato) revealed a slower monoxenic coloniser, only reaching complete gut colonisation between 48h and 72h post-exposure, but not in the kynu-1 mutant, which displayed a much lower rate and lesser extent of gut colonisation throughout (Figure 29). Remarkably, haao-1 mutant worms exhibited earlier and greater gut colonisation

by *Enterobacter ludwigii* (MYb174-dTomato) between 24h and 72h post-exposure. Interestingly, kmo-1 mutants exhibited a higher initial gut colonisation at 6h post-exposure, but not from 12h onwards.

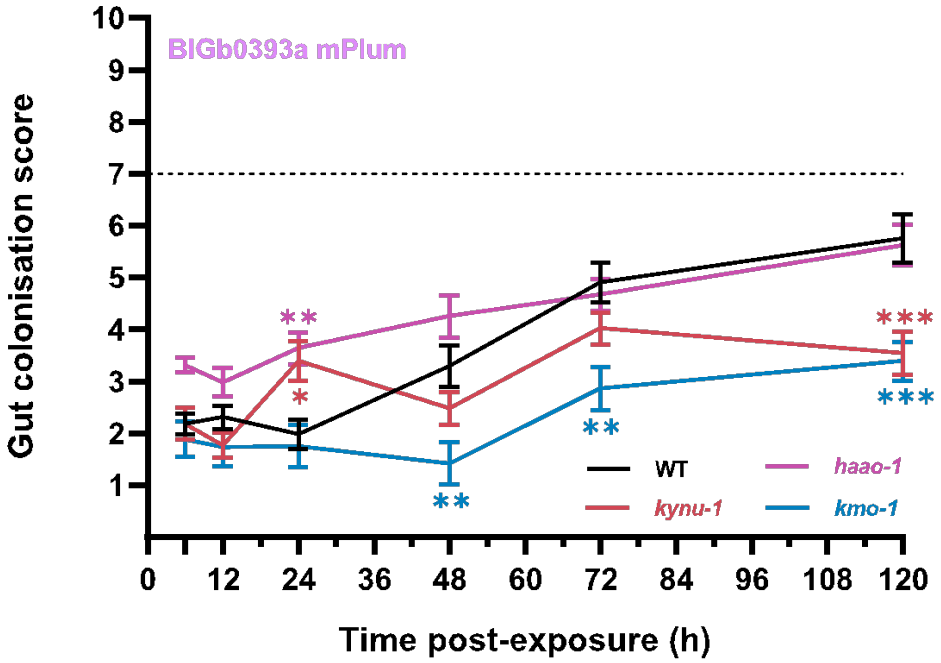

Figure 30. Gut colonisation rate of monoxenic *Pantoea nemavictus* in naïve control versus kynurenine pathway mutant *C. elegans* adults. *C. elegans* day 1 adult worms were raised on *E. coli* OP50 bacteria and transferred onto NGM plate seeded with fluorescently-tagged isolate of the CeMbio community *P. nemavictus*, expressing the genetically-encoded fluorescent protein mPlum (https://www.fpbase.org/protein/mplum/) (see methods). Fluorescence images were acquired at 6, 12, 24, 48, 72 and 120 hours post-exposure, and a visual score of 0-12 was given to quantify the extent of the gut colonisation (see Table 10). The experiment was carried out once due to time restrictions (N=1), imaging and measuring 25-50 worms per condition. Error bars indicate the standard error of the mean. Differences were assessed by 2-way ANOVA with post-hoc Tukey's correction for multiple comparisons. Differences were deemed significant for $p<0.05$. Asterisks indicate significant differences compared to wild-type control: * $p<0.05$, ** $p<0.01$, *** $p<0.001$.

Next, *Pantoea nemavictus* (BIGb0393a-mPlum) displayed a slow monoxenic colonisation ability for the first 24h, before gradually progressing from a spotty gut colonisation pattern to full gut colonisation in wildtype worms (Figure 30). Interestingly, it colonised haao-1 more readily initially, gradually progressing throughout to reach the same maximal colonisation level as in wild type worms at 72h and 120h. More surprisingly, *Pantoea nemavictus* (BIGb0393a-mPlum) appeared to colonise kmo-1, and to a lesser extent kynu-1, mutant guts with more difficulty.

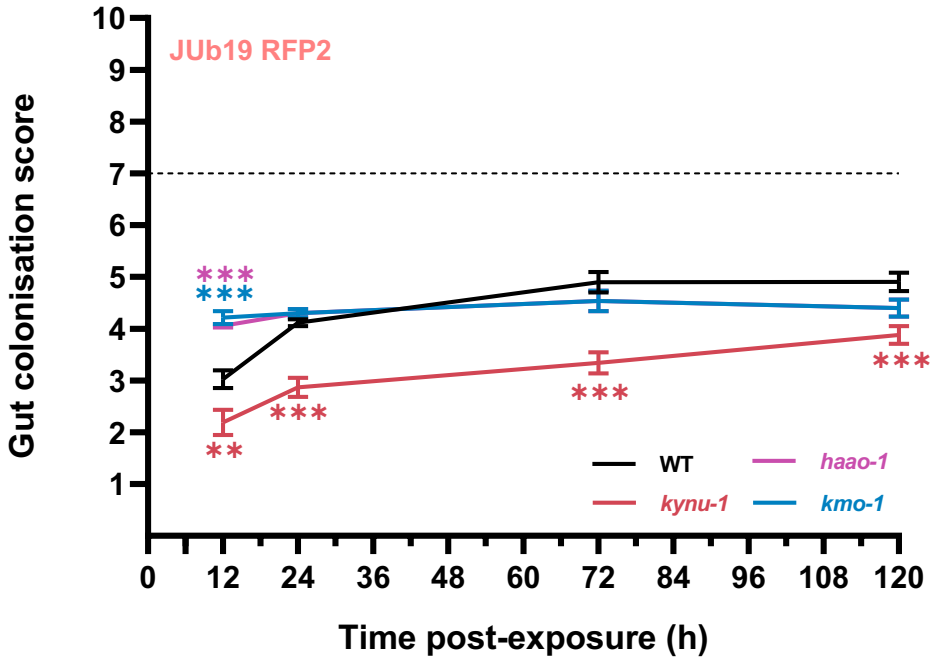

Figure 31. Gut colonisation rate of monoxenic *Stenotrophomonas indicatrix* in naïve control versus kynurenine pathway mutant *C. elegans* adults. *C. elegans* day 1 adult worms were raised on *E. coli* OP50 bacteria and transferred onto NGM plate seeded with fluorescently-tagged isolate of the CeMbio community *S. indicatrix*, expressing the genetically-encoded fluorescent protein RFP2 (https://www.fpbase.org/protein/dcyrfp2s/) (see methods). Fluorescence images were acquired at 6, 12, 24, 48, 72 and 120 hours post-exposure, and a visual score of 0-12 was given to quantify the extent of the gut colonisation (see Table 10). The experiment was carried out on two different weeks (N=2), imaging and measuring 25-50 worms per condition. Error bars indicate the standard error of the mean. Differences were assessed by 2-way ANOVA with post-hoc Tukey's correction for multiple comparisons. Differences were deemed significant for $p<0.05$. Asterisks indicate significant differences compared to wild-type control: *$p<0.05$, **$p<0.01$, ***$p<0.001$.

Finally, *Stenotrophomonas indicatrix* (JUb19-RFP2) displayed the lowest colonisation levels of all four microbial strain studied (Figure 31). Despite colonising the worm gut uniformly within 12h, it never led to intestinal bloating in either of the worm strain studied. Yet, it showed a faster initial rate of gut colonisation in haao-1 and kmo-1 mutants, and a much reduced colonisation rate in kynu-1 mutants.

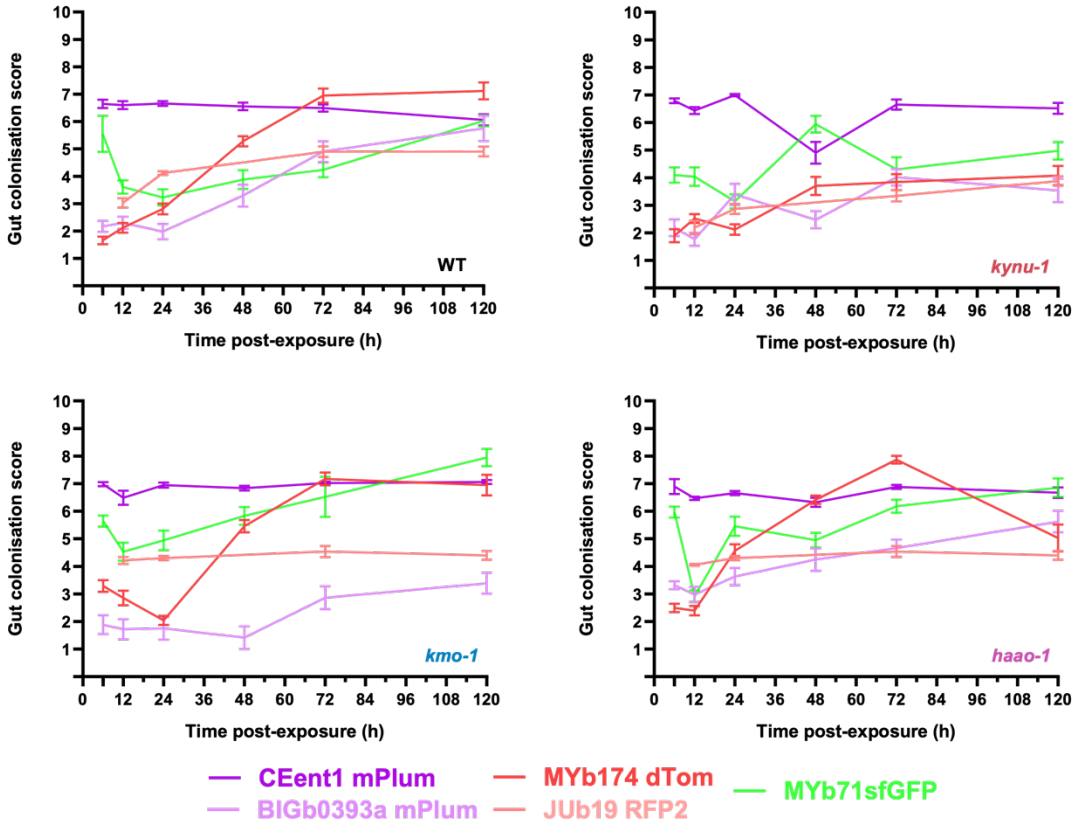

Figure 32. Comparative extent of gut colonisation by fluorescently tagged isolates of CeMbio community across *C. elegans* kynurenine pathway mutant strains in monoxenic condition. The graph above shows differential colonisation pattern induced by each kynurenine pathway mutants, across the fluorescent CeMbio bacteria. Fluorescence images were acquired at 6, 12, 24, 48, 72 and 120 hours post-exposure, and a visual score of 0-12 was given to quantify the extent of the gut colonisation (see Table 10). Data was assembled from various bacterial monoxenic experiments, each conducted on two independent days, resulting in two independent replicates per condition (N=2), except for BIGb0393a mPlum (N=1), imaging and measuring 25-50 worms per condition. Error bars indicate the standard error of the mean.

Combined, results from these gut colonisation experiments in monoxenic conditions paint a complex picture where KP pathway mutants all differ from wild type animals and from each other in their relative abilities to support gut colonisation by the CeMbio+ commensals studied here.

Together these results further highlight differing gut colonisation strategies by the isolates studied, at least when in monoxenic conditions. Contrasting with *Enterobacter* and *Ochrobactrum* species that immediately fill the worm gut, *Pantoea nemavictus* (BIGb0393a mPlum) and *Stenotrophomonas indicatrix* (JUb19 RFP2) colonise the worm gut much slower initially. They also do not lead to intestinal distension or pathogenicity as seen with *Enterobacter ludvigii* (MYb174 dTom) and *Ochrobactrum vermis* (MYb71 sfGFP).

5.4 Inter-Bacterium And/Or Host-Bacterium Interactions In Polyxenic Conditions Lead To A Temporary Reduction Of Gut Microbial Colonization In *Caenorhabditis Elegans*, Worsened In Kynurenine Pathway Mutants

While previous experiments focused on monoxenic conditions, studying *C. elegans* under polyxenic conditions better reflects natural environments where multiple bacterial species contribute to the gut microbiota. In such microbial communities, inter-strain competition and metabolic inter-dependencies shape gut colonization dynamics, determine bacterial persistence, and define the impact of the gut microbiota on the host physiology.

Hence while the monoxenic conditions studied earlier afford simpler analyses of host genetics-gut microbe interactions, these conditions are unlikely to occur in the wild and to have shaped host-microbe evolution. We thus next asked how similar bacterial gut colonisation rates and the influence of the host kynurenine pathway would be in a more natural context where worms are exposed to a mix of commensal gut microbes.

We selected *Enterobacter cloacae* (CEent1-mPLum), *Ochrobactrum vermis* (MYb71 sfGFP), and *Stenotrophomonas indicatrix* (JUb19-RFP2) as they are core members of the CeMbio selection tagged with non-overlapping fluorophores, thus allowing for their co-imaging *in vivo*. Young adult worms (day one) were transferred to plates seeded with equal amounts of each of the three fluorescent isolates and imaged by fluorescence stereomicroscopy at regular intervals over the next five days.

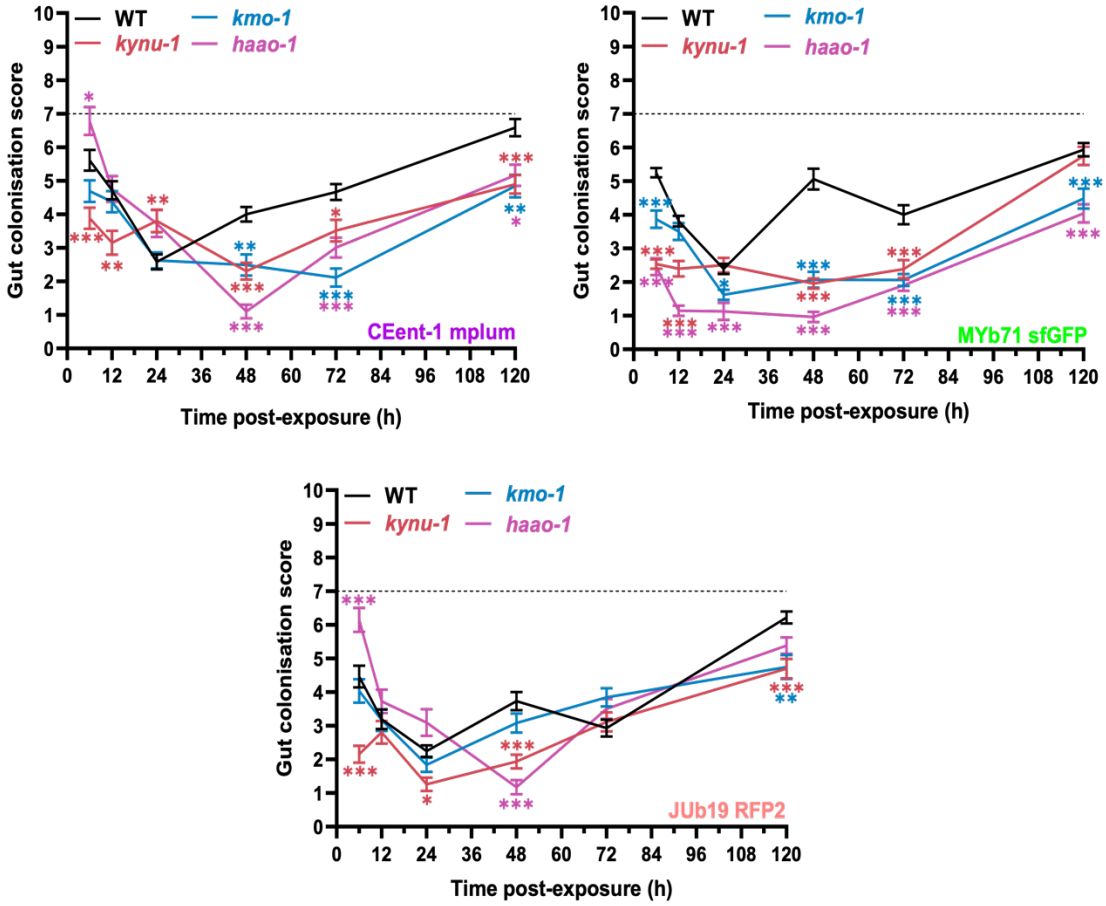

Figure 33. Differential gut colonisation pattern of naïve control and kynurenine pathway mutant *C. elegans* adults on *Ochrobactrum vermis*, *Enterobacter hormaechei* and *Stenotrophomonas indicatrix* under polyxenic condition. *C. elegans* day 1 adult worms were raised on *E. coli* OP50 bacteria and transferred onto NGM plate seeded with three fluorescently tagged isolates of the CeMbio community *O. vermis, E. hormaechei* and *S. indicatrix*, expressing the genetically-encoded fluorescent protein sfGFP, mPlum and RFP2 respectively. Fluorescence images were acquired at 6, 12, 24, 48, 72 and 120 hours post-exposure, and a visual score of 0-12 was given to quantify the extent of the gut colonisation (see Table 10). The experiment was carried out on two different weeks (N=2), imaging and measuring 25-50 worms per condition. Error bars indicate the standard error of the mean. Differences were assessed by 2-way ANOVA with post-hoc Tukey's correction for multiple comparisons. Differences were deemed significant for $p<0.05$. Asterisks indicate significant differences compared to wild-type control: * $p<0.05$, ** $p<0.01$, *** $p<0.001$.

All three strains were found to colonise the *C. elegans* gut in the four worm genotypes tested, establishing tripartite gut microbial communities. Wild type *C. elegans* were the most readily colonised by the bacterial cocktail with colonisation scores around 6 after 120h, while the *kynu-1* and the *kmo-1* mutants averaged gut colonisation scores around 4.5 and 5 respectively and *haao-1* mutants had an intermediate phenotype (with CEent1-mPlum and JUb19 RFP2 score around 5 and MYb71 sfGFP scores around 4) (Figure 33)

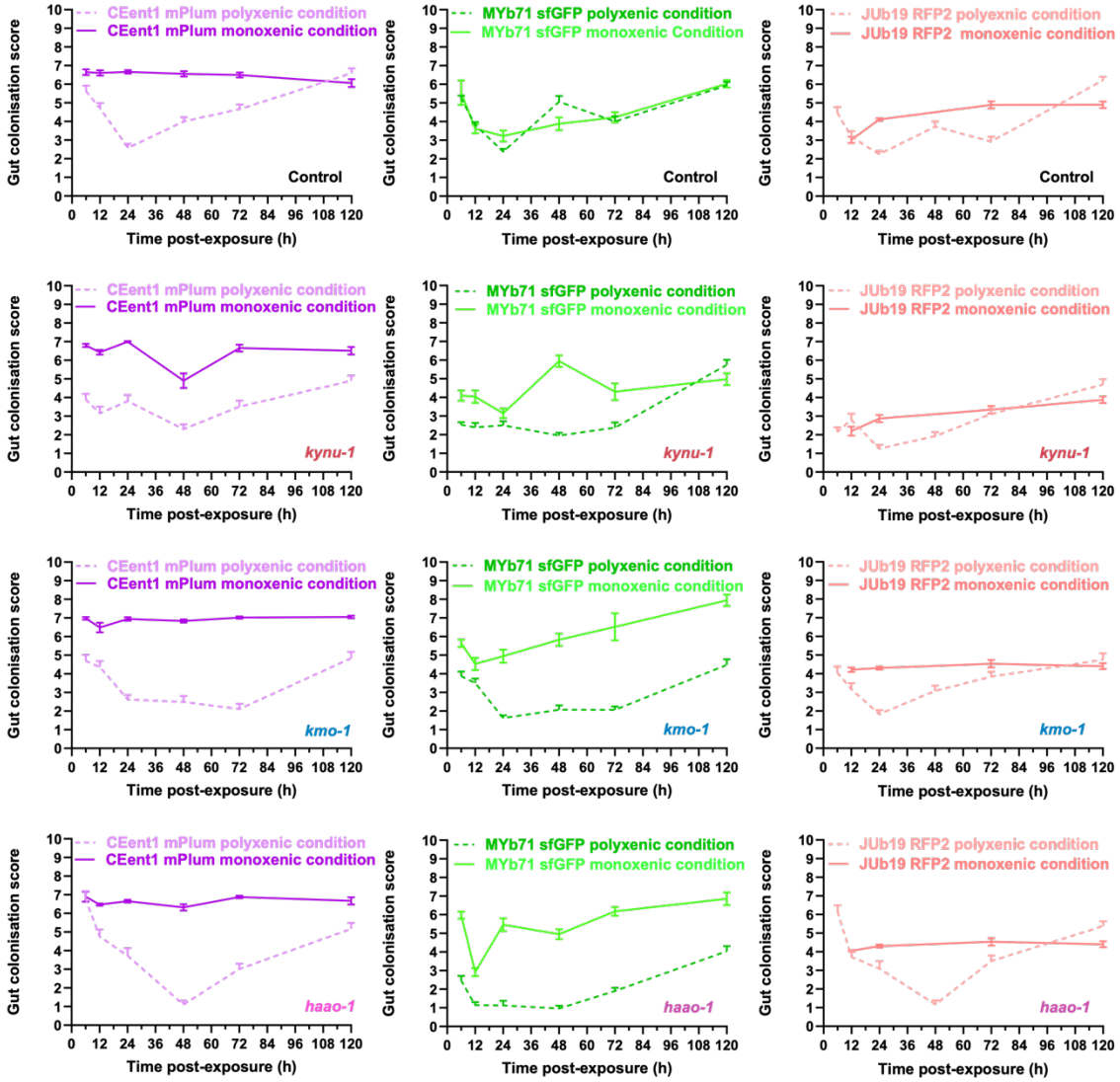

Figure 34. Comparative analysis of gut colonizing fluorescently tagged CeMbio bacterial isolates in naïve control and kynurenine pathway mutant *C. elegans* under monoxenic vs. polyxenic culture condition. Fluorescence images were acquired at 6, 12, 24, 48, 72 and 120 hours post-transfer, and a visual score of 0-12 was given to quantify the extent of the gut colonisation. The experiment was carried out on two different weeks (N=2), imaging and measuring 25-50 worms per condition. Error bars indicate the standard error of the mean.

Compared to monoxenic conditions, gut colonisation in polyxenic conditions seemed to follow a common trend regardless of host genotype, including a fast initial gut colonisation, followed by a decrease over the first 24-48h depending on the strain of worm and bacterial isolate, and a moderate but steady increase in gut bacterial load afterwards until 120h (Figure 34).

The bacterium isolates with the most differing behaviour between monoxenic and polyxenic conditions was *Enterobacter cloacae* (CEent1-mPlum) possibly because as a fast monoxenic coloniser, it is sensitive to competition in polyxenic conditions. Yet, after 120h, it caught back

with the colonisation levels achieved in monoxenic conditions. *Ochrobactrum vermis* (MYb71-sfGFP) and *Stenotrophomonas indicatrix* (JUB19-RFP2) were less affected by polyxenic conditions in wild type animals, with both reaching at least equivalent levels of gut colonisation as in monoxenic conditions by 120h.

However, both *Enterobacter cloacae* (CEent1-mPlum) and *Ochrobactrum vermis* (MYb71-sfGFP) gut colonisation patterns in polyxenic conditions were strongly impacted by host KP enzyme mutations, failing to reach the same colonisation levels as in monoxenic conditions in KP mutants. Although a slower coloniser, *Stenotrophomonas indicatrix* (JUB19-RFP2) appeared less affected by the interaction between the host KP activity and polyxenic conditions, reaching at least equivalent levels of gut colonisation as in monoxenic conditions by 120h for all worm genotypes.

Interestingly, *kmo-1* and *haao-1* mutants, which displayed an increased propensity for rapid and extent gut colonisation by *Ochrobactrum vermis* (MYb71-sfGFP), displayed an opposite behaviour in polyxenic conditions. Hence, the combination of a host-mutation and co-occurrence of other gut bacteria changed *Ochrobactrum vermis* (MYb71-sfGFP) colonisation behaviour.

Comparing the gut colonisation ability of CeMbio isolates in monoxenic *versus* polyxenic conditions thus evidenced a significant interaction between host KP metabolism and gut microbiota composition.

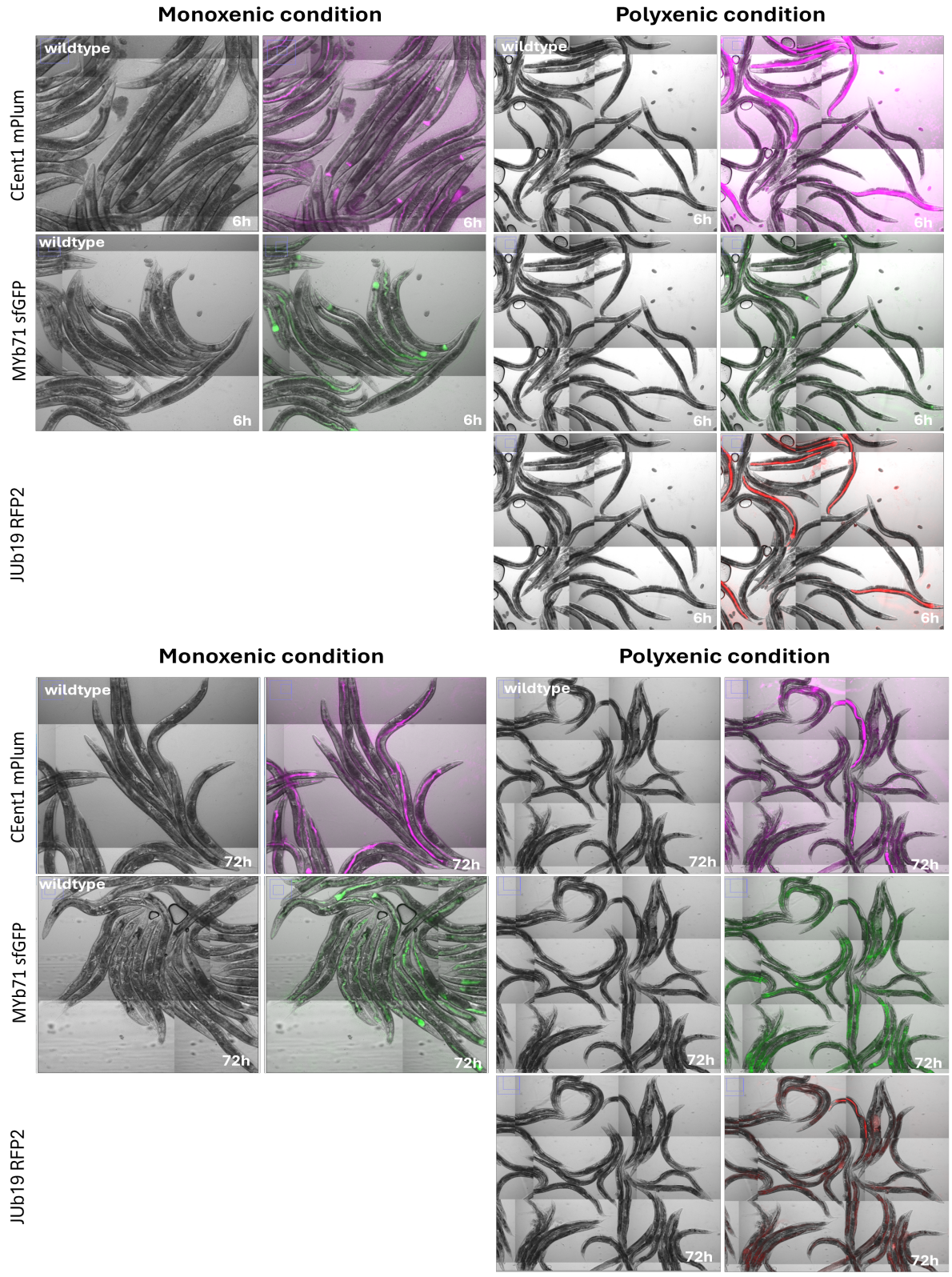

Figure 35. Fluorescent microscopic images as a visual representation of bacterial load present in wildtype *C.elegans* when exposed to *Enterobacter hormaechei, Ochrobactrum vermis* and *Stenotrophomonas indicatrix* in monoxenic vs. polyxenic conditions. Images taken post-transfer at 6 hours and 72 hours for wildtype worms, when in varying conditions shows the intensity of the bacteria present at the given time. These images are taken from a single repeat which may may not directly comply with the graphical representation in the figure above as it includes multiple repeats. JUb19 RFP2 images are unavailable at the moment*

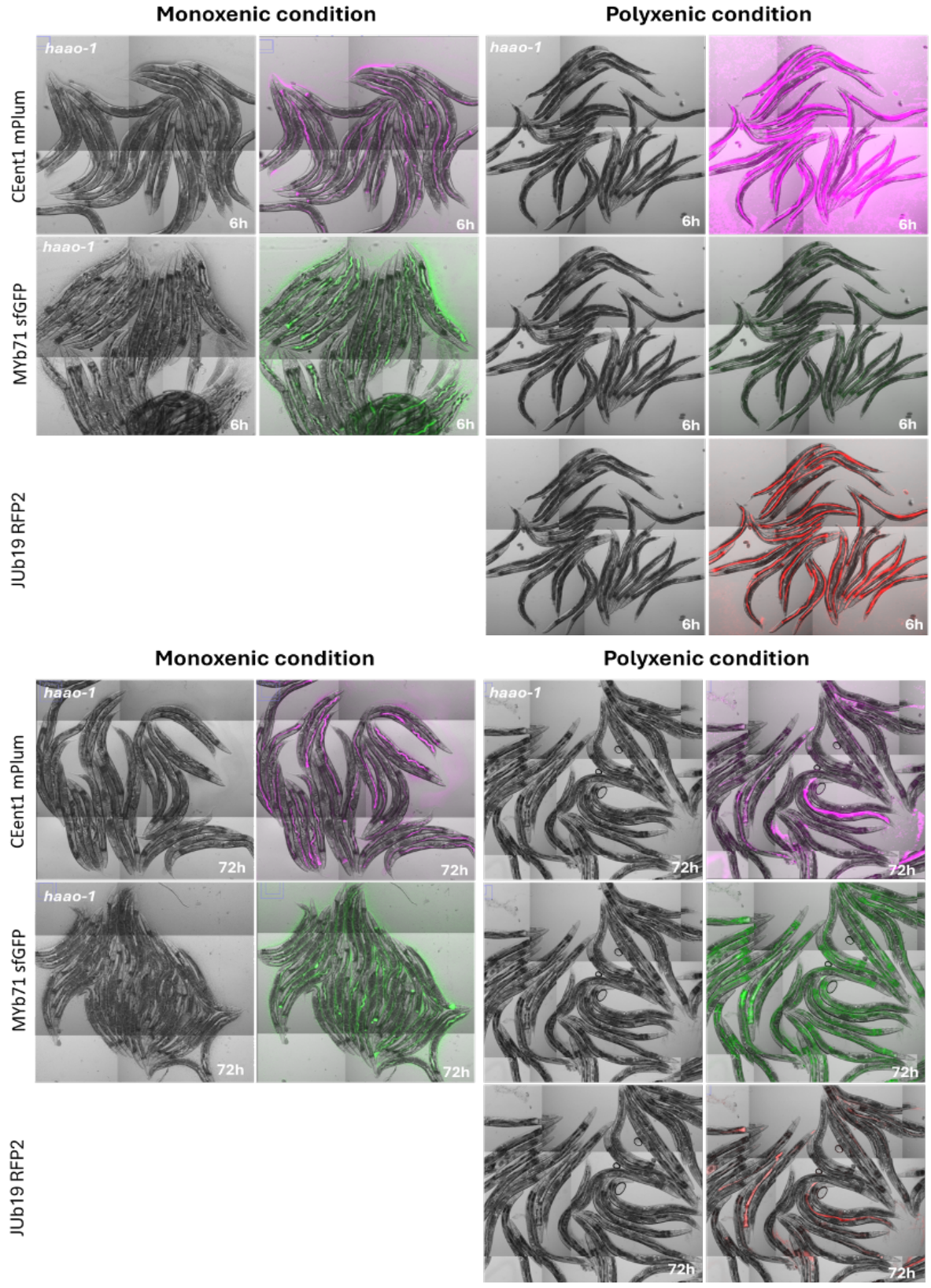

Figure 36. Fluorescent microscopic images as a visual representation of bacterial load present in *haao-1* mutant *C.elegans* when exposed to *Enterobacter hormaechei, Ochrobactrum vermis* and *Stenotrophomonas indicatrix* in monoxenic vs. polyxenic conditions. Images taken post-transfer at 6 hours and 72 hours for *haao-1* mutant worms, when in varying conditions shows the intensity of the bacteria present at the given time. These images are taken from a single repeat which may may not directly comply with the graphical representation in the figure above as it includes multiple repeats. JUb19 RFP2 images are unavailable at the moment*

5.4.1 Age-associated intestinal atrophy is reduced in polyxenic conditions

Age-associated intestinal atrophy, characterized by damage to the gut lining and pharynx alongside bacterial accumulation, is a significant hallmark of aging in *C. elegans* (Zhao et al., 2017). By examining intestinal atrophy under polyxenic conditions, such as exposure to different CeMbio strains, we aim to assess how microbial diversity influences gut morphology and function during aging (Van Der Goot et al., 2012). This study focuses on quantifying intestinal atrophy and microbial impacts, providing insights into potential interventions for mitigating age-related gastrointestinal decline (Zhao et al., 2017).

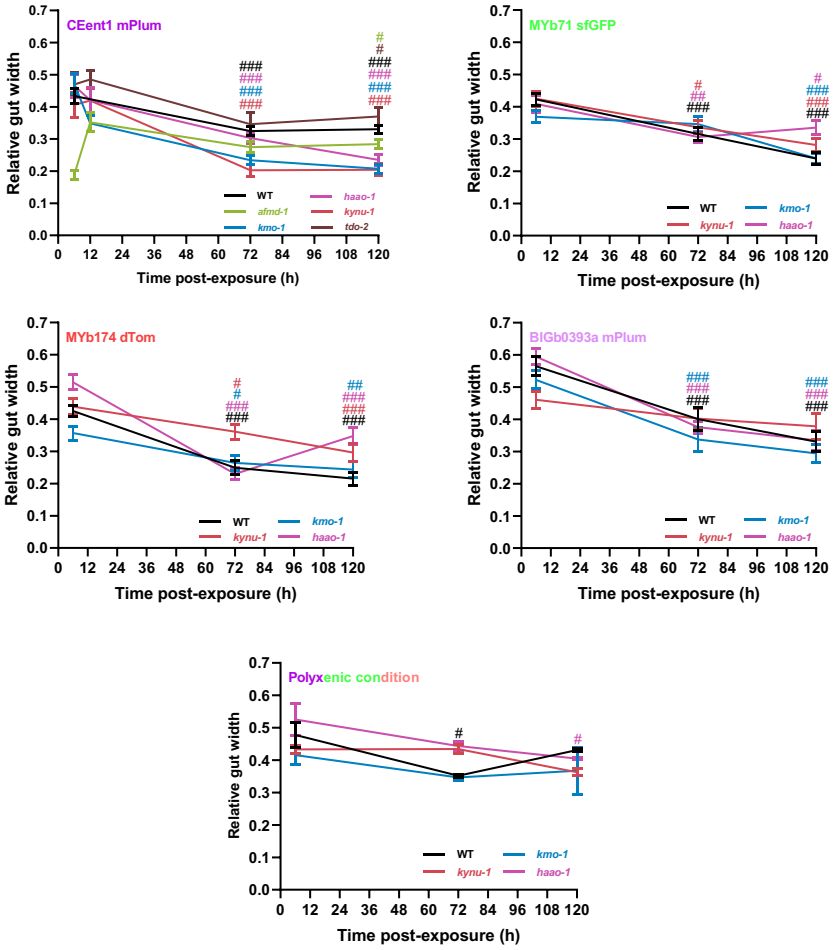

Figure 37. Quantification of intestinal gut atrophy of kynurenine pathway mutant *C.elegans* post-exposure to fluorescently tagged isolates of CeMbio in monoxenic and polyxenic conditions. Bright field images acquired at 6,72 and 120 hours post-exposure were analysed for development of intestinal atrophy. At the posterior end of the worm, using tools from Fiji, measurement of intestinal lumen width (L), intestinal width (I), and body width were recorded, and relative gut width was determined. Relative Gut Width=(Lumen-Intestinal)/body width. Two independent repeats were carried out on different weeks (N=2), 12 worms per condition were randomly quantified for measuring ageing pathologies. Error bars represent standard error of the mean (SEM). Statistical analysis was performed using 2way ANOVA followed by Tukey's multiple comparisons test. Hashtags indicate significant differences when compared to the 6-hour time point. #p>0.05, ##p>0.01, ###p>0.001. Polyxenic condition: CEent1 mPlum + MYb71 sfGFP + JUb19 RFP2.

To make a valid comparison, we referenced previous work that had quantitatively measured intestinal atrophy of *C. elegans* under monoxenic conditions with *E. coli* OP50 at 15°C, 20°C and 25°C of temperatures (Ezcurra, Benedetto et al, 2018). The results revealed progressive thinning of the intestinal tissue with age, with corresponding increased gut morphological deterioration and accumulation of PLP (Pseudocoelomic Lipoprotein Pools). As this effect has been well characterized, I decided to investigate the effect of microbial diversity under monoxenic and polyxenic conditions rather than re-measure OP50. The results obtained displayed a progressive thinning of the gut tissue (Figure 37) that align with those of previous reports.

Exposure to the fast coloniser *Enterobacter cloacae* (CEent1-mPlum) led to more variable effects on age-associated intestinal atrophy across KP mutants, compare to other isolates, with *kynu-1* and *kmo-1* exhibiting the most severe phenotypes. Conversely, exposure to the phylogenetically related *Enterobacter ludwigii* (MYb174-dTomato) led to accelerated intestinal atrophy for wild type and *kmo-1* mutant. Interestingly, polyxenic conditions seemed favourable to wild type worms as intestinal atrophy was minimal over the first 6 days of adulthood (the mean relative gut width remained around 45%) and KP metabolism did not impact majorly on intestinal atrophy in this context, mirroring previous observations on bacterial gut colonisation rate and suggesting a link between gut colonisation patterns and age-associated gut atrophy.

5.4.1 Gut colonisation alone does not fully determine gut lumen width

As bacteria colonise the worm gut, filling its lumen, they may extend it, mechanically stressing the intestine and leading to its relative thinning. The fact that gut lumen width enters the calculation of relative intestinal width may also lead to a negative correlation between relative gut width and bacterial gut colonisation. To verify this, I next plotted gut lumen width and gut colonisation scores (Figure 38). While both measures appeared broadly positively corelated, the evolution of gut lumen width over time in worms exposed to gut commensals did not perfectly track gut bacterial load, indicating that other factors than gut bacterial colonisation drive gut lumen enlargement and likely intestinal atrophy, as described for *E. coli* in (Ezcurra, Benedetto et al, 2018).

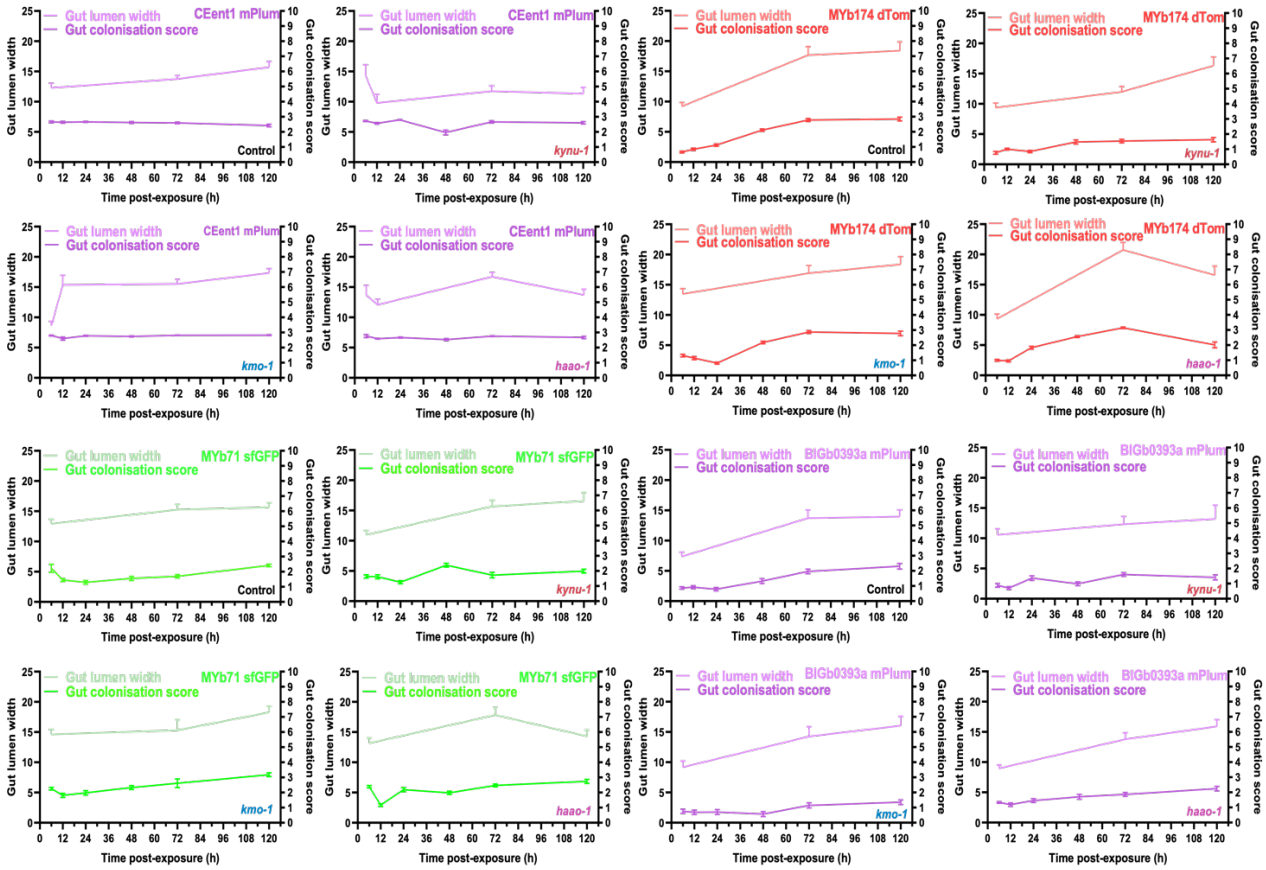

Figure 38. Correlative analysis between bacterial colonization scores vs. gut lumen width of kynurenine pathway mutant *C.elegans*, post exposure to fluorescently tagged isolated of CeMbio community, across different time points.

5.4.2 Pharyngeal enlargement correlates with pharyngeal infection and increasing gut colonization rate in *kmo-1* and *haao-1* mutants exposed to *Enterobacter ludwigii* and in *kynu-1* mutant exposed to *Ochrobactrum vermis*

Age-related deterioration of the pharynx is another critical pathological feature in *C. elegans* ageing, potentially acting as a life-limiting factor as pharyngeal pumping span correlates with lifespan (Collins, Huang, Hughes, & Kornfeld, 2007) and pharynges atrophy with age in worms fed an *E. coli* diet (Ezcurra, Benedetto et al, 2018). Another pharyngeal phenotype with an age component has also been highlighted by (Zhao et al., 2017) who identify pharyngeal swelling caused by opportunistic bacterial infection following pharyngeal mechanical tear. In their article, the authors phenotype dead worms and introduce the concepts of "Big P" (P) and "small p" (p) death in *C. elegans*.

A. "Big P" (P): It is typically associated with the end of life in young or middle-aged worms. The pharynx of immunocompromised *C. elegans* is susceptible to bacterial infection and proliferation of the bacteria can induce swelling of the posterior pharyngeal bulb that limits worm lifespan. This explains the early death of worm i.e. P death.

B. "small p" (p): This is identified as late death in aged *C. elegans*, characterized by a gradual decline in health and function. Small p showed marked atrophy of the posterior bulb, with up to a 70% decrease compared to Big P. On infection with fluorescent bacteria p corpses typically contained very less to almost no fluorescence bacteria indicating a controlled invasion (Zhao et al., 2017).

However, *E. coli* is not a naturally occurring gut microbe for *C. elegans.* I thus investigated whether either of the above phenotypes occurred in worms exposed to commensal microbes, measuring pharyngeal sizes and noting whether bacteria had invaded the posterior pharyngeal bulb by looking at the pharynx fluorescence signal.

When exposed to fluorescently tagged isolates of CeMbio+ bacterial strains, wildtype and KP mutant *C. elegans* showed progressively increasing pharyngeal sizes post-exposure/with age, except for *Ochrobactrum vermis* sfGFP (MYb71-sfGFP) (as seen below in Figure 39). In case of *Ochrobactrum vermis* sfGFP, *kynu-1* and wildtype shows a significant rise in pharyngeal size at 72h, whereas for these two mutants along with *kmo-1* and *haao-1* the pharyngeal size at 120h eventually falls back to normal or even lesser when compared to 6h timepoint, which also suggests age-associated atrophy.

Similar patterns were observed for wild type and *haao-1* mutant *C. elegans* with *Enterobacter ludwigii* dTomato, (as seen below in Figure 39) where an initial increasing pharyngeal size was observed from 6h to 72h followed by a slightly significant reduction in the pharyngeal bulb size.

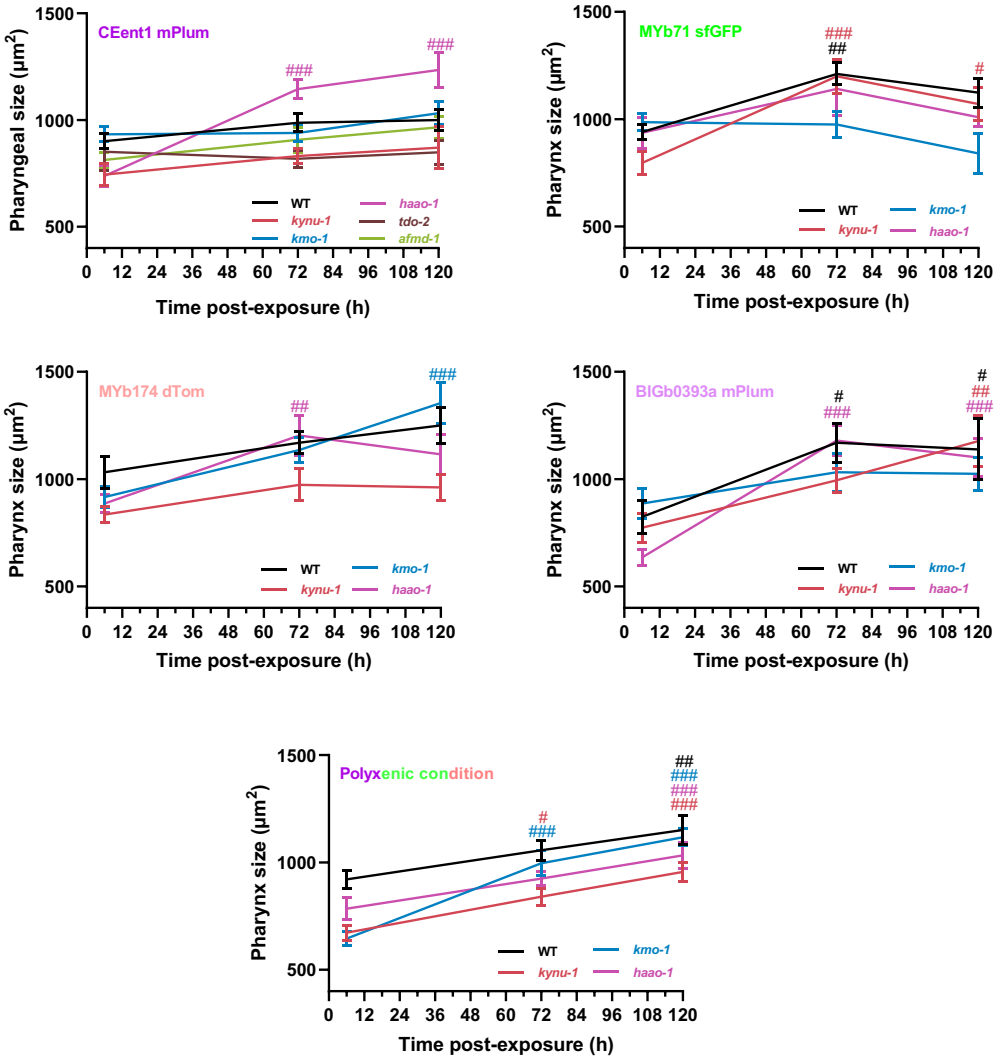

Figure 39. Analysis of pharyngeal morphological changes across kynurenine pathway mutant C. elegans post exposure to fluorescently tagged microbes in monoxenic and polyxenic conditions. Bright field images acquired at 6,72 and 120 hours post-exposure were analysed for measuring pharyngeal changes. Pharynx size were quantified by manual tracing of pharyngeal circumference to determine cross-sectional area at defined time points. The experiment was carried out on two different weeks (N=2), 12 worms per condition were randomly quantified for measuring pharyngeal size. Error bars represent standard error of the mean (SEM). Statistical analysis was performed using 2way ANOVA followed by Tukey's multiple comparisons test. Hashtags indicate significant differences when compared to the 6-hour time point. #p>0.05, ##p>0.01, ###p>0.001. Polyxenic condition: CEent1 mPlum + MYb71 sfGFP + JUb19 RFP2.

As infected pharynges (cf. big P pharynges above) tend to be rounder and larger, I next wondered whether an increased pharyngeal size correlates with increased infection and increased gut bacterial colonisation. To visualise it, I plotted the pharyngeal section surface against the gut colonisation score for all microbial condition tested for the different KP mutant genotypes studied (Figure 40). This revealed a general positive correlation between pharyngeal size and gut colonisation score across conditions.

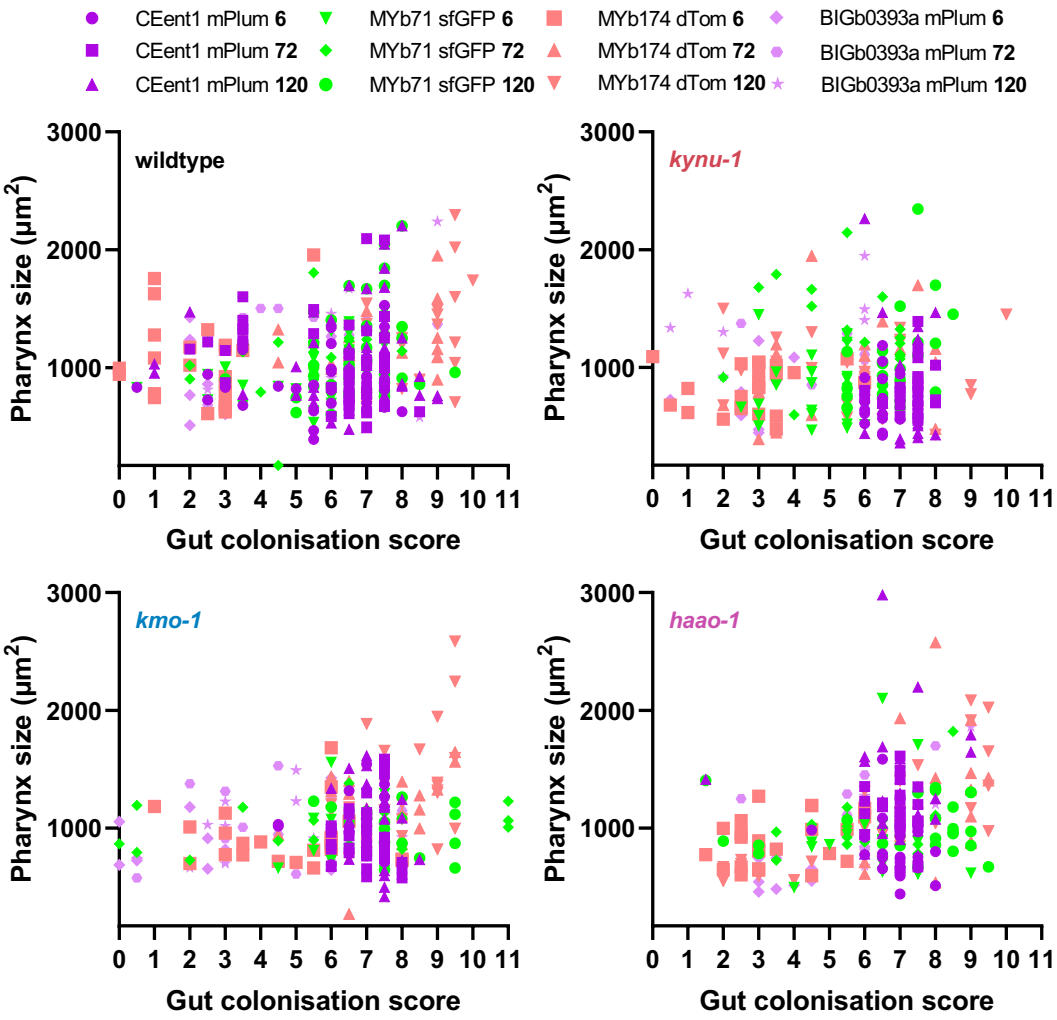

Figure 40. Correlative analysis of bacterial colonization scores vs. pharyngeal size of naïve and kynurenine pathway mutant *C.elegans*, post exposure to four fluorescently tagged isolated of CeMbio community in monoxenic condition. Fluorescence and brightfield images were acquired at 6, 12, 24, 48, 72 and 120 hours post-transfer, and a visual score of 0-12 was given to quantify the extent of the gut colonisation. Pharynx size were quantified by manual tracing of pharyngeal circumference to determine cross-sectional area at defined time points using bright field images. The experiment was carried out on two different weeks (N=2), imaging and measuring 25-50 worms for gut colonisation score and 12 worms per condition were randomly quantified for measuring pharyngeal size.

To delve deeper into these correlations, I next plotted pharyngeal sizes against individual microbial colonisation scores for each mutant at 72h and at 120h and performed spearman correlation analysis.

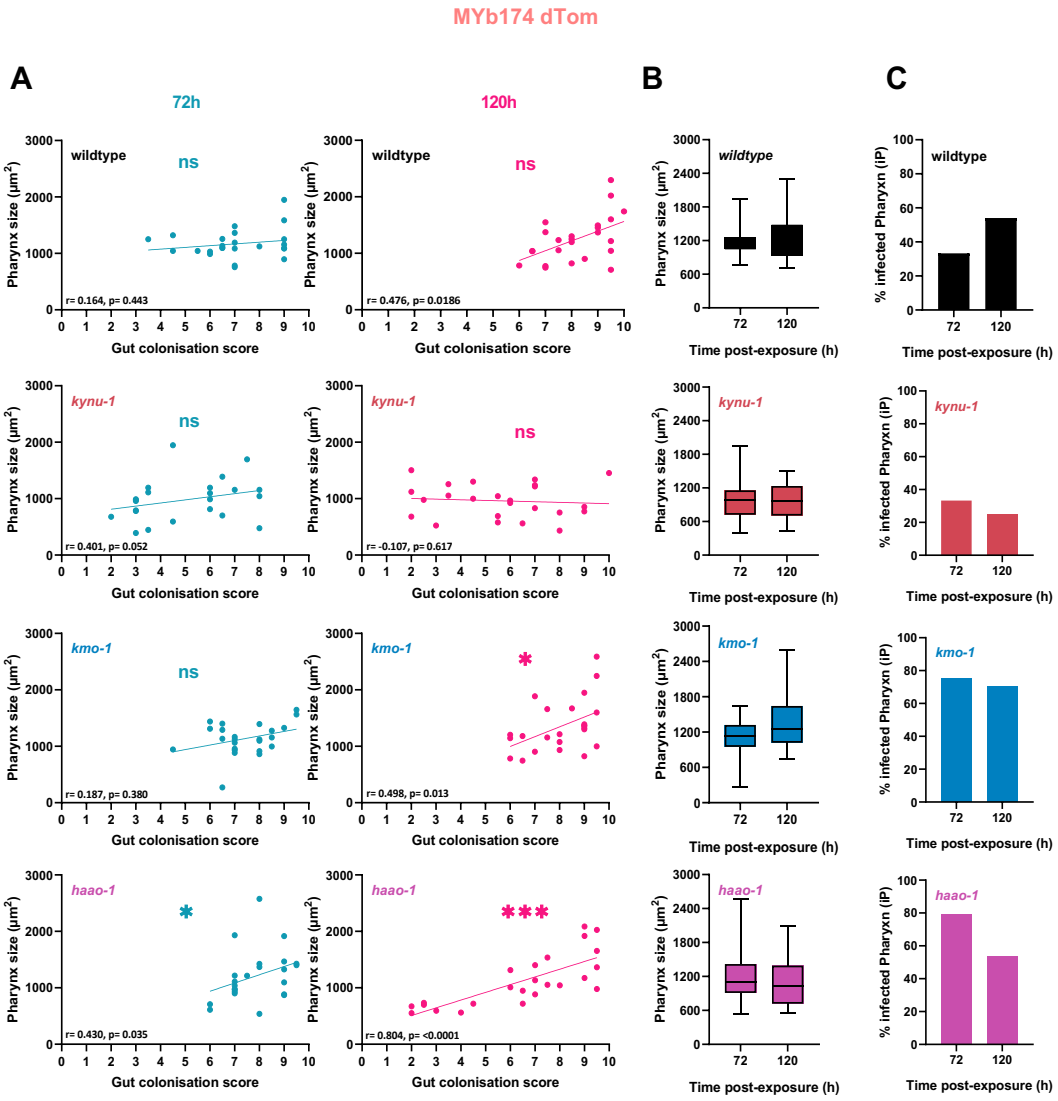

Figure 41. Quantitative analysis of pharyngeal morphology and bacterial colonization in naïve and kynurenine pathway mutant *C. elegans* post exposure to fluorescently tagged isolate of *Enterobacter ludwigii* expressing fluorescent protein dTomato in monoxenic condition. A. Correlative analysis of bacterium colonization scores versus pharyngeal size **B.** Proportional distribution of P/p pharynx morphotypes plotted against pharyngeal size. Base on the extent of bacterial infection and pharyngeal morphology *C. elegans* were labelled P (swollen pharynx with bacterial infection) or p (no bacterial invasion) pharynx. The experiment was carried out on two different weeks (N=2), imaging and measuring 25-50 worms for gut colonisation score and 12 worms per condition were randomly quantified for measuring pharyngeal morphologies. Error bars represent standard error of the mean (SEM). Pearson's linear regression with 95% confidence intervals was plotted to visualize trend. Statistical analysis was performed using nonparametric spearman correlation test to assess the strength and significance of the relationship between pharyngeal size and bacterial colonization scores. Significance levels: * p<0.05, ** p<0.01, *** p<0.001.

Strikingly, I found that at 120h on *Enterobacter ludwigii* (MYb174-dTomato), for all worm genotypes, except for *kynu-1*, pharyngeal size correlates positively with gut colonisation score (Figure 41. A), suggesting a role for gut colonisation in pharyngeal swelling. Interestingly, the only mutant for which no correlation was found between gut colonisation levels and pharyngeal size (*kynu-1*) exhibited smaller pharynges on average (Figure 41. B) and revealed less susceptible to pharyngeal infections (Figure 41. C). Conversely, *haao-1* and *kmo-1* that

showed high levels of gut colonisation and large pharynges also showed high rates of severe pharyngeal infection (Figure 41. C)

This suggests that when exposed to *Enterobacter ludwigii* (MYb174-dTomato) a positive correlation between gut colonisation and pharyngeal size is indicative of susceptibility to pharyngeal infection.

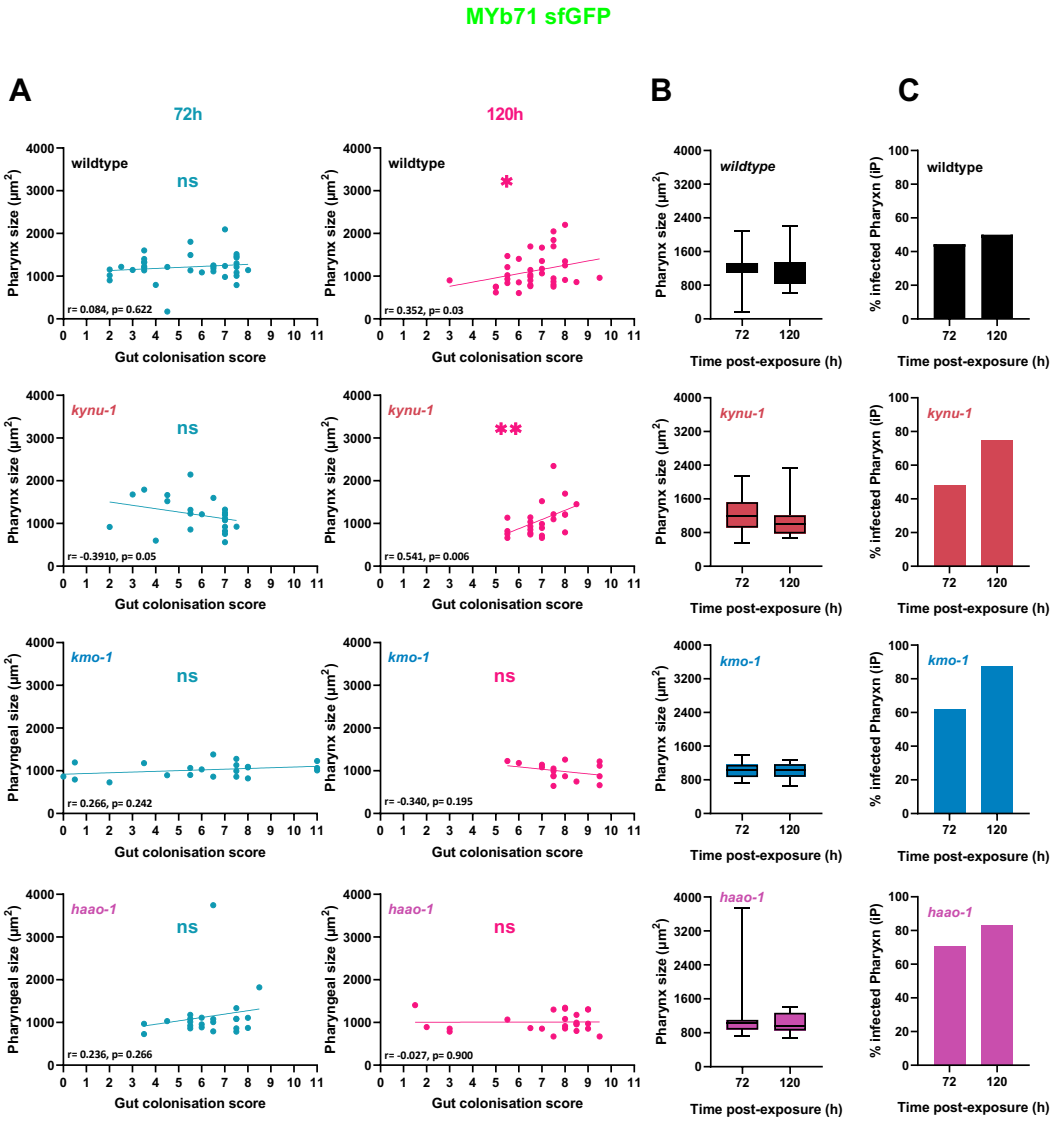

Figure 42. Quantitative analysis of pharyngeal morphology and bacterial colonization in naïve and kynurenine pathway mutant *C. elegans* post exposure to fluorescently tagged isolate of *Ochrobactrum vermis* expressing fluorescent protein sf GFP in monoxenic condition. A. Correlative analysis of bacterium colonization scores versus pharyngeal size **B.** Proportional distribution of P/p pharynx morphotypes plotted against pharyngeal size. Base on the extent of bacterial infection and pharyngeal morphology *C. elegans* were labelled P (swollen pharynx with bacterial infection) or p (no bacterial invasion) pharynx. The experiment was carried out on two different weeks (N=2), imaging and measuring 25-50 worms for gut colonisation score and 12 worms per condition were randomly quantified for measuring pharyngeal morphologies. Error bars represent standard error of the mean (SEM). Pearson's linear regression with 95% confidence intervals was plotted to visualize trend. Statistical analysis was performed using nonparametric spearman correlation test to assess the strength and significance of the relationship between pharyngeal size and bacterial colonization scores. Significance levels: * p<0.05, ** p<0.01, *** p<0.001.

Surprisingly, this does not appear to apply to gut colonisation by *Ochrobactrum vermis* (MYb71 sfGFP), as for *kmo-1* and *haao-1*, the most susceptible strains to pharyngeal infection in this context (Figure 42), no positive correlation was found between gut colonisation score and pharyngeal size, possibly because the differing nature of the pharyngeal infection process leads to smaller infected pharynges. Whereas for *kynu-1* at 120h, there appears to be a significant level of correlation between gut colonisation and pharyngeal size, in case of *Ochrobactrum vermis* sfGFP (MYb71 sfGFP).

5.4.1 *Caenorhabditis elegans* exhibits increase tumor formations in polyxenic conditions compared to monoxenic conditions

Beyond intestinal atrophy and pharyngeal degeneration, another biomarker of ageing in *C. elegans* hermaphrodites is the development of large uterine tumours (Ezcurra, Benedetto et al, 2018). Therefore, I next measured the development of uterine tumors. (Ezcurra et al., 2018)(Wang et al., 2018)

When exposed to fluorescently tagged isolates of CeMbio bacterial strains, wild type and KP mutant *C. elegans* showed progressively increasing development of uterine tumors starting from around 48h, with a gradually increasing size when observed at 120h timepoint.

Interestingly, KP mutants displayed smaller tumours on average than wild type worms, irrespective of the CeMbio+ bacterial exposure (Figure 43), possibly because age-matched adult KP mutants tend to be smaller, and possibly due to tryptophan metabolism issues that may not support optimal uterine tumour growth.

Another interesting observation is that on polyxenic cultures, tumour sizes are generally increased, possibly reflecting the positive impact of a richer gut microbiota on host metabolism.

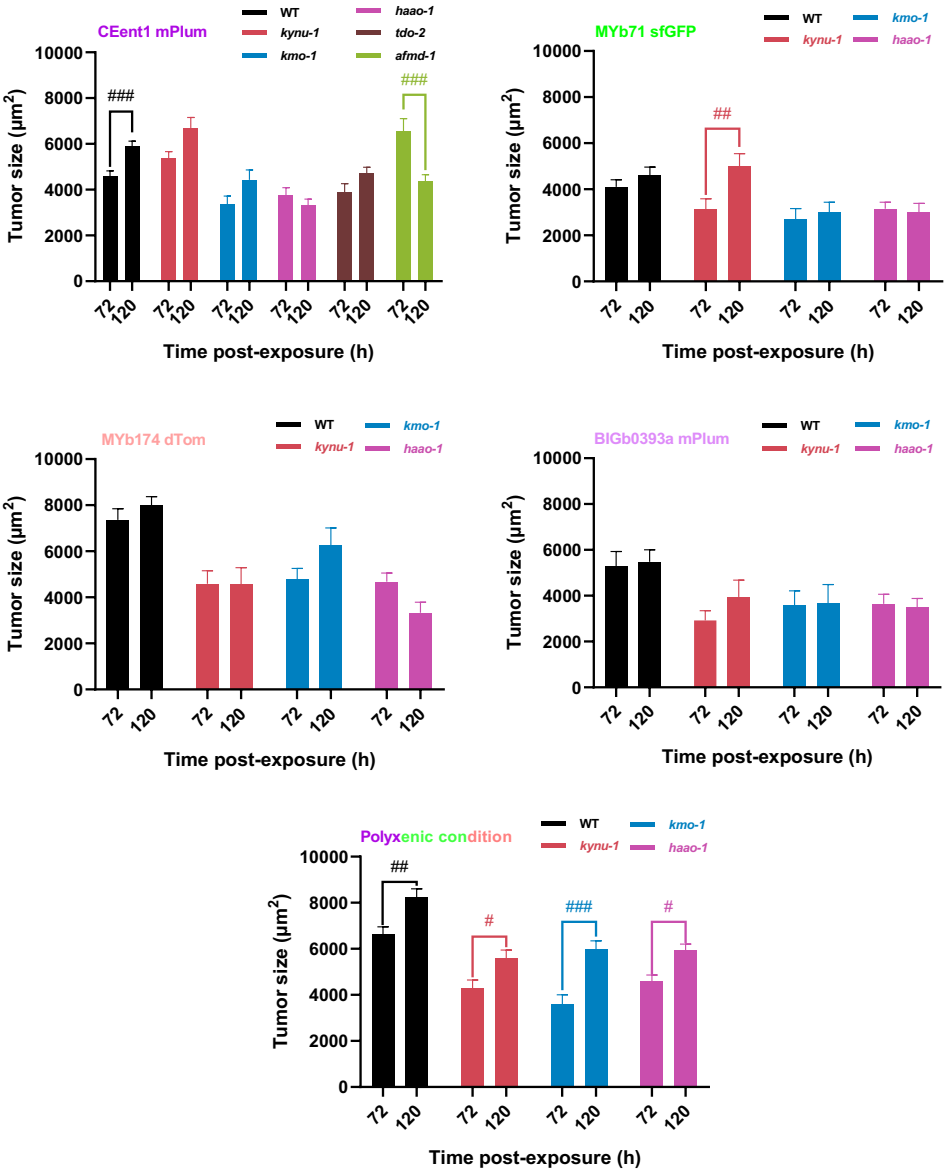

Figure 43. Uterine tumor development in wildtype and kynurenine pathway mutant *C.elegans* strains post-exposure to fluorescently tagged isolates of CeMbio community in monoxenic and polyxenic conditions. Tumor's size was quantified by manual tracing of tumor boundaries to determine cross-sectional area at defined time points. The experiment was carried out on two different weeks (N=2), 12 worms per condition were randomly quantified for measuring tumors. Error bars represent standard error of the mean (SEM). Statistical analysis was performed using 2way ANOVA followed by Bonferroni's multiple comparison test. Hashtags indicate significant differences observed between the 72h and 120h timepoints. #p>0.05, ##p>0.01, ###p>0.001. Polyxenic condition: CEent1 mPlum + MYb71 sfGFP + JUb19 RFP2.

5.5 Dual Transcriptomic Analysis Of *Caenorhabditis elegans* And Associated Bacterial Strains

Dual RNA sequencing (dual-RNAseq) is an advanced technique that allows for the simultaneous profiling of transcriptomes from two interacting organisms, typically a host and a pathogen or symbiont in real-time. This unbiased approach can uncover novel interaction mechanisms, regulatory networks, and previously unknown genes or RNA molecules involved in the interaction. It is particularly valuable in studying infectious diseases, symbiotic relationships, and host-microbe interactions in various biological systems (Westermann, Gorski, & Vogel, 2012).

In this study, we performed dual-RNA sequencing to investigate the transcriptional responses of *C. elegans* on exposure to various gut bacteria including the CeMbio bacterial strains studied in this report (Table 13), in a bid to identify host genes involved in gut bacterial colonisation, such as KP genes.

Following total RNA extraction (4.9.2), RNA quality was checked by electrophoresis, displaying distinct RNA bands with minimal degradation (Figure 44). Samples were subsequently sent for rRNA depletion and dual-RNA sequencing to capture the host and bacterial transcriptional dynamics. Due to time constraints, comprehensive analysis of the sequencing data has not yet been completed, and the results are pending.

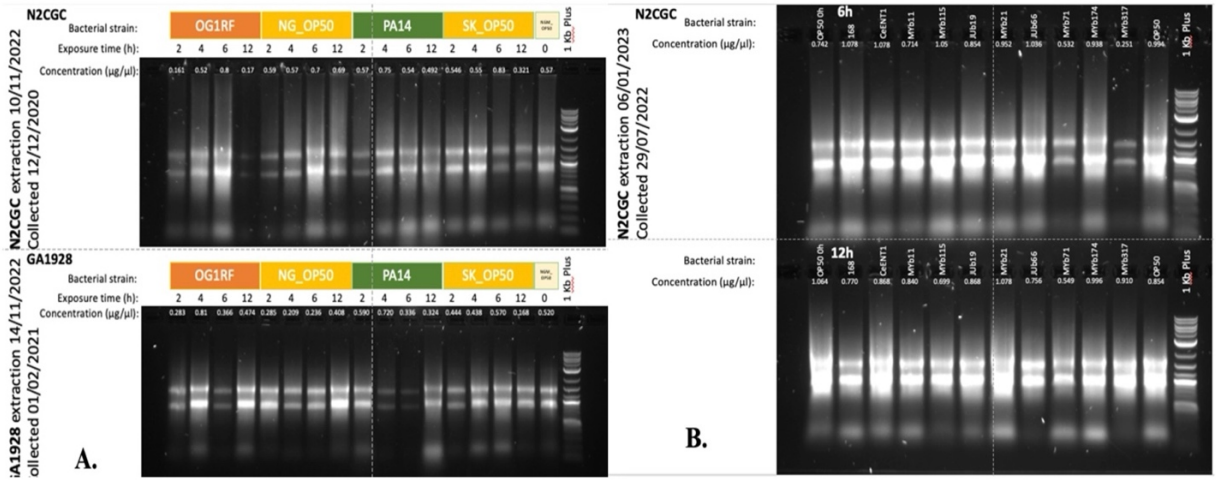

Figure 44. Agarose gel electrophoresis of total RNA extracted from *C. elegans* exposed to different bacterial strains at various time points. A. RNA extraction from N2CGC and GA1928 strains after exposure to *E. faecalis* OG1RF, *E. coli* NG_OP50, *P. aeruginosa* PA14, and E. coli SK_OP50. Samples were collected at 2, 4, 6, and 12 hours post-exposure. **B.** RNA extraction at 6 and 12 hours post-exposure to multiple bacterial strains, showing distinct RNA bands at varying concentrations and highlighting overall high-quality RNA integrity. RNA concentrations (µg/µl) are indicated above each lane. 1Kb plus DNA ladder weight marker is included on the far right.

Table 14. Interesting Bacterial Candidates for dual RNAseq with *Caenorhabditis elegans*

RNA samples collected	Strain Name	CeM bio	Strain Taxonomy	Strain Source (Lab of Origin)	OTU Taxonomy	Reason	Genome assembly	Protein-coding genes	References
Yes	MYb11	Yes	*Pseudomonas lurida*	wild *C. elegans* from compost (Schulenburg)	*Pseudomonadaceae; Pseudomonas*	Persistence in worm gut, protection from infection by *Bacillus thuringiensis* and *Pseudomonas aeruginosa*	PRJNA400855	5500	(Dirksen et al., 2020)(Zimmermann et al., 2019)(Kissoyan et al., 2022)
Yes	MYb115	No	*Pseudomonas fluorescens*	member of the native microbiome of the nematode Caenorhabditis elegans	*Pseudomonadaceae; Pseudomonas*	Persistence in worm gut, protection from infection by *Bacillus thuringiensis* and *Pseudomonas aeruginosa*	PRJNA400855	6000	(Dirksen et al., 2020)(Zimmermann et al., 2019)(Kissoyan et al., 2022)
Yes	MYb71	Yes	*Ochrobactrum vermis*	wild *C. elegans* from compost (Schulenburg)	*Brucellaceae; Ochrobactrum*	Persistence in worm gut, possible immunomodulatory effect predicted from genome sequence	PRJNA400855	-	(Dirksen et al., 2020)(Yang et al., 2019)
Yes	MYb21	No	*Comamonas sp.*	member of the native microbiome of the nematode Caenorhabditis elegans	*Comamonadaceae; Comamonas*	Persistence in worm gut, forms persistent gut infections in C. elegans	Illumina 36 contigs (16S KX079720.1) (Schulenburg)	3200	(Zárate-Potes, Ali, Ribeiro Camacho, Brownless, & Benedetto, 2022)
Yes	168	No	*Bacillus subtilis*	X-ray mutagenised Marburg strain tryptophan auxotroph (Parry)	*Bacillaceae; Bacillus*	Persistence in worm gut, possible protective effect against heat and oxidative stress	PRJNA57675, PRJNA76	4900	(Zeigler, 2011)(Zárate-Potes, Ali, Ribeiro Camacho, Brownless, & Benedetto, 2022)
No	ATCC 6538	No	*Staphylococcus aureus*	initially isolated from a human lesion prior to the introduction of the widespread use of antimicrobials	*Staphylococcaceae; Staphylococcus*	Persistence in worm gut, forms persistent gut infections in C. elegans	PRJNA378149	2800	(Zárate-Potes, Ali, Ribeiro Camacho, Brownless, & Benedetto, 2022)
Yes	CEent1	Yes	*Enterobacter hormaechei*	*C. elegans* N2 from mesocosm (Shapira)	*Enterobacteriaceae*	Persistence in worm gut; fluroscent strain available	PRJEB37895	-	(Dirksen et al., 2020)
Yes	JUb19	Yes	*Stenotrophomonas indicatrix*	rotting pear with wild *C. elegans* (Félix)	*Xanthomonadaceae; Stenotrophomonas*	Persistence in worm gut; fluroscent strain available	PRJEB37895	-	(Dirksen et al., 2020)
Yes	JUb66	Yes	*Lelliottia amnigena*	rotting apple with wild *C. elegans* (Félix)	*Enterobacteriaceae*	Persistence in worm gut; fluroscent strain available	GCF_003752235.1	8400	(Dirksen et al., 2020)
Yes	MYb174	No	*Enterobacter ludwigii*	wild isolate (Schulenburg)	*Enterobacteriaceae*	Persistence in worm gut; fluroscent strain available	Illumina 29 contigs (Schulenburg)	4800	-
Yes	MYb317	No	*Chryseobacterium sp.*	isolated from MY2768 wild isolate (Schulenburg) by J. Johnke	*Bacterioidetes*	Seems to be pathogenic according to previous data from lab	NCBI:txid2745220	-	-
Yes	BIGb170	Yes	*Sphingobacterium multivorum*	Isolated from wild C. elegans from rotting apple (Samuel)	*Sphingobacteriaceae; Sphingobacterium*	Persistence in worm gut; extend healthspan	PRJNA624308	-	(Dirksen et al., 2020)

5.6 *kmo-1* Kynurenine Pathway Mutation Influences Both Bacterial Colonization And Longevity In *Caenorhabditis elegans* On *Ochrobactrum vermis*

Caenorhabditis elegans, wildtype and *kmo-1* KP mutant, were used, to assess lifespan alterations when colonized with isolate of CeMbio community. *Ochrobactrum vermis* (MYb71) was chosen as bug of interest, as this bacterium is known to be abundant within the *C. elegans* microbiome and capable of persistently colonizing the gut even under stressful conditions (Petersen, et al., 2021). Studying the lifespan of *C. elegans* colonized by *O. vermis* allows for the assessment of whether this bacterium has any beneficial or detrimental effects on the host's longevity. This is particularly relevant given the potential involvement of the kynurenine pathway, a metabolic pathway that has been linked to aging and age-related diseases (Sas, et al., 2007).

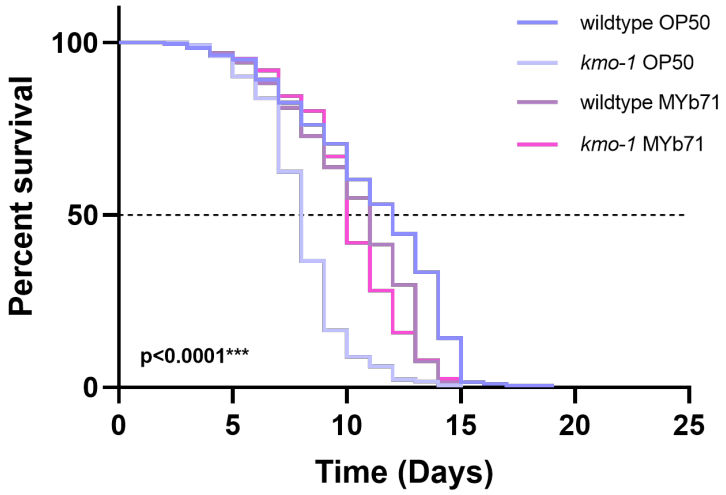

Figure 45. Lifespan of *C. elegans* wildtype and *kmo-1* mutants on *Escherichia coli* and *Ochrobactrum vermis*. Percent survival of naïve control (wild-type) and *kmo-1* (OW478) mutant *C. elegans* strains when grown on lawn of *Ochrobactrum vermis*. Worm strains were age synchronised by egg-lay technique and were transferred onto *E.coli* OP50 and *Ochrobactrum vermis* seeded NGM plates, incubated at 25 °C and counted everyday till last worm survive (see method 4.8.1). Survival curves were compared using the log-rank (Mantel-Cox) test (χ^2 = 216.6, df = 3, $p < 0.0001$). The median survival (in days) for each condition was: WT OP50: 12 days, kmo-1 OP50: 8 days, WT MYb71: 11 days,kmo-1 MYb71: 10 days. The experiment was carried out on two different weeks (N=2), and 120 worms per condition were assayed.

In our study as well, we found that fluorescently tagged isolate of *Ochrobactrum vermis* (MYb71-sfGFP)(Figure 28) showed significantly higher gut colonisation rate in *kmo-1* mutant *C. elegans* compared to wildtype, when in monoxenic condition at 120h. Whereas at the same time with higher gut colonisation score this mutant showed a decrease in pharyngeal size (Figure 39), it became of an interest to investigate the effect of *Ochrobactrum vermis* (MYb71) on lifespan of *kmo-1* mutants.

To determine the lifespan of *C. elegans* N2 wildtype and *kmo-1* mutant on *Ochrobactrum vermis*, worms were exposed to both OP50 *E.coli* (control) and *Ochrobactrum vermis* (4.8.1) and counted every day until the last worm died. The lifespan graph represents percent survival across all four conditions. It can be observed that, wildtype *C. elegans* on OP50 *E.coli* and MYb71 are reported to be living longer compared to *kmo-1* mutant, by a median survival rate of 12 and 11 days respectively. Thus, it can be stated that *kmo-1* mutation can alter the lifespan of *C. elegans* on OP50 *E.coli* as well as *Ochrobactrum* vermis (MYb71) (probably reducing the lifespan). But however, *kmo-1* mutant on *Ochrobactrum* vermis (MYb71) survives longer than *kmo-1* on OP50 *E.coli*. Which, suggests that the mutant with bacterium of interest has a little impact on survival rate compared to when in control.

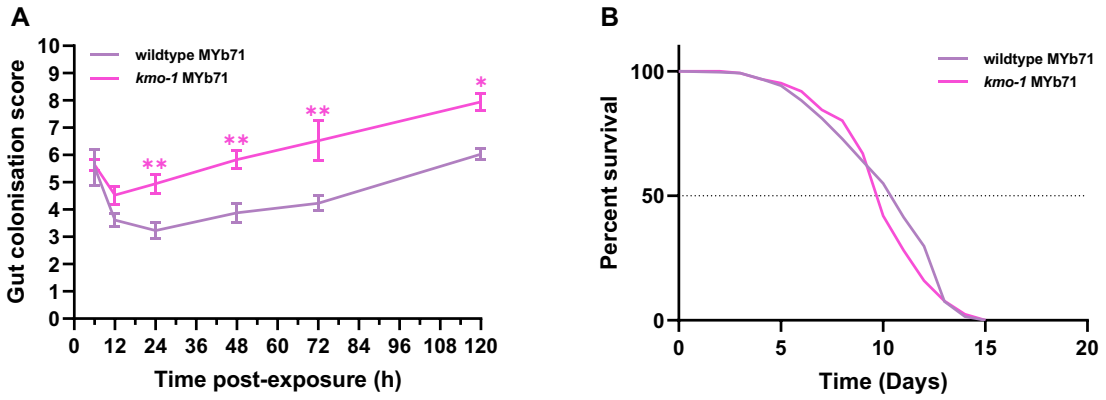

Figure 46. Gut colonisation score vs. Lifespan assay of wildtype and *kmo-1* Kynurenine Pathway mutant *C. elegans* on fluorescently-tagged *Ochrobactrum vermis* mPlum (MYb71-sfGFP) and *Ochrobactrum vermis* (parental strain) respectively. A. Gut colonisation score of monoxenic Ochrobactrum vermis in naïve control (wild-type) and kmo-1 (OW478) mutant C. elegans. Fluorescent images were acquired at 6,12,24,48,72 and 120 hours post-exposure and a visual score of 0-12 was given to quantify the extent of the gut colonisation. The experiment was carried out on two different weeks (N=2), imaging and measuring 25-40 worms per condition. Error bars indicate standard error of the mean. Differences were tested using a 2way ANOVA with Tukey's corrections for multiple comparisons. Asterisks indicate significant differences compared to wild-type control: *p<0.05, **p<0.01, ***p>0.001. **B.** Percent survival of same, naïve control (wild-type) and *kmo-1* (OW478) mutant *C. elegans* strains when grown on lawn of *Ochrobactrum vermis* (see method 4.8.1)**.** The experiment was carried out on two different weeks (N=2), and 120 worms per condition were assayed for lifespan.

The differential gut colonization patterns observed between wildtype and *kmo-1* mutant *C. elegans* when exposed to *Ochrobactrum vermis* sfGFP (MYb71-sfGFP) suggest a mechanistic link between colonization efficiency and host longevity. The reduced colonization rates in wildtype worms correlate with extended lifespan (even though with minor difference of median survival by 1 day apart, needs additional repeats and investigation) when cultured with *Ochrobactrum vermis*, indicating that colonization intensity may be inversely related to

longevity. The enhanced bacterial colonization observed in *kmo-1* mutants appears to influence survival capacity, potentially through altered host-microbe interactions. This observation aligns with previous studies where increased bacterial load in the *C. elegans* intestine has been associated with reduced lifespan (Portal-Celhay, et al., 2012). The kynurenine pathway, disrupted in *kmo-1* mutants, may play a regulatory role in bacterial colonization resistance. Due to time restrictions this experiment could only be performed twice; to establish more definitive conclusions and better understanding of the corelation between bacterial colonisation vs. lifespan, additional replicates and bacterial species would be required.

6 DISCUSSION

The intricate relationship between host organisms and their gut microbiome represents a critical frontier in understanding biological complexity and organismal health. This study explores the complex interactions between *Caenorhabditis elegans* and its commensal bacterial communities, focusing on the Kynurenine Pathway (KP) and its role in host-microbe dynamics. Using fluorescently tagged bacterial strains from the CeMbio community generated in the lab, I gained insights into bacterial colonization patterns, their connection to age-related pathologies, and how the kynurenine pathway modulates host gut microbial interactions *in vivo*.

I first validated our fluorescently-tagged microbial models used to visualise host-gut microbe interactions *in vivo*, by confirming that they are sufficiently similar genetically and phenotypically to their parental strains using Biolog Ecoplate assay. I found that *Stenotrophomonas indicatrix* RFP2 (JUb19-RFP2), *Enterobacter ludwigii* dTomato (MYb174-dTomato), and *Ochrobactrum vermis* sfGFP (MYb71-sfGFP) exhibited metabolic profiles (5.2) closely resembling their parental strains suggesting that the fluorescent versions reliably represent the behaviour of their non-fluorescent counterparts.

Secondly, I validated the gut colonisation experiment by analysing the extent of bacterial proliferation within the *C. elegans* gut using a scoring system (mentioned in Table 10). The comparative analysis of monoxenic and polyxenic bacterial conditions demonstrated that specific kynurenine pathway (KP) mutant *C. elegans*, namely *kmo-1*, *kynu-1*, and *haao-1*, shows unique gut colonization patterns compared to wildtype (N2OW) with fluorescently tagged CeMbio strains i.e. *Enterobacter cloacae* mPlum (CEent1-mPlum), *Ochrobactrum vermis* sfGFP (MYb71-sfGFP), *Pantoea nemavictus* mPlum (BIGb0393a-mPlum), *Enterobacter ludwigii* dTom (MYb174-dTom) and *Stenotrophomonas indicatrix* RFP2 (JUb19-RFP2).

Notably, Enterobacter cloacae-mPlum (CEent1-mPlum), *Ochrobactrum vermis-sfGFP* (MYb71-sfGFP), and *Enterobacter ludwigii-dTom* (MYb174-dTom) were identified as the most efficient colonizers in the wild-type, *kmo-1*, and *kynu-1* mutant strains. In contrast, *Pantoea nemavictus*-mPlum (BIGb0393a-mPlum) and *Stenotrophomonas indicatrix*-RFP2 (JUb19-RFP2) exhibited significantly lower colonization levels across all KP mutant strains. However, an exception was observed in *haao-1* mutants, where gut colonization by *Pantoea nemavictus*

mPlum progressively increased. Additionally, *haao-1* mutants showed a distinct interaction with *Enterobacter ludwigii*-dTom (MYb174-dTom) as the bacteria within the gut was found highly colonised at the 72 and 120-hour time point. These findings highlight the differential impact of KP mutations on the colonization capacity of various bacterial species within the *C. elegans* gut, underscoring the nuanced interactions between host metabolic pathways and microbial colonization.

The quantitative assessment of developing age-associated pathologies further revealed delayed intestinal atrophy under polyxenic conditions, with wild-type worms maintaining ~45% gut width over six days at 25°C, whereas *E. cloacae* (CEent1-mPlum) and *E. ludwigii* (MYb174-dTomato) showed increase tissue-specific deterioration across specific KP mutants. CeMbio strains caused progressive pharyngeal enlargement with age for most strains except *Ochrobactrum vermis* (MYb71-sfGFP), with *E. ludwigii* (MYb174-dTom) linking gut colonization to pharyngeal swelling. Uterine tumors appeared earlier (around 48h) and were generally larger under polyxenic conditions, compared to monoxenic condition where KP mutants exhibited smaller tumors regardless of bacterial strain.

Finally, I processed worm-bacterium samples for dual-RNA sequencing to shed light on the gene expression changes that co-occur in specific gut bacteria and their worm host during the gut colonisation process. Quality-checks were performed, libraries were prepared and samples processed on an Illumina NovaSeq platform, but results of the analysis are still pending.

Building upon previous investigations in the Benedetto lab, my work has now provided clearer evidence for a direct role of the Kynurenine pathway into mediating host-gut bacterial interactions during early ageing. It has also enabled the development of new experimental protocols utilising fluorescent bacteria to study host-microbial dynamics in various context. While doing so, it has opened new avenues of investigation but also highlighted several experimental limitations or challenges that future work will need to address, and which are discussed below.

6.1 Limitations Of The Study

6.1.1 Lack of OP_{50} *Escherichia coli* control data set

A significant limitation of this study is the absence of a paired OP50 control dataset for gut colonization assays and aging pathologies. OP_{50} *E. coli* is the standard bacterial diet in *C. elegans* research, and substantial published data is available for comparison. However, due to time constraints, experiments with OP_{50} were not conducted, limiting the ability to directly contrast findings with existing datasets. This gap prevents robust comparisons and conclusions regarding how CeMbio strains differ from OP_{50} in influencing gut colonization and aging pathologies. Additionally, while N2(CGC) was used as the *C. elegans* control, many studies utilize N2(OW), which could exhibit subtle behavioural or physiological differences. Including OP_{50} controls in future experiments would provide a more comprehensive comparative framework and enhance the interpretability of findings in the context of existing literature.

6.1.2 Limitations of using *Caenorhabditis elegans* as a model for studying anaerobic microbes

C. elegans has an inability to regulate body temperature, as it passively adopts the ambient environmental temperature. This precludes its suitability for studying gut microbes that require the homeostatic temperature conditions found in mammals or thermoregulated invertebrates, such as fish or bees, where gut temperatures range between 25–30°C. The gut lumen of *C. elegans* is speculated to have higher oxygen levels compared to mammalian intestines, where oxygen tension is very low (~1–2% compared to atmospheric 21%). Although facultative anaerobes capable of surviving in both aerobic and anaerobic conditions can be studied, the absence of true anaerobic conditions limits the full exploration of human gut microbiota. This could make *C. elegans* unsuitable for studying strictly anaerobic microbes, which thrive in hypoxic environments.

6.1.3 Bacterial transformation challenges, metabolic differences and optimization strategies

The Tn7 transformation approach encountered significant hurdles, even after number of repeats not a single successful bacterial transformation was obtained (when done by me). These challenges provide critical insights into the complexities of bacterial genetic modification and highlights the need for methodological refinement. To improve the efficiency of bacteria transformation in future experiments, several optimization steps were suggested and referenced (Wiles et al., 2018).

Transformation success varied across CeMbio strains, as the method optimized for *Pseudomonas aeruginosa* proved less effective for others. Strain-specific mating inefficiencies were a major hurdle, with many attempts failing to produce fluorescent clones. Extending mating incubation, modifying conjugation conditions, and prolonging post-mating outgrowth may enhance gentamicin resistance expression and integration efficiency (Wiles et al., 2018).

Partially transformed clones acquiring antibiotic resistance but lacking fluorescent genes were common. Increasing transformation replicates and refining selection protocols could improve success rates (Wiles et al., 2018). Additionally, fluorescence stability was inconsistent, suggesting incomplete chromosomal integration. Isolating multiple colonies, rigorous screening, and alternative genetic integration methods may improve stability (Wiles et al., 2018).

Unexpectedly, helper bacteria and untransformed parental strains were identified instead of intended transformants. This underscores the need for stringent verification via colony morphology comparison, PCR, sequencing, and MALDI-TOF analysis.

To overcome these limitations, future experiments should consider optimizing electroporation parameters, exploring alternative integration techniques, and developing strain-specific modification protocols (Dower et al., 1988). A systematic, adaptable approach tailored to bacterial diversity will improve transformation reliability and advance microbiome research.

6.1.4 Assessing early aging pathologies and the need for lifespan analysis in *Caenorhabditis elegans* exposed to CeMbio+ strains

L4+24-hour-old worms exposed to CeMbio+ strains were assessed for gut colonization level and aging pathologies over the first six days of adulthood at 25°C. While this timeframe captures early age-pathology development, as observed in worms raised on OP50, it does not provide a complete picture of all age-related pathologies or lifespan trajectories. Tracking worms until death would be preferable for a comprehensive understanding of aging pathologies, as it would encompass late-stage declines and provide lifespan data, similar to the approach in (Ezcurra, Benedetto et al. 2018), where late-life senescent pathologies, such as intestinal atrophy, yolk-related damage, and self-digestion, were identified. Future studies could extend experimental timelines and incorporate lifespan tracking to better correlate gut colonization with the full spectrum of age-related pathologies in *C. elegans*.

6.1.5 Limitations of fluorescent microscopy for studying bacterial co-localization in *Caenorhabditis elegans*

The use of fluorescent microscopy to assess bacterial colonization within the *C. elegans* gut was constrained by both the limited number of available fluorophore proteins and the channels required for simultaneous imaging in the current lab setup. In this study, the system could only accommodate three fluorophores at a time (sfGFP/mPlum/dTomato and LRO) along with a brightfield channel, restricting the ability to study the co-localization of multiple bacterial strains. For evaluating all three proteins (for example: sfGFP, mPlum, and dTomato) alongside LRO and brightfield would require at least six channels. This limitation hinders the clear observation and analysis of bacterial interactions within the *C. elegans* gut in a laboratory setting, especially when compared to the more complex gut microbiota environment that worms experience in nature. To improve this, the lab is working towards expanding the list of available fluorophore proteins which could enable more comprehensive studies. However, even with this expansion, current optical systems can reliably distinguish a maximum of 5-8 colors, and further advancements in microscopy may be required to reliably assess more complex co-colonization scenarios.

6.1.6 Need for an automated system for bacterial gut colonization scoring

After exposing the worms and imaging them using fluorescent microscopy, a manual scoring system was adopted to assess bacterial load intensity. In this system, worms for each condition were manually scored by visual observation, which might would have introduced potential variations due to factors like difference in the time required to score one condition versus another over the course of several months, due to the large number of images (250+) processed, screen resolution, lighting conditions, and subjective interpretation. While the current scoring system is functional for the study's purposes, but an automated and unbiased objective approach would improve consistency and accuracy. To address this, the lab is currently developing an automated segmentation and fluorescence analysis pipeline to streamline and standardize an automated gut colonization analysis.

6.1.7 Preconditioning of *Caenorhabditis elegans* with OP_{50} *Escherichia coli*

Preconditioning *C. elegans* with *E. coli* at the L4 stage prior to introducing fluorescent bacteria serves an important experimental purpose. In natural environments, *C. elegans* are exposed to diverse microbial communities rather than monoxenic conditions, which can influence their gut colonization dynamics and host responses. Pre-feeding ensures a consistent baseline, mimicking a microbial priming effect similar to natural conditions where worms encounter a variety of bacteria. This approach allows for controlled colonization studies while maintaining ecological relevance.

A study by (Dirksen et al., 2016) highlights that *C. elegans* in nature interacts with a range of microbial species, emphasizing the ecological relevance of studying gut colonization with multiple bacterial strains under controlled laboratory conditions. Including pre-feeding ensures the worms are not in a naive state, which better reflects real-world microbial exposure.

However, a potential limitation of this preconditioning approach is that it introduces a controlled, yet artificial, microbial community, which may not fully replicate the complexity or diversity of natural environments. Secondly, the presence of *E. coli* may alter the way subsequent bacteria interact with the host, introducing bias in the study of bacterial co-colonization. Furthermore, it can be challenging to account for how the pre-feeding impacts

(and that too be a specific strain of *E. coli* that may may not fully represent the diverse and dynamic microbiota *C. elegans* encounters in nature) the long-term dynamics of bacterial colonization, as the worms may undergo physiological changes due to prior exposure.

An alternate approach could involve the use of a broader range of bacterial strains during the preconditioning step or even the use of natural microbial consortia that more closely replicate the diverse environments *C. elegans* encounters in the wild. This would allow for a more ecologically relevant representation of gut microbiota, though it may require more advanced techniques for managing and analysing microbial communities in the lab.

6.2 Exploiting Metabolic Variability: Host Adaptations To Bacterial Differences

6.2.1 Biolog analysis highlights differential substrate utilization by transformed and parental bacterial strains

The metabolic differences between bacterial strains can significantly influence their colonization dynamics within the host, as evidenced by Biolog EcoPlate data demonstrating varied substrate preferences among different bacterial isolates. These differences imply that bacteria may not colonize the gut of *C. elegans* at the same rate, potentially affecting the overall microbial community structure and its interaction with the host. For instance, the strain *Enterobacter cloacae* mPlum (CEent1-mPlum) exhibited significant variation in metabolic characteristics compared to its parent strain, which could lead to altered effects on the host. Conversely, strains such as *Stenotrophomonas indicatrix* RFP2 (JUb19-RFP2), *Enterobacter ludwigii* dTomato (MYb174-dTomato), and *Ochrobactrum vermis* sfGFP (MYb71-sfGFP) appear to closely reflect the metabolic behaviour of their non-fluorescent counterparts, suggesting that their fluorescent tagging does not significantly alter their functional properties. However, *Lelliottia amnigena* GFP (JUb66-GFP) may differ enough from JUb66 based on EcoPlate results to warrant further investigation, despite lacking statistical significance in this study. Additional replicates could clarify these metabolic distinctions.

A critical limitation in studying these bacterial strains is the common use of transformation techniques involving transposable elements for inserting fluorescent tags into bacterial genomes. This method often results in unpredictable insert locations, which can disrupt

endogenous gene expression (Gebrie, 2023). Such disruptions may alter the metabolic behaviour of the bacteria, similar to how foreign protein expression can impact *C. elegans* physiology. In studies concerning the gut-brain axis, these metabolic differences stemming from transgenesis can complicate interpretations of how tagged strains interact with the host and influence its health (Borre et al., 2014). Therefore, it is crucial to consider that tagged strains may not perfectly replicate the behaviour of their natural isolates.

To improve upon these limitations, generating new integrated strains using more precise genetic engineering techniques could be beneficial. For example, employing CRISPR/Cas9 technology could allow for targeted modifications that minimize unintended phenotypic changes (Song et al., 2016) . This approach could facilitate the development of fluorescent microbes that more closely resemble their parental strains, particularly for CEent1-mPlum and JUb66. Additionally, sequencing the genomic regions surrounding fluorescent tag insertions could provide insights into any affected genes and elucidate potential reasons for observed metabolic differences in EcoPlate tests. By employing these strategies, researchers can enhance our understanding of bacterial metabolism and its implications for host interactions.

6.2.2 Kynurenine Pathway mutations differentially influence bacterial gut colonization dynamics in *Caenorhabditis elegans* under monoxenic condition

The Kynurenine Pathway generates several metabolites, including Kynurenine, 3-Hydroxykynurenine (3 HK), and 3-Hydroxyanthranilic acid (3 HAA), each of which plays a role in regulating various physiological processes (Savitz, 2019). Studies on *C. elegans*, a model organism, have shown that mutations in KP genes (e.g., *kmo-1*, *kynu-1*, and *haao-1*) can significantly affect bacterial colonization in the gut and impact the worm's health and longevity (Dang et al., 2023).

In our study, mutations in the Kynurenine Pathway (KP) genes, particularly *kmo-1* and *haao-1*, significantly influenced bacterial gut colonization dynamics in *C. elegans* under monoxenic conditions. The *kmo-1* mutants exhibited higher colonization rates for *Enterobacter ludwigii* dTomato (MYb174-dTomato) *Ochrobactrum vermis* sfGFP (MYb71-sfGFP) and *Enterobacter cloacae* mPlum (CEent1-mPlum), correlating with the accumulation of kynurenine. This

suggests that elevated kynurenine levels may enhance microbial persistence or alter host gut integrity, facilitating colonization.

Interestingly, *Pantoea nemavictus* mPlum (BIGb0393a-mPlum) and *Stenotrophomonas indicatrix* RFP2 (JUb19-RFP2), seems to be amongst the lower colonisers with least gut colonizing levels among most of the KP mutant strains, indicating a potential role of kynurenine in controlling the growth of specific bacterial species.

The *haao-1* mutants, which accumulate 3-Hydroxyanthranilic acid (3-HAA), displayed increased colonization levels again for *Ochrobactrum vermis* sfGFP (MYb71-sfGFP) and *Enterobacter cloacae* mPlum (CEent1-mPlum). Conversely, they appeared to inhibit the colonization of certain microbes, such as *Enterobacter ludwigii* dTomato (MYb174-dTom), particularly at later time points (72-120h). This duality underscores the complex role of KP metabolites in modulating host-microbe interactions. Notably, 3-HAA has been shown to be a powerful ROS scavenger due to its aromatic hydroxyl group (Zhuravlev, et al., 2016a). While its antioxidant and context-dependent pro-oxidant properties may influence host–microbe interactions, direct antibacterial effects of 3-HAA appear limited.

The *kynu-1* mutants, which accumulate 3-Hydroxykynurenine (3-HK) presented a distinct and highly fluctuating colonization pattern across all bacterial strains. In cases involving *Ochrobactrum vermis* sfGFP (MYb71-sfGFP), *Pantoea nemavictus* mPlum (BIGb0393a-mPlum), *Enterobacter ludwigii* dTom (MYb174-dTom) and *Stenotrophomonas indicatrix* RFP2 (JUb19-RFP2), *kynu-1* mutants exhibited lower colonization levels compared to *Enterobacter cloacae* mPlum (CEent1-mPlum). This suggests that the accumulation of 3-Hydroxykynurenine (3-HK) may possess bacteria inhibiting properties or that *kynu-1* plays a specific role in regulating bacterial colonization.

These findings align with previous research highlighting the role of KP metabolites in modulating host-microbe interactions. For instance, 3-HK has been shown to enhance host survival during bacterial infections by restricting bacterial expansion in macrophages, despite lacking direct antibacterial activity. (Parada-Kusz et al., 2023) Additionally, the KP has been implicated in various disorders associated with impaired mitochondrial function, suggesting a broader impact on host physiology (Zhuravlev, Z et al.a, 2016b).

In conclusion, our study demonstrates that KP mutations in *C. elegans* differentially influence bacterial gut colonization dynamics under monoxenic conditions. The accumulation of specific KP metabolites, such as kynurenine, 3-HK, and 3-HAA, plays a role in modulating these interactions. These findings do not imply a uniform or systematic effect across all conditions, suggesting that other factors might be interfering these interactions. Future research should explore the mechanistic underpinnings of these interactions to better understand the complex interplay between host metabolic pathways and microbial colonization.

6.2.3 Differences in impact when microbes are in cocktail vs. monoxenic conditions

The colonization dynamics in monoxenic versus polyxenic (cocktail) conditions revealed important microbial interactions and ecological trade-offs. In monoxenic conditions, individual bacterial strains such as *Enterobacter cloacae* mPlum (CEent1-mPlum) achieved higher colonization rates, particularly in KP mutants like *kmo-1* and *haao-1*, which may provide less resistance to bacterial persistence. The absence of competition in single-strain environment, might allow microbes to maximize resource utilization and host colonization potential.

In contrast, under polyxenic conditions, bacterial colonization was reduced overall, reflecting inter-microbial competition for resources and niches within the gut. For example, *Enterobacter cloacae* mPlum (CEent1-mPlum) consistently emerged as the dominant strain during initial time points, but its colonization was tempered by competition with *Ochrobactrum vermis* sfGFP (MYb71-sfGFP) and *Stenotrophomonas indicatrix* RFP2 (JUb19-RFP2). This behavioural preference was also observed during manual microscopy, where worms tended to migrate towards the *Enterobacter cloacae* mPlum (CEent1-mPlum*)* lawn first, with *Stenotrophomonas indicatrix* RFP2 (JUb19-RFP2) being the second choice of bacteria to feed upon. These findings are consistent with reports that *C. elegans* can exhibit altered preferences toward specific microbiota members after preconditioning, as shown in studies with *O. vermis MYb71* (Petersen, et al., 2021). Interestingly, JUb19-RFP2 displayed a delayed but significant increase in colonization at 120 hours, suggesting its competitive resilience in the gut microbiota community. Such competitive dynamics align with ecological theories like the competitive exclusion principle, where co-existing microbes limit each other's proliferation (Eldridge et al., 2017).

The differences in colonization between monoxenic and cocktail conditions highlight the importance of microbial interactions in shaping host-microbe relationships. Notably, *kmo-1* and *haao-1* mutants exhibited controlled colonization of *Ochrobactrum vermis* sfGFP (MYb71-sfGFP) in cocktail conditions, suggesting a role for kynurenine and 3-HAA in regulating microbial competition and proliferation. This observation emphasizes that microbial community complexity—and not just single-strain effects—plays a critical role in influencing host physiology.

Age-related vulnerability of pharyngeal tissues, combined with this bacterial stress and constant defensive activity, may accelerate muscle deterioration and reduce repair capacity (Chow, et al., 2008) which explains the pharyngeal deterioration. Interestingly, while polyxenic conditions exhibited a more diverse microbiota, they resulted in less intestinal atrophy, increased pharyngeal size and larger tumour formations compared to monoxenic conditions. This suggests that certain microbial communities may play a protective role in maintaining gut integrity despite the increased complexity.

In conclusion, worms exposed to microbial cocktails are more susceptible to pronounced ageing phenotypes, including tumor formation and intestinal deterioration, compared to those exposed to single bacterial strains. These findings underscore the importance of microbial diversity in modulating host ageing trajectories. While single strains can elicit specific host responses, the combined effects of bacterial cocktails appear to amplify these responses, leading to more severe ageing pathologies.

6.2.4 What is a beneficial microbe after all?

Beneficial microbes play a crucial role in maintaining host health, offering a diverse range of functions such as enhancing immune responses, promoting gut integrity, and defending against pathogenic infections. Recent studies have focused on the interaction between host metabolic pathways and the gut microbiota, particularly how metabolites influence microbial behaviour and health outcomes. The Kynurenine Pathway (KP), a primary route for tryptophan metabolism, has been implicated in lifespan extension, health span enhancement, and microbiome regulation.

In the context of *C. elegans*, certain bacterial strains from the CeMbio+ community exhibit clear beneficial effects on host physiology. For example, *Enterobacter cloacae* mPlum

(CEent1-mPlum) demonstrated robust gut colonization across multiple time points, indicating its ability to persist in the host environment. Interestingly, in polyxenic condition (*Enterobacter cloacae* mPlum, *Ochrobactrum vermis* sfGFP and *Stenotrophomonas indicatrix* RFP2) displayed reduced intestinal atrophy , while strains such as *Ochrobactrum vermis* sfGFP (MYb71-sfGFP) and *Pantoea nemavictus* mPlum (BIGb0393a-mPlum) were associated with smaller tumor sizes compared to other bacterial strains. This suggests that specific microbial communities can confer protective effects against age-related pathologies in *C. elegans*, potentially through mechanisms involving KP metabolites. Further research and studies involving measuring aging pathologies and lifespan assay on these bacteria may provide role of specific bacterial species as a probiotic.

6.2.5 Can *Caenorhabditis elegans* be used to study gut microbes in other animals?

The findings from this study reinforce the utility of *C. elegans* as a model for gut microbe-host interactions relevant to other animals. Although *C. elegans* lacks an adaptive immune system, its simplified gut microbiome and transparent body enable direct observation of microbial colonization and associated host responses. The absence of an endogenous microbiota allows for precise control over microbial colonization under monoxenic or polyxenic conditions, which is particularly useful for dissecting the individual and combinatorial effects of bacterial strains on host physiology, including aging, stress resistance, and pathology development (e.g., tumors and intestinal atrophy as seen in our results). Such mechanistic insights are often difficult to obtain in more complex systems.

Similarities between *C. elegans* and other animals, such as bees and fish, include the role of microbial metabolites (e.g., KP intermediates like 3-HAA) in modulating gut integrity and resistance to colonization. Moving forward, *C. elegans* should be used to investigate specific aspects of gut microbial dynamics—such as host genetic factors, bacterial colonization patterns, and microbe-induced aging phenotypes—that are broadly applicable to other systems. For studies requiring more physiological relevance to mammals or thermoregulated invertebrates, alternative models like zebrafish or rodents may be more appropriate.

6.2.6 Microbes of interest for further study

The CeMbio+ strains identified in this study present promising candidates for further investigation. *Enterobacter cloacae* (CEent1-mPlum) demonstrated consistent colonization across various host mutants and conditions, making it a robust model for understanding host-microbe dynamics. Similarly, *Ochrobactrum vermis* (MYb71-sfGFP) and *Stenotrophomonas indicatrix* (JUb19-RFP2) showed competitive resilience in cocktail conditions, suggesting their adaptability within complex microbiota environments.

These strains also displayed differential colonization across KP mutants, highlighting their potential for studying microbial metabolite interactions with host metabolic pathways. Future studies could explore the role of specific metabolites (e.g., kynurenine, 3-HAA) in modulating host health, stress resistance, and longevity. Advanced omics techniques such as metabolomics and transcriptomics would provide deeper insights into the molecular mechanisms underlying these interactions.

In conclusion, the findings from this study underscore the importance of understanding how specific bacterial strains can influence host health through probiotic mechanisms within the framework of kynurenine pathway-driven gut colonization dynamics.

6.3 Trade-Offs Between Reproductive Output And Health/Stress Resistance Or Longevity/Ageing Rate: Implications For Research On Ageing

From an evolutionary perspective, the trade-offs between reproductive output, stress resistance, and longevity are complex. Metabolites like 3-Hydroxyanthranilic acid (3-HAA) and 3-Hydroxykynurenine (3-HK) may enhance stress resistance and potentially extend lifespan, but these benefits could reduce reproductive output or energy allocation. In *C. elegans*, microbial colonization interacts with host health, revealing clear trade-offs. Kynurenine pathway (KP) mutants, such as *kmo-1* and *kynu-1*, show distinct gut colonization patterns, where increased bacterial load correlates with intestinal atrophy, demonstrating antagonistic pleiotropy—traits that are advantageous early in life may accelerate aging later (Park & Wang, 2018)

For example, in *kmo-1* mutants exposed to *Ochrobactrum vermis* (MYb71), greater gut colonization leads to significant gut lumen widening, a marker of intestinal atrophy, mirroring

the progressive deterioration of gut epithelial integrity seen in aging *C. elegans*. Chronic microbial colonization accelerates aging-related gut pathologies and systemic tissue decline. These findings suggest the need for tight regulation of microbial colonization to balance the benefits of stress resistance and nutrient provisioning against potential aging effects (Caballero-Flores, et al., 2022).

The microbiota plays a crucial role in modulating stress resistance and aging in *C. elegans*, with controlled microbiota contributing to healthier aging (Kumar et al., 2019). However, imbalances—especially in KP mutants—disrupt these dynamics, leading to premature aging pathologies. Such interactions underscore the evolutionary cost of host-microbe associations, where early-life benefits may predispose the host to accelerated aging. Understanding how gut microbiota dynamics influence aging and associated pathologies could provide new insights into aging progression, potentially identifying specific bacterial strains or metabolites that modulate healthspan and longevity.

6.4 Lifespan Assay: Impact Of Bacterial Colonization And Ageing Pathologies

The lifespan assay (5.6) demonstrates a significant relationship between bacterial colonization patterns and host longevity in *C. elegans*, providing further insights into microbial influences on ageing.

Interestingly, worms exposed to *Ochrobactrum vermis* (MYb71-sfGFP) showed comparatively improved longevity, suggesting a potential strain-specific effect where this bacterial colonization may induce beneficial host responses, such as improved stress resistance or reduced tissue damage. These findings indicate that microbial strains can differentially influence lifespan, likely through their metabolic activity and their ability to colonize the intestinal lumen.

In mutants such as *kmo-1*, the lifespan assay revealed further lifespan reduction, indicating a heightened sensitivity to bacterial colonization in worms with compromised kynurenine pathway function. This finding aligns with earlier observations that *kmo-1* mutants experience severe intestinal atrophy and tissue degeneration under bacterial exposure, particularly at high colonization levels. Such results suggest that disrupted host-microbe homeostasis, exacerbated by genetic mutations, accelerates ageing processes.

The accumulation of bacterial metabolites, including those associated with the kynurenine pathway (e.g., 3-HAA, 3-HK), may also contribute to the observed reduction in lifespan. While these metabolites can confer short-term benefits, such as antibacterial properties, their over-accumulation might drive long-term tissue damage and ageing-related decline

This study provides important insights into the role of bacterial colonization in regulating host longevity. The lifespan assay emphasizes how specific bacterial strains—through their persistence, metabolic products, and ability to colonize the gut—can modulate ageing pathologies, such as intestinal deterioration and reproductive tissue tumors. It also demonstrates the role of host factors, such as the kynurenine pathway, in mediating susceptibility to microbial colonization and subsequent lifespan reduction.

7 CONCLUSION

Despite its limitations, this study establishes a solid foundation for exploring the CeMbio+ bacterial collection to better understand gut microbiota-host interactions. The findings underscore the importance of maintaining a balanced microbiota for overall host health and highlight the potential of microbial modulation to address ageing-related pathologies, such as intestinal atrophy, pharyngeal damages and uterine tumor development. Beneficial bacterial strains identified through this study may extend lifespan, enhance stress resistance, and mitigate age-related disorders, offering clues for probiotic therapies aimed at promoting gut health.

Experiments with Biolog plates, which could have provided critical metabolic insights into bacterial nutrient utilization and host-microbe interactions, could not be fully analysed within the available time frame. These assays would allow for a deeper understanding of bacterial metabolism and its effects on *C. elegans* health and ageing. Similarly, Dual-RNA sequencing experiments, aimed at analysing the host and microbial transcriptomes simultaneously, were initiated but remain incomplete due to time limitations. The results from this experiment are anticipated to reveal important insights into how bacterial colonization influences host gene expression and metabolic pathways, particularly those linked to ageing, stress resistance, and gut pathologies. The completion and analysis of these experiments would provide a systems-level understanding of host-microbe interactions and allow for identifying critical microbial genes that modulate host physiology. This data would also highlight host responses to specific bacterial strains, thus offering promising directions for future research.

Due to time constraints/ limited availability of fluorescently tagged CeMbio+ bacterial strains several experiments, such as lifespan assays and bacterial colonization studies with all CeMbio+ strains, were only conducted once or twice. For robust statistical conclusions, biological replicates (at least in triplicates) are essential to ensure the reproducibility and reliability of results. Without sufficient replication, certain trends and observations remain preliminary and require further validation.

7.1 Future Direction

Future research on *C. elegans* gut microbiota can be greatly advanced with a combination of cutting-edge techniques and alternative models. Dual-RNA sequencing will provide deeper insights into host-microbe interactions by profiling both microbial and host gene expression, while Biolog plate assays will reveal microbial metabolic activity, helping us understand how microbes influence aging and stress resistance. Germ-free and gnotobiotic *C. elegans* models will also be invaluable for studying the effects of specific microbial communities on host aging and health, allowing for more precise investigations of microbial contributions to gut health.

Live imaging, including time-lapse fluorescence microscopy, will enable real-time observation of microbial dynamics within the gut and their relationship to aging phenotypes such as intestinal atrophy. The development of fluorescent probes to track bacterial activity and metabolite production could further enhance this approach. Additionally, CRISPR/Cas9 gene editing in *C. elegans* will help identify host genes that regulate microbial colonization and aging, offering insight into the genetic basis of host-microbe interactions.

Metabolomics, combined with isotope labelling, will allow researchers to track metabolic exchanges between the host and microbiota, identifying key microbial metabolites that influence host longevity and stress resistance. Microbiome profiling using next-generation sequencing will help track microbial diversity over the lifespan of *C. elegans*, identifying shifts that correlate with aging. Models like zebrafish or mice, which more closely mimic mammalian gut conditions, can provide a more physiologically relevant context for studying these interactions.

Finally, artificial intelligence and machine learning can help analyse large-scale microbiome data, uncovering novel microbial-host interactions and potential therapeutic targets. Ultimately, these studies can bridge the gap between basic microbial research and translational applications, advancing therapeutic strategies to maintain gut homeostasis and combat ageing-related disorders in humans.

8 REFERENCES

1. Abou-Dahech, M. S., & Williams, F. E. (2024). Aging, age-related diseases, and the zebrafish model. *Journal of Dementia and Alzheimer's Disease, 1*(1), 48. doi:10.3390/jdad1010004
2. Azmitia, E. C. (2020). Chapter 1 - Evolution of serotonin: sunlight to suicide. *Handbook of Behavioral Neuroscience, 31*, 3–22. 10.1016/B978-0-444-64125-0.00001-3
3. Backes, C., Martinez-Martinez, D., & Cabreiro, F. (2021). C. elegans: A biosensor for host–microbe interactions. *Lab Animal, 50*(5), 127. doi:10.1038/s41684-021-00724-z
4. Biragyn, A., & Ferrucci, L.Gut dysbiosis: A potential link between increased cancer risk in ageing and inflammaging.
5. Borre, Y. E., O'keeffe, G. W., Clarke, G., Stanton, C., Dinan, T. G., & Cryan, J. F. (2014). Microbiota and neurodevelopmental windows: Implications for brain disorders. *Trends in Molecular Medicine, 20*(9), 509. doi:10.1016/j.molmed.2014.05.002
6. Brenner, S.*The genetics of caenorhabdztzs elegans*
7. Browning, D. F., Wells, T. J., França, F. L. S., Morris, F. C., Sevastsyanovich, Y. R., Bryant, J. A., . . . Henderson, I. R. (2013). Laboratory adapted escherichia coliK-12 becomes a pathogen of caenorhabditis elegans upon restoration of O antigen biosynthesis. *Molecular Microbiology, 87*(5), 939. doi:10.1111/mmi.12144
8. Buffenstein, R., Edrey, Y.H., Larsen, P.L. (2008). Animal Models in Aging Research. In: Conn, P.M. (eds) Sourcebook of Models for Biomedical Research. Humana Press. https://doi.org/10.1007/978-1-59745-285-4_52
9. Byerly, L., Cassada, R. C., & Russell, R. L.The life cycle of the nematode caenorhabditis elegans I. wild-type growth and reproduction.
10. Caballero-Flores, G., Pickard, J. M., & Núñez, G. (2022). Microbiota-mediated colonization resistance: Mechanisms and regulation. *Nature Reviews Microbiology, 21*(6), 347. doi:10.1038/s41579-022-00833-7
11. Cabreiro, F., & Gems, D. (2013). Worms need microbes too: Microbiota, health and aging in caenorhabditis elegans. *EMBO Molecular Medicine, 5*(9), 1300. doi:10.1002/emmm.201100972

12. Cani, P. D., & Delzenne, N. M.The role of the gut microbiota in energy metabolism and metabolic disease.
13. Cervenka, I., Agudelo, L. Z., & Ruas, J. L. (2017). Kynurenines: Tryptophan's metabolites in exercise, inflammation, and mental health. *Science (New York, N.Y.), 357*(6349), eaaf9794. https://doi.org/10.1126/science.aaf9794.
14. Cho, J., & Park, Y. (2024). Development of aging research in caenorhabditis elegans: From molecular insights to therapeutic application for healthy aging. *Current Research in Food Science, 9* doi:10.1016/j.crfs.2024.100809
15. Chow, D. K., Glenn, C. F., Johnston, J. L., Goldberg, I. G., & Wolkow, C. A. (2008). Sarcopenia in the caenorhabditis elegans pharynx correlates with muscle contraction rate over lifespan. *Experimental Gerontology, 41*(3), 252. doi:10.1016/j.exger.2005.12.004
16. Clark, L. C., & Hodgkin, J. (2016). Caenorhabditis microbiota: Worm guts get populated. *BMC Biology, 14*(1) doi:10.1186/s12915-016-0260-7
17. Clark, R. I., & Walker, D. W. (2017). Role of gut microbiota in aging-related health decline: Insights from invertebrate models. *Cellular and Molecular Life Sciences, 75*(1), 93. doi:10.1007/s00018-017-2671-1
18. Clayton, T. A., Baker, D., Lindon, J. C., Everett, J. R., & Nicholson, J. K. (2008). Pharmacometabonomic identification of a significant host-microbiome metabolic interaction affecting human drug metabolism.
19. Coburn, C., Allman, E., Mahanti, P., Benedetto, A., Cabreiro, F., Pincus, Z., . . . Gems, D. (2013). Anthranilate fluorescence marks a calcium-propagated necrotic wave that promotes organismal death in C. elegans. *PLoS Biology, 11*(7) doi:10.1371/journal.pbio.1001613
20. Coburn, C., & Gems, D. (2013). The mysterious case of the C. elegans gut granule: Death fluorescence, anthranilic acid and the kynurenine pathway. *Frontiers in Genetics, 4* doi:10.3389/fgene.2013.00151
21. Cohen, A. A. (2017). Aging across the tree of life: The importance of a comparative perspective for the use of animal models in aging. *Biochimica Et Biophysica Acta (BBA) - Molecular Basis of Disease, 1864*(9), 2680. doi:10.1016/j.bbadis.2017.05.028

22. Collins, J. J., Huang, C., Hughes, S., & Kornfeld, K. (2007). *WormBook* WormBook. doi:10.1895/wormbook.1.137.1
23. Conlon, M. A., & Bird, A. R. (2014). The impact of diet and lifestyle on gut microbiota and human health. *Nutrients, 7*(1), 17. doi:10.3390/nu7010017
24. Dang, H., Castro-Portuguez, R., Espejo, L., Backer, G., Freitas, S., Spence, E., . . . Sutphin, G. L. (2023). On the benefits of the tryptophan metabolite 3-hydroxyanthranilic acid in caenorhabditis elegans and mouse aging. *Nature Communications, 14*(1) doi:10.1038/s41467-023-43527-1
25. Dejong, E. N., Surette, M. G., & Bowdish, D. M. E. (2020). The gut microbiota and unhealthy aging: Disentangling cause from consequence. *Cell Host &Amp; Microbe, 28*(2), 180. doi:10.1016/j.chom.2020.07.013
26. Dirksen, P., Assié, A., Zimmermann, J., Zhang, F., Tietje, A., Marsh, S. A., . . . Samuel, B. S. (2020). CeMbio - TheCaenorhabditis elegansMicrobiome resource. *G3 Genes|Genomes|Genetics, 10*(9), 3025. doi:10.1534/g3.120.401309
27. Dirksen, P., Marsh, S. A., Braker, I., Heitland, N., Wagner, S., Nakad, R., . . . Schulenburg, H. (2016). The native microbiome of the nematode caenorhabditis elegans: Gateway to a new host-microbiome model. *BMC Biology, 14*(1) doi:10.1186/s12915-016-0258-1
28. Donato, V., Ayala, F. R., Cogliati, S., Bauman, C., Costa, J. G., Leñini, C., & Grau, R. (2017). Bacillus subtilis biofilm extends caenorhabditis elegans longevity through downregulation of the insulin-like signalling pathway. *Nature Communications, 8*(1) doi:10.1038/ncomms14332
29. Dower, W. J., Miller, J. F., & Ragsdale, C. W. (1988). High efficiency transformation of E. coli by high voltage electroporation. *Nucleic acids research*, *16*(13), 6127–6145. https://doi.org/10.1093/nar/16.13.6127
30. Eldridge, D. J., Delgado-baquerizo, M., Travers, S. K., Val, J., Oliver, I., Hamonts, K., & Singh, B. K. (2017). Competition drives the response of soil microbial diversity to increased grazing by vertebrate herbivores. *Ecology, 98*(7), 1922. doi:10.1002/ecy.1879
31. Elvers, K. T., Wilson, V. J., Hammond, A., Duncan, L., Huntley, A. L., Hay, A. D., & van der Werf, E. T. (2020). Antibiotic-induced changes in the human gut microbiota for the

most commonly prescribed antibiotics in primary care in the UK: a systematic review. *BMJ open*, *10*(9), e035677. https://doi.org/10.1136/bmjopen-2019-035677

32. Espejo, L. S., Denicola, D., Chang, L. M., Hofschneider, V., Haskins, A. E., Balsa, J., . . . Sutphin, G. L. (2024). The emerging role of 3-hydroxyanthranilic acid onC. elegansAging immune function. doi:10.1101/2024.01.07.574394
33. Ezcurra, M., Benedetto, A., Sornda, T., Gilliat, A. F., Au, C., Zhang, Q., . . . Gems, D. (2018). C. elegans eats its own intestine to make yolk leading to multiple senescent pathologies. *Current Biology, 28*(20), 3352. doi:10.1016/j.cub.2018.10.003
34. Fay, D. (2005). Genetic mapping and manipulation: Chapter 1-introduction and basics. *WormBook,* doi:10.1895/wormbook.1.90.1
35. Fries, J. F. (2015). Aging, natural death, and the compression of morbidity. *New England Journal of Medicine, 303*(3), 130. doi:10.1056/nejm198007173030304
36. Franceschi, C., Garagnani, P., Parini, P., Giuliani, C., & Santoro, A. (2018). Inflammaging: a new immune-metabolic viewpoint for age-related diseases. Nature reviews. Endocrinology, 14(10), 576–590. https://doi.org/10.1038/s41574-018-0059-4
37. Gao, J., Xu, K., Liu, H., Liu, G., Bai, M., Peng, C., . . . Yin, Y. (2018). *Impact of the gut microbiota on intestinal immunity mediated by tryptophan metabolism* Frontiers Media SA. doi:10.3389/fcimb.2018.00013
38. Garigan, D., Hsu, A., Fraser, A. G., Kamath, R. S., Ahringer, J., & Kenyon, C.Genetic analysis of tissue aging in caenorhabditis elegans: A role for heat-shock factor and bacterial proliferation.
39. Gebrie, A. (2023). Transposable elements as essential elements in the control of gene expression. *Mobile DNA, 14*(1) doi:10.1186/s13100-023-00297-3
40. Genome, M., & Consortium, S.Initial sequencing and comparative analysis of the mouse genome.
41. Gordon, A. L., Witham, M. D., Henderson, E. J., Harwood, R. H., & Masud, T. (2021). Research into ageing and frailty. *Future Healthcare Journal, 8*(2), e237. doi:10.7861/fhj.2021-0088
42. Guo, J., Huang, X., Dou, L., Yan, M., Shen, T., Tang, W., & Li, J. (2022). Aging and aging-related diseases: From molecular mechanisms to interventions and treatments. *Signal Transduction and Targeted Therapy, 7*(1) doi:10.1038/s41392-022-01251-0

43. *Gut microbiota and ageing + 1.4*
44. Han, B., Sivaramakrishnan, P., Lin, C. J., Neve, I. A. A., He, J., Tay, L. W. R., . . . Wang, M. C. (2017). Microbial genetic composition tunes host longevity. *Cell, 169*(7), 1249. doi:10.1016/j.cell.2017.05.036
45. Hans Hedrich. (2012). *The laboratory mouse. 2nd edition. the laboratory mouse.* Elsevier Ltd;.
46. Haran, J. P., & Mccormick, B. A. (2021). Aging, frailty, and the Microbiome—How dysbiosis influences human aging and disease. *Gastroenterology, 160*(2), 507. doi:10.1053/j.gastro.2020.09.060
47. Holmes, D. J., & Kristan, D. M. (2008). Comparative and alternative approaches and novel animal models for aging research. *AGE, 30*(2-3), 63. doi:10.1007/s11357-008-9068-x
48. Hugon, P., Dufour, J., Colson, P., Fournier, P., Sallah, K., & Raoult, D. (2015). *A comprehensive repertoire of prokaryotic species identified in human beings* Elsevier BV. doi:10.1016/s1473-3099(15)00293-5
49. Issi, L., Rioux, M., & Rao, R. (2017). The nematode caenorhabditis elegans - A versatile in vivo model to study host-microbe interactions. *Journal of Visualized Experiments,* (128) doi:10.3791/56487
50. *The jackson laboratory handbook on genetically standardized mice*
51. Johnson, S. C., Rabinovitch, P. S., & Kaeberlein, M. (2013). mTOR is a key modulator of ageing and age-related disease. *Nature, 493*(7432), 338. doi:10.1038/nature11861
52. Kamada, N., Chen, G. Y., Inohara, N., & Núñez, G. (2014). Control of pathogens and pathobionts by the gut microbiota. *Nature Immunology, 14*(7), 685. doi:10.1038/ni.2608
53. Kearns, R. (2024). The kynurenine pathway in gut permeability and inflammation. *Inflammation,* doi:10.1007/s10753-024-02135-x
54. Keith, S. A., Amrit, F. R. G., Ratnappan, R., & Ghazi, A. (2014). The C. elegans healthspan and stress-resistance assay toolkit. *Methods, 68*(3), 476. doi:10.1016/j.ymeth.2014.04.003
55. Kennedy, P. J., Cryan, J. F., Dinan, T. G., & Clarke, G. (2016). Kynurenine pathway metabolism and the microbiota-gut-brain axis. *Neuropharmacology, 112*, 399. doi:10.1016/j.neuropharm.2016.07.002

56. Kissoyan, K. A. B., Peters, L., Giez, C., Michels, J., Pees, B., Hamerich, I. K., . . . Dierking, K. (2022). Exploring effects of C. elegans protective natural microbiota on host physiology. *Frontiers in Cellular and Infection Microbiology, 12* doi:10.3389/fcimb.2022.775728
57. Koenig, J. E., Spor, A., Scalfone, N., Fricker, A. D., Stombaugh, J., Knight, R., . . . Ley, R. E. (2010). Succession of microbial consortia in the developing infant gut microbiome. *Proceedings of the National Academy of Sciences, 108*(supplement_1), 4578. doi:10.1073/pnas.1000081107
58. Kumar, S., Egan, B. M., Kocsisova, Z., Schneider, D. L., Murphy, J. T., Diwan, A., & Kornfeld, K. (2019). Lifespan extension in C. elegans caused by bacterial colonization of the intestine and subsequent activation of an innate immune response. *Developmental Cell, 49*(1), 100. doi:10.1016/j.devcel.2019.03.010
59. Lee, S., & Min, K. (2019). Drosophila melanogaster as a model system in the study of pharmacological interventions in aging. *Translational Medicine of Aging, 3*, 98. doi:10.1016/j.tma.2019.09.004
60. Lin, L., Lemieux, G. A., Enogieru, O. J., Giacomini, K. M., & Ashrafi, K. (2020). Neural production of kynurenic acid in caenorhabditis elegans requires the AAT-1 transporter. *Genes &Amp; Development, 34*(15-16), 1033. doi:10.1101/gad.339119.120
61. López-Otín, C., Blasco, M. A., Partridge, L., Serrano, M., & Kroemer, G. (2023). Hallmarks of aging: An expanding universe. *Cell, 186*(2), 243. doi:10.1016/j.cell.2022.11.001
62. Macfarlane, S., & Macfarlane, G. T. (2003). Regulation of short-chain fatty acid production. *Proceedings of the Nutrition Society, 62*(1), 67. doi:10.1079/pns2002207
63. Maier, L., Diard, M., Sellin, M. E., Chouffane, E., Trautwein-Weidner, K., Periaswamy, B., . . . Hardt, W. (2014). Granulocytes impose a tight bottleneck upon the gut luminal pathogen population during salmonella typhimurium colitis. *PLoS Pathogens, 10*(12) doi:10.1371/journal.ppat.1004557
64. Markaki, M., & Tavernarakis, N. (2020). Caenorhabditis elegans as a model system for human diseases. *Current Opinion in Biotechnology, 63*, 118. doi:10.1016/j.copbio.2019.12.011

65. Mcgee, M. D., Weber, D., Day, N., Vitelli, C., Crippen, D., Herndon, L. A., . . . Melov, S. (2011). Loss of intestinal nuclei and intestinal integrity in aging C. elegans. *Aging Cell, 10*(4), 699. doi:10.1111/j.1474-9726.2011.00713.x

66. Metwaly, A., Kriaa, A., Hassani, Z. *et al.* A Consensus Statement on establishing causality, therapeutic applications and the use of preclinical models in microbiome research. *Nat Rev Gastroenterol Hepatol* (2025). https://doi.org/10.1038/s41575-025-01041-3

67. Min'an Zhao, Jiayi Chu, Shiyao Feng, Chuanhao Guo, Baigong Xue, Kan He, Lisha Li, Immunological mechanisms of inflammatory diseases caused by gut microbiota dysbiosis: A review,Biomedicine & Pharmacotherapy, Volume 164, 2023, 114985, ISSN 0753-3322,https://doi.org/10.1016/j.biopha.2023.114985. https://www.sciencedirect.com/science/article/pii/S0753332223007758)

68. Nagy-Grócz, G., Spekker, E., & Vécsei, L. (2024). *Kynurenines, neuronal excitotoxicity, and mitochondrial oxidative stress: Role of the intestinal flora* MDPI AG. doi:10.3390/ijms25031698

69. Nguyen, T. L. A., Vieira-Silva, S., Liston, A., & Raes, J. (2015). *How informative is the mouse for human gut microbiota research?*. The Company of Biologists. 10.1242/dmm.017400

70. O'Toole, P. W., & Jeffery, I. B. (2015). Gut microbiota and aging. *Science (New York, N.Y.)*, *350*(6265), 1214–1215. https://doi.org/10.1126/science.aac8469

71. O'toole, P. W., Marchesi, J. R., & Hill, C. (2017). *Next-generation probiotics: The spectrum from probiotics to live biotherapeutics* Springer Science and Business Media LLC. doi:10.1038/nmicrobiol.2017.57

72. O'toole, P. W., & Jeffery, I. B. (2024). *Gut microbiota and aging*

73. Okuda, S., Nishiyama, N., Saito, H., & Katsuki, H. (1998). 3-Hydroxykynurenine, an endogenous oxidative stress generator, causes neuronal cell death with apoptotic features and region selectivity. *Journal of Neurochemistry, 70*(1), 299. doi:10.1046/j.1471-4159.1998.70010299.x

74. Pandey UB, Nichols CD. Human disease models in Drosophila melanogaster and the role of the fly in therapeutic drug discovery. Pharmacol Rev. 2011 Jun;63(2):411-36. doi: 10.1124/pr.110.003293. Epub 2011 Mar 17. PMID: 21415126; PMCID: PMC3082451.

75. Parada-Kusz, M., Clatworthy, A. E., Goering, E. R., Blackwood, S. M., Salm, E. J., Choi, C., . . . Hung, D. T. (2023). *A tryptophan metabolite modulates the host response to bacterial infection via kainate receptors* Cold Spring Harbor Laboratory. doi:10.1101/2023.08.16.553532
76. Park, M., & Wang, M. C. (2018). Aging: Antagonistic pleiotropy supported by gut eating. *Current Biology, 28*(16), R890. doi:10.1016/j.cub.2018.07.011
77. Petersen, C., Pees, B., Martínez Christophersen, C., & Leippe, M. (2021). Preconditioning with natural microbiota strain *Ochrobactrum vermis* MYb71 influences caenorhabditis elegans behavior. *Frontiers in Cellular and Infection Microbiology, 11* doi:10.3389/fcimb.2021.775634
78. Platten, M., Nollen, E. A. A., Röhrig, U. F., Fallarino, F., & Opitz, C. A. (2019). *Tryptophan metabolism as a common therapeutic target in cancer, neurodegeneration and beyond* Springer Science and Business Media LLC. doi:10.1038/s41573-019-0016-5
79. Popkes, M., & Valenzano, D. R. (2020). Microbiota–host interactions shape ageing dynamics. *Philosophical Transactions of the Royal Society B: Biological Sciences, 375*(1808) doi:10.1098/rstb.2019.0596
80. Portal-Celhay, C., Bradley, E. R., & Blaser, M. J.Control of intestinal bacterial proliferation in regulation of lifespan in caenorhabditis elegans.
81. Radeke, L. J., & Herman, M. A. (2021). *Take a walk to the wild side of caenorhabditis elegans-pathogen interactions* doi:10.1128/MMBR
82. Rollins, J. A., Howard, A. C., Dobbins, S. K., Washburn, E. H., & Rogers, A. N. (2017). Assessing health span in caenorhabditis elegans: Lessons from short-lived mutants. *The Journals of Gerontology: Series A, 72*(4), 473. doi:10.1093/gerona/glw248
83. Rony, M. K. K., Parvin, M. R., Wahiduzzaman, M. D., Akter, K., & Ullah, M. (2024). Challenges and advancements in the health-related quality of life of older people. *Advances in Public Health, 2024*, 1. doi:10.1155/2024/8839631
84. Rydell-Törmänen, K., & Johnson, J. R. (2019). *The applicability of mouse models to the study of human disease* Springer New York. doi:10.1007/978-1-4939-9086-3_1
85. Sai, M., Jandhyala, R., Talukdar, C., Subramanyam, H., Vuyyuru, M., Sasikala, . . . Reddy. (2015). Role of the normal gut microbiota. *World Journal of Gastroenterology, 21*(29) doi:10.3748/wjg.v21.i29.8787

86. Sas, K., Robotka, H., Toldi, J., & Vécsei, L. (2007). Mitochondria, metabolic disturbances, oxidative stress and the kynurenine system, with focus on neurodegenerative disorders. *Journal of the Neurological Sciences, 257*(1-2), 221. doi:10.1016/j.jns.2007.01.033
87. Savitz, J. (2019). The kynurenine pathway: A finger in every pie. *Molecular Psychiatry, 25*(1), 131. doi:10.1038/s41380-019-0414-4
88. Scharf, A., Pohl, F., Egan, B. M., Kocsisova, Z., & Kornfeld, K. (2021). Reproductive aging in caenorhabditis elegans: From molecules to ecology. *Frontiers in Cell and Developmental Biology, 9* doi:10.3389/fcell.2021.718522
89. Schindelin, J., Arganda-Carreras, I., Frise, E., Kaynig, V., Longair, M., Pietzsch, T., . . . Cardona, A. (2013). Fiji: An open-source platform for biological-image analysis. *Nature Methods, 9*(7), 676. doi:10.1038/nmeth.2019
90. Schupack, D. A., Mars, R. A. T., Voelker, D. H., Abeykoon, J. P., & Kashyap, P. C. (2022). The promise of the gut microbiome as part of individualized treatment strategies. *Nature Reviews Gastroenterology &Amp; Hepatology, 19*(1), 7. doi:10.1038/s41575-021-00499-1
91. Sekirov, I., Russell, S. L., Antunes, L. C., & Finlay, B. B. (2010). Gut microbiota in health and disease. *Physiological reviews*, *90*(3), 859–904. https://doi.org/10.1152/physrev.00045.2009.
92. Shubin, M., Schaufler, K., Tedin, K., Vehkala, M., & Corander, J. (2016). *Identifying multiple potential metabolic cycles in time-series from biolog experiments* Public Library of Science (PLoS). doi:10.1371/journal.pone.0162276
93. Singh, A., & Luallen, R. J. (2024). Understanding the factors regulating host–microbiome interactions using caenorhabditis elegans. *Philosophical Transactions of the Royal Society B: Biological Sciences, 379*(1901) doi:10.1098/rstb.2023.0059
94. Song, G., Jia, M., Chen, K., Kong, X., Khattak, B., Xie, C., . . . Mao, L. (2016). CRISPR/Cas9: A powerful tool for crop genome editing. *The Crop Journal, 4*(2), 75. doi:10.1016/j.cj.2015.12.002
95. Stiernagle, T. (2006). Maintenance of C. elegans. *WormBook,* doi:10.1895/wormbook.1.101.1
96. Tashiro, T., Murakami, Y., Mouri, A., Imamura, Y., Nabeshima, T., Yamamoto, Y., & Saito, K. (2016). Kynurenine 3-monooxygenase is implicated in antidepressants-

responsive depressive-like behaviors and monoaminergic dysfunctions. *Behavioural Brain Research, 317*, 279. doi:10.1016/j.bbr.2016.09.050

97. Tremaroli, V., & Bäckhed, F. (2012). Functional interactions between the gut microbiota and host metabolism. *Nature, 489*(7415), 242. doi:10.1038/nature11552
98. Van Der Goot, A. T., & Nollen, E. A. A. (2013). Tryptophan metabolism: Entering the field of aging and age-related pathologies. *Trends in Molecular Medicine, 19*(6), 336. doi:10.1016/j.molmed.2013.02.007
99. Van Der Goot, A. T., Zhu, W., Vázquez-Manrique, R. P., Seinstra, R. I., Dettmer, K., Michels, H., . . . Nollen, E. A. A. (2012). Delaying aging and the aging-associated decline in protein homeostasis by inhibition of tryptophan degradation. *Proceedings of the National Academy of Sciences, 109*(37), 14912. doi:10.1073/pnas.1203083109
100. Verhaar, B. J. H., Hendriksen, H. M. A., De Leeuw, F. A., Doorduijn, A. S., Van Leeuwenstijn, M., Teunissen, C. E., . . . Van Der Flier, W. M. (2022). *Gut microbiota composition is related to AD pathology* Frontiers Media SA. doi:10.3389/fimmu.2021.794519
101. Wang, X., Zhang, X., Zhang, Z., Lang, H., & Zheng, H. (2018). Honey bee as a model organism to study gut microbiota and diseases. *Drug Discovery Today: Disease Models, 28*, 35. doi:10.1016/j.ddmod.2019.08.010
102. Wang, Zhao, Ezcurra, Benedetto, Gilliat, Hellberg, . . . Gems. (2018). A parthenogenetic quasi-program causes teratoma-like tumors during aging in wild-type C. elegans. *Npj Aging and Mechanisms of Disease, 4*(1) doi:10.1038/s41514-018-0025-3
103. Westermann, A. J., Gorski, S. A., & Vogel, J. (2012). Dual RNA-seq of pathogen and host. *Nature Reviews Microbiology, 10*(9), 618. doi:10.1038/nrmicro2852
104. Wiles, T. J., Wall, E. S., Schlomann, B. H., Hay, E. A., Parthasarathy, R., Guillemin, K., & Graf, J. (2018). Modernized tools for streamlined genetic manipulation and comparative study of wild and diverse proteobacterial lineages. doi:10.1128/mBio
105. Wu, C., Davis, S., Saudagar, N., Shah, S., Zhao, W., Stern, A., . . . Yang, H. (2024). *Caenorhabditis elegans as a convenient animal model for microbiome studies* MDPI AG. doi:10.3390/ijms25126670
106. Wurm, S., Diehl, M., Kornadt, A. E., Westerhof, G. J., & Wahl, H. (2021). How do views on aging affect health outcomes in adulthood and late life? explanations for

an established connection. *Developmental Review, 46*, 27. doi:10.1016/j.dr.2017.08.002

107. Yang, W., Petersen, C., Pees, B., Zimmermann, J., Waschina, S., Dirksen, P., . . . Schulenburg, H. (2019). The inducible response of the nematode caenorhabditis elegans to members of its natural microbiota across development and adult life. *Frontiers in Microbiology, 10* doi:10.3389/fmicb.2019.01793

108. Zárate-Potes, A., Ali, I., Ribeiro Camacho, M., Brownless, H., & Benedetto, A. (2022). Meta-analysis of caenorhabditis elegans transcriptomics implicates hedgehog-like signaling in host-microbe interactions. *Frontiers in Microbiology, 13* doi:10.3389/fmicb.2022.853629

109. Zeigler, D. R. (2011). The genome sequence of bacillus subtilis subsp. spizizenii W23: Insights into speciation within the B. subtilis complex and into the history of B. subtilis genetics. *Microbiology, 157*(7), 2033. doi:10.1099/mic.0.048520-0

110. Zhang, F., Berg, M., Dierking, K., Félix, M., Shapira, M., Samuel, B. S., & Schulenburg, H. (2017). Caenorhabditis elegans as a model for microbiome research. *Frontiers in Microbiology, 8* doi:10.3389/fmicb.2017.00485

111. Zhang, S., Li, F., Zhou, T., Wang, G., & Li, Z. (2020). Caenorhabditis elegans as a useful model for studying aging mutations. *Frontiers in Endocrinology, 11* doi:10.3389/fendo.2020.554994

112. Zhao, D., Wang, Y., Wong, N. D., & Wang, J. (2024). Impact of aging on cardiovascular diseases. *JACC: Asia, 4*(5), 345. doi:10.1016/j.jacasi.2024.02.002

113. Zhao, Gilliat, Ziehm, Turmaine, Wang, Ezcurra, . . . Gems. (2017). *Two forms of death in ageing caenorhabditis elegans* Springer Science and Business Media LLC. doi:10.1038/ncomms15458

114. Zheng, H., Steele, M. I., Leonard, S. P., Motta, E. V. S., & Moran, N. A. (2018). Honeybees as models for gut microbiota research. *Lab Animal, 47*(11), 317. doi:10.1038/s41684-018-0173-x

115. Zhuravlev, A. V., Zakharov, G. A., Shchegolev, B. F., & Savvateeva-Popova, E. V. (2016). *Antioxidant properties of kynurenines: Density functional theory calculations* Public Library of Science (PLoS). doi:10.1371/journal.pcbi.1005213

116. Zimmermann, J., Obeng, N., Yang, W., Pees, B., Petersen, C., Waschina, S., . . . Schulenburg, H. (2019). The functional repertoire contained within the native

microbiota of the model nematodeCaenorhabditis elegans. *The ISME Journal, 14*(1), 26. doi:10.1038/s41396-019-0504-y

117. Zimmermann, J., Piecyk, A., Sieber, M., Petersen, C., Johnke, J., Moitinho-Silva, L., . . . Schulenburg, H. (2023). *Gut-associated functions are favored during microbiome assembly acrossC. eleganslife* Cold Spring Harbor Laboratory. doi:10.1101/2023.03.25.534195

9 ACKNOWLEDGEMENT

Completing this Master's degree has been a transformative journey, one filled with challenges, growth, and self-discovery. This accomplishment would not have been possible without the support and encouragement of so many wonderful individuals. First and foremost, I extend my deepest gratitude to God for granting me the opportunity to pursue this degree and for guiding me toward opportunities I never thought possible.

I am immensely grateful to everyone who has contributed to my academic journey and the successful completion of this thesis.

My sincerest and most heartfelt thanks go to **Dr. Alexandre Benedetto**, whose mentorship has been indispensable to my academic and personal growth. From helping me navigate administrative processes to guiding me through the challenges of transitioning to a new country, you have been an exceptional mentor. The advanced scientific techniques I have acquired and my development as a researcher are a direct result of your unwavering patience, dedication, and support. I will always be grateful for your guidance. I would also like to express my sincere thanks to **Dr. Susan Broughton**, for providing me an opportunity to work with flies and for extending your knowledge and motivation.

I would also like to express my gratitude to **Dr. Alejandra Zarate-Potes** for your thorough guidance and training in the technical aspects of my project. Your mentorship extended far beyond the lab, offering invaluable advice on research and career prospects, for which I am deeply appreciative. **Irtiqa Ali**, your technical help in the lab and your emotional and mental support throughout this journey have been truly invaluable. Your friendship has made this experience all the more enjoyable, and I will forever be thankful for your encouragement. **Dr. Jack Martin**, thank you for your expertise in microbiology and *C. elegans* research. Your contributions have been critical to the smooth progress of my work, and I truly appreciate your support. **Justin Ng**, I am deeply grateful for your help in the lab, your assistance with thesis-writing, and your overall guidance.

Special thanks to **Dr. Poorna Murali**—my fly buddy, mentor, and life coach. Thank you for your expert guidance in lab techniques, presentation skills, and for being a pillar of support during my mental breakdowns. Your generosity in cooking for me and treating me like family,

along with your unwavering help with my writing, has had an immeasurable impact on this work.

To my colleagues from other groups, thank you for your support and collaboration. Whether it was sharing equipment or providing technical expertise, your contributions made a significant difference. Special thanks to **Dr. Dimitra Papatziamou**, Thomas Slater, and **Dr. Natalia Da Silva Jardim** for your camaraderie and insightful discussions. Natalia, your enthusiasm and expertise have added a valuable dimension to this work.

I am grateful to **Dr. David Clancy** for agreeing to examine my thesis, and to **Dr. Harsh Pawar** for your career guidance and for all the delicious home-cooked meals.

I would like to extend my thanks to the BLS staff, particularly Dr. Elizabeth Shaw for microscopy training, David Andrew for your general technical support, and Dr. Jayde Whittingham-Dowd for your technical training. Your contributions have been integral to the success of my research.

My heartfelt gratitude goes to my parents for their unwavering belief in me, their constant encouragement, and their financial support. Despite being miles apart, you have always been present in every way that matters. Dad, thank you for adjusting to time zones to ensure my safety during late-night work, and Mum, thank you for being my source of emotional strength and motivation throughout this journey.

To my sister Heli, thank you for your love, your persistent reminders to meet deadlines, and for managing family responsibilities in my absence. Your support kept me grounded and focused, and I am eternally grateful for it. My dear friends Khushi and Saumi, thank you for being my family away from home. Your encouragement, unwavering belief in me, and constant support have been a source of strength and inspiration.

Finally, I want to thank Devarsh for being my constant source of comfort and support. Your love and presence have kept me sane, and your encouragement has meant more to me than words can express.

This thesis is a testament to the collective efforts of all these incredible individuals. Without you, this journey would not have been possible. I thank you all from the bottom of my heart.

10 APPENDIX

10.1 Bacterial profile

No.	Bacteria	Identifier	Function/Context	Genome sequence
1.	*Escherichia coli* SM10/pTn7xKS-dTomato	SM10/pTn7xKS-dTomato	Donor Bacteria (Transformation)	CGCCAGCAACGCGGCCTTTTTACGGTTCCTGGCCTTTTGCTGGCCTTTTGCTCACATGTTCTTT CCTGCGTTATCAGGGGATTCCTTAAGGTATACTTTCCGCTGCATAACCCTGCTTCGGGGTCAT TATAGCGATTTTTTCGGTATATCCATCCTTTTTCGCACGATATACAGGATTTTGCCAAAGGGT TCGTGTAGACTTTCCTTGGTGTATCCAACGGCGTCAGCCGGGCAGGATAGGTGAAGTAGGC CCACCCGCGAGCGGGTGTTCCTTCTTCACTGTCCCTTATTCGCACCTGGCGGTGCTCAACGG GAATCCTGCTCTGCGAGGCTGGCCGATAAGCTCTGATACCGCTCGCCGCAGCCGAACGACC GAGCGCAGCGGGTCAGTGAGCGAGGAAGCGGAAGAGCGCCCAATACGCAAACCGCCTCTC CCCGCGCGTTGGCCGATTCATTAATGCAGCGCCCAAACATAACAGGAAGAAAAATGCCCCG CTGTGGGCGGACAAAATAGTTGGGAACTGGGAGGGGTGGAAATGGAGTTTTTAAGGATTA TTTAGGGAAGAGTGACAAAATAGATGGGAACTGGGTGTAGCGTCGTAAGCTAATACGAAA ATTAAAAATGACAAAATAGTTTGGAACTAGATTTCACTTATCTGGTTGGCCTGCAAGGCCTTC GCGAGGTACCGGGCCCAAGCTTCTCGAGGAATTCCTGCAGCCCGGGGGATCCACTAGCTAG GCCGAGAAAAAAAAGCCCGCTCATTAGGCGGGCTAGCTCATTATTTGTAGAGCTCATCCATG CCATGTGTAATCCCAGCAGCAGTTACAAACTCAAGAAGGACCATGTGGTCACGCTTTTCGTT GGGATCTTTCGAAAGGGCAGATTGTGTCGACCAGCTATCGATCCATGGGGCCCGCGGCCGC TTACTTGTACAGCTCGTCCATGCCGTACAGGAACAGGTGGTGGCGGCCCTCGGAGCGCTCG TACTGTTCCACGATGGTGTAGTCCTCGTTGTGGGAGGTGATGTCCAGCTTGGTGTCCACGTA GTAGTAGCCGGGCAGTTGCACGGGCTTCTTGGCCATGTAGATGGTCTTGAACTCCACCAGGT AGTGGCCGCCGTCCTTCAGCTTCAGGGCCTGGTGGATCTCGCCCTTCAGCACGCCGTCGCGG GGGTACAGGCGCTCGGTGGAGGCCTCCCAGCCCATGGTCTTCTTCTGCATTACGGGGCCGTC GGGGGGGAAGTTGGTGCCGCGCATCTTCACCTTGTAGATCAGCGTGCCGTCCTGCAGGGAG GAGTCCTGGGTCACGGTCACCAGACCGCCGTCCTCGAAGTTCATCACGCGCTCCCACTTGAA GCCCTCGGGGAAGGACAGCTTCTTGTAATCGGGGATGTCGGCGGGGTGCTTCACGTACGCC TTGGAGCCGTACATGAACTGGGGGGACAGGATGTCCCAGGCGAAGGGCAGGGGGCCGCCC TTGGTCACCTTCAGCTTGGCGGTCTGGGTGCCCTCGTAGGGGCGGCCCTCGCCCTCGCCCTC GATCTCGAACTCGTGGCCGTTCATGGAGCCCTCCATGCGCACCTTGAAGCGCATGAACTCTT TGATGACCTCCTCGCCCTTGCTCACCATATGTATATCTCCTTCTTAAAGTTAAACAAAATTATT TCTAGGGATCCTCCACACATTATACGAGCCGATGATTAATTGTCAAGAATTCTAGTGAGCTC ATGCATGATCGAATTAGCTTCAAAAGCGCTCTGAAGTTCCTATACTTTCTAGAGAATAGGAA CTTCGGAATAGGAACTTCAAGATCCCCTGATTCCCTTTGTCAACAGCAATGGATCGAATTGA CATAAGCCTGTTCGGTTCGTAAACTGTAATGCAAGTAGCGTATGCGCTCACGCAACTGGTCC AGAACCTTGACCGAACGCAGCGGTGGTAACGGCGCAGTGGCGGTTTTCATGGCTTGTTATG ACTGTTTTTTTGTACAGTCTATGCCTCGGGCATCCAAGCAGCAAGCGCGTTACGCCGTGGGT CGATGTTTGATGTTATGGAGCAGCAACGATGTTACGCAGCAGCAACGATGTTACGCAGCAG GGCAGTCGCCCTAAAACAAAGTTAGGTGGCTCAAGTATGGGCATCATTCGCACATGTAGGC TCGGCCCTGACCAAGTCAAATCCATGCGGGCTGCTCTTGATCTTTTCGGTCGTGAGTTCGGA GACGTAGCCACCTACTCCCAACATCAGCCGGACTCCGATTACCTCGGGAACTTGCTCCGTAG TAAGACATTCATCGCGCTTGCTGCCTTCGACCAAGAAGCGGTTGTTGGCGCTCTCGCGGCTT ACGTTCTGCCCAGGTTTGAGCAGCCGCGTAGTGAGATCTATATCTATGATCTCGCAGTCTCC GGCGAGCACCGGAGGCAGGGCATTGCCACCGCGCTCATCAATCTCCTCAAGCATGAGGCCA ACGCGCTTGGTGCTTATGTGATCTACGTGCAAGCAGATTACGGTGACGATCCCGCAGTGGCT CTCTATACAAAGTTGGGCATACGGGAAGAAGTGATGCACTTTGATATCGACCCAAGTACCGC CACCTAACAATTCGTTCAAGCCGAGATCGGCTTCCCGGCCGCGGAGTTGTTCGGTAAATTGT CACAACGCCGCGGCCAATTCGATCTAGAATTCCATTGAGTAAGTTTTTAAGCACATCAGCTTC AAAAGCGCTCTGAAGTTCCTATACTTTCTAGAGAATAGGAACTTCGGAATAGGAACTTCAAG ATCCCCAATTCGATCGTCCGGGCCGCAAGCTCCTAGCGGCGGATTTGTCCTACTCAGGAGAG CGTTCACCGACAAACAACAGATAAAACGAAAGGCCCAGTCTTTCGACTGAGCCTTTCGTTTT ATTTGATGCCTCAAGCTAGAGAGTCATTACCCCAGGCGTTTAAGGGCACCAATAACTGCCTT AAAAAAATTACGCCCCGCCCTGCCACTCATCGCAGTCTAGCTTGGATTCTCACCAATAAAAAA CGCCCGGCGGCAACCGAGCGTTCTGAACAAATCCAGATGGAGTTCTGAGGTCATTACTGGA TCTATCAACAGGAGTCCAAGCTCAGCTAATTAAGCTAGCTTATCGATACCGTCGACCTCGAA CCCCACGCCCCTCTTTAATACGACGGGCAATTTGCACTTCAGAAAATGAAGAGTTTGCTTTAG CCATAACAAAAGTCCAGTATGCTTTTTCACAGCATAACTGGACTGATTTCAGTTTACAACTAT TCTGTCTAGTTTAAGACTTTATTGTCATAGTTTAGATCTATTTTGTTCAGTTTAAGACTTTATT GTCCGCCCACACCCGCTTACGCAGGGCATCCATTTATTACTCAACCGTAACCGATTTTGCCAG GTTACGCGGCTGGTCCTCTAGCTGGCGTAATAGCGAAGAGGCCCGCACCGATCGCCCTTCCC AACAGTTGCGCAGCCTGAATGGCGAATGGCGATCCGAGCCGGAAGCATAAAGTGTAAAGC CTGGGGTGCCTAATGAGTGAGCTAACTCACATTAATTGCGTTGCGCTCACTGCCCGCTTTCCA GTCGGGAAACCTGTCGTGCCAGCTGCATTAATGAATCGGCCAACGCGCGGGGAGAGGCGG TTTGCGTATTGGGCGCCAGGGTGGTTTTTCTTTTCACCAGTGAGACGGGCAACAGCTGATTG CCCTTCACCGCCTGGCCCTGAGAGAGTTGCAGCAAGCGGTCCACGCTGGTTTGCCCCAGCAG

				GCGAAAATCCTGTTTGATGGTGGTTAACGGCGGGATATAACATGAGCTGTCTTCGGTATCGT CGTATCCCACTATCGAGATATCCGCACCAACGCGCAGCCCGGACTCGGTAATGGCGCGCATT GCGCCCAGCGCCATCTGATCGTTGGCAACCAGCATCGCAGTGGGAACGATGCCCTCATTCA GCATTTGCATGGTTTGTTGAAAACCGGACATGGCACTCCAGTCGCCTTCCCGTTCCGCTATCG GCTGAATTTGATTGCGAGTGAGATATTTATGCCAGCCAGCCAGACGCAGACGCGCCGAGAC AGAACTTAATGGGCCCGCTAACAGCGCGATTTGCTGGTGACCCAATGCGACCAGATGCTCC ACGCCCAGTCGCGTACCGTCTTCATGGGAGAAAATAATACTGTTGATGGGTGTCTGGTCAGA GACATCAAGAAATAACGCCGGAACATTAGTGCAGGCAGCTTCCACAGCAATGGCATCCTGG TCATCCAGCGGATAGTTAATGATCAGCCCACTGACGCGTTGCGCGAGAAGATTGTGCACCG CCGCTTTACAGGCTTCGACGCCGCTTCGTTCTACCATCGACACCACCACGCTGGCACCCAGTT GATCGGCGCGAGATTTAATCGCCGCGACAATTTGCGACGGCGCGTGCAGGGCCAGACTGG AGGTGGCAACGCCAATCAGCAACGACTGTTTGCCCGCCAGTTGTTGTGCCACGCGGTTGGG AATGTAATTCAGCTCCGCCATCGCCGCTTCCACTTTTTCTCGCGTTTTCGCAGAAACGTGGCT GGCCTGGTTCACCACGCGAGAAACGGTCTGATAAGAGACACCGGCATACTCTGCGACATCG TATAGCGTTACTGGTTTCACATTCACCACCCTGAATTGACTCTCTTCCGGGCGCTATCATGCC ATACCACGAAAGGTTTTGCACCATTCGATGCGCCTGATGCGGTATTTTCTCCTTACGCATCTG TGCGGTATTTCACACCGCATATCGAGGAGCTGTTGACAATTAATCATCGGCTCGTATAATGT GTGGAATTGTGAGCGGATAACAATTTCACACGGCCGGCCAAGGAGAAAGGCTATGAAGCA CAACCCTCTGGTGGTGTGTCTGCTCATTATCTGCATTACGATTCTGACATTCACACTCCTGACC CGACAAACGCTCTACGAACTGCGGTTCCGGGACGGTGATAAGGAGGTTGCTGCGCTCATGG CCTGCACGTCCAGGTAATCGCGAGTCGACAGGAAGGATAAGAAGAACATAAAAAATGGCA CTATTCTCTAAAATATTAATTTTTTATGTGATTGGTGTGAACATATCCTTTGTCATTATCTGGT TTATCTCACATGAGAAAACACATATTCGTTTACTTAGTGCATTCCTGGTCGGAATAACCTGGC CAATGAGTCTGCCTGTGGCATTACTTTTTTCTCTCTTTTAGGTCGACGGCGCCAGGAGACGCG TATGAACCTGGTGGATATCGCCATTCTTATCCTCAAACTCATTGTTGCAGCACTGCAACTGCT TGATGCTGTTCTGAAATACCTGAAGTAATACTTAATTAAGGGCAAGCGCGGGGATTTTCCCC GCGCATTTCCCGGGTCAGTATGGTGCACTCTCAGTACAATCTGCTCTGATGCCGCATAGTTA AGCCAGCCCCGACACCCGCCAACACCCGCTGACGCGCCCTGACGGGCTTGTCTGCTCCCGGC ATCCGCTTACAGACAAGCTGTGACCGTCTCCGGGAGCTGCATGTGTCAGAGGTTTTCACCGT CATCACCGAAACGCGCGAGACGAAAGGGCCTCGTGATACGCCTATTTTTATAGGTTAATGTC ATGATAATAATGGTTTCTTAGACGTCAGGTGGCACTTTTCGGGGAAATGTGCGCGGAACCCC TATTTGTTTATTTTTCTAAATACATTCAAATATGTATCCGCTCATGAGACAATAACCCTGATAA ATGCTTCAATAATATTGAAAAAGGAAGAGTATGAGTATTCAACATTTCCGTGTCGCCCTTATT CCCTTTTTTGCGGCATTTTGCCTTCCTGTTTTTGCTCACCCAGAAACGCTGGTGAAAGTAAAA GATGCTGAAGATCAGTTGGGTGCACGAGTGGGTTACATCGAACTGGATCTCAACAGCGGTA AGATCCTTGAGAGTTTTCGCCCCGAAGAACGTTTTCCAATGATGAGCACTTTTAAAGTTCTGC TATGTGGCGCGGTATTATCCCGTATTGACGCCGGGCAAGAGCAACTCGGTCGCCGCATACA CTATTCTCAGAATGACTTGGTTGAGTACTCACCAGTCACAGAAAAGCATCTTACGGATGGCA TGACAGTAAGAGAATTATGCAGTGCTGCCATAACCATGAGTGATAACACTGCGGCCAACTTA CTTCTGACAACGATCGGAGGACCGAAGGAGCTAACCGCTTTTTTGCACAACATGGGGGATC ATGTAACTCGCCTTGATCGTTGGGAACCGGAGCTGAATGAAGCCATACCAAACGACGAGCG TGACACCACGATGCCTGTAGCAATGGCAACAACGTTGCGCAAACTATTAACTGGCGAACTAC TTACTCTAGCTTCCCGGCAACAATTAATAGACTGGATGGAGGCGGATAAAGTTGCAGGACC ACTTCTGCGCTCGGCCCTTCCGGCTGGCTGGTTTATTGCTGATAAATCTGGAGCCGGTGAGC GTGGGTCTCGCGGTATCATTGCAGCACTGGGGCCAGATGGTAAGCCCTCCCGTATCGTAGTT ATCTACACGACGGGGAGTCAGGCAACTATGGATGAACGAAATAGACAGATCGCTGAGATA GGTGCCTCACTGATTAAGCATTGGTAACTGTCAGACCAAGTTTACTCATATATACTTTAGATT GATTTAAAACTTCATTTTTAATTTAAAAGGATCTAGGTGAAGATCCTTTTTGATAATCTCATG ACCAAAATCCCTTAACGTGAGTTTTCGTTCCACTGAGCGTCAGACCCCGTAGAAAAGATCAA AGGATCTTCTTGAGATCCTTTTTTTCTGCGCGTAATCTGCTGCTTGCAAACAAAAAAACCACC GCTACCAGCGGTGGTTTGTTTGCCGGATCAAGAGCTACCAACTCTTTTTCCGAAGGTAACTG GCTTCAGCAGAGCGCAGATACCAAATACTGTCCTTCTAGTGTAGCCGTAGTTAGGCCACCAC TTCAAGAACTCTGTAGCACCGCCTACATACCTCGCTCTGCTAATCCTGTTACCAGTGGCTGCT GCCAGTGGCGATAAGTCGTGTCTTACCGGGTTGGACTCAAGACGATAGTTACCGGATAAGG CGCAGCGGTCGGGCTGAACGGGGGGTTCGTGCACACAGCCCAGCTTGGAGCGAACGACCT ACACCGAACTGAGATACCTACAGCGTGAGCTATGAGAAAGCGCCACGCTTCCCGAAGGGAG AAAGGCGGACAGGTATCCGGTAAGCGGCAGGGTCGGAACAGGAGAGCGCACGAGGGAGC TTCCAGGGGGAAACGCCTGGTATCTTTATAGTCCTGTCGGGTTTCGCCACCTCTGACTCGAG CGTCGATTTTTGTGATGCTCGTCAGGGGGGCGGAGCCTATGGAAAAA (Wiles et al., 2018)(pTn7xKS-dTomato was a gift from Karen Guillemin(Addgeneplasmid#117395;*http://n2t.net/addgene:117395*;RRID:Addgene_117395)
2.	*Escherichia coli* SM10/pTn7xKS-mPlum	SM10/pTn7x KS-mPlum	Donor Bacteria (Transformation)	CGCCAGCAACGCGGCCTTTTTACGGTTCCTGGCCTTTTGCTGGCCTTTTGCTCACATGTTCTTT CCTGCGTTATCAGGGGATTCCTTAAGGTATACTTTCCGCTGCATAACCCTGCTTCGGGGTCAT TATAGCGATTTTTTCGGTATATCCATCCTTTTTCGCACGATATACAGGATTTTGCCAAAGGGT TCGTGTAGACTTTCCTTGGTGTATCCAACGGCGTCAGCCGGGCAGGATAGGTGAAGTAGGC CCACCCGCGAGCGGGTGTTCCTTCTTCACTGTCCCTTATTCGCACCTGGCGGTGCTCAACGG GAATCCTGCTCTGCGAGGCTGGCCGATAAGCTCTGATACCGCTCGCCGCAGCCGAACGACC GAGCGCAGCGGGTCAGTGAGCGAGGAAGCGGAAGAGCGCCCAATACGCAAACCGCCTCTC CCCGCGCGTTGGCCGATTCATTAATGCAGCGCCCAAACATAACAGGAAGAAAAATGCCCCG CTGTGGGCGGACAAAATAGTTGGGAACTGGGAGGGGTGGAAATGGAGTTTTTAAGGATTA

				TTTAGGGAAGAGTGACAAAATAGATGGGAACTGGGTGTAGCGTCGTAAGCTAATACGAAA ATTAAAAATGACAAAATAGTTTGGAACTAGATTTCACTTATCTGGTTGGCCTGCAAGGCCTTC GCGAGGTACCGGGCCCAAGCTTCTCGAGGAATTCCTGCAGCCCGGGGGATCCACTAGCCGG TAAACCGAAAGGCAGGAACAGGAGAGCGCACGAGGGAGCCGCCAGGGGGAAACGCCTGG TATCTTTATAGTCCTGTCGGGTTTCGCCACCACTGATTTGAGCGTCAGATTTCGTGATGCTTG TCAGGGGGGCGGAGCCTATGGAAAAACGGCTTTGCCGCGGCCCTCTCACTTCCCTGTTAAGT ATCTCCTAGGCCGAGAAAAAAAAGCCCGCTCATTAGGCGGGCTAGCTCATTATTTGTAGAGC TCATCCATGCCATGTGTAATCCCAGCAGCAGTTACAAACTCAAGAAGGACCATGTGGTCACG CTTTTCGTTGGGATCTTTCGAAAGGGCAGATTGTGTCGACCAGCTATCGATCCATGGGGCCC GCGGCCGCCTAGGCGCCGGTGGAGTGGCGGCCCTCGGCGCGCTCGTACTGTTCCACGATGG TGTAGTCCTCGTTGTGGGAGGTGATGTCCAGCTTGATGTCGGTCTTGTAGGCGCCGGGCAG CTGCACGGGCTTCTTGGCCATGTAGGTGGTCTTGACCTCGGCGTCGTAGTGGCCGCCGTCCT TCAGCCTCAGCCTCATCTTCATCTCGCCCTTCAGGGCGCCGTCCTCGGGGTACATCCGCTCGG AGGAGGCCTCCCAGCCCATGGTCTTCTTCTGCATTACGGGGCCGTCGGAGGGGAAGTTGGT GCCGCGCACCTTCACCTTGTAGATAACTCGCCGTCCTGCAGGGAGGAGTCCTGGGTCACGGT CACCACGCCGCCGTCCTCGAAGTTCATCACGCGCTCCCACTTGAAGCCCTCGGGGAAGGACA GCTTCAAGTAGTCGGGGATGTCGGCGGGGTGCTTCACGTAGGCCTTGGAGCCGTACATGAT CTGAGGGGACAGGATGTCCCAGGCGAAGGGCAGGGGGCCACCCTTGGTCACCTTCAGCCT GGCGGTCTGGGTGCCCTCGTAGGGGCGCCCTCGCCCTCGCCCTCGATCTCGAACTCGTGGCC GTTCACGGAGCCCTCCATGTGCTCCTTGAAGCGCATGAACTCCTTGATGACCTCCTCGCCCTT GCTCACCATATGTATATCTCCTTCTTAAAGTTAAACAAAATTATTTCTAGGGATCCTCCACACA TTATACGAGCCGATGATTAATTGTCAAGAATTCTAGTGAGCTCATGCATGATCGAATTAGCTT CAAAAGCGCTCTGAAGTTCCTATACTTTCTAGAGAATAGGAACTTCGGAATAGGAACTTCAA GATCCCCTGATTCCCTTTGTCAACAGCAATGGATCGAATTGACATAAGCCTGTTCGGTTCGTA AACTGTAATGCAAGTAGCGTATGCGCTCACGCAACTGGTCCAGAACCTTGACCGAACGCAG CGGTGGTAACGGCGCAGTGGCGGTTTTCATGGCTTGTTATGACTGTTTTTTTGTACAGTCTAT GCCTCGGGCATCCAAGCAGCAAGCGCGTTACGCCGTGGTCGATGTTTGATGTTATGGAGCA GCAACGATGTTACGCAGCAGCAACGATGTTACGCAGCAGGGCAGTCGCCCTAAAACAAAGT TAGGTGGCTCAAGTATGGGCATCATTCGCACATGTAGGCTCGGCCCTGACCAAGTCAAATCC ATGCGGGCTGCTCTTGATCTTTTCGGTCGTGAGTTCGGAGACGTAGCCACCTACTCCCAACA TCAGCCGGACTCCGATTACCTCGGGAACTTGCTCCGTAGTAAGACATTCATCGCGCTTGCTG CCTTCGACCAAGAAGCGGTTGTTGGCGCTCTCGCGGCTTACGTTCTGCCCAGGTTTGAGCAG CCGCGTAGTGAGATCTATATCTATGATCTCGCAGTCTCCGGCGAGCACCGGAGGCAGGGCA TTGCCACCGCGCTCATCAATCTCCTCAAGCATGAGGCCAACGCGCTTGGTGCTTATGTGATCT ACGTGCAAGCAGATTACGGTGACGATCCCGCAGTGGCTCTCTATACAAAGTTGGGCATACG GGAAGAAGTGATGCACTTTGATATCGACCCAAGTACCGCCACCTAACAATTCGTTCAAGCCG AGATCGGCTTCCCGGCCGCGGAGTTGTTCGGTAAATTGTCACAACGCCGCGGCCAATTCGAT CTAGAATTCCATTGAGTAAGTTTTTAAGCACATCAGCTTCAAAAGCGCTCTGAAGTTCCTATA CTTTCTAGAGAATAGGAACTTCGGAATAGGAACTTCAAGATCCCCAATTCGATCGTCCGGGC CGCAAGCTCCTAGCGGCGGATTTGTCCTACTCAGGAGAGCGTTCACCGACAAACAACAGAT AAAACGAAAGGCCCAGTCTTTCGACTGAGCCTTTCGTTTTATTTGATGCCTCAAGCTAGAGA GTCATTACCCCAGGCGTTTAAGGGCACCAATAACTGCCTTAAAAAAATTACGCCCCGCCCTG CCACTCATCGCAGTCTAGCTTGGATTCTCACCAATAAAAAACGCCCGGCGGCAACCGAGCGT TCTGAACAAATCCAGATGGAGTTCTGAGGTCATTACTGGATCTATCAACAGGAGTCCAAGCT CAGCTAATTAAGCTAGCTTATCGATACCGTCGACCTCGAACCCCACGCCCCTCTTTAATACGA CGGGCAATTTGCACTTCAGAAAATGAAGAGTTTGCTTTAGCCATAACAAAAGTCCAGTATGC TTTTTCACAGCATAACTGGACTGATTTCAGTTTACAACTATTCTGTCTAGTTTAAGACTTTATT GTCATAGTTTAGATCTATTTTGTTCAGTTTAAGACTTTATTGTCCGCCCACACCCGCTTACGCA GGGCATCCATTTATTACTCAACCGTAACCGATTTTGCCAGGTTACGCGGCTGGTCCTCTAGCT GGCGTAATAGCGAAGAGGCCCGCACCGATCGCCCTTCCCAACAGTTGCGCAGCCTGAATGG CGAATGGCGATCCGAGCCGGAAGCATAAAGTGTAAAGCCTGGGGTGCCTAATGAGTGAGC TAACTCACATTAATTGCGTTGCGCTCACTGCCCGCTTTCCAGTCGGGAAACCTGTCGTGCCAG CTGCATTAATGAATCGGCCAACGCGCGGGGAGAGGCGGTTTGCGTATTGGGCGCCAGGGT GGTTTTTCTTTTCACCAGTGAGACGGGCAACAGCTGATTGCCCTTCACCGCCTGGCCCTGAG AGAGTTGCAGCAAGCGGTCCACGCTGGTTTGCCCCAGCAGGCGAAAATCCTGTTTGATGGT GGTTAACGGCGGGATATAACATGAGCTGTCTTCGGTATCGTCGTATCCCACTATCGAGATAT CCGCACCAACGCGCAGCCCGGACTCGGTAATGGCGCGCATTGCGCCCAGCGCCATCTGATC GTTGGCAACCAGCATCGCAGTGGGAACGATGCCCTCATTCAGCATTTGCATGGTTTGTTGAA AACCGGACATGGCACTCCAGTCGCCTTCCCGTTCCGCTATCGGCTGAATTTGATTGCGAGTG AGATATTTATGCCAGCCAGCCAGACGCAGACGCGCCGAGACAGAACTTAATGGGCCCGCTA ACAGCGCGATTTGCTGGTGACCCAATGCGACCAGATGCTCCACGCCCAGTCGCGTACCGTCT TCATGGGAGAAAATAATACTGTTGATGGGTGTCTGGTCAGAGACATCAAGAAATAACGCCG GAACATTAGTGCAGGCAGCTTCCACAGCAATGGCATCCTGGTCATCCAGCGGATAGTTAATG ATCAGCCCACTGACGCGTTGCGCGAGAAGATTGTGCACCGCCGCTTTACAGGCTTCGACGCC GCTTCGTTCTACCATCGACACCACCACGCTGGCACCCAGTTGATCGGCGCGAGATTTAATCG CCGCGACAATTTGCGACGGCGCGTGCAGGGCCAGACTGGAGGTGGCAACGCCAATCAGCA ACGACTGTTTGCCCGCCAGTTGTTGTGCCACGCGGTTGGGAATGTAATTCAGCTCCGCCATC GCCGCTTCCACTTTTTCTCGCGTTTTCGCAGAAACGTGGCTGGCCTGGTTCACCACGCGAGA AACGGTCTGATAAGAGACACCGGCATACTCTGCGACATCGTATAGCGTTACTGGTTTCACAT TCACCACCCTGAATTGACTCTCTTCCGGGCGCTATCATGCCATACCACGAAAGGTTTTGCACC ATTCGATGCGCCTGATGCGGTATTTTCTCCTTACGCATCTGTGCGGTATTTCACACCGCATAT

				CGAGGAGCTGTTGACAATTAATCATCGGCTCGTATAATGTGTGGAATTGTGAGCGGATAAC AATTTCACACGGCCGGCCAAGGAGAAAGGCTATGAAGCACAACCCTCTGGTGGTGTGTCTG CTCATTATCTGCATTACGATTCTGACATTCACACTCCTGACCCGACAAACGCTCTACGAACTG CGGTTCCGGGACGGTGATAAGGAGGTTGCTGCGCTCATGGCCTGCACGTCCAGGTAATCGC GAGTCGACAGGAAGGATAAGAAGAACATAAAAAATGGCACTATTCTCTAAAATATTAATTTT TTATGTGATTGGTGTGAACATATCCTTTGTCATTATCTGGTTTATCTCACATGAGAAAACACA TATTCGTTTACTTAGTGCATTCCTGGTCGGAATAACCTGGCCAATGAGTCTGCCTGTGGCATT ACTTTTTTCTCTCTTTTAGGTCGACGGCGCCAGGAGACGCGTATGAACCTGGTGGATATCGC CATTCTTATCCTCAAACTCATTGTTGCAGCACTGCAACTGCTTGATGCTGTTCTGAAATACCTG AAGTAATACTTAATTAAGGGCAAGCGCGGGGATTTTCCCCGCGCATTTCCCGGGTCAGTATG GTGCACTCTCAGTACAATCTGCTCTGATGCCGCATAGTTAAGCCAGCCCCGACACCCGCCAA CACCCGCTGACGCGCCCTGACGGGCTTGTCTGCTCCCGGCATCCGCTTACAGACAAGCTGTG ACCGTCTCCGGGAGCTGCATGTGTCAGAGGTTTTCACCGTCATCACCGAAACGCGCGAGAC GAAAGGGCCTCGTGATACGCCTATTTTTATAGGTTAATGTCATGATAATAATGGTTTCTTAGA CGTCAGGTGGCACTTTTCGGGGAAATGTGCGCGGAACCCCTATTTGTTTATTTTTCTAAATAC ATTCAAATATGTATCCGCTCATGAGACAATAACCCTGATAAATGCTTCAATAATATTGAAAAA GGAAGAGTATGAGTATTCAACATTTCCGTGTCGCCCTTATTCCCTTTTTTGCGGCATTTTGCCT TCCTGTTTTTGCTCACCCAGAAACGCTGGTGAAAGTAAAAGATGCTGAAGATCAGTTGGGTG CACGAGTGGGTTACATCGAACTGGATCTCAACAGCGGTAAGATCCTTGAGAGTTTTCGCCCC GAAGAACGTTTTCCAATGATGAGCACTTTTAAAGTTCTGCTATGTGGCGCGGTATTATCCCGT ATTGACGCCGGGCAAGAGCAACTCGGTCGCCGCATACACTATTCTCAGAATGACTTGGTTGA GTACTCACCAGTCACAGAAAAGCATCTTACGGATGGCATGACAGTAAGAGAATTATGCAGT GCTGCCATAACCATGAGTGATAACACTGCGGCCAACTTACTTCTGACAACGATCGGAGGACC GAAGGAGCTAACCGCTTTTTTGCACAACATGGGGGATCATGTAACTCGCCTTGATCGTTGGG AACCGGAGCTGAATGAAGCCATACCAAACGACGAGCGTGACACCACGATGCCTGTAGCAAT GGCAACAACGTTGCGCAAACTATTAACTGGCGAACTACTTACTCTAGCTTCCCGGCAACAAT TAATAGACTGGATGGAGGCGGATAAAGTTGCAGGACCACTTCTGCGCTCGGCCCTTCCGGC TGGCTGGTTTATTGCTGATAAATCTGGAGCCGGTGAGCGTGGGTCTCGCGGTATCATTGCAG CACTGGGGCCAGATGGTAAGCCCTCCCGTATCGTAGTTATCTACACGACGGGGAGTCAGGC AACTATGGATGAACGAAATAGACAGATCGCTGAGATAGGTGCCTCACTGATTAAGCATTGG TAACTGTCAGACCAAGTTTACTCATATATACTTTAGATTGATTTAAAACTTCATTTTTAATTTA AAAGGATCTAGGTGAAGATCCTTTTTGATAATCTCATGACCAAAATCCCTTAACGTGAGTTTT CGTTCCACTGAGCGTCAGACCCCGTAGAAAAGATCAAAGGATCTTCTTGAGATCCTTTTTTTC TGCGCGTAATCTGCTGCTTGCAAACAAAAAAACCACCGCTACCAGCGGTGGTTTGTTTGCCG GATCAAGAGCTACCAACTCTTTTTCCGAAGGTAACTGGCTTCAGCAGAGCGCAGATACCAAA TACTGTCCTTCTAGTGTAGCCGTAGTTAGGCCACCACTTCAAGAACTCTGTAGCACCGCCTAC ATACCTCGCTCTGCTAATCCTGTTACCAGTGGCTGCTGCCAGTGGCGATAAGTCGTGTCTTAC CGGGTTGGACTCAAGACGATAGTTACCGGATAAGGCGCAGCGGTCGGGCTGAACGGGGGG TTCGTGCACACAGCCCAGCTTGGAGCGAACGACCTACACCGAACTGAGATACCTACAGCGT GAGCTATGAGAAAGCGCCACGCTTCCCGAAGGGAGAAAGGCGGACAGGTATCCGGTAAGC GGCAGGGTCGGAACAGGAGAGCGCACGAGGGAGCTTCCAGGGGGAAACGCCTGGTATCTT TATAGTCCTGTCGGGTTTCGCCACCTCTGACTCGAGCGTCGATTTTTGTGATGCTCGTCAGGG GGGCGGAGCCTATGGAAAAA (Wiles et al., 2018) (pTn7xKS-mPlum was a gift from Karen Guillemin (Add gene plasmid # 117396 *; http://n2t.net/addgene:117396* ; RRID:Addgene_117396)
3.	*Escherichia coli* SM10/pTn7xKS-sfGFP	SM10/pTn7x KS-sfGFP	Donor Bacteria (Transformation)	CGCCAGCAACGCGGCCTTTTTACGGTTCCTGGCCTTTTGCTGGCCTTTTGCTCACATGTTCTTT CCTGCGTTATCAGGGGATTCCTTAAGGTATACTTTCCGCTGCATAACCCTGCTTCGGGGTCAT TATAGCGATTTTTTCGGTATATCCATCCTTTTTCGCACGATATACAGGATTTTGCCAAAGGGT TCGTGTAGACTTTCCTTGGTGTATCCAACGGCGTCAGCCGGGCAGGATAGGTGAAGTAGGC CCACCCGCGAGCGGGTGTTCCTTCTTCACTGTCCCTTATTCGCACCTGGCGGTGCTCAACGG GAATCCTGCTCTGCGAGGCTGGCCGATAAGCTCTGATACCGCTCGCCGCAGCCGAACGACC GAGCGCAGCGGGTCAGTGAGCGAGGAAGCGGAAGAGCGCCCAATACGCAAACCGCCTCTC CCCGCGCGTTGGCCGATTCATTAATGCAGCGCCCAAACATAACAGGAAGAAAAATGCCCCG CTGTGGGCGGACAAAATAGTTGGGAACTGGGAGGGGTGGAAATGGAGTTTTTAAGGATTA TTTAGGGAAGAGTGACAAAATAGATGGGAACTGGGTGTAGCGTCGTAAGCTAATACGAAA ATTAAAAATGACAAAATAGTTTGGAACTAGATTTCACTTATCTGGTTGGCCTGCAAGGCCTTC GCGAGGTACCGGGCCCAAGCTTCTCGAGGAATTCCTGCAGCCCGGGGGATCCACTAGCTAG GCCGAGAAAAAAAAGCCCGCTCATTAGGCGGGCTAGCTCATTATTTGTAGAGCTCATCCATG CCATGTGTAATCCCAGCAGCAGTTACAAACTCAAGAAGGACCATGTGGTCACGCTTTTCGTT GGGATCTTTCGAAAGGGCAGATTGTGTCGACCAGCTATCGATCCATGGGGCCCGCGGCCGC TCACTTGTACAGCTCGTCCATGCCGAGAGTGATCCCGGCGGCGGTCACGAACTCCAGCAGG ACCATGTGATCGCGCTTCTCGTTGGGGTCTTTGCTCAGGACGGACTGGGTGCTCAGGTAGTG GTTGTCGGGCAGCAGCACGGGGCCGTCGCCGATGGGGGTGTTCTGCTGGTAGTGGTCGGC GAGCTGCACGCTGCCGTCCTCGACGTTGTGGCGGATCTTGAAGTTCACCTTGATGCCGTTCT TCTGCTTGTCGGCCATGATATAGACGTTGTGGCTGTTGAAGTTGTACTCCAGCTTGTGCCCCA GGATGTTGCCGTCCTCCTTGAAGTCGATGCCCTTCAGCTCGATGCGGTTCACCAGGGTGTCG CCCTCGAACTTCACCTCGGCGCGGGTCTTGTAGGTGCCGTCGTCCTTGAAGAAGATGGTGCG CTCCTGGACGTAGCCTTCGGGCATGGCGGACTTGAAGAAGTCGTGCTGCTTCATGTGGTCG GGGTAGCGGCTGAAGCACTGCACGCCGTAGGTCAGGGTGGTCACGAGGGTGGGCCAGGG CACGGGCAGCTTGCCGGTGGTGCAGATGAACTTCAGGGTCAGCTTGCCGTTGGTGGCATCG CCCTCGCCCTCGCCGCGCACGCTGAACTTGTGGCCGTTTACGTCGCCATCCAGCTCGACCAG

				GATGGGCACCACCCCGGTGAACAGCTCCTCGCCCTTGCTCATATGTATATCTCCTTCTTAAAG TTAAACAAAATTATTTCTAGGGATCCTCCACACATTATACGAGCCGATGATTAATTGTCAAGA ATTCTAGTGAGCTCATGCATGATCGAATTAGCTTCAAAAGCGCTCTGAAGTTCCTATACTTTC TAGAGAATAGGAACTTCGGAATAGGAACTTCAAGATCCCCTGATTCCCTTTGTCAACAGCAA TGGATCGAATTGACATAAGCCTGTTCGGTTCGTAAACTGTAATGCAAGTAGCGTATGCGCTC ACGCAACTGGTCCAGAACCTTGACCGAACGCAGCGGTGGTAACGGCGCAGTGGCGGTTTTC ATGGCTTGTTATGACTGTTTTTTTGTACAGTCTATGCCTCGGGCATCCAAGCAGCAAGCGCGT TACGCCGTGGGTCGATGTTTGATGTTATGGAGCAGCAACGATGTTACGCAGCAGCAACGAT GTTACGCAGCAGGGCAGTCGCCCTAAAACAAAGTTAGGTGGCTCAAGTATGGGCATCATTC GCACATGTAGGCTCGGCCCTGACCAAGTCAAATCCATGCGGGCTGCTCTTGATCTTTTCGGT CGTGAGTTCGGAGACGTAGCCACCTACTCCCAACATCAGCCGGACTCCGATTACCTCGGGAA CTTGCTCCGTAGTAAGACATTCATCGCGCTTGCTGCCTTCGACCAAGAAGCGGTTGTTGGCG CTCTCGCGGCTTACGTTCTGCCCAGGTTTGAGCAGCCGCGTAGTGAGATCTATATCTATGATC TCGCAGTCTCCGGCGAGCACCGGAGGCAGGGCATTGCCACCGCGCTCATCAATCTCCTCAA GCATGAGGCCAACGCGCTTGGTGCTTATGTGATCTACGTGCAAGCAGATTACGGTGACGAT CCCGCAGTGGCTCTCTATACAAAGTTGGGCATACGGGAAGAAGTGATGCACTTTGATATCG ACCCAAGTACCGCCACCTAACAATTCGTTCAAGCCGAGATCGGCTTCCCGGCCGCGGAGTTG TTCGGTAAATTGTCACAACGCCGCGGCCAATTCGATCTAGAATTCCATTGAGTAAGTTTTTAA GCACATCAGCTTCAAAAGCGCTCTGAAGTTCCTATACTTTCTAGAGAATAGGAACTTCGGAA TAGGAACTTCAAGATCCCCAATTCGATCGTCCGGGCCGCAAGCTCCTAGCGGCGGATTTGTC CTACTCAGGAGAGCGTTCACCGACAAACAACAGATAAAACGAAAGGCCCAGTCTTTCGACT GAGCCTTTCGTTTTATTTGATGCCTCAAGCTAGAGAGTCATTACCCCAGGCGTTTAAGGGCA CCAATAACTGCCTTAAAAAAATTACGCCCCGCCCTGCCACTCATCGCAGTCTAGCTTGGATTC TCACCAATAAAAAACGCCCGGCGGCAACCGAGCGTTCTGAACAAATCCAGATGGAGTTCTG AGGTCATTACTGGATCTATCAACAGGAGTCCAAGCTCAGCTAATTAAGCTAGCTTATCGATA CCGTCGACCTCGAACCCCACGCCCCTCTTTAATACGACGGGCAATTTGCACTTCAGAAAATG AAGAGTTTGCTTTAGCCATAACAAAAGTCCAGTATGCTTTTTCACAGCATAACTGGACTGATT TCAGTTTACAACTATTCTGTCTAGTTTAAGACTTTATTGTCATAGTTTAGATCTATTTTGTTCA GTTTAAGACTTTATTGTCCGCCCACACCCGCTTACGCAGGGCATCCATTTATTACTCAACCGT AACCGATTTTGCCAGGTTACGCGGCTGGTCCTCTAGCTGGCGTAATAGCGAAGAGGCCCGC ACCGATCGCCCTTCCCAACAGTTGCGCAGCCTGAATGGCGAATGGCGATCCGAGCCGGAAG CATAAAGTGTAAAGCCTGGGGTGCCTAATGAGTGAGCTAACTCACATTAATTGCGTTGCGCT CACTGCCCGCTTTCCAGTCGGGAAACCTGTCGTGCCAGCTGCATTAATGAATCGGCCAACGC GCGGGGAGAGGCGGTTTGCGTATTGGGCGCCAGGGTGGTTTTTCTTTTCACCAGTGAGACG GGCAACAGCTGATTGCCCTTCACCGCCTGGCCCTGAGAGAGTTGCAGCAAGCGGTCCACGC TGGTTTGCCCCAGCAGGCGAAAATCCTGTTTGATGGTGGTTAACGGCGGGATATAACATGA GCTGTCTTCGGTATCGTCGTATCCCACTATCGAGATATCCGCACCAACGCGCAGCCCGGACT CGGTAATGGCGCGCATTGCGCCCAGCGCCATCTGATCGTTGGCAACCAGCATCGCAGTGGG AACGATGCCCTCATTCAGCATTTGCATGGTTTGTTGAAAACCGGACATGGCACTCCAGTCGC CTTCCCGTTCCGCTATCGGCTGAATTTGATTGCGAGTGAGATATTTATGCCAGCCAGCCAGA CGCAGACGCGCCGAGACAGAACTTAATGGGCCCGCTAACAGCGCGATTTGCTGGTGACCCA ATGCGACCAGATGCTCCACGCCCAGTCGCGTACCGTCTTCATGGGAGAAAATAATACTGTTG ATGGGTGTCTGGTCAGAGACATCAAGAAATAACGCCGGAACATTAGTGCAGGCAGCTTCCA CAGCAATGGCATCCTGGTCATCCAGCGGATAGTTAATGATCAGCCCACTGACGCGTTGCGCG AGAAGATTGTGCACCGCCGCTTTACAGGCTTCGACGCCGCTTCGTTCTACCATCGACACCAC CACGCTGGCACCCAGTTGATCGGCGCGAGATTTAATCGCCGCGACAATTTGCGACGGCGCG TGCAGGGCCAGACTGGAGGTGGCAACGCCAATCAGCAACGACTGTTTGCCCGCCAGTTGTT GTGCCACGCGGTTGGGAATGTAATTCAGCTCCGCCATCGCCGCTTCCACTTTTTCTCGCGTTT TCGCAGAAACGTGGCTGGCCTGGTTCACCACGCGAGAAACGGTCTGATAAGAGACACCGGC ATACTCTGCGACATCGTATAGCGTTACTGGTTTCACATTCACCACCCTGAATTGACTCTCTTCC GGGCGCTATCATGCCATACCACGAAAGGTTTTGCACCATTCGATGCGCCTGATGCGGTATTT TCTCCTTACGCATCTGTGCGGTATTTCACACCGCATATCGAGGAGCTGTTGACAATTAATCAT CGGCTCGTATAATGTGTGGAATTGTGAGCGGATAACAATTTCACACGGCCGGCCAAGGAGA AAGGCTATGAAGCACAACCCTCTGGTGGTGTGTCTGCTCATTATCTGCATTACGATTCTGACA TTCACACTCCTGACCCGACAAACGCTCTACGAACTGCGGTTCCGGGACGGTGATAAGGAGG TTGCTGCGCTCATGGCCTGCACGTCCAGGTAATCGCGAGTCGACAGGAAGGATAAGAAGAA CATAAAAAATGGCACTATTCTCTAAAATATTAATTTTTTATGTGATTGGTGTGAACATATCCTT TGTCATTATCTGGTTTATCTCACATGAGAAAACACATATTCGTTTACTTAGTGCATTCCTGGTC GGAATAACCTGGCCAATGAGTCTGCCTGTGGCATTACTTTTTTCTCTCTTTTAGGTCGACGGC GCCAGGAGACGCGTATGAACCTGGTGGATATCGCCATTCTTATCCTCAAACTCATTGTTGCA GCACTGCAACTGCTTGATGCTGTTCTGAAATACCTGAAGTAATACTTAATTAAGGGCAAGCG CGGGGATTTTCCCCGCGCATTTCCCGGGTCAGTATGGTGCACTCTCAGTACAATCTGCTCTGA TGCCGCATAGTTAAGCCAGCCCCGACACCCGCCAACACCCGCTGACGCGCCCTGACGGGCTT GTCTGCTCCCGGCATCCGCTTACAGACAAGCTGTGACCGTCTCCGGGAGCTGCATGTGTCAG AGGTTTTCACCGTCATCACCGAAACGCGCGAGACGAAAGGGCCTCGTGATACGCCTATTTTT ATAGGTTAATGTCATGATAATAATGGTTTCTTAGACGTCAGGTGGCACTTTTCGGGGAAATG TGCGCGGAACCCCTATTTGTTTATTTTTCTAAATACATTCAAATATGTATCCGCTCATGAGACA ATAACCCTGATAAATGCTTCAATAATATTGAAAAAGGAAGAGTATGAGTATTCAACATTTCC GTGTCGCCCTTATTCCCTTTTTTGCGGCATTTTGCCTTCCTGTTTTTGCTCACCCAGAAACGCT GGTGAAAGTAAAAGATGCTGAAGATCAGTTGGGTGCACGAGTGGGTTACATCGAACTGGA TCTCAACAGCGGTAAGATCCTTGAGAGTTTTCGCCCCGAAGAACGTTTTCCAATGATGAGCA

				CTTTTAAAGTTCTGCTATGTGGCGCGGTATTATCCCGTATTGACGCCGGGCAAGAGCAACTC GGTCGCCGCATACACTATTCTCAGAATGACTTGGTTGAGTACTCACCAGTCACAGAAAAGCA TCTTACGGATGGCATGACAGTAAGAGAATTATGCAGTGCTGCCATAACCATGAGTGATAACA CTGCGGCCAACTTACTTCTGACAACGATCGGAGGACCGAAGGAGCTAACCGCTTTTTTGCAC AACATGGGGGATCATGTAACTCGCCTTGATCGTTGGGAACCGGAGCTGAATGAAGCCATAC CAAACGACGAGCGTGACACCACGATGCCTGTAGCAATGGCAACAACGTTGCGCAAACTATT AACTGGCGAACTACTTACTCTAGCTTCCCGGCAACAATTAATAGACTGGATGGAGGCGGATA AAGTTGCAGGACCACTTCTGCGCTCGGCCCTTCCGGCTGGCTGGTTTATTGCTGATAAATCT GGAGCCGGTGAGCGTGGGTCTCGCGGTATCATTGCAGCACTGGGGCCAGATGGTAAGCCCT CCCGTATCGTAGTTATCTACACGACGGGGAGTCAGGCAACTATGGATGAACGAAATAGACA GATCGCTGAGATAGGTGCCTCACTGATTAAGCATTGGTAACTGTCAGACCAAGTTTACTCAT ATATACTTTAGATTGATTTAAAACTTCATTTTTAATTTAAAAGGATCTAGGTGAAGATCCTTTT TGATAATCTCATGACCAAAATCCCTTAACGTGAGTTTTCGTTCCACTGAGCGTCAGACCCCGT AGAAAAGATCAAAGGATCTTCTTGAGATCCTTTTTTTCTGCGCGTAATCTGCTGCTTGCAAAC AAAAAAACCACCGCTACCAGCGGTGGTTTGTTTGCCGGATCAAGAGCTACCAACTCTTTTTC CGAAGGTAACTGGCTTCAGCAGAGCGCAGATACCAAATACTGTCCTTCTAGTGTAGCCGTAG TTAGGCCACCACTTCAAGAACTCTGTAGCACCGCCTACATACCTCGCTCTGCTAATCCTGTTA CCAGTGGCTGCTGCCAGTGGCGATAAGTCGTGTCTTACCGGGTTGGACTCAAGACGATAGT TACCGGATAAGGCGCAGCGGTCGGGCTGAACGGGGGGTTCGTGCACACAGCCCAGCTTGG AGCGAACGACCTACACCGAACTGAGATACCTACAGCGTGAGCTATGAGAAAGCGCCACGCT TCCCGAAGGGAGAAAGGCGGACAGGTATCCGGTAAGCGGCAGGGTCGGAACAGGAGAGC GCACGAGGGAGCTTCCAGGGGGAAACGCCTGGTATCTTTATAGTCCTGTCGGGTTTCGCCA CCTCTGACTCGAGCGTCGATTTTTGTGATGCTCGTCAGGGGGGCGGAGCCTATGGAAAAA (Wiles et al., 2018)(pTn7xKS-sfGFP was a gift from Karen Guillemin (Add gene plasmid #117394; RRID:Addgene_117394, *https://www.addgene.org/117394/sequences/*)
4.	*Escherichia coli SM10/pTNS2*	SM10/pTNS2	Helper Bacteria (Transformation	No data available
5.	*Sphingobacterium multivorum*	BIGb0170	Recipient Bacteria (CeMbio)	GATCCTGGCTCAGGATGAACGCTAGCGGCAGGCCTAATACATGCAAGTCGGACGGGATCCG TCGAGAGCTTGCTCGAAGACGGTGAGAGTGGCGCACGGGTGCGTAACGCGTGAGCAACCT ACCTCTATCAGGGGGATAGCCTCTCGAAAGAGAGATTAACACCGCATAACATATCTGACCGG CATCGGTTRGCTATTAAATATTTATAGGATAGAGATGGGCTCGCGTGACATTAGCTAGTTGG TAGGGTAACGGCTTACCAAGGCGACGATGTCTAGGGGCTCTGAGAGGAGAATCCCCCACAC TGGTACTGAGACACGGACCAGACTCCTACGGGAGGCAGCAGTAAGGAATATTGGTCAATGG GCGGAAGCCTGAACCAGCCATGCCGCGTGCAGGATGACTGCCCTATGGGTTGTAAACTGCT TTTGTCCAGGAATAAACCTTTCTACGTGTAGGAAGCTGAATGTACTGGAAGAATAAGGATCG GCTAACTCCGTGCCAGCAGCCGCGGTAATACGGAGGATCCGAGCGTTATCCGGATTTATTG GGTTTAAAGGGTGCGTAGGCGGCCTATTAAGTCAGGGGTGAAATACGGTGGCTCAACCATC GCAGTGCCTTTGATACTGATGGGCTTGAATCCATTTGAAGTGGGCGGAATAAGACAAGTAG CGGTGAAATGCATAGATATGTCTTAGAACTCCGATTGCGAAGGCAGCTCACTAAGCTGGTAT TGACGCTGATGCACGAAAGCGTGGGGATCGAACAGGATTAGATACCCTGGTAGTCCACGCC CTAAACGATGATAACTCGATGTTGGCGATAGACAGCCAGCGTCCAAGCGAAAGCGTTAAGT TATCCACCTGGGGAGTACGCCCGCAAGGGTGAAACTCAAAGGAATTGACGGGGGCCCGCA CAAGCGGAGGAGCATGTGGTTTAATTCGATGATACGCGAGGAACCTTACCCGGGCTTGAAA GTTAGTGAAGAATGCAGAGACGCATTCGTCCTTCGGGACACGAAACTAGGTGCTGCATGGC TGTCGTCAGCTCGTGCCGTGAGTGTTGGGTTAAGTCCCGCAACGAGCGCAACCCCTATGTTT AGTTGCCAGCATGTAATGGTGGGGACTCTAAACAGACTGCCTGTGCAAACAGTGAGGAAGG TGGGGACGACGTCAAGTCATCATGGCCCTTACGTCCGGGGCTACACACGTGCTACAATGGA TGGTACAGCGGGCAGCTACATAGCAATATGATGCTAATCTCTAAAAGCCATTCACAGTTCGG ATTGGGGTCTGCAACTCGACCCCATGAAGTTGGATTCGCTAGTAATCGCGTATCAGCAATGA CGCGGTGAATACGTTCCCGGGCCTTGTACACACCGCCCGTCAAGCCATGAAAGTTGGGGGT ACCTAAAGCATGTTACCGCGAGGAGCG
6.	*Comamonas piscis*	BIGb0172	Recipient Bacteria (CeMbio)	GCGCCCTCCTTGCGGTTAGGCTACCTACTTCTGGCGAGACCCGCTCCCATGGTGTGACGGGC GGTGTGTACAAGACCCGGGAACGTATTCACCGTGACATTCTGATCCACGATTACTAGCGATT CCGACTTCACGCAGTCGAGTTGCAGACTGCGATCCGGACTACGACTGGCTTTATGGGATTAG CTCCCCCTCGCGGGTTGGCAACCCTTTGTACCAGCCATTGTATGACGTGTGTAGCCCCACCTA TAAGGGCCATGAGGACTTGACGTCATCCCCACCTTCCTCCGGTTTGTCACCGGCAGTCCCATT AGAGTGCCCAACTAAATGTAGCAACTAATGGCAAGGGTTGCGCTCGTTGCGGGACTTAACC CAACATCTCACGACACGAGCTGACGACAGCCATGCAGCACCTGTGTTACGGTTCTCTTTCGA GCACATGTCCATCTCTGGTCACTTCCGTACATGTCAAAGGTGGGTAAGGTTTTTCGCGTTGCA TCGAATTAAACCACATCATCCACCGCTTGTGCGGGTCCCCGTCAATTCCTTTGAGTTTCAACC TTGCGGCCGTACTCCCCAGGCGGTCAACTTCACGCGTTAGCTTCGTTACTGAGAAAGTTAAT TCCCAACAACCAGTTGACATCGTTTAGGGCGTGGACTACCAGGGTATCTAATCCTGTTTGCTC CCCACGCTTTCGT GCATGAGCGTCAGTACAGGTCCAGGGGATTGCCTTCGCCATCGGTGTTCCTCCGCATATCTA CGCATTTCACTGCTACACGCGGAATTCCATCCCCCTCTACCGTACTCTAGCTATGCAGTCACA AAGGCAGTTCCCAGGTTGAGCCCGGGGATTTCACCTCTGTCTTACATAACCGCCTGCGCACG CTTTACGCCCAGTAATTCCGATTAACGCTTGCACCCTACGTATTACCGCGGCTGCTGGCACGT AGTTAGCCGGTGCTTATTCTTACGGTACCGTCATGGACCCTCTTTATTAGAAAGAGTCTTTTC GTTCCGTACAAAAGTAGTTTACAACCCGAGGGCCTTCATCCTACACGCGGCATTGCTGGATC AGGCTTTCGCCCATTGTCCAAAATTCCCCACTGCTGCCTCCCGTAGGAGTCTGGACCGTGTCT CAGTTCCAGTGTGGCTGGTCGTCCTCTCAGACCAGCTACAGATCGTCGGCTTGGTAAGCTTT

				TATCCCACCAACTACCTAATCTGCCATCAGCCGCTCTAGTAGCACAAGGTCTTGCGATCCCCT GCTTTCATCCTTAGATCTCATGCGGTATTAGCTACTCTTTCGAGTAGTTATCCCCCACTACTAG GCACGTTCCGATGTATTACTCACCCGTTCGCCACTCGTCAGCATCCGAAGACCTGTTACCGTT CGACTTGCATGTGTAAAGCATGCCGCCAGCGTTCAATCTGAGC
7.	*Comamonas sp. B-9*	MYb21	Recipient Bacteria (CeMbio)	GGCTGGCGGCATGCTTTTACACATGCAAGTCGAACGGTAACAGGTCTTCGGATGCTGACGA GTGGCGAACGGGTGAGTAACACATCGGAACGTGCCTAGTAGTGGGGGATAACTACTCGAA AGAGTAGCTAATACCGCATGAGATCTAAGGATGAAAGCAGGGGACCTTCGGGCCTTGCGTA CTAGAGCGGCTGATGGCAGATTAGGTAGTTGGTGGGATAAAAGCTTACCAAGCCGACGATC TGTAGCTGGTCTGAGAGGACGACCAGCCACACTGGGACTGAGACACGGCCCAGACTCCTAC GGGAGGCAGCAGTGGGGAATTTTGGACAATGGGCGAAAGCCTGATCCAGCAATGCCGCGT GTAGGATGAAGGCCCTCGGGTTGTAAACTACTTTTGTACGGAACGAAAAGACTCTTTCTAAT AAAGAGGGTCCATGACGGTACCGTAAGAATAAGCACCGGCTAACTACGTGCCAGCAGCCGC GGTAATACGTAGGGTGCAAGCGTTAATCGGAATTACTGGGCGTAAAGCGTGCGCAGGCGG TTATGTAAGACAGAGGTGAAATCCCCGGGCTCAACCTGGGAACGGCCTTTGTGACTGCATA GCTAGAGTACGGTAGAGGGGGATGGAATTCCGCGTGTAGCAGTGAAATGCGTAGATATGC GGAGGAACACCGATGGCGAAGGCAATCCCCTGGACCTGTACTGACGCTCATGCACGAAAGC GTGGGGAGCAAACAGGATTAGATACCCTGGTAGTCCACGCCCTAAACGATGTCAACTGGTT GTTGGGAATTAACTTTCTCAGTAACGAAGCTAACGCGTGAAGTTGACCGCCTGGGGAGTAC GGCCGCAAGGTTGAAACTCAAAGGAATTGACGGGGACCCGCACAAGCGGTGGATGATGT7. GGTTTAATTCGATGCAACGCGAAAAACCTTACCCACCTTTGACATGTACGGAAGTGACCAGA GATGGACATGTGCTCGAAAGAGAACCGTAACACAGGTGCTGCATGGCTGTCGTCAGCTCGT GTCGTGAGATGTTGGGTTAAGTCCCGCAACGAGCGCAACCCTTGCCATTAGTTGCTACGAAA GGGCACTCTAATGGGACTGCCGGTGACAAACCGGAGGAAGGTGGGGATGACGTCAAGTCC TCATGGCCCTTATAGGTGGGGCTACACACGTCATACAATGGCTGGTACAAAGGGTTGCCAA CCCGCGAGGGGGAGCTAATCCCATAAAGCCAGTCGTAGTCCGGATCGCAGTCTGCAACTCG ACTGCGTGAAGTCGGAATCGCTAGTAATCGTGGATCAGAATGTCACGGTGAATACGTTCCC GGGTCTTGTACACACCGCCCGTCACACCATGGGAGCGGGTCTCGCCAGAAGTAGGTAGCCT AACCGTAAGGAGGGCGCTTACCACGGCGG
8.	*Chryseobacterium sp.*	MYb317	Recipient Bacteria (CeMbio)	TATATTGAATGGCATCATTCGATATTGAAAACTCCGGTGGATAGAGATGGGCACGCGCAAG ATTAGATAGTTGGTGAGGTAACGGCTCACCAAGTCTRCGATCTTTAGGGGGCCTGAGAGGG TGATCCCCCACACTGGTACTGAGACACGGACCAGACTCCTACGGGAGGCAGCAGTGAGGAA TATTGGACAATGGGTGAGAGCCTGATCCAGCCATCCCGCGTGAAGGACGACGGCCCTATGG GTTGTAAACTTCTTTTGTATAGGGATAAACCTAGATACGTGTATCTAGCTGAAGGTACTATAC GAATAAGCACCGGCTAACTCCGTGCCAGCAGCCGCGGTAATACGGAGGGTGCAAGCGTTAT CCGGATTTATTGGGTTTAAAGGGTCCGTAGGCGGATCTGTAAGTCAGTGGTGAAATCTCACA GCTTAACTGTGAAACTGCCATTGATACTGCAGGTCTTGAGTGTTGTTGAAGTAGCTGGAATA AGTAGTGTAGCGGTGAAATGCATAGATATTACTTAGAACACCAATTGCGAAGGCAGGTTAC TAANGCAACAACTGACGCTGATGGACGAAAGCGTGGGGAGCGAACAGGATTAGATACCCT GGTAGTCCACGCCGTAAACGATGCTAACTCGTTTTTGGGATTTAGGTTTCAGAGACTAAGCG AAAGTGATAAGTTAGCCACCTGGGGAGTACGTTCGCAAGAATGAAACTCAAAGGAATTGAC GGGGGCCCGCACAAGCGGTGGATTATGTGGTTTAATTCGATGATACGCGAGGAACCTTACC AAGGCTTAAATGGGAAATGACAGGTTTAGAAATAGACTTTTCTTCGGACATTTTTCAAGGTG CTGCATGGTTGTCGTCAGCTCGTGCCGTGAGGTGTTAGGTTAAGTCCTGCAACGAGCGCAAC CCCTGTCACTAGTTGCCATCATTAAGTTGGGGACTCTAGTGAGACTGCCTACGCAAGTAGAG AGGAAGGTGGGGATGACGTCAAATCATCACGGCCCTTACGCCTTGGGCCACACACGTAATA CAATGGCCAGTACAGAGGGCAGCTACACAGCGATGTGATGCAAATCTCGAAAGCTGGTCTC AGTTCGGATTGGAGTCTGCAA

10.2 Protocol for Gut Colonisation assay

1. *C. elegans* strains

STRAIN	BACKGROUND
OW454	*kynu-1(tm4924) X*
OW477	*afmd-1(tm4547) IV*
OW478	*kmo-1(tm4529) V*
Ow479	*haao-1(tm4627)*
OW717	*tdo-2(zg217) III*
N2 (OW)	N2 from OW lab

2. Bacterial strain

Enterobacter cloacae mPlum (CeENT-1 mPlum)

Ochrobactrum vermis sfGFP (MYb71 sfGFP)

Enterobacter ludwigii dTom (MYb174 dTom)

Pantoea nemavictus mPlum (BIGb0393a mPlum)

Stenotrophomonas indicatrix RFP2 (JUb19 RFP2)

Maintain bacterial strain CeEnt1-mPlum (any fluorescently tagged bacterial isolate) at 15C on LB + G60 (gentamicin 60ug/mL) + IPTG (to eliminate any *E. coli* donor contamination) plates by re-streaking weekly.

1st day

- Pick 15-20 L4 worms from a clean never-starved plate and transfer them onto another pre-seeded (at least 3 days earlier and kept at 20-25C) OP50 plate (60mm)
- **Label with strain name, date, researcher initials, and day0**
- **Use different colour pens for different strains to avoid mixing them!**
- Incubate at 15 °C for 24 h
- Make 2 or 3 separate bacterial suspensions from clean clones of *CeENT1-mPlum* in LB G60 broth + IPTG (clones taken from a 1-week-old plate that is clean and confirmed to be homogeneously fluorescent, IPTG may or may not be added depending on the confidence you have that the *E. coli* donor has been eliminated) and incubate it 48h at 25 °C under agitation (make sure to leave enough oxygen, do not fill the tubes: about 9-10 mL in a 14mL tube or 30mL in a 50mL tube!).

2nd day

- Pick the 15-20 day1 young adult worms from the previous plate and transfer to another pre-seeded OP50 plate (60mm) labelled as day1
- Incubate at 15 °C for 24 h
- Let your CeENT1-mPlum bacteria keep growing at 25C under agitation.

3rd day

- Pick the 15-20 day2 adult worms from the previous plate and transfer to another pre-seeded op50 plate (60mm) labelled day2
- Incubate at 15 °C for 24 h
- Check the colour of the 2 or 3 separate bacterial suspensions of *CeENT1- mPlum* in LB G60 broth (check that the fluorophore starts to be expressed, you will normally favour the clone with the best expression), seed enough plates for 1 days' worth of experiment for all clones and make sure to specify the clone number on each plate (calculate how many you might need). Grow at 25C for 1 day.

4th day

- Pick the 15-20 day3 adult worms from the previous plate and transfer to another pre-seeded op50 plate (60mm) labelled day3
- Incubate at 15 °C for 24 h
- Also pick the 15-20 L4 worms from an earlier plate and transfer to another pre-seeded op50 plate (60mm) labelled day0 (starting a new series of egg lays)
- Incubate at 15 °C for 24 h
- Check the colour of the 2 or 3 separate bacterial suspensions of *CeENT1- mPlum* in LB G60 broth (check that the fluorophore starts to be expressed, you will normally favour the clone with the best expression)
- Inoculate 100 µL of bacterial suspension of *CeENT1-mPlum* culture per NGM plate (60mm). **Make sure the NGM plates have been poured at least 2 days earlier so that they are dry enough.** Make sure to seed enough plates for 1 days' worth of experiment for each clone (assume some clones might be contaminated) and make sure to specify the clone number on each plate (calculate how many you might need).
- Grow at 25C for 24 h.

5th day

- On this day, day0 or day1 plates from the first series of egg lays would have L4 that are useable for experiments and can be transferred for 24h onto new OP50 plates at

25C. However, if you did not prepare *CeENT1-mPum* bacterial plates early enough, you might need to wait further.

- Kill all the adult worms from the plates labelled day3
- Pick the 15-20 day1 adult worms from the new plates labelled day0 and transfer to another pre-seeded op50 plate (60mm) labelled day1
- Incubate at 15 °C for 24 h
- Check NGM bacterial plates from 4th day for contaminations and check for homogeneous fluorescence. Discard plates that are not satisfactory (this is why you grow 2-3 bacterial clones and only see 1 day worth of plates on the 4th day).
- Keep them growing at 15-20C for 48 h.
- If at least one bacterial culture is clean with homogeneous fluorescence, inoculate 100 µL of bacterial suspension of *CeENT1-mPlum* culture per NGM plate (60mm). **Make sure the NGM plates have been poured at least 2 days earlier so that they are dry enough.** Make sure to seed enough plates for the full remaining experiment (calculate how many you should need including the useable plates seeded on the 4th day, but seed 15% more plates in case you have unanticipated transfers to do or some plates get contaminated with fungi) and make sure to specify the clone number on each plate.
- Grow at 15-20C for 24 h.

6th day

- day0-2 plates from the first series of egg lays should have L4 that are useable for experiments and can be transferred onto new OP50 plates at 25C. Make sure to note the time at which the transfer and temperature switch are done and that worms are all L4 across the different worm strains being compared. **Make sure to have enough worms for your experiments (plan to have almost twice as many worms as you expect to mount: ~250-300 worms per strain, as some may die toward the last couple of days of the experiment, and you might have to redo some slides). I suggest you put 50-60 worms per plate and thus have 5 plates for each condition. I also suggest you aim to do that at 9am in the morning to make your life easier for the erst of the experiment.**

- Grow these worms 24h at 25C on the OP50-seeded GM plates.
- Pick the 15-20 day2 adult worms from the new plates labelled day1 and transfer to another pre-seeded op50 plate (60mm) labelled day2
- Incubate at 15 °C for 24 h
- Keep growing clean CeENT1-mPlum plates from 4th day at 15-20C for a further 24 h.
- Check the CeENT1-mPlum plates inoculated on the 5th day that are at 25C and transfer them to 15-20C for 48 h.

7th day

- You can finally tranter day 1 adult worms (L4 +24h grown at 25C on OP50) onto *CeENT1-mPlum* plates (50-60 worms per plate). Use the plates from the 4th day. Transfer worms manually, depositing the worms all in the same location on the plate, making sure to remove eggs and OP50 bacteria after worms wiggle out of the spot where you transferred them. **Note the time precisely for each strain, this is your time 0h! It is good to have your strains staggered so that it makes mounting them for imaging less stressful later.**
- Keep worms on *CeENT1-mPlum* at 25C from now on until the end of the experiment.
- Pick the 15-20 day3 adult worms from the new plates labelled day2 and transfer to another pre-seeded op50 plate (60mm) labelled day3.
- Incubate at 15 °C for 24 h
- Also pick the 15-20 L4 worms from an earlier plate and transfer to another pre-seeded op50 plate (60mm) labelled day0 (starting a new series of egg lays)
- Incubate at 15 °C for 24 h
- Keep growing clean CeENT1-mPlum plates from 5th day at 15-20C for a further 24 h.
- Around timepoint 6h, you can practice mounting and acquire a few worm images per condition (10-15 worms max). This timepoint is not essential for the KP paper but is used to adjust imaging parameters for both fluorescence and transmitted light if needed (I will try to come to the axiozoom when you have slides ready then).

7th day, timepoint 10-11h

- Start the heat-block to melt the 2% agarose in M9 (set it at 100C)

- Prepare your slides, coverslip, tape, silicone grease, and anaesthetic.
- When a strain reaches timepoint 11.5-12h (you can start 30min early), start mounting worms onto slides. Mount strains in the order in which you have placed them on the *CeENT1-mPlum* plates 12 h earlier (check the time of your timepoint 0h). Once mounted and sealed, keep plates in a tip box as demonstrated at 15C.
- Image on the AxioZoom once all your slides have been prepared. This is your first required timepoint (you will aim to image 30 worms per time point using the Zeiss AxioZoom setup for timepoints 12h, 24, 48h, 72h and 120h).

8th day

- Before timepoint 24h, start the heat-block to melt the 2% agarose in M9 (set it at 100C)
- Prepare your slides, coverslip, tape, silicone grease, and anaesthetic.
- At timepoint 23-24h start mounting worms for imaging again.
- After this, transfer all worms onto new CeENT1-mPlum NGM plates to get rid of larvae and eggs, and keep at 25C again. Discard old *CeENT1-mPlum* plates you removed the ageing worms from.
- Kill all the adult worms from the egg lay plates labelled day3
- Pick the 15-20 day1 adult worms from the new plates labelled day0 and transfer to another pre-seeded op50 plate (60mm) labelled day1
- Incubate at 15 °C for 24 h

9th day

- Before timepoint 48h, start the heat-block to melt the 2% agarose in M9 (set it at 100C)
- Prepare your slides, coverslip, tape, silicone grease, and anaesthetic.
- At timepoint 47-49h (the timing is a bit more flexible then) start mounting worms for imaging again.
- After this, transfer all worms onto new CeENT1-mPlum NGM plates to get rid of larvae and eggs, and keep at 25C again. Discard old *CeENT1-mPlum* plates you removed the ageing worms from.

- Pick the 15-20 day2 adult worms from the new plates labelled day1 and transfer to another pre-seeded op50 plate (60mm) labelled day2
- Incubate at 15 °C for 24 h

Make sure to transfer your worms on new CeENT1-mPlum (or freshly seeded bacteraial plate) daily until they stop having young larvae. Note that as you go through your worms, you need less and less plates as you can keep 50-60 worms per plate and by the 3rd time point, you will only have half of your worms left.

10.3 Macros For Image Analysis

10.3.1 CEent-1 mPlum (monoxenic condition)

Language: ImageJ macro

```
/*
 * Macro template to process multiple images in a folder
 */
#@ File (label = "Input directory", style = "directory") input
#@ File (label = "Output directory", style = "directory") output
#@ String (label = "File suffix", value = ".czi") suffix
// See also Process_Folder.py for a version of this code
// in the Python scripting language.
processFolder(input);
// function to scan folders/subfolders/files to find files with correct suffixfunction
processFolder(input) {list = getFileList(input);list = Array.sort(list);for (i = 0; i < list.length; i++)
{if(File.isDirectory(input + File.separator + list[i]))processFolder(input + File.separator +
list[i]);if(endsWith(list[i], suffix))processFile(input, output, list[i]);}}function
processFile(input, output, file) {setBatchMode(true);
        // Do the processing here by adding your own code.
        // Leave the print statements until things work, then remove them.
        print("Processing: " + input + File.separator + file);
```

```
        //open with bioformats run("Bio-Formats Importer",
"open=["+input+File.separator+file+"] color_mode=Default view=Hyperstack
stack_order=XYCZT");
        //trim the suffix from the files - some files have dots in the names
        //file = substring(file, 0, file.length-4);
        //set LUTs for composite of 3 channels
        //Stack.setDisplayMode("composite");
        //Stack.setChannel(3);
        //run("Grays");
        //Stack.setChannel(2);
        //run("Green");
        //Stack.setChannel(1);
        //run("Blue");
// THIS MACRO WILL PROCESS IMAGES WITH 2 FLUORESCENCE CHANNELS AND ONE
BRIGHTFIELD CHANNEL
// CHANNELS WOULD HAVE BEEN TYPICALLY ACQUIRED IN THE FOLLOWING ORER ON THE
AXIOZOOM SYSTEM:
// (1) LRO AUTOFLUORESCENCE
// (2) FLUORESCENT GUT BACTERIUM
// (3) WORM ANATOMY BY CONTRASTED BRIGHTFIELD IMAGING
// IT PROCEEDS TO PREPARE A SINGLE BRIGHTFIEDL IMAGE TAKEN IN TEH MIDDLE OF TEH Z-
STACK
// THEN IT REDUCES EACH FLUO STACK TO A SINGLE PROJECTED 8-BIT IMAGE TO FACILITATE
// (1) CHANNEL RE-MERGING FOR GUT COLONISATION SCORING
// (2) ANALYSIS OF LRO AA-DEPENDENT AUTOFLUORESCENCE IN RESPONSE TO GUT
BACTERIA
// NUMBERS IN BLUE IN PARENTHESIS CAN BE ADJUSTED DEPENDING ON THE BACETRIUM
AND WORM GENETIC BACKGROUND
// BUT THEY MUST BE CONSISTENTLY APPLIED ACCROSS ALL CONDITIONS COMPARED
// (SAME FOR ALL TIME POINTS AND WORM GENOTYPES FOR A GIVEN BACTERIUM)
//split channels
run("Split Channels");
```

```
//keep middle slice only and smootrun("Slice Keeper", "first=9 last=9 increment=2");
run("Median...", "radius=2");
//make last channel 8-bit run("8-bit");
//apply intensity correction on brightfield for composite/merge display
run("Brightness/Contrast..."); setMinAndMax(40, 450);
//ensure Brightfield image is gray run("Grays");
//save the channel (BF here) and close it saveAs("Tiff", output+File.separator+file+"BF.tif");
run("Close"); print("Saving to: " + output); run("Close"); close();
//process next fluorescence channel (ceENT1_mPlum here)
//smooth image run("Median...", "radius=2");
//perform Z-projection on ChN-1 channel run("Z Project...", "start=2 stop=16
projection=[Average Intensity]");
//Apply intensity corrections run("Brightness/Contrast..."); setMinAndMax(90, 1200);
run("Apply LUT");
//make 8-bit run("8-bit");
//ensure fluorescence image is Yellow to allow for easier visual scoring (the human eye
perceives yellows better than blues and reds for instance) run("Yellow");
//save the channel (CEent1-mPlum here) and close it saveAs("Tiff",
output+File.separator+file+"M.tif");run("Close");print("Saving to: " +
output);run("Close");close();
//process next fluorescence channel (LRO blue fluorescence here)
//smooth image run("Median...", "radius=2");
//perform Z-projection on ChN-2 channel (1st channel in a 3-channel image) run("Z
Project...", "start=3 stop=15 projection=[Average Intensity]");
//Apply intensity corrections run("Brightness/Contrast..."); setMinAndMax(330, 3000);
run("Apply LUT");
//make 8-bitrun("8-bit");
//ensure fluorescence image is blue run("Blue");
//save last channel and close any other saveAs("Tiff", output+File.separator+file+"LRO.tif");
run("Close");print("Saving to: " + output); run("Close All");setBatchMode(false);}
```

Macros for other conditions were changed according to the fluorescent channel exposure time, brightness and contrast etc.